

# Rheology, Chemistry and Microstructure of *Oil* and *Tempera* Paints

Zur Erlangung des akademischen Grades einer  
DOKTORIN DER INGENIEURWISSENSCHAFTEN (DR.-ING.)

von der KIT-Fakultät für Chemieingenieurwesen und Verfahrenstechnik  
des Karlsruher Instituts für Technologie (KIT)

genehmigte

## DISSERTATION

von  
Dipl. -Ing. Ophélie Ranquet  
aus Colmar, Frankreich

Erstgutachter: Prof. Dr. Norbert Willenbacher  
Zweitgutachterin: Prof. Dr. Ilaria Bonaduce  
Tag der mündlichen Prüfung: 26.05.2023



# Preface

This dissertation consists of two peer-reviewed scientific journal articles, published in multidisciplinary journals including an article in a journal of high impact. These include the main results of my experimental work at the *Karlsruhe Institute of Technology* (KIT, Germany), Institute for Mechanical Process Engineering and Mechanics, Applied Mechanics Group, and at the *University of Pisa* (Italy), Department of Chemistry and Industrial Chemistry, from January 2019 until August 2022.

The main part of this thesis follows a general introduction and a description of the materials and methods used and it includes the following adapted publications:

- Ranquet, O., Duce, C., Bramanti, E., Dietemann, P., Bonaduce, I. & Willenbacher, N. A holistic view on the role of egg yolk in Old Masters' oil paints. *Nature Communications*. **14**, 1534 (2023)
- Ranquet, O., Duce, C., Caroti, G., Dietemann, P., Bonaduce, I. & Willenbacher, N. *Tempera* and *Tempera Grassa* – from wet paints to solid films. *ACS Appl. Polym. Mater.* **5**, 4664–4677 (2023)

Moreover, an additional chapter gathering further studies on the presented topic is included.

This thesis concludes with an overall summary, an outlook and a bibliography. The bibliography includes all references of the publications. Furthermore, some graphs and images are modified in terms of size and color.





# Acknowledgments

These following pages are the fruit of a work that began in January 2019.

These three and a half years of research were intense, interesting, intellectually and emotionally enriching. I spent time in three different cities around Europe: Pisa, Karlsruhe and Munich, learned a new language and improved two others, which I can now professionally use, went through most of my PhD during a global pandemic and worked on a topic I loved from the beginning to the end.

These achievements would not have been possible without the help and the support of the people around me: all of them contributed differently to the success of the work presented in the following pages, and especially I would like to express my gratitude to:

- Prof. Dr. Norbert Willenbacher, my Doktorvater, for giving me the opportunity to do my doctorate under his guidance at the Institute of Mechanical Process Engineering and Mechanics (MVM) - Applied Mechanics Group (AME) at the Karlsruhe Institute of Technology. Norbert, ich danke dir für dein Vertrauen, deine Ermutigung, meine Ideen zu vertreten, und deine Unterstützung, meine Kreativität auszuüben, wenn es nötig war.
- Prof. Dr. Ilaria Bonaduce, my supervisor, for welcoming me in the Analytical Chemistry for Cultural Heritage Group of the Department of Chemistry and Industrial Chemistry at the University of Pisa. Ilaria, grazie a te per la tua fiducia, per avermi insegnato tutte queste conoscenze, per i nostri scambi e per tutto il tempo trascorso a lavorare con una persona interessante come te.
- Finally, I would like to thank Dr. Patrick Diemann, my mentor, for the possibility of working at and with the Doerner Institut, Bayerische Staatsgemäldesammlungen in Munich during this project. Patrick, ich danke dir, dass du mich mit deiner Leidenschaft angesteckt hast, dass du mir diesen magischen Ort, das Doerner Institut, mit all den leidenschaftlichen Menschen, die dort arbeiten, gezeigt hast. Danke für deine so wertvollen Ratschläge und Ermutigungen.

I am grateful to have had the opportunity to work with you on such an interesting topic from three different perspectives, for the access to your working areas and laboratories, for your advices, our long discussions and open-minded fruitful exchanges. But especially thank you, all the three of you, for helping me grow as a scientist.

- I would like to thank Prof. Celia Duce for her support, her kindness, her time and all of our exchanges along the years. Silvia, grazie a te for your support and the long discussions at

work but also *alle Bandierine* in front of a plate of spaghetti. Grazie also to Dr. E. Bramanti for the work together and the access to the equipments in her laboratories at the CNR in Pisa.

- I would also like to thank the *INSTM*, the *DAAD France*, the *KCT* and the *KHYS* for their financial support.
- Many thanks to the academic staff of the Department of Chemistry and Industrial Chemistry of the University of Pisa, especially R. Carosi, A. Andreotti, E. Pulidori, Prof. E. Ribecchini., Prof. I. Degano, Prof. F. Modugno, Prof. M.P. Colombini, Prof. L. Bernazzani, Prof. M.R. Tinè for the opportunity to work with you, using your equipment and your valuable time and expertise. A very special thanks to Francescina, Federica, Silvia, Francesca, Marco, Silvia and Giulia, my dear friends and colleagues, for your warm welcome, your support, your incredible input of the Italian culture and all of these special and wonderful moments I had with you all. Grazie Mille.
- Merci Justine de m'avoir accompagnée en ce début de thèse et pour toutes nos aventures à la découverte de l'Italie.
- U. Baumer, Dr. H. Stege and the staff of the Doerner Institut thank you for showing me around, seeing your work among these incredible pieces of art.
- Thanks to my students Lou Spanneut, Thayane Cantoni da Rocha, Rizwan Mehmood, Helena Telle Jiménez and Kubilay Baki for writing their Bachelor- or Master Thesis on my topics and/or being my research assistants. It was a great pleasure to work with you.
- At the KIT in Karlsruhe, vielen Dank to Dr. B. Hochstein for your help on technical issues and your great advice. The technical staff of the MVM, K. Sasso, K. Bertsch, K. Hirsch, A. Huber and R. Mall for your valuable time and expertise. Merci à toi Claude pour tes conseils, ta bonne humeur et tes blagues qui m'ont été tellement bénéfiques.
- Thanks to my AME colleagues and those who became my friends David, Annika, Kevin, Jonas, Moritz, Yiliang, Wolf, Maxilein, Karlita, Johannes, Bruna, Felipe, Bo, Hongye, Katrin, Karim, for being supportive and sometimes crazy with me. We went through a pandemic together, organized Coffee-lists competitions, did some cheese and wine evenings, a lot of singing along or coffee breaks under the sunny balcony, shared (un)memorable times during the group seminars. I became your "Ophélie Rakete". Thank you all for taking care of me.
- Meriem, Ronald, Aïcha, thanks for the great evenings, cooking, dancing and deep discussions, and Simon and Sam, les rois des cailloux, for all the quality time I had with you.
- Kasia, Chouchou, dziękuję za wspólne chwile, gotowanie, śmiech i podróże. Rozjaśniłeś moje codzienne życie podczas ostatnich dwóch lat pracy magisterskiej.
- Annika, Schatzi, ich danke dir, dass du deine Freude und Energie mit mir geteilt hast und dass du mir in jedem Moment eine so wertvolle Freundin warst!

- Merci à mes amis de toujours, notamment Mallaury, Tom, Diboune, Bambi, Lucas, Pauline, Kauffer, Fengdi, Laroche, Manon, Mathilde, Pauline, Hélène, Emilie, Estelle, Sarah, pour leur soutien sans failles à travers les épreuves et les joies.
- Last, but not least, merci to my family, for your never-ending love and support. Vous m'avez accompagnée, encouragée et soutenue tout au long de cette aventure, ce marathon, dans les joies comme dans les peines. Je vous aime et j'espère vous rendre fiers.

Merci à vous tous.

Ophélie Ranquet



# Abstract

Old Masters such as Botticelli, da Vinci, Dürer, Rembrandt or Vermeer frequently used paints containing both egg and oil as binders to create their paintings, but the way and the reason this was done is still not understood. Indeed, these two binders can be added in the paint in many different ways, resulting in considerably diverse behavior of the wet paints, and also affects the drying behavior and the curing reactions. Identifying how the paints have been prepared in the past is useful to understand how to restore them in the present, and be able to preserve them for the future. Studying the techniques used in artistic painting by chemical analysis has been commonly performed using a top-down approach consisting on analytical techniques to identify the pigment and binder compositions and art technical studies. But very little work has been done to study the flow and physico-chemical properties of the prepared paints. In recent years, consideration of principles of colloid chemistry lead to a new perspective in our understanding of the properties of paints and how they can be applied on paintings. Some studies have been conducted on the rheological characterization of paints, showing the need of connecting the formulation of ancient paint recipes with their flow properties and their final appearance on a canvas. However, the paints systems are complex, and when the studies are based on paints reconstructions, multiple parameters are usually simultaneously varied, blurring the information regarding important criteria ruling the flow properties of such systems such as the volume fraction of the disperse phase or the pigment-binder interactions. Also, knowledge about chemical reactions taking place during ageing of oil paints has been recently advancing, with the development of models associated with these complex chemical pathways. Despite this, very little is known about systems involving both siccativ oils and proteins, which are components commonly present in the paint mixtures prepared by the Old Masters.

This thesis, consisting of a preparation of various mock-up paints, focuses on the influence of the repartition of the binder in paints and examines how the preparation of these paints can be used to manipulate their microstructures, resulting in paints having different flow behaviors, drying and ageing properties, influencing the aspect of the final appearance of the paints we can observe in museums. Several strategies to modify oil paints with egg additions have been studied. Here, egg yolk and linseed oil were used in combination with two pigments, lead white and ultramarine blue, to evaluate how different repartition of proteinaceous and lipid binders can be used to control the flow behavior as well as drying kinetics and chemistry of paints. Steady shear experiments were employed to determine the yield stress and the high shear viscosity, which influence the brushability, brush stroke profile and impasto of a paint. Results were combined with gravimetric

and thermogravimetric analysis, differential scanning calorimetry, but also mechanical texture analysis and spectrometric techniques to gain understanding of the drying and curing processes going on in such paint layers.

In an effort to shed light on the role of proteinaceous material additions in oil paints, pure oil paints were compared to capillary suspensions (CapS) and egg-coated pigments in oil (PCP) of identical disperse volume fractions  $\phi$ . Capillary suspensions develop if egg yolk (or water) is mixed into oil paints, e.g. with a brush, or even due to the uptake of humidity. The aqueous component forms with the pigments a percolating fractal network, resulting in stiff paints with a high yield stress, ideal for creating impasto, but paint stiffening due to undesired uptake of humidity from the environment can also be suppressed, depending on proteinaceous binder distribution and colloidal paint microstructure. Egg-coated pigments in oil are formed when pigments are ground with egg added as a wetting and anticaking agent, before dispersing the coated pigment in oil. Adding egg during the preparation of the paints can be used to increase the pigment-binder ratio, avoiding problems caused by traces of humidity naturally occurring in the pigments during storage, and minimizing binder-caused ageing problems such as darkening and crack formation. Brushability at high pigment loading can be improved when reducing the high shear viscosity of the paints, and wrinkling can be suppressed adjusting a high yield stress. Egg acts as antioxidant: it slows down the onset of curing and the dry-to-touch and promotes the formation of cross-linked networks less prone to oxidative degradation compared to oil alone, which might have improved the preservation of invaluable artworks.

Then, paints bound with egg (the so-called *tempera* paints) and the influence of added oil on microstructure, rheology, drying kinetics and chemistry is investigated. When oil is added in egg *tempera* paints, these systems are called fatty *tempera*, or *tempera grassa* (TG), and are believed to play an intermediate role between oil and *tempera* paints. However, despite their hydrophobic nature, pigments remain outside the emulsified oil droplets due to the adsorption of egg proteins on the pigment surface. The flow behavior of both paint types can be described using classical concepts of colloidal dispersion rheology, including not only the pigment but also the added egg yolk and oil into the calculation of the disperse phase volume fraction  $\phi$ . Small differences in viscosity and yield stress are attributed to the broader particle size distribution for *tempera grassa* paints. *Tempera* paints are known to dry quickly, and the dry-to-touch is controlled by the evaporation of water in both, *tempera* and *tempera grassa* paints. The added oil does not influence the painting behavior in general, however, on absorbent substrates different brushability is observed due to the remaining oil in *tempera grassa*. After the dry to the touch state is reached, the oil cross-linking sets in, leading to a second hardening step. The distribution of protein, water and oil in paints correlates with the flow properties and the drying and curing behavior of paints, demonstrating, that *tempera grassa* paints behaves like *tempera* and cannot explain observations from paintings showing characteristics “in between” *tempera* and oil techniques.

Ultimately, we investigated the role of the disperse volume fraction and the influence of the thickness of oil paint layers on their drying and aging properties. Particularly, the wrinkle formation as well as the onset of drying time increases for paints having a lower yield stress, which is intensified when the layer thickness increases. Flow properties, drying kinetics and color modifications are mostly affected by a change of the chemical composition of the pigment surface rather than the pigment shape and size distribution in oil paints for the pigment systems investigated here. Finally, color modifications, curing and oxidative degradation reactions seem to be influenced by the paint microstructure on the long-term, which need to be conducted in longer-term experiments (> 3 years) in a controlled and systematic way.

In total, this thesis offers a multi-disciplinary and multi-analytical approach based on rheology, physical and analytical chemistry, carried out to study the chemical composition as well as the mechanical and physico-chemical properties of various paints. The focus was not only on wet paints, but also on their drying and curing behavior, in order to correlate them with effects observed on *tempera* and oil paintings. Samples with different applications of egg yolk and linseed oil mixed binders with lead white and ultramarine blue pigments were prepared and analyzed by a broad range of chemical and mechanical methods. This project involving art technology, chemistry and rheology shifts the focus from a sole investigation of paint chemical composition towards a holistic understanding of the formation of microstructures with varying distribution of paint ingredients on a micrometer length scale or below, depending on the preparation of materials and their colloidal interactions.

These new insights, obtained in a research frame conducted in a systematic way, are the first pillars of a groundwork which will help to connect these fields of expertise, usually kept apart, helpful to contribute to a better conservation and preservation of invaluable artworks.





# Zusammenfassung

Alte Meister wie Botticelli, da Vinci, Dürer, Rembrandt oder Vermeer verwendeten häufig Malfarben, die sowohl Ei als auch Öl als Bindemittel enthielten, um ihre Gemälde zu schaffen, aber die Art und Weise und der Grund dafür sind immer noch nicht verstanden. In der Tat können diese beiden Bindemittel der Malfarben auf viele verschiedene Arten zugesetzt werden, was zu einem sehr unterschiedlichen Verhalten der nassen Malfarben führt und auch das Trocknungsverhalten und die Härtingsreaktionen beeinflusst. Zu wissen, wie die Malfarben in der Vergangenheit zubereitet wurden, ist hilfreich um zu verstehen, wie sie besser für die Zukunft bewahrt werden können. Bei der Untersuchung der in der künstlerischen Malerei verwendeten Techniken mittels chemischer Analytik wurde in der Regel ein Top-Down-Ansatz verfolgt, der auf analytischen Verfahren zur Ermittlung der Pigment- und Bindemittelzusammensetzung beruht. Das Fließverhalten und die physikalisch-chemischen Eigenschaften der zubereiteten Malfarben wurde jedoch nur wenig untersucht. In den letzten Jahren hat die Berücksichtigung der Prinzipien der Kolloidchemie zu einer neuen Perspektive für unser Verständnis der Eigenschaften von Malfarben und ihrer Anwendung auf Gemälden geführt. Es wurden einige Studien zur rheologischen Charakterisierung von Malfarben durchgeführt, die zeigen, dass es notwendig ist, die Formulierung alter Rezepte mit ihren Fließeigenschaften und ihrem endgültigen Aussehen auf der Leinwand zu verbinden. Die Systeme sind jedoch komplex, und wenn die Studien auf Rekonstruktionen von Malfarben beruhen, werden in der Regel mehrere Parameter gleichzeitig variiert, wodurch die Informationen über wichtige Kriterien, die die Fließeigenschaften solcher Systeme bestimmen, wie der Volumenanteil der dispersen Phase oder die Pigment-Bindemittel-Wechselwirkungen, verwischt werden. Auch das Wissen über die chemischen Reaktionen, die während der Alterung von Ölfarben ablaufen, hat in letzter Zeit Fortschritte gemacht, indem weiterführende Modelle für diese komplexen chemischen Vorgänge entwickelt wurden. Dennoch ist nur sehr wenig über Systeme bekannt, an denen sowohl trocknende Öle als auch Proteine beteiligt sind, die in den von den Alten Meistern hergestellten Farbmischungen häufig vorkommen.

In dieser Arbeit wird durch Rekonstruktion verschiedener Malfarben der Einfluss der Verteilung des Bindemittels untersucht und geprüft, wie die Zubereitung der Malfarben zur Manipulation ihrer Mikrostruktur verwendet werden kann, und wie dies ihr Fließverhalten, sowie die Trocknungs- und Alterungseigenschaften verändert, welche das endgültige Aussehen der Malfarben beeinflussen, die wir in Museen sehen können. Es wurden mehrere Strategien zur Veränderung von Ölfarben mit Eizusätzen untersucht. Hier wurden Eigelb und Leinöl in Kombination mit zwei Pigmenten, Bleiweiß und Ultramarinblau, verwendet, um zu untersuchen, wie sich das Fließverhalten, die

Trocknungskinetik und die Chemie von Malfarben durch eine unterschiedliche Verteilung von proteinhaltigen und lipidhaltigen Bindemitteln steuern lassen. Mit Hilfe von Experimenten mit konstanter Scherung wurden die Fließspannung und die hohe Scherviskosität bestimmt, die die Streichfähigkeit, das Pinselstrichprofil und die Pastositäten einer Malfarbe beeinflussen. Die Ergebnisse wurden mit gravimetrischen und thermogravimetrischen Analysen, dynamischer Differenzkalorimetrie, aber auch mit mechanischer Texturanalyse und spektrometrischen Techniken kombiniert, um ein Verständnis für die Trocknungs- und Aushärtungsprozesse in solchen Farbschichten zu gewinnen.

In dem Bemühen, die Rolle von Protein-Zusätzen in Ölfarben zu beleuchten, wurden reine Ölfarben mit Kapillarsuspensionen (CapS) und mit Ei beschichteten Pigmenten in Öl (PCP) mit identischen dispersen Volumenanteilen  $\phi$  verglichen. Kapillarsuspensionen entstehen, wenn Eigelb (oder Wasser) in Ölfarben eingemischt wird, z. B. mit einem Pinsel, oder auch durch die Aufnahme von Feuchtigkeit. Die wässrige Komponente bildet mit den Pigmenten ein perkolierendes fraktales Netzwerk, was zu steifen Malfarben mit hoher Fließspannung führt (ideal für die Erzeugung von Pastositäten). Im Gegensatz dazu kann aber auch die unerwünschte Versteifung der Malfarben durch Feuchtigkeitsaufnahme aus der Umgebung je nach proteinhaltiger Bindemittelverteilung und kolloidalem Farbgefüge unterdrückt werden. Mit Ei beschichtete Pigmente in Öl entstehen, wenn Pigmente mit zugesetztem Ei als Netz- und Antiklumpmittel gerieben werden, bevor das beschichtete Pigment in Öl dispergiert wird. Durch die Zugabe von Ei bei der Herstellung der Malfarben kann das Pigment-Bindemittel-Verhältnis erhöht und dadurch Probleme vermieden werden, die durch Spuren von Feuchtigkeit entstehen, die während der Lagerung natürlicherweise in den Pigmenten vorkommen. Gleichzeitig können durch das Bindemittel verursachte Alterungsprobleme wie Nachdunkeln und Rissbildung minimiert werden. Die Streichbarkeit bei hohem Pigmentanteil kann durch Verringerung der hohen Scherviskosität der Malfarben verbessert und die Runzelbildung durch Einstellung einer hohen Fließspannung unterdrückt werden. Ei wirkt als Antioxidans: Es verlangsamt den Beginn der Aushärtung und die Trockenzeit und fördert die Bildung von vernetzten Netzwerken, die im Vergleich zu Öl allein weniger anfällig für oxidativen Abbau sind, was die Erhaltung wertvoller Kunstwerke verbessert haben könnte.

Dann werden mit Ei gebundene Malfarben (die so genannten *Temperafarben*) und der Einfluss des zugesetzten Öls auf Mikrostruktur, Rheologie, Trocknungskinetik und Chemie untersucht. Wenn *Eitemperafarben* Öl zugesetzt wird, werden diese Systeme als *fette Tempera* oder *Tempera grassa* (TG) bezeichnet, und man ging davon aus, dass sie eine Zwischenstellung zwischen Öl- und *Temperafarben* einnehmen. Trotz ihrer hydrophoben Beschaffenheit bleiben die Pigmente jedoch außerhalb der emulgierten Öltröpfchen, da die Eiproteine an der Pigmentoberfläche adsorbiert werden. Das Fließverhalten beider Malfarbentypen kann mit den klassischen Konzepten der kolloidalen Dispersionsrheologie beschrieben werden, wobei nicht nur das Pigment, sondern auch das zugesetzte Eigelb und Öl in die Berechnung des Volumenanteils  $\phi$  der dispersen Phase einbezogen werden. Die geringen Unterschiede in der Viskosität und der Fließspannung werden

auf die breitere Teilchengrößenverteilung bei *Temperafarben* zurückgeführt. *Temperafarben* sind dafür bekannt, dass sie schnell trocknen, und die Trockenzeit wird sowohl bei *Tempera-* als auch bei *Tempera-Grassa-Farben* durch die Verdunstung von Wasser gesteuert. Das zugesetzte Öl hat im Allgemeinen keinen Einfluss auf das Malverhalten, auf saugfähigen Untergründen wird jedoch aufgrund des verbleibenden Öls in *Tempera Grassa* eine unterschiedliche Streichfähigkeit beobachtet. Nach Erreichen des griffrockenen Zustands setzt die Ölvernetzung ein, was zu einem zweiten Härtungsschritt führt. Die Verteilung von Eigelb, Wasser und Öl korreliert mit den Fließeigenschaften und dem Trocknungs- und Aushärtungsverhalten der Malfarben, was zeigt, dass sich *Tempera-Grassa-Farben* wie *Tempera* verhalten und die Beobachtungen von Gemälden mit Eigenschaften "zwischen" *Tempera-* und Öltechniken nicht erklären können.

Schließlich untersuchten wir die Rolle des dispersen Volumenanteils und den Einfluss der Schichtdicke von Ölfarben auf deren Trocknungs- und Alterungseigenschaften. Insbesondere die Runzelbildung sowie der Beginn der Trocknungszeit nehmen bei Malfarben mit einer geringeren Fließspannung zu, was sich mit zunehmender Schichtdicke noch verstärkt. Die Fließeigenschaften, die Trocknungskinetik und die Farbveränderungen werden bei den hier untersuchten Pigmentsystemen hauptsächlich durch eine Änderung der chemischen Zusammensetzung der Pigmentoberfläche und weniger durch die Pigmentform und -größenverteilung in Ölfarben beeinflusst. Schließlich scheinen Farbveränderungen, Aushärtung und oxidative Abbaureaktionen langfristig von der Malfarbenmikrostruktur beeinflusst zu werden, was in längerfristigen Experimenten (> 3 Jahre) kontrolliert und systematisch untersucht werden muss.

Insgesamt bietet diese Arbeit einen multidisziplinären und multianalytischen Ansatz auf der Grundlage von Rheologie, physikalischer und analytischer Chemie, um die chemische Zusammensetzung sowie die mechanischen und physikalisch-chemischen Eigenschaften verschiedener Malfarben zu untersuchen. Der Schwerpunkt lag dabei nicht nur auf den nassen Malfarben, sondern auch auf ihrem Trocknungs- und Aushärtungsverhalten, um sie mit den bei *Tempera-* und Ölgemälden beobachteten Effekten zu korrelieren. Es wurden Proben mit verschiedenen Anwendungen von Eigelb- und Leinöl-Mischbindemitteln mit Bleiweiß- und Ultramarinblau-Pigmenten hergestellt und mit einer breiten Palette von chemischen und mechanischen Methoden analysiert. Dieses Projekt, an dem Kunsttechnologie, Chemie und Rheologie beteiligt sind, verlagert den Schwerpunkt von der alleinigen Untersuchung der chemischen Zusammensetzung von Malfarben hin zu einem ganzheitlichen Verständnis der Bildung von Mikrostrukturen mit unterschiedlicher Verteilung der Farbbestandteile auf einer Mikrometer-Längenskala oder darunter, je nach der Verarbeitung der Materialien und ihrer kolloidalen Wechselwirkungen.

Diese neuen Erkenntnisse, die im Rahmen einer systematisch durchgeführten Forschung gewonnen wurden, sind die ersten Grundpfeiler einer Arbeit, die dazu beitragen wird, diese normalerweise getrennten Fachgebiete miteinander zu verbinden, um so zu einer besseren Konservierung und Erhaltung wertvoller Kunstwerke beizutragen.



# Table of Contents

Preface.....	I
Acknowledgments.....	III
Abstract .....	VII
Zusammenfassung.....	XI
<b>1. State of the Art .....</b>	<b>1</b>
1.1. Succinct history of artistic painting .....	1
1.2. Terminology .....	2
1.3. <i>Tempera</i> and Oil painting techniques.....	7
1.4. Studies on artist paint formulations and properties .....	16
1.5. Motivation.....	20
<b>2. Materials and methods.....</b>	<b>23</b>
2.1. Materials .....	23
2.2. Paints preparation.....	29
2.3. Experimental methods and devices .....	32
<b>3. A holistic view on the role of egg yolk in Old Masters' oil paints .....</b>	<b>43</b>
3.1. Abstract.....	43
3.2. Introduction .....	44
3.3. Results and discussion .....	47
3.4. Conclusion .....	58
3.5. Acknowledgments.....	59
3.6. Competing interests.....	59
3.7. Supplementary information.....	59
<b>4. <i>Tempera</i> and <i>Tempera Grassa</i> – from wet paints to solid films.....</b>	<b>73</b>
4.1. Abstract.....	73
4.2. Introduction .....	74
4.3. Results and discussion .....	76
4.4. Summary and Conclusion .....	93
4.5. Acknowledgments.....	94
4.6. Competing interests.....	94

4.7. Supplementary information.....	95
<b>5. From the flow properties to the final aspect of paints: complementary investigations on paint modifications.....</b>	<b>107</b>
5.1. Further investigation on the flow behavior, drying kinetics and wrinkling of oil paints..	108
5.2. Colorimetric study of paints having a similar composition but different microstructures .....	116
5.3. Study of the influence of the particle size distribution of ultramarine blue pigment on the flow behavior, drying kinetics and color of oil paints .....	119
5.4. Oxidation, crosslinking and complex oil-protein interactions in <i>tempera grassa</i> and oil paints .....	133
<b>Summary .....</b>	<b>143</b>
<b>Outlook .....</b>	<b>147</b>
<b>Appendix .....</b>	<b>149</b>
<b>Notations .....</b>	<b>153</b>
Abbreviations.....	153
Symbols .....	154
<b>Bibliography.....</b>	<b>157</b>

# 1. State of the Art

This chapter offers a brief overview on the necessary background regarding artistic painting for this work. First, a summary of the historical context and the corresponding artistic intentions and aims of painting through the eras is presented, prior to introduce *oil* and *tempera* painting techniques and the complexity they represent in terms of definition and interpretation for curators, art conservators and scientists. Eventually, an overview of the scientific studies performed on artists' paint formulations and properties is given, including a discussion of the challenges in this field.

## 1.1. Succinct history of artistic painting

For thousands of years, painting has been a source of expression whose varied techniques have continued to evolve over time and geographical locations. From the Upper Paleolithic, with the remarkable works discovered in the Chauvet Cave in Ardèche (France) for example, to modern techniques, human beings have never ceased to discover, create, improve and perfect their methods of pictorial representation, sometimes still a mystery today. This diversity and technical complexity, which is part of the charm of artistic painting, is intertwined with the intrinsic properties of paint as a material: its texture, its flowing properties, its color, its drying behavior, and much more. All of these aspects are very closely linked to the painting technique employed.

Since Antiquity, a great variety of pigments and paint binders have been used in painting, including for instance wax, resins, animal glue, honey, milk, etc, and were applied on a wide range of surfaces, such as walls, wood, parchment, canvas or textiles. Some murals, but also painted objects such as potteries and ceramics dated from the Antiquity testify about the materials used and the various painting techniques. Pliny the Elder (1<sup>st</sup> century) describes painting with egg as a binder, but also several other techniques such as encaustic, which uses molten waxes with pigments.<sup>1</sup> Later, in medieval panel painting, there are different traditions in the North and South of Europe. Whereas oil seems the predominant binder in the North, egg was preferred in the South.

During the early Renaissance, *Il libro dell'arte, o Trattato della pittura* from Cennino Cennini (c. 1400) is a manuscript which describes in much detail the preparation of paints, the way of painting and it collects many recipes used in Italy at that time.<sup>2</sup> Back then, the *tempera* technique was dominant in Italy for painting on panels. One of the major transitions in Europe regarding the painting technique took place during the 15<sup>th</sup> century in Italy, when Italian artists such as Giovanni Bellini (1430 -1516) or Leonardo da Vinci started to turn from egg *tempera* towards adopting

Northern *oil painting*.<sup>3-6</sup> However oil paints were known in Italy for more than a century: oil binders have been identified in Italian 14<sup>th</sup> century paints<sup>3,4,6,7</sup> and the preparation of oil paints have been described by Cennino Cennini in his famous treatise<sup>2</sup>. Yet, these paints did not need blending or complex paint application, which indicates that oil painting seems to be more than painting with oil paints<sup>8</sup>, where additions of other materials such as proteins might have been helpful to modify the oil paints' properties, allowing more sophisticated usage of paint.

In the past, the "invention" of *oil painting* has been attributed to the Flemish painter Jan Van Eyck in the 15<sup>th</sup> century, however, this has been disproved as a myth. Several sources such as Theophilus (12<sup>th</sup> century) convey the use of oil in paintings centuries earlier<sup>9-11</sup>. From the 16<sup>th</sup> century to the industrialization, oil seemed to be more or less the dominant binder for painting both in North and South Europe. Only during the second half of the 19<sup>th</sup> century *tempera* was rediscovered by some artists, especially in Germany<sup>12</sup>, but also in other countries. Then during the 19<sup>th</sup> and 20<sup>th</sup> centuries, industrialization took over with first the invention of paint tubes and then the development of new synthetic binders such as acrylic paints or polyvinyl acetate, which revolutionized the painting approach.<sup>9</sup> Buying paint tubes became easy, but unfortunately came along with the loss of precious knowledge regarding the preparation of painting media among the artists using them.

The technical knowledge of paint preparation was initially passed down by Old Masters in workshops, but most of it is lost today. Know-how was handed down mostly orally and by observing the work processes. Few manuscripts, however, such as the *Liber diversarum artium* (c. 1300)<sup>13</sup> and the famous *Il libro dell'arte, o Trattato della pittura* by Cennino Cennini<sup>2</sup>, give detailed descriptions of precious medieval and Renaissance recipes; but due to the evolution of the language and the way of explaining and detailing the recipes, invaluable information got lost upon these centuries. Today, modern analytical methods (invasive or non-invasive) allow identification of materials in paint layers with a very high specificity and sensitivity, and the technical art examination facilitates the differentiation between the various painting techniques used, however, in insufficient detail. There is clearly more to the preparation of a paint than just mixing the pigment with a binder. As will be shown in this thesis, the properties of paints can be manipulated with adding small amounts of additives, or by the specific formulation of the paint, which is neither included in sufficient detail in the written recipes, nor can be accessed by chemical analysis.

## 1.2. Terminology

The definition of *tempera* is blurred. From today's view, it may refer to the visual appearance of a painting, a technique and/or to specific materials (Table 1.1).<sup>14</sup> The term "*tempera*" itself differs considerably with time and with language<sup>3,15</sup>: the word '*tempera*' comes from the Latin *temperare*, which means either 'mixing of paint' or simply 'to bind', and was generally employed during Renaissance in Italy to describe an (aqueous) egg paint, but other binders such as animal glue,



casein or gums were also used across centuries<sup>3,16–18</sup>. Since painting in Italy initially was performed with aqueous binders, the term *tempera* was transferred to painting with egg.

For instance, in French, a *tempera* is always translated as “*détrempe*”, distemper, which corresponds to the definition of ‘mixing’. However; according to the Encyclopédie Française Larousse, the word *tremper*, close to *détrempe*, means ‘soaking in a liquid’ which involves the use of water, and suggests the utilization of an aqueous binder in the field of painting. On the other hand, “*peinture à l’oeuf*”, i.e. egg paint, is closer to the second definition of *tempera* given by Cennini. In Spanish, *temple* is made from pigments ground with water and binding media (egg, gum or animal glue), whereas in Italy, both definitions of ‘emulsion’ and ‘mixing of binding media’ coexist. In German, this word is defined as any type of painting technique employing an emulsion. Finally, ‘*tempera*’ (for the use of egg yolk), ‘distemper’ (for a glutinous binder) and ‘emulsion’ (colloidal material, probably inspired by the German definition) are commonly used to describe *tempera* paints in English technical paint literature. In the 19<sup>th</sup> century, “*tempera*” and “distemper” were often used equivalently<sup>15</sup>. Only later the terms became more differentiated, but a broad variety of different and inconsistent nomenclature systems were developed, which rather obscured the meaning of the term “*tempera*”. All in all, most definitions in European languages define *tempera* as systems that can be diluted with water, in contrast to oil paints, which can be diluted with oil of turpentine but not water.<sup>12,15,19,20</sup> The definition of a *tempera* is not exclusive as suggests its multiple translations and historical terminologies with for instance “oil-*tempera*”, “aqueous *tempera*”, “fatty- or lean *tempera*”.<sup>12</sup> These terms are not used in this manuscript, because of their lack of precision and clarity, sometimes even inconsistency. To avoid any confusion, the word *tempera* refers in the rest of this study to the traditional Italian definition: an aqueous paint, where water is the continuous phase and contains egg yolk, water and pigments.

“Oil painting” is more than painting with a material, a drying oil in this case, it is also a technique (Table 1.1). Drying oils with high level of polyunsaturations such as linseed, poppyseed or walnut oil were employed for oil-containing paintings<sup>16</sup>, and several recipes recommended to place the painted panel or other painted surface under the sun to let the paint or varnish dry, more accurately to set and harden<sup>4</sup>. In contrast to *tempera* painting, the drying times required for oils are quite long, and some described recipes where the oil was previously boiled to accelerate this process. However, this also effected in changing the aspect of the paint since the oil became thicker, stickier and harder to paint with in thin layers as were the requirements at that time.<sup>21</sup> From the 15<sup>th</sup> century, the oil painting technique have improved with the Van Eyck brothers and the use of transparency provided by the oil medium. Due to the longer drying times of the oil and the paint’s flow properties, quick hatched brushstrokes were no longer needed, and oil brushstrokes, when applied side by side, could be blended together. The *oil paint* drying time is long enough to be able to modify and manipulate the brushstroke<sup>3,21</sup>, and allow softer transitions from one color to another when the paint is still wet, which is called “wet-in-wet” painting technique.

Painted artworks are usually classified into “watercolor”, “fresco”, “*tempera*” or “oil”, and simplified assumptions are made regarding the binder compositions: the term “oil painting” refers for example to a painting technique taking advantage of properties typical for oil paints, such as wet-in-wet color mixing when the paints are still wet, - and to a composition: the paint contains mostly oil. This is confusing, because here “oil” both denotes a material and a technique, which we now have evidence that this cannot be always true (see below). However, it has been shown that oil paints may contain typical *tempera* binders such as proteins, and vice versa.<sup>14,22,23</sup> Thus a definition purely based on materials does not necessarily work. On the other hand, written sources and artists’ statements usually refer to the solubility of paints, thus *tempera* paints can be diluted with water, but not oil of turpentine, for oil paint it is the other way around. From a modern point of view, the solubility corresponds to the continuous phase of the paint, which depends on its microstructure. On an entirely different level, whether a painting is an oil or *tempera* painting is usually decided by specialists such as art historians or conservators, based on the visual appearance of an artwork.

The terminology applied for describing these two types of paints is plural and leads to constant confusion between the different level of meanings. A more detailed terminology is therefore necessary to consider the different levels of these words. This was proposed by Dietemann et. al (2015)<sup>14</sup>, giving a triple definition of the terms “*tempera*” and “oil”, which takes into account the different meanings of the terms, listed in Table 1.1:

Table 1.1 – Definition of ‘oil’ and ‘tempera’ at different level of meaning, adapted from Dietemann et al. (2015)<sup>14</sup>

Term	Criteria	Definition
<i>oil / tempera painting</i>	Visual appearance	An <b>oil painting</b> looks as we expect it to appear. A <b>tempera painting</b> looks as we expect it to appear.
<i>oil / tempera paint</i>	Miscibility, dilutability	An <b>oil paint</b> can be diluted with oil of turpentine, but not with water. A <b>tempera paint</b> can be diluted with water but not with oil of turpentine.
<i>oil / tempera composition</i>	Material	<b>Oils</b> consist of lipids, mainly triacylglycerols. <b>Tempera</b> binders usually contain aqueous binders such as proteins or polysaccharides.

The visual appearance corresponds to typical properties of *tempera* or oil paints, respectively: oil paints are more transparent and can be mixed wet-in-wet, whereas *tempera* paints dry too quickly to be mixed wet-in-wet, and are rather opaque. Thus, besides optical aspects, the appearance of a painting depends to a great deal on rheological and drying properties of paints. In the past it was assumed that the three terms proposed in Table 1.1 correlate directly: oil paintings were painted with oil paints, which contained oil as a binder, and the same is true for *tempera*. As has been demonstrated by Dietemann et. al (2015)<sup>14</sup>, paints can be multicomponent complex systems, which can contain both *tempera* binders and oil. The microstructure of these materials determines the continuous phase, which depends not only on the materials used, but also on their formulation. As a consequence, from a modern point of view, the different levels of meaning in Table 1.1 correlate mainly by colloid chemistry and rheology, as is depicted in Figure 1.1):

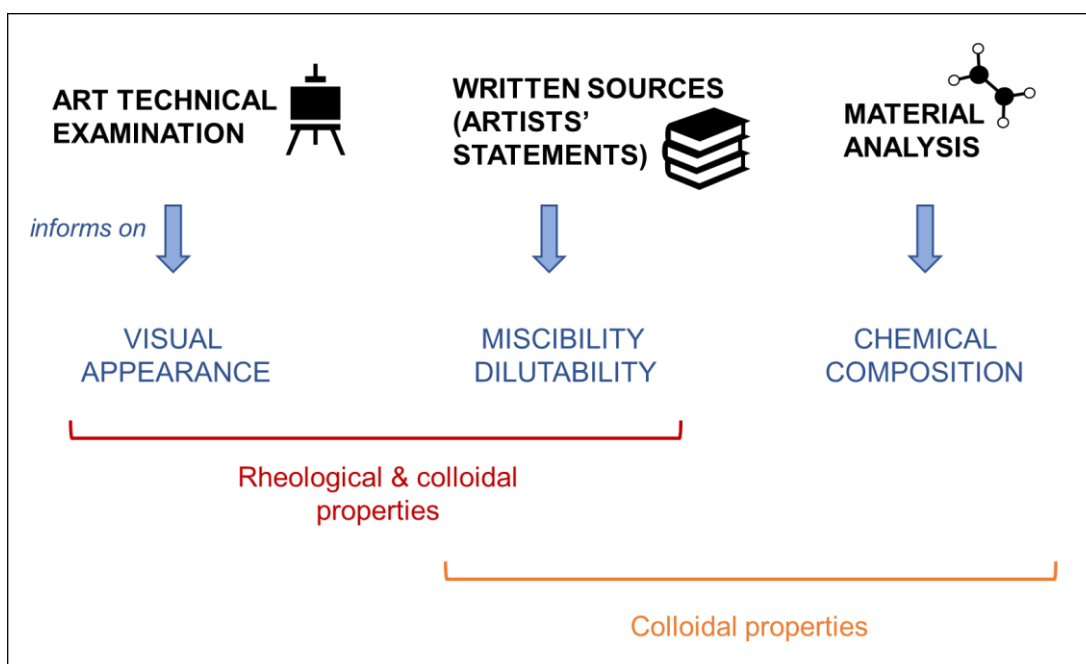


Figure 1.1 - Correlations between the information obtained from technical studies of artistic paints, adapted from Dietemmann et al. (2014)<sup>20</sup>

The correlations between material composition, microstructure (including phase distribution) and rheological as well as drying properties of paints are not sufficiently known and understood so far. In addition to this, the current chemical analytical techniques do not always make it possible to determine the exact compositions of these paints which can be complex multicomponent systems. A sample of several micrograms is not always representative of the entire painting, but sampling a bigger quantity is not realizable, due to ethical reasons that we do not need to state here. Besides, even if the exact composition of the dry paint is known, we do not know its colloidal structure and the distribution of the ingredients among the different phases. However, these colloidal features are essential to determine the wet paint properties such as flow behavior and brushability, but also the drying and curing behavior of the paints, including crosslinking, oxidation reactions, but also crack formation or wrinkling.

A better understanding of these correlations is beneficial for the improvement of art technological studies and conservation purposes, with a strong interdisciplinary cooperation. This dissertation offers a multi-disciplinary and multi-analytical approach based on rheology, physical and analytical chemistry, carried out to investigate the chemical composition as well as the mechanical and physico-chemical properties of various paints.

The following sections will help the reader to understand in more detail how the two major painting techniques used during Renaissance are described by art historians and technical art historians, prior to giving an overview of the scientific works done on the topic during the last years.

### 1.3. *Tempera* and Oil painting techniques

The former altarpiece of Santa Maria Novella in Florence painted by Domenico Ghirlandaio and his Workshop between 1490 and 1494 (Figure 1.2) has been painted in both *tempera* and *oil*, and will serve as support for the description of the different painting techniques. Originally made of eight panels, three of them remained in the collection of the Bavarian State Painting Collections. Domenico Ghirlandaio died before the achievement of the altarpiece, and his brother came back from France where he was living to finish it. It is believed that the altarpiece was originally planned to be painted in *tempera*, which is the predominant technique used there: the right panel is completely painted in *tempera*, except for the green draperies of Saint Lawrence which are in *oil*, and the central panel is mostly painted in *tempera*. Only details from the middle panel are painted in *oil* (the clothing of Saint Thomas (mark-up **A**), the foot of Saint John (**B**), and the hands of Saint Dominic holding the book). The left panel representing Saint Catherine is fully painted in *oil*. This altarpiece painted with multiple techniques will help to support the description of both *tempera* and *oil* painting techniques in the following sections.

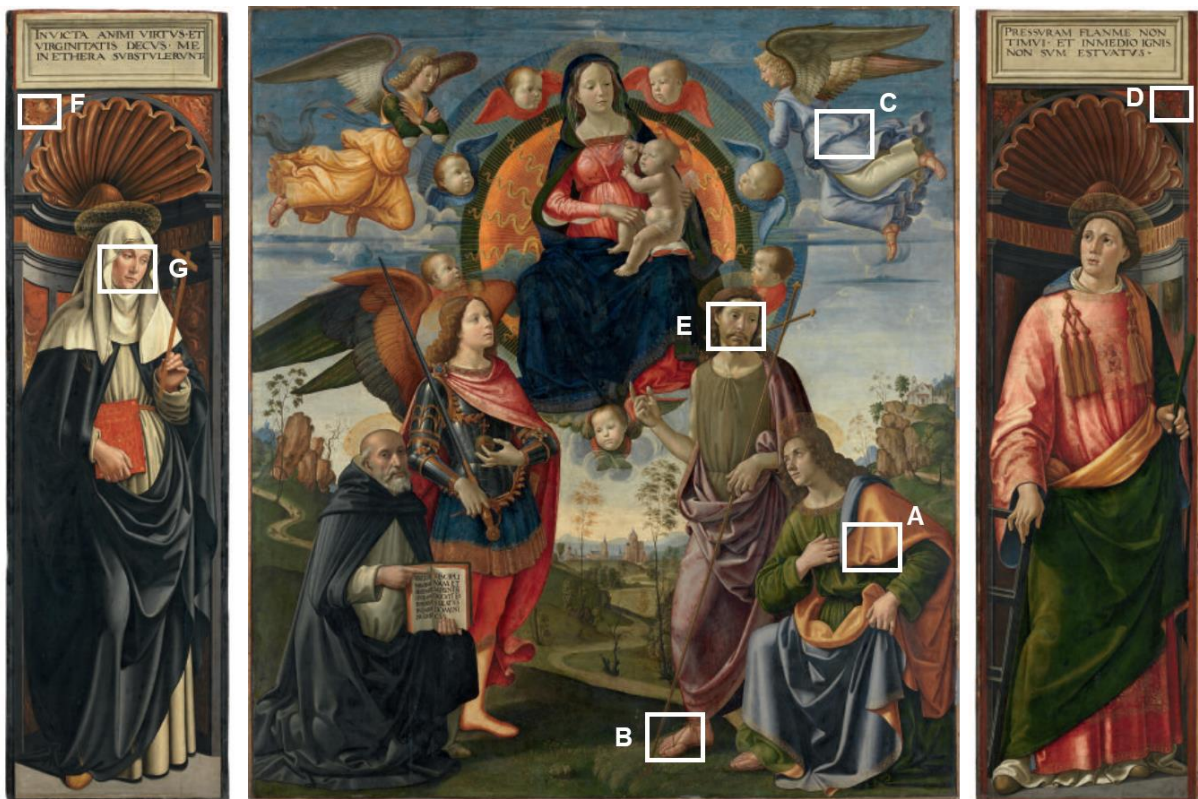


Figure 1.2 - Domenico Ghirlandaio and Workshop, Former High altarpiece of S. Maria Novella, Florence (1490-1494), Bavarian State Painting Collections, Inv. No. 1077, 1078, 1076. 3 panels of initially 8 panels (not a triptych). 223,9 x 201,4 cm (middle panel), c. 212 x 57 cm (side panels) © Bavarian State Painting Collections, Munich. Photo: Sibylle Forster

### 1.3.1. *Tempera painting*

The painting technique of traditional *egg tempera* leads to a particular look than can be distinguished from other techniques<sup>15,21</sup>: the wet *tempera* paint dries quickly through the evaporation of water, and thus two paints of different hue cannot be mixed to form a color transition. Instead, the paint is applied in thin layers with weak hiding power, and thus a color transition is formed with many brushstrokes.<sup>3,15,21,22</sup>

Another technique was applied especially in large works that are usually seen from a distance, such as altarpieces (Figure 1.2): if an area of color is hatched with another color, the two colors will fuse due to lack of resolution at a certain distance. For example in Figure 1.3, the dark blue hatching will darken the shadows painted with a middle tone blue. Figure 1.4 shows that paints could also easily be applied on top of each other due to the rather quick drying times. This was an efficient technique if color transitions did not need to be smooth, unlike in faces or flesh.

Techniques were of course combined: for instance, in flesh, the skin colors were often applied on top of a uniformly green first layer, which was left visible in the shadows (Figure 1.5).

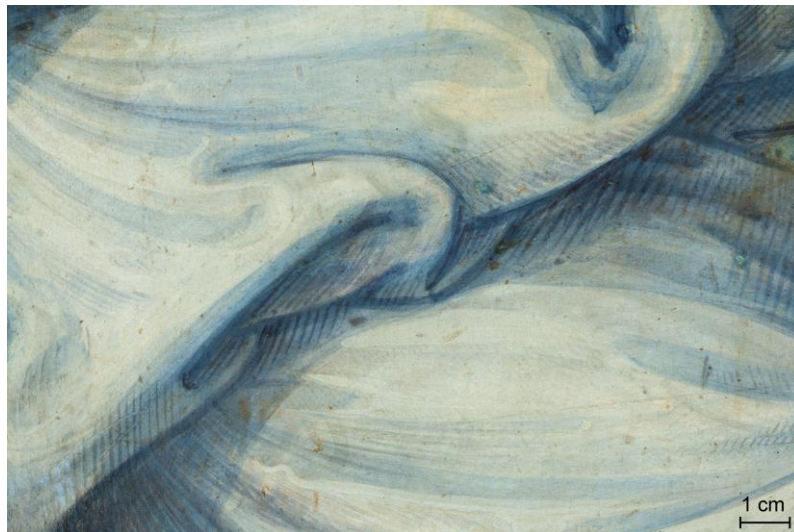


Figure 1.3 - Detail C of the middle panel 223,9 x 201,4 cm, where the brushstrokes and sharp color transitions are clearly pronounced. Domenico Ghirlandaio and Workshop. The entire altarpiece is visible in Figure 1.2. © Bavarian State Painting Collections, Munich. Photo: Daniela Karl



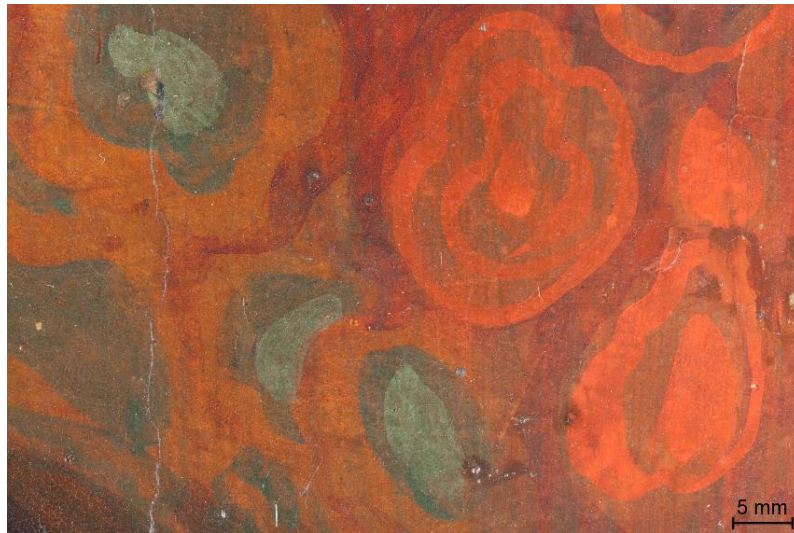


Figure 1.4 – Detail **D** of the right panel (212 x 57 cm), painted in the “layer-on-layer” technique. Domenico Ghirlandaio and Workshop. The entire altarpiece is visible in Figure 1.2. © Bavarian State Painting Collections, Munich. Photo: Daniela Karl

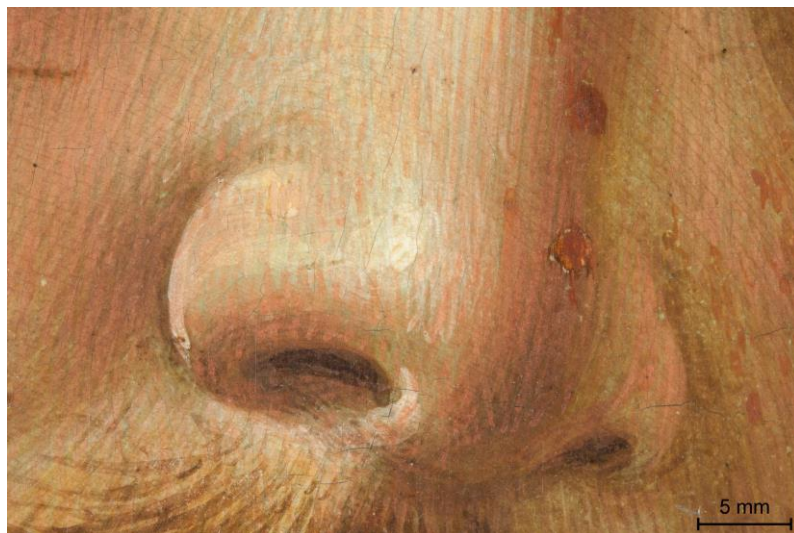


Figure 1.5 - Detail **E** of the middle panel 223,9 x 201,4 cm, of the flesh of Saint John. Domenico Ghirlandaio and Workshop. The entire altarpiece is visible in Figure 1. © Bavarian State Painting Collections, Munich. Photo: Daniela Karl

### 1.3.2. Oil painting

The *oil paint* drying time is long enough to be able to modify and manipulate the brushstroke<sup>3,21</sup>, and allow softer transitions from one color to another when the paint is still wet, that is called “wet-in-wet” painting technique, illustrated with a detail of the altarpiece painted by Ghirlandaio and his workshop in Figure 1.6. This detail corresponds to the detail painted in *tempera* (Figure 1.4): both are supposed to look similar from a distance, although they look different from close up.



Figure 1.6 - Detail **F** of the left panel (212 x 57 cm), painted in the “wet-in-wet” technique. Domenico Ghirlandaio and Workshop. The entire altarpiece is visible in Figure 1.2. © Bavarian State Painting Collections, Munich. Photo: Daniela Karl

The brushstroke might now be intentionally visible or completely soften and blended, as shows the perfect color transition in the flesh in the same painting, visible in Figure 1.7, which is completely different from the one performed in *tempera* in the same altarpiece, showed previously in Figure 1.4.





Figure 1.7 - Detail **G** of the left panel (212 x 57 cm) of the flesh of Saint Catherine. Domenico Ghirlandaio and Workshop. The entire altarpiece is visible in Figure 1.2. © Bavarian State Painting Collections, Munich. Photo: Daniela Karl

The aspect of draperies and other types of fabric can be painted in highly realistic way, by playing with the color transitions and the aspect of the brushstrokes (Figure 1.8).<sup>23</sup> To modify the flow properties of the oil paint in making it even more liquid to ensure a lighter brushstroke, without altering drastically its drying, some painters such as the Van Eyck used volatile solvents such as turpentine or naphtha. This information, however, has to be treated with caution: it is unclear, since when solvents like turpentine or naphtha have been used to dilute oil paints. No analysis could detect the former presence of these volatile solvents in these paints, and there are no indications for the use of volatile solvents (for oil paints) until the 16th century.<sup>21</sup>

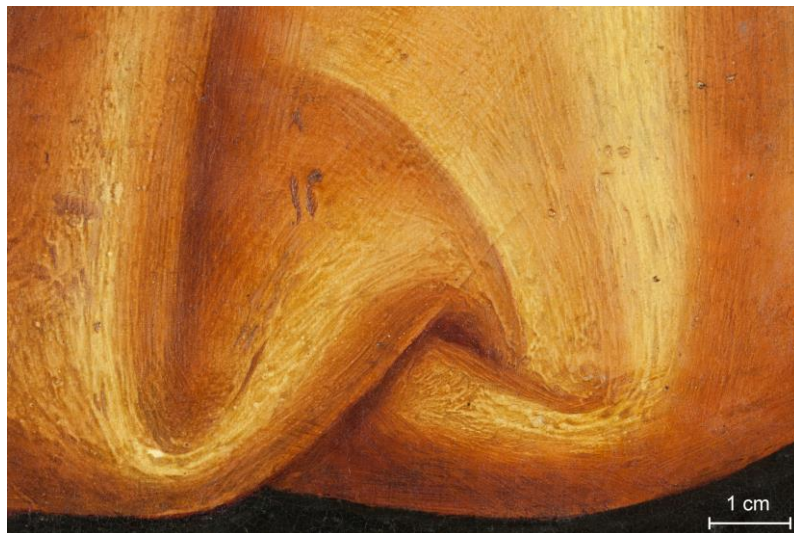


Figure 1.8 - Detail **A** of the middle panel 223,9 x 201,4 cm of the drapery of Saint Thomas. Domenico Ghirlandaio and Workshop. The entire altarpiece is visible in Figure 1.2. © Bavarian State Painting Collections, Munich. Photo: Daniela Karl

The transition from *tempera* to oil painting technique in Italy was probably gradual. Several painters of the Italian Renaissance, such as Domenico Ghirlandaio or Sandro Botticelli used both techniques in a same painting, adapting the type of technique to the subject or the pigment. During the 15<sup>th</sup> century in Italy, artists started to turn from egg *tempera* towards adopting Northern oil painting, but they seemed to have had some problems, as the wrinkling in an early painting by Leonardo da Vinci testifies (see chapter 3).

This transition from *tempera* to *oil painting* in the fifteenth century in Italy has been theorized by many people, including art historians, conservators and scientists, without being sure if the hypotheses made were actually working, in terms of flow properties, drying and ageing of the paint. For instance, it is often assumed that one needs to add oil to a *tempera* in order to obtain a so-called *tempera grassa*, e.g. a fatty *tempera*, which will be the “in-between system” observed in several historical artists paints. This paint should take long time enough to dry, in order to be able to paint in the wet-in-wet technique and have a certain texture, and yet dry fast enough to apply quickly another layer on the top of it.<sup>3,4</sup> However, as J. Dunkerton points it out, “the presence of both oil and egg does not necessary mean that a *tempera grassa* has been used”<sup>4</sup>, for the very reason that both composition and microstructures are not directly related in that simplistic way, as discussed previously. From the 16<sup>th</sup> in Europe, except for the icons, *oil* painting became the dominating technique for easel paintings, sufficiently developed and mastered, and was acclaimed both in Northern and Southern Europe due to its multiple possibilities and its incredible realistic finish.<sup>21</sup>

The difference between an oil and a *tempera* painting depends on complex properties, which are not determined by the composition only, but first and foremost is governed by visual characteristics of the painting; it relates to aspects such as transparency/opacity, gloss, type of execution of color transitions (i.e. wet-on-wet or not), formation of “impasto” which is related to the flow properties of the paint, type of application (with brush or also e.g. with spatula), etc.<sup>12,14</sup> These paint properties are closely related to the colloidal structure of the material (see Table 1.1 and Figure 1.1), which may be described with the help of rheology and chemistry, but are so far very little studied in a systematic way. However, these physico-chemical concepts have been throughout the centuries poorly understood and lead to contradictory terms describing “oil” and “*tempera*” systems, which are still used today and lead to misleading painting descriptions.

### 1.3.3. Proteinaceous material additions in oil paintings

As emphasized previously, the paint systems that we usually describe are not strictly related to their composition, neither to one single painting technique: the level of meaning in Table 1.1 is decisive to understand how a paint system should be described. For instance, proteinaceous materials have been detected in several traditional artists' *oil paintings*, in Italy (Leonardo da Vinci, Sandro Botticelli, and others<sup>5,6</sup>) but also in the North of Europe (Johannes Vermeer, Rembrandt, Albrecht Dürer, and many others<sup>7-10</sup>) and in works dated from several centuries, while it is usually assumed that traditional Old Masters' *oil paints* only contain oil as a binding medium (with eventual additions of some resins)<sup>1-4</sup>.

An artwork may look like an oil painting in terms of visual appearance (involving the color, the gloss, etc) and its flow properties may correlate to the traditional way of defining a typical oil painting technique, yet the composition may not completely fit with the standard material of an oil painting: additions of proteinaceous materials have also been detected. The detection of these materials can be difficult, because usually extremely small amounts of paints (some micrograms) are analyzed, in which proteinaceous materials such as egg are not dominant components. Even when analytical methods could demonstrate the presence of both oil and egg, it did not necessary mean that a *tempera grassa* (i.e a *tempera* in which oil has been emulsified) has been used, as usually described<sup>4,14,23</sup>: the composition does not obligatory define the colloidal structure of a painting system, even if they are related. Other systems containing these ingredients are possible, with flow properties resembling strongly to pure protein-free oil paints, or not.<sup>12</sup>

Often, the detection of these proteinaceous species is attributed to impurities and not further investigated, because it is conventionally assumed that proteinaceous materials do not belong to traditional *oil paintings*, but several written sources, arising from the artists themselves, prove the contrary. Indeed, old art technical manuscripts such as *Il libro dell'arte* from Cennini<sup>2</sup> (c. 1400) or the so-called *Strasburg Manuscript* (15<sup>th</sup> century) do not describe the addition of proteins to oil paints. This omission is, however, not surprising because the preparation of a pigment, which is a labor-intensive and time-consuming process, is often described in a different chapter, or completely left out. Indeed, the pigments themselves, many of them deriving from minerals, had to be crushed and dispersed, cleaned and purified. Many recipes describe the cleaning and preparation of blue pigments such as azurite or natural ultramarine, which sometimes require the addition of materials such as egg, glue, polysaccharide gums or honey<sup>2,13,24</sup>. These procedures are mostly mentioned in context of illumination painting techniques on paper or parchment, which are based on aqueous binders, not for *oil paints*, which would cause stains. The *Liber diversarum arcium* (Figure 1.9), i.e. the famous "Montpellier Manuscript" (c. 1300-1400) which is presumably the most complete codification of medieval traditional *oil painting*<sup>13</sup>, gives the only recipe according to our knowledge describing the addition of a proteinaceous binder to *oil painting*. The translation of the recipe 1.3.9B states<sup>13</sup>: "first grind with water and combine with three drops of glaire, and leave to dry in the sun, and once with time it is dried, repeat, and do this three or four times; afterwards temper it with oil

[or] gum water, and use it." It is here described the coating of pigments with egg white (glaire) as part of the grinding process, prior to disperse the particles with the oil. Such proteinaceous additions might also be useful for other pigments than the delicate and expensive blue pigments: various other systems may be formed with egg yolk or other aqueous proteinaceous solutions, drying oil and pigments, depending on paint preparation.<sup>12,23</sup>



Figure 1.9 - First and second pages of the "Liber diversarum arcium". Montpellier, fonds ancien, Bibliothèque Interuniversitaire Historique de Médecine, Manuscript H 277, 81v and 82r.

### 1.3.4. Oil additions in *tempera* paintings

Additions of siccativ oils to *tempera* paints is usually described as forming a type of paint called *tempera grassa*, e.g. fatty *tempera*.<sup>16,21,25</sup> Sometimes it is assumed that by mixing different binders in quick drying *tempera* paints, such as oils, the drying times of these paint systems will increase and will allow the obtention of paint properties closer to the ones of pure *oil* paints. However, from a colloidal point of view, this simplistic approach in which the properties of one system (*tempera*) will be gradually transferred to another one (*oil* paint) by increasing the amount of binder (oil) is not always consistent, because other important parameters influencing the paint system microstructure are neglected, as stated above.<sup>8</sup> Sometimes even in paintings ascribed to *tempera* systems, little amounts of drying oils have been detected with chromatographic techniques in paintings dated from the 15<sup>th</sup> century, questioning the definition of a *tempera grassa* paint and its properties.<sup>4</sup>



As a matter of fact, the definition of the *tempera grassa* painting technique itself is blurred: the detection of this type of paint typically in Italian Renaissance paintings is usually described in literature on a composition basis, where relatively high amounts of both proteins (usually egg yolk) and lipids from drying oils are detected, together with the visual observation of paints brushstrokes, which are less pronounced than in “pure” *tempera paints*.<sup>3,4,16</sup> Several paintings of Sandro Botticelli and Carlo Crivelli (see Figure 1.10) are believed to have been painted (partly) in *tempera grassa*.<sup>3</sup>



Figure 1.10 - Carlo Crivelli, *Madonna and Child Enthroned with Donor*, 1470, National Gallery of Art, Washington, 125.3 x 50.7 cm, Samuel H. Kress Collection, Accession Number 1952.5.6

However, it has not been proven yet that *tempera grassa* paints take longer times to dry than pure *tempera* ones, and at the same time allow wet-in-wet painting techniques or even to paint thicker layers to obtain a stable impasto, without crack formations. Some technical art studies<sup>8,12,23</sup> tried to describe in more details what has been interpreted as *tempera* painting systems having “in-between” properties, but the assumptions concerning the microstructure of these systems show that there are still conflicts between the conclusions drawn on the observed painting systems and fundamental rules of rheology and colloid chemistry (principles of miscibility, Bancroft’s rule, etc). A deeper scientific understanding of the principles ruling the mixing of these paints, cross-

referenced with the chemical reactions taking place in these systems are useful aspects, which might help to contribute to a better conservation and preservation of these invaluable artworks.

## 1.4. Studies on artist paint formulations and properties

Numerous studies regarding the binding media and the preparation of oil and *tempera* paints, the painting techniques, but also on the transition from *tempera* to oil paintings already exist from the point of view of technical art history<sup>3-5,8</sup>. These are mostly based on the study of historical sources such as ancient books on the topic and treaties, which are then connected with the work and experience of art curators and conservators who are daily confronted with precious and invaluable pieces of art. However, these studies do not fully manage to connect important aspects of painting media, such as how a wet paint structure transforms into a dry paint film. Common concepts in modern conservation science of how paints were prepared and applied, are in conflict with basic principles of rheology and colloid chemistry<sup>22</sup>. Therefore, there is a need to unite knowledge from art technology, analytical chemistry and rheology to understand painting in deeper detail, which might help to improve efficient and targeted conservation strategies and for the preservation and restoration of unique, delicate artworks, and advance our knowledge of our ancient art history.

Most of the time, these aspects are treated separately by conservation specialists, rheologists or chemists, probably for practical reasons, but also due to different approaches of the topic. Here, an overview of some scientific publications focused on the topic are presented.

### 1.4.1. Rheological studies on paintings

Few studies have been conducted on the rheological characterization of artist paints, varying their composition and preparation methods in order to connect them with the appearance of impasto on artistic paintings. Most of the scientific publications on the subject show the need to connect the formulation of ancient paint recipes with their flow properties and their final appearance on a canvas. Yet, the studied systems are complex; when they are based on paints reconstructions, they comprise numerous ingredients, and multiple parameters are usually varied simultaneously<sup>26,27</sup>: the type of pigment, binder and solvent<sup>28</sup>, their quantity, or the introduction of charges<sup>29</sup>. Indeed, the solids content or the pigment-binder interactions, which are important criteria ruling the flow properties of suspensions, are not taken into consideration in these works. As a result, trying to fully copy a recipe without studying systematically the influence of one or two parameters in simplified systems complicates the understanding of the role of each component in a paint. Some research groups tried this approach, by investigating the flow behavior of mock-up oil paints in a more systematic way by varying the pigment loading of simple paint formulations and

comparing them to similar paints prepared with other pigments (lead white and zinc white)<sup>30</sup>, but complementary research on drying and chemical characterization might be needed to understand the entire painting process and to extend this to other paint systems.

It is very rare to find rheological studies on *tempera* paints. Fanost et al. (2021) investigated the structure of *tempera* prepared with green earth by combining oscillatory shear rheological measurements of wet paints and NMR experiments of the dried structures obtained. They could demonstrate that surface interactions are taking place between the proteins of the egg yolk and the green earth used as pigment.<sup>31</sup> However, this study did not pretend to vary the composition of the paint and to study the influence of each component to draw these conclusions, neither investigating the structure of these complex systems. They compared indeed two types of paints with the same pigment but dispersed them in completely different media: water, which acts as a solvent, or egg yolk, which is a binder, and contains also solid particles<sup>32–34</sup>. These parameters are a little investigated in the thesis of the same author<sup>35</sup>, where the pigment content is varied, but again, these systems prepared with water and egg yolk are directly compared without paying attention to their composition. The journey is still very long to connect the flow behavior of the paints an artist used with the appearance of the final art work. Further techniques and knowledge in different fields of research such as conservation art science and chemistry are necessary to reach this goal.

#### 1.4.2. *Drying behavior of mock-up artist paints*

The transformation of liquid paints to solid films is driven by several complex mechanisms, investigated in some studies, mentioned in the following section. It requires to join knowledge on colloidal interactions taking place in the complex paint mixtures with the kinetic and thermodynamic stability of these liquid systems, which may flow, evaporate, cure and/or continue to transform mechanically and chemically upon time.<sup>36,37</sup> The continuous phase of the system has an important influence on the drying behavior of the paint layers, but the interactions taking place between the different ingredients and the environmental conditions are also fundamental in the study of the process. Beyond the formation of a solid film, further changes in the dried paint layers may appear: crack formations<sup>38</sup>, wrinkling<sup>39,40</sup>, shrinkage,<sup>41</sup> changes of color<sup>42,43</sup>, etc. Micro-heterogeneities might also influence the drying process and affect the stability of the paints over time.<sup>44</sup> These are strongly connected to the paint flow properties and the chemical reactions ruling the paint drying kinetics, but little work has been done on the topic.

Some interesting studies focus on the influence of pigments, binders and additives on the long-term evolution of mechanical properties during drying of oil and alkyd paints. They tried to connect them to the chemical composition of the pigment and binders and the resulting chemical reactions taking place in such complex systems.<sup>45,46</sup> These works are necessary to understand the changes observed in the mechanical performances of the paint films which might appear upon long ageing times.

### 1.4.3. Chemical characterizations of artistic paintings

The drying of an oil paint layer is a chemically driven process, involving the oxidation and cross-linking of the constituting polyunsaturated triglycerides (curing). It is influenced by several factors, such as the environmental conditions (light, temperature, humidity) and the intrinsic properties of the film such as its chemical composition (binder and pigment) and the layer thickness<sup>17,47–50</sup>. The curing mechanism of oil paints has been investigated for about a hundred years<sup>51–54</sup>, and is still not fully understood.

Works combining thermal analysis, spectrometric techniques and non-invasive imaging methods helped decisively to disclose key reactions involved in these complex mechanisms involved in the curing of siccative oil under the influence of diverse pigments and binders.<sup>17,48,55–57</sup> These advances lead to the constitution of molecular and kinetic models helpful for the understanding of the complex mechanisms taking place in these paints.<sup>47,48,58,59</sup> Mock-up paint systems are usually prepared for these studies to simplify the investigation of the chemical reactions and interactions taking place in the paints upon ageing. However, the molecular characterization of cross-linked fractions and polymeric networks formed in paint layers containing drying oils remains one of the greatest challenges in this discipline, which gets even more complicated for multi-components systems.

In addition to this, few scientific studies on the additions of proteins in oil paints have been reported to our knowledge.<sup>8,10,60–65</sup> Indeed, proteins have been detected in ancient paintings and archeological objects<sup>2,66,67</sup>, but it might sometimes be very difficult to find them due to strong degradation phenomena<sup>68,69</sup>. Several factors such as the presence of certain pigments, heat treatments, pH variations, chemical changes, contact to active species containing oxygen accelerate protein degradation through aggregation and denaturation processes and might challenge their detection in these artworks.<sup>70–72</sup> Research on model systems based on combinations of different pigments and proteinaceous materials showed that proteins can undergo structural modifications, depending on the nature of the pigment and the age of the paint layer<sup>73</sup>. Reactions between lipid oxidation products and proteins have been reported<sup>74–76</sup>, and may cause polymeric network modifications<sup>77</sup> and co-polymerization<sup>78</sup> in paints containing these substances.

In paintings, proteins originating from animals such as egg, casein (from milk) and glue (obtained by boiling the bones and the skin of mammals or fish), were frequently used as binders for pigments in the *tempera* technique, and their degradation has also been studied in some painting systems<sup>68,70,79–83</sup>. Egg yolk in particular was a popular binder for preparing *tempera* paints, and most of the research regarding the yolk stability upon storage, temperature or pH variations for instance have been investigated for the food chemical and processing field.

However, other reactions relevant for the cultural heritage, in particular to artistic painting with the interaction of the egg yolk with pigments or drying oils, might also play important role in transformations and degradations of its proteins<sup>84</sup>. Besides the environmental conditions<sup>85</sup>, the



pigments used to prepare *tempera* play a fundamental role in the degradation of the paint layers<sup>42</sup>. It has been shown that historically relevant pigments such as azurite or lead white greatly influence the degradation of the egg lipids in *tempera* paints, especially in the presence of basic carbonate such as in lead white.<sup>77,86</sup> Increasing the amount of this pigment may reduce the thermal stability of the paint medium (whole egg),<sup>87</sup> whereas egg *tempera* paints containing azurite pigments have shown to be sensitive towards thermal ageing and environmental conditions.<sup>86</sup> The oxidation of cholesterol is also accelerated by the presence of inorganic pigments.<sup>88</sup> Few studies focused on the fate of proteins in egg *tempera* paints, and it has been shown that they may be also subject to both cross-linking and hydrolysis upon ageing, and to a lesser extent, to oxidation of the side chains.<sup>89</sup>

Still, there is a need for research focusing on the addition of these proteinaceous materials on the flow properties of the obtained paints and their impact on the chemical changes taking place in the paints upon curing and ageing.

## 1.5. Motivation

The conservation and restoration of works of art, such as paintings, is of unique importance, as it allows to preserve these ancient artworks through the ages and to perpetuate these artistic testimonies of infinite value. This work aims to increase our knowledge and to understand how the artists prepared their paints and created their artworks, and which technical knowledge was developed and improved by the painters of the Renaissance. This might help to understand how the technical transition from egg tempera to oil painting took place during Renaissance, and by extension, might contribute to research into new paint formulations based on traditional media.

In order to fill this important knowledge gap, between the masterpieces we can still admire in museums and the material science behind it, we address the following aspects in this work:

- What is the role of egg yolk as binder in *oil* paints, and vice-versa, what is the role of oil in *tempera* paints?
- How do the mixing properties of paint systems affect their microstructure? And how does this influence the flow behavior of the liquid paints, particularly regarding the repartition of the binders? Which parameters have an influence on the modification of the flow properties?
- How does the flow properties of liquid paints correlate with their drying kinetics? Which factors may influence it?
- Additionally, do the above-mentioned parameters affect the chemical and physical stability of aging paints, in terms of visible changes such as the modification of the surface or the color? And how can this be limited or even better, avoided?

To simplify the systems in this study, the use of additives or solvents different than water are not being studied in the scope of this thesis. Mock-up paints with defined compositions and conditions are prepared in order to study systematically their flow properties, drying and chemical behavior.

The interdisciplinarity of the study, crossing path between rheology, chemistry and art conservation will help to draw conclusions regarding phenomena which are so far not well understood. This thesis is composed of 5 chapters which will address these different key aspects.

Chapter 1 of this manuscript introduced the topic and gave an overview of the fundamentals and important aspects regarding artistic paintings, necessary to comprehend the aspects discussed in this thesis.

In chapter 2 the materials used in this work are presented. The preparation of mock-up paints studied in this thesis is then detailed, prior to give an overview of all the methods employed along this thesis.

The publication in chapter 3 focuses on additions of egg yolk in oil-based paints and how this influences the paint properties, from their wet state until they transform into solid films and age.

Chapter 4 is adapted from another scientific article where *tempera* paint systems are investigated. Here we investigate how the flow properties and drying behavior of *tempera* paints can be modified, by means of oil additions or changes in the water content.

Then, chapter 5 addresses several aspects influencing the flow behavior, the drying kinetics and finally the physico-chemical properties of both *tempera* and oil aged paints.

Finally, the final chapters *Summary* and *Outlook* gather the main conclusions of the thesis and give an outlook of this work for further studies, addressing additional points of interest which may be interesting for future research on the topic.



## 2. Materials and methods

This chapter provides an overview of the materials used for the preparation of paints investigated in the next chapters of this thesis. A detailed explanation of the paint preparation procedures is then given to finally give an overview of all the technical and analytical methods employed.

### 2.1. Materials

#### 2.1.1. Pigments

Two historically relevant pigments, used for artistic paintings for centuries are used for this present study: lead white and ultramarine blue, the synthetic pigment of lapis lazuli. Old Masters used pigments, many of them deriving from minerals, which had to be crushed and dispersed, cleaned and purified.<sup>2,13,24</sup> Nowadays, the pigment preparation is less laborious for the artists, who can buy them on their final form. However, often these procedures are only mentioned for blue pigments and in context of painting techniques based on aqueous binders. Here we will describe the specificities of these two major pigments used alongside this study. The methods associated with the measurements described here are to be found in the next part of this chapter.

#### Lead White

Lead white pigment (LW) has been the major white pigment used in artistic painting and cosmetics since antiquity. Described by authors such as Plato or Aristophanes, its synthesis, based on a relatively simple reaction between lead and acetic acid (vinegar) in a carbon dioxide-rich atmosphere, was already detailed in the 4<sup>th</sup> century B.C and is known today as the “Dutch method”.<sup>90,91</sup> This white pigment, also referred as *psimythium* (Greek) or *cerussa* (Latin), remained the most used pigment until the 20<sup>th</sup> century despite its strong toxicity, already known for centuries (Pliny the Elder). Besides its use in painting, it was also commonly used as a whitening cosmetic due to its soft texture<sup>92</sup>. In France for instance, regulations were implemented in 1915 to restrict its access but the pigment was still in use until the end of the 20<sup>th</sup> century.<sup>90</sup> Nowadays, it is nonetheless quite common to find this pigment in artists workshops, however its use has been mostly replaced by non-toxic titanium white and zinc white pigments.<sup>9</sup>

Lead white is generally composed of cerussite ( $\text{PbCO}_3$ ) or hydrocerussite ( $\text{Pb}_3(\text{CO}_3)_2(\text{OH})_2$ ), sometimes a mixture of both<sup>90,91,93</sup>, with a reference density =  $6.7 \text{ g/cm}^3$ . The pigment used in this study was purchased from *Kremer Pigmente* (Germany). Its grains, analyzed by Scanning Electron Microscopy (SEM) (Figure 2.1), are relatively isometric, with an average diameter size  $x_{50} = 2 \mu\text{m}$  and a narrow mono-modal particle size distribution (Figure 2.2).

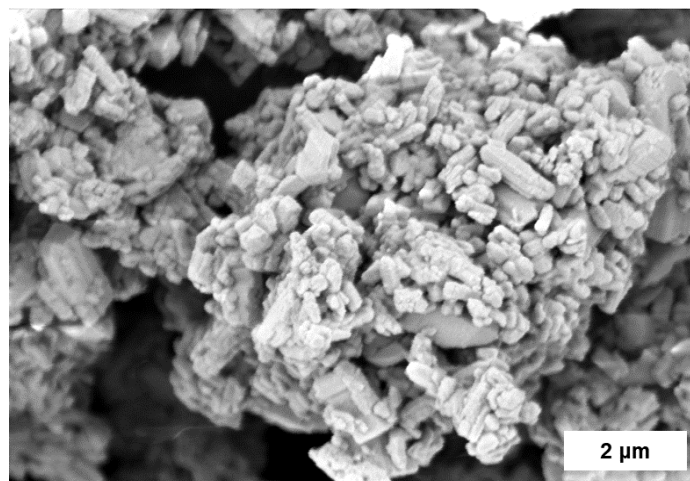


Figure 2.1 - Scanning electron microscope (SEM) pictures of LW pigment used in this study.

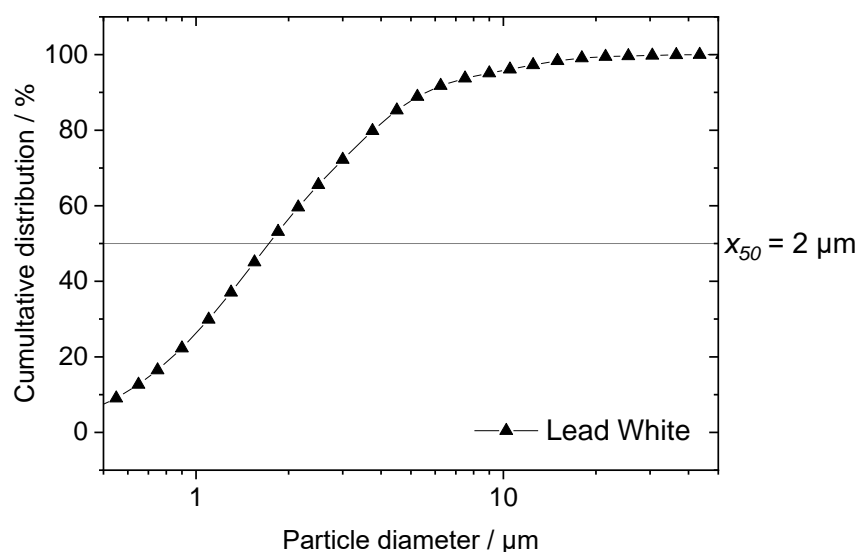


Figure 2.2 - Particle size distribution of LW pigment used in this study.

The crystal structure of LW may vary depending on its composition and presents generally a certain degree of disorder according to crystallographic studies. It has been shown that when hydrocerussite is the major type of crystal in LW, its structure is rather hexagonal rhombohedral, from the space group  $R3m^{90}$ , and when cerussite is the major type of crystal, its structure is orthorhombic from the space group  $Pm\bar{c}n^{94}$ . X-ray diffraction (XRD) analysis (Figure 2.3) revealed

that the main crystalline phase of the LW pigment used for this study is cerussite, a lead carbonate (peaks marked marked by ?). Traces of other unidentified crystalline phases, not related to other lead compounds (i.e hydrocerussite, plumbonacrite, lead acetate, lead oxides) are also present. The shape of the pigment particles observed from SEM data together with the XRD pattern of the LW pigment confirm that the relative roundness of the pigment particles correlates with its crystallographic structure, studied also in literature.

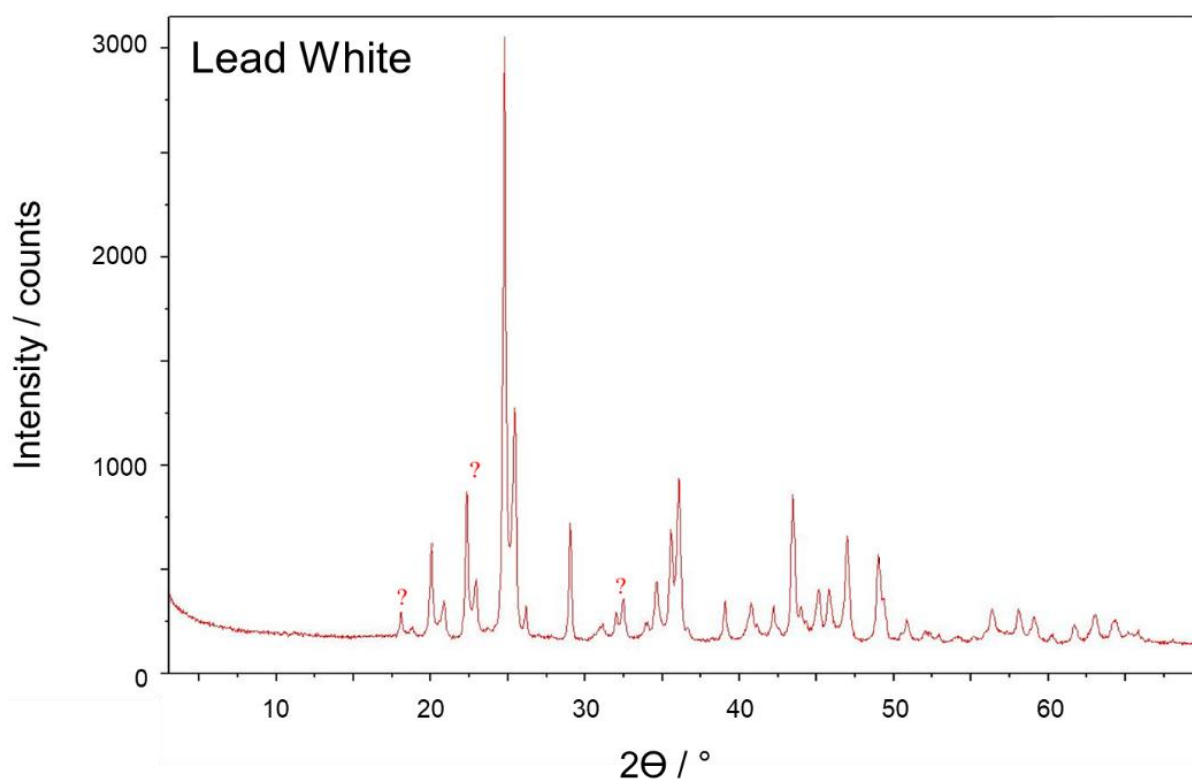


Figure 2.3 - XRD pattern of LW pigment used in this study. Analysis performed by E. Cantisani (ICVBC, CNR in Florence)

### Ultramarine Blue

UB pigment was made originally from the semi-precious stone lapis lazuli, collected exclusively in Afghanistan, through a long and fastidious process, improved through the centuries, and probably unchanged since Cennini's description.<sup>2,95</sup> Detected in decorative buildings and archeological objects from the early Egyptian times, the first proof of its actual use in paintings is dated from the 6<sup>th</sup> – 7<sup>th</sup> century in Afghanistan. It was then identified in several artistic paintings or illuminated manuscripts in Persia, China, India and Europe. In Italy from the 14<sup>th</sup> century, natural ultramarine pigment was used almost exclusively for the robes of the Christ and the Virgin, due to its extremely high price, aligned to the one of gold.<sup>95–97</sup> The different preparation steps, including grinding, washings, crushing and mixing with wax, resins and/or oils, were very long and could require some

weeks of work. The blue particles of lazurite could be separated from the colorless crystalline material and impurities, remaining in the wax, repeating this process several times. The bigger lazurite particles were obtained first, and the remaining smallest ones are known as ultramarine ash, containing a higher amount of colorless material, resulting in greyish pigment fractions. Some natural impurities such as calcite remain in the pigment, helpful to differentiate it from the synthetic UB pigment.<sup>95</sup>

UB became more affordable and thus accessible to a broader community in the 19th century thanks to the production of synthetic ultramarine blue in 1826 by Jean-Baptiste Guimet, giving the designation *french ultramarine* to this pigment.<sup>96</sup> Due to the synthetic industrial process, the impurities, size and particle size distribution of the pigment can be better controlled, which is the reason why synthetic UB pigment was chosen in the scope of this study. Of course for Old Masters, natural ultramarine was the only available source of this pigment. Highly heterogeneous particles (some of which are very large, much more than 10  $\mu\text{m}$  in diameter) typically present in natural ultramarine, however, would have disturbed rheological measurements, and would have added a higher degree of variability in the experimental parameters.

UB is a complex sulfur-containing sodium aluminum silicate, its approximate formula is  $\text{Na}_{8-10}\text{Al}_6\text{Si}_6\text{O}_{24}\text{S}_{2-4}$  and it may also contain some chloride and calcium. Its structure is probably the most complex among all pigments<sup>95</sup>, and not resolved yet.<sup>97</sup> With a reference density of  $2.35 \text{ g/cm}^3$ , the pigment is referred in the Color Index as PB29, the deep blue color coming from its polysulfides and radical anion  $\text{S}_3^-$ , also present in the crystal structure of natural ultramarine (lapis lazuli).<sup>98</sup> This latter contains mostly hextetrahedral isometric crystals, from the space group  $P43n$ .<sup>99</sup> The UB pigment used in this study was purchased from *Abralux Colori Beghè* (Italy). Its grains, analyzed by Scanning Electron Microscopy (Figure 2.4), are relatively isometric, with an average diameter size  $x_{50} = 2 \mu\text{m}$  and a narrow mono-modal particle size distribution (Figure 2.5).



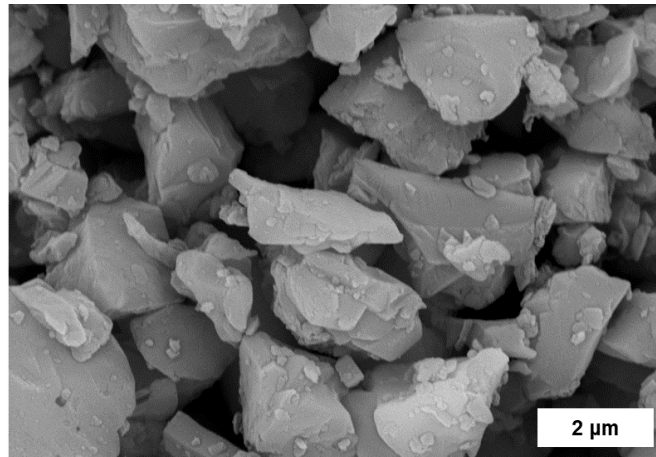


Figure 2.4 - Scanning electron microscope (SEM) pictures of UB pigment used in this study.

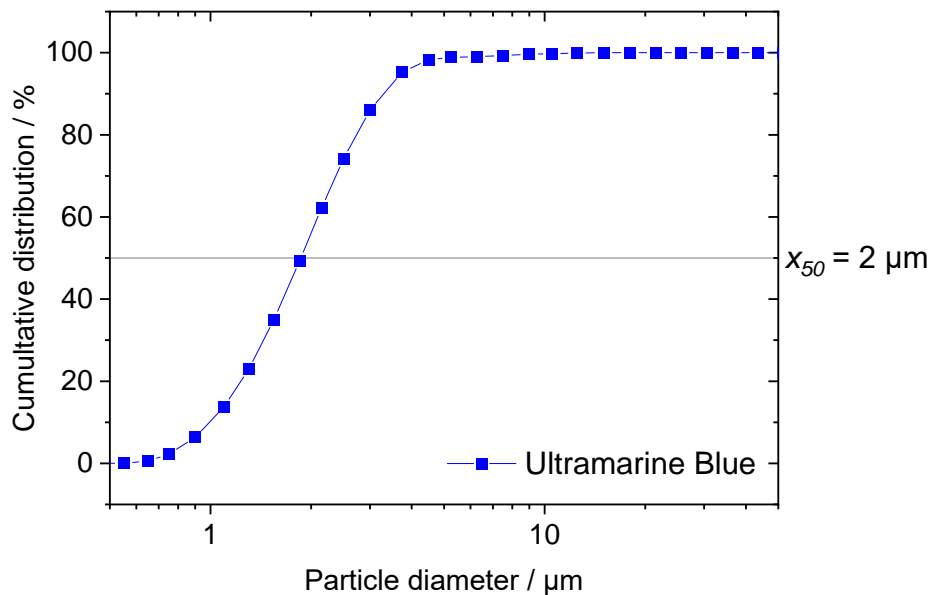


Figure 2.5 - Particle size distribution of UB pigment used in this study.

X-ray diffraction analysis (Figure 2.6) revealed that all peaks refer to the crystalline phase of synthetic ultramarine blue, a sodium aluminum silicate containing sulfur, with the exception of the peak at  $2\theta$   $26,70^\circ$ , which is related to quartz ( $\text{SiO}_2$ , marked with the circle). The crystal structure of artificial ultramarine is indeed complex and not resolved yet. The crystalline structure of natural UB, due to its high content of impurities, might contain calcite, sodalite, and pyrite crystals.<sup>97</sup>

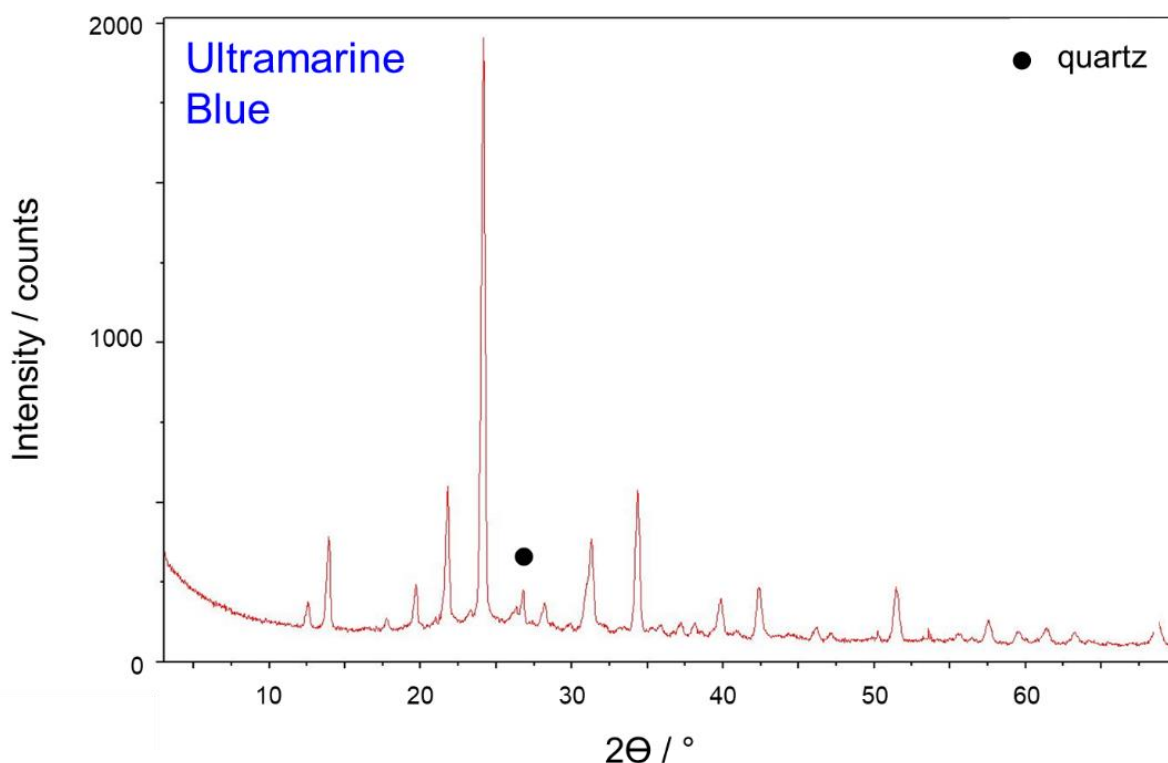


Figure 2.6 - XRD pattern of UB pigment used in this study. Analysis performed by E. Cantisani (ICVBC, CNR in Florence)

### 2.1.2. Linseed oil as drying oil

Linseed oil, obtained from the seeds of the flax plant (*Linum usitatissimum*), has been used since the Ancient Egypt and is still commonly used today, forming resistant films appropriate for paintings. In paintings, varnishes and coatings, other vegetable oils, such poppyseed or walnut oils, were also used. However, the higher content of linolenic acid in linseed oil makes it a faster drying oil compared to the other ones.<sup>16,100</sup> Aged drying oil paint films generally contain high amounts of dicarboxylic acids, where azelaic acid is usually being the most abundant. Natural degradation of these lipids can be accelerated when the material is exposed to high temperatures and also oxidizing conditions. Light and oxygen, but also oil pre-treatments, such as boiling processes or addition of additives may influence its curing kinetics.<sup>16</sup> Linseed oil tends to yellow upon ageing<sup>101,102</sup>, causing color alterations in artistic paintings if not appropriately handled. The curing mechanism of linseed oil in paints has been investigated for hundreds of years, but is still not fully understood yet.<sup>47,103</sup>

The linseed oil used in this present study was purchased from *Maimeri* (Italy), stored at room temperature conditions in a closet and freshly opened for curing and long-term drying experiments. Its reference density is 0.93 g/cm<sup>3</sup>.

### 2.1.3. Egg yolk as proteinaceous binder

The use of hen egg yolk as binder in paintings such as *tempera* is ancient. With about 50 wt% of dry matter, the EY is composed of about 31 wt% of lipids, 17 wt% of proteins and 2 wt% of carbohydrates and ash.<sup>32</sup> What remains is water, which makes the EY an aqueous binder. Its microstructure is sophisticated: proteins and lipids are presents in complexes in two major forms: the insoluble granular aggregates ( $d = 0.3\text{-}2\ \mu\text{m}$ ) containing high density lipoprotein complexes (HDL) and the water-soluble plasma, composed mostly of low-density-lipoprotein (LDL) micelles ( $d = 13\text{-}50\ \text{nm}$ ).<sup>33,34,104</sup> The complex microstructure of EY is a dispersion of protein-stabilized lipid particles and droplets, and we can describe the entire system as a concentrated oil-in-water emulsion, stabilized by proteins.<sup>105,106</sup>

Modifications of the storage conditions affect the EY properties: long storage times lead to a decrease of the permeability of the membrane separating the yolk from the albumen, resulting in an increase of the water content in the yolk. Also, the membrane breaks more easily, which complexifies the separation between the egg yolk and the white.<sup>107</sup> This increase of the water content leads to a modification of the flow properties of the yolk.<sup>108,109</sup> Other important effects, such as the modification of the storage temperature conditions, have shown to modify the pH of the yolk<sup>110</sup>, and this impacts its rheological and chemical properties<sup>33,107,111</sup>. In addition to this, it has been demonstrated that salt additions influence the protein secondary structures in EY<sup>84</sup>, as in several foodstuffs. Dehydration (freeze-drying) and freezing of the egg also deliver yolks with other properties, which are not relevant in the frame of this thesis.<sup>32,84,112</sup>

These changes, together with the natural variability of each egg depending on the animal, its type, its diet, and so many other parameters, might influence the composition of each EY used in this study. The differences observed regarding the egg's quality due to the hens' diet were known already during the Renaissance, since Cennini made a clear difference between the eggs coming from the towns, which are whiter, and the ones from the farms, which are more red.<sup>2,113</sup> Considering this, organic hen's fresh eggs were purchased in local supermarkets and used within 3 days after purchase. In addition to this, the quantity of water, measured gravimetrically, was set as determining parameter, used as reference for calculating the amount of each group of compounds (proteins, lipids, ...) based on the above-mentioned average quantities.

## 2.2. Paints preparation

### 2.2.1. Preparation of the yolk

Fresh organic hen's eggs, stored no longer than 3 days after their purchase were used for this study. Conserved at room temperature, a fresh egg yolk (EY) is first separated from its white. The yolk is cautiously deposited on an absorbing paper to remove excess water and egg white residuals, without breaking its skin. The yolk is transferred into the hand and its skin pierced gently,

prior to empty it into a beaker while still holding the skin between the fingers. An amount of around 13 g was collected. A magnetic bar is added and the beaker is quickly closed and sealed with a stretchable piece of plastic *Parafilm* so avoid excessive water evaporation, and placed on a water-cooling bath (RT) on magnetic stirrer to ensure the homogenization of the liquid EY at room temperature.

### 2.2.2. Oil-based paints

#### Oil paints

The pigments are ground on a glass plate together with the linseed oil with a glass muller for 10 minutes until the paint is homogeneous and does not show any grains anymore.

#### Capillary Suspensions Paints (CapS)

An oil paint is prepared in which a few drops (from 1 to 4 vol%) of a secondary fluid, either distilled water or fresh EY are added, the paint is then mixed with a palette knife for 1 min, resulting in a very stiff paint.

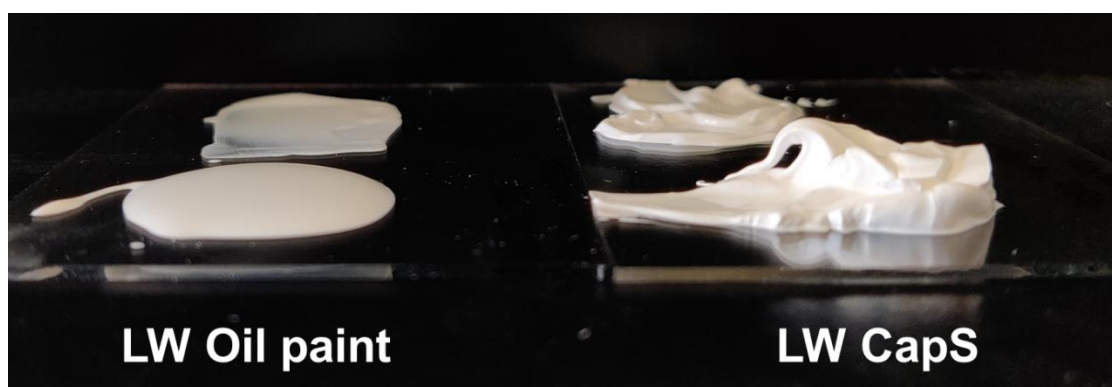


Figure 2.7 – Visual aspect of a LW-based oil paint (left) and a LW-based capillary suspension paint (right) after their preparation.  $\phi = 32$  vol% for both paints, and the LW CapS paint contains about 2 vol% of water.

#### Protein Coated Pigment Paints (PCP)

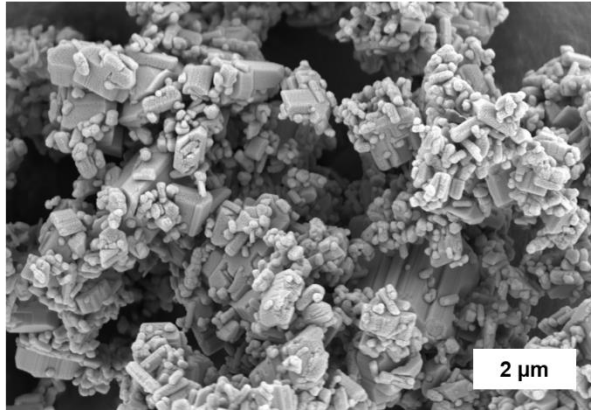
Several steps are necessary for the preparation of a PCP paint:

1. Fresh homogenized EY is diluted with distilled water, and the EY dried matter are quantified gravimetrically.
2. The pigment is ground with an adjusted quantity of diluted EY for 10 minutes, and left to dry (c. 30 min at 30 °C). When the water has evaporated, all non-volatile EY components must be deposited on the surface of the pigment particles. The existence of a protein layer on the surface of the pigments was confirmed by scanning electron microscopy images

(Figure 2.8). This protein surface layer is included when calculating the volume solids content  $\phi$  for the *PCP* paints.

3. The pigments coated with dried EY are ground again with the linseed oil for 10 min until the paint is homogeneous and does not show any grains anymore (Figure 2.9).

**Lead White**



**Coated Lead White**

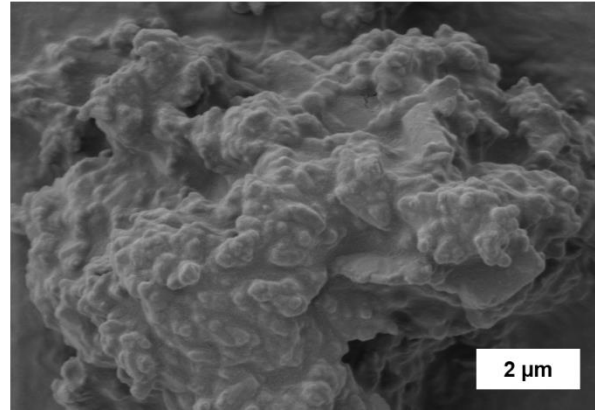


Figure 2.8 - SEM pictures of uncoated LW (left) and LW coated with a  $\approx 1 \mu\text{m}$  egg yolk layer (right).

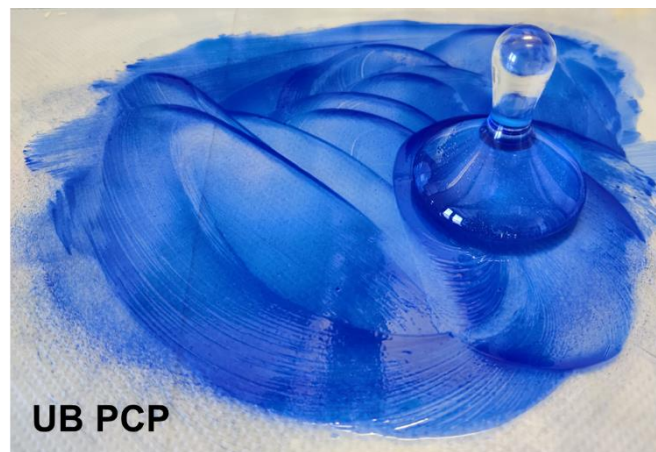


Figure 2.9 – Step 3 of a UB PCP paint preparation: the pigments coated with dried EY are ground together with linseed oil for 10 minutes in order to obtain a homogeneous paint.

### 2.2.3. Water-based Paints

#### **Tempera**

Pigments, fresh egg yolk and water were ground on a glass plate with a flat muller for 10 minutes, until enough water evaporated to be able to transfer the paint from this surface to another with the palette knife. The dried matter of each egg yolk was determined gravimetrically and the quantity of water in the paint was adjusted by adding distilled water to the existing water naturally contained in the fresh egg yolk.

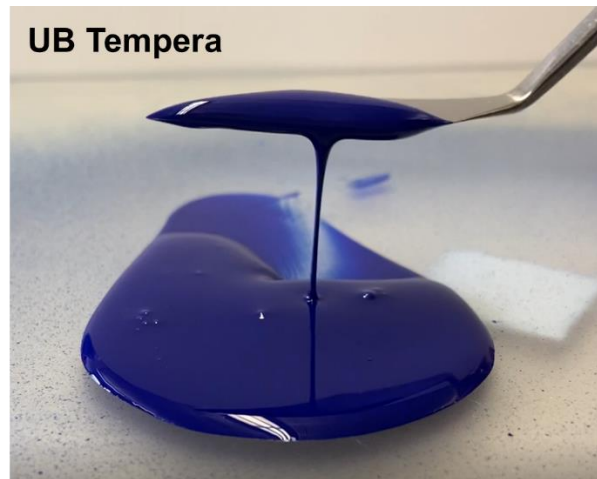


Figure 2.10 – UB-based tempera in the liquid state. This paint is composed of  $\varphi = 50$  vol% of disperse fraction (including 1/3 of pigment and 2/3 of EY dried matter) and 50 vol% of water.

### **Tempera Grassa (TG)**

To prepare a *tempera grassa*, linseed oil was then slowly added to the existing *tempera* paint, while continuing homogenizing this the flat muller, until enough water evaporated to be able to transfer the paint from this surface to another with the palette knife.

For rheological and hardness measurements only, both types of water-based paint samples were homogenized using a non-contact planetary mixer (SpeedMixer DAC 150.1 FVC, Hauschild Engineering, Germany) in sealed containers (75 mL) to avoid the evaporation of water. Pigments, fresh egg yolk and distilled water were first mixed at 2000 rpm during 120 s. For TG paints, linseed oil was then added, and the samples were homogenized again at 3000 rpm during 60 s.

## **2.3. Experimental methods and devices**

### *2.3.1. Characterization of the raw materials*

#### **Contact angle measurements**

Contact angle measurements were performed according to the norm ISO 19403-2:2017 using the sessile drop method (DataPhysics Instruments GmbH, OCA15, Filderstadt, Germany). Previously dried pigments were placed as a thin layer on a double-side tape on a flat surface on which a drop of liquid was deposited. For the egg yolk measurements, a thin layer of diluted egg yolk was placed on a glass slide and let to dry prior to the deposition of a drop of liquid (distilled water or linseed oil). The value of the contact angle for each liquid is calculated as the arithmetic mean of the at least 7 measured values.



## Humidity storage

Pigments were ground prior to be disposed as thin layers (around 2 mm) in aluminum containers in desiccators containing saturated solution of salts ( $\text{MgCl}_2$  or  $\text{NaCl}$ ) or drying medium (silica gel) during 14 days. Relative humidity at  $T = 20.0 \pm 0.5$  °C was determined with a temperature and humidity sensor (Digi-Sense™ USB Datalogger, Cole-Parmer). The moisture taken up by the pigments was determined gravimetrically as follows: the weight of the pigments stored at laboratory conditions ( $T = 20.0 \pm 0.5$  °C) before storage in desiccators was subtracted from the weight of the samples after 2 weeks storage in desiccators containing saturated solution of salts ( $\text{MgCl}_2$  or  $\text{NaCl}$ ) or drying medium (silica gel).

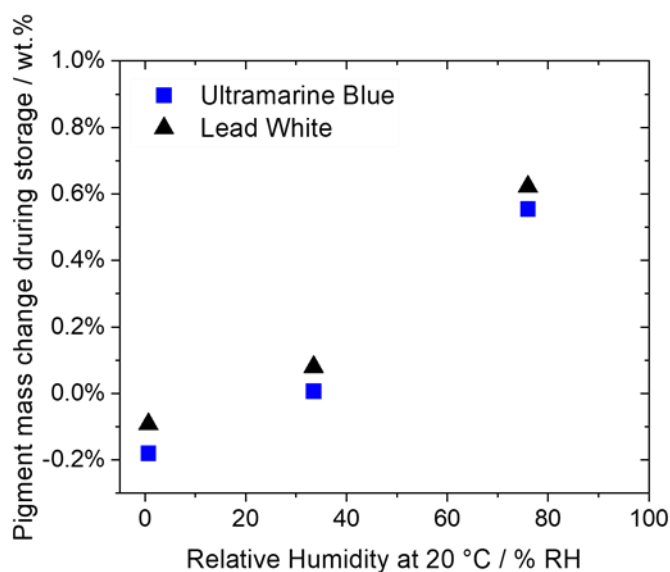


Figure 2.11 - Pigment mass change after 2 weeks of storage at different humidity conditions at 20 °C.

## Particle size distribution (PSD)

The particle size distribution was determined through Fraunhofer diffraction (Helos H0309; Sympatec GmbH, Clausthal-Zellerfeld, Germany) using water for particle dispersion in an ultrasonic wet dispersing unit (Quixel and Cuvette, Sympatec GmbH) for both UB and LW pigments.

## X-ray diffraction (XRD)

An X'Pert Pro diffractometer equipped with an X'Celerator detector with a Cu X-ray tube ( $\lambda = 1.54$  Å) was used with a Ni-filtered Cu-K $\alpha$  radiation source (Malvern Panalytical, United Kingdom). The X-ray tube was operated at 40 kV and 30 mA. The diffraction patterns were collected under the following conditions:  $2\theta$  range 3–70°, step size 0.02°. Soller and anti-scatter slits were used on the incident and diffracted beams; a divergent slit was used on the incident beam. A zero-background sample stage was used. Few mg of UB and LW pigments were analysed, and the phase

identification of the samples was performed using the X'Pert HighScore program and the ICCD database. The analyses have been performed by E. Cantisani (ICVBC, CNR in Florence).

### 2.3.2. Characterization of the wet paints

#### Brush strokes analysis

Automated paint brush strokes on painting paper (Fabriano, Hot Press, 25% Cotton 300 g/m<sup>3</sup>) were performed with a universal testing machine (Texture Analyzer TA.XT Plus, Stable Micro Systems, UK) with a custom-made paint brush holder keeping an angle of 60° between the brush (Gussow Oil Painting Brush, 15 mm width, flat, Gerstaecker, Germany) and the painting surface (see Figure 2.12). Brush strokes of 20 x 150 mm were performed in triplicate at a speed of 20 mm/s.

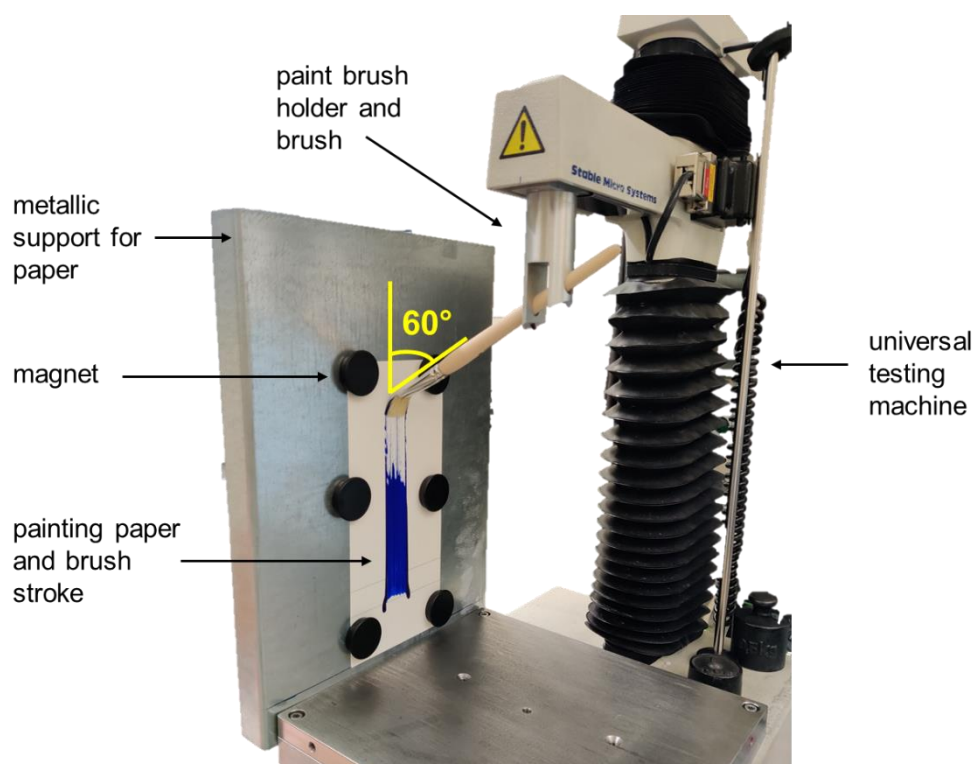


Figure 2.12 - Custom-made equipment on a universal testing machine to make automated paint brush strokes.

#### Confocal laser microscopy (LSM)

Automated paint brush stroke profiles of fresh paints were analyzed with a 3D confocal laser microscope with a magnification of 10x (Keyence VK-X100, Japan) to determine the roughness  $R_z$  of the paint brush strokes. The single image size of the LSM had a size of 1406  $\mu\text{m}$  x 1054  $\mu\text{m}$  (x- and y-dimension, with a resolution of 0.05  $\mu\text{m}$ ), and 24 to 25 images were acquired per cross-section. The resolution in z-direction perpendicular to the image was 0.02  $\mu\text{m}$ .



### **Centrifugation experiments**

Centrifugation experiments were performed using an Eppendorf Centrifuge 5430R (Germany). About 12 mL of homogenized samples were centrifugated at 20°C for 1 h at 7000 rpm (g-force  $\approx 6000 \text{ m.s}^{-2}$ ) in order to separate the different phases of the paint. Aliquots collected from each phase, dried on microscope slides, were then analyzed using ATR-FTIR (Perkin Elmer Spectrum One FTIR Spectrophotometer, equipped with a universal attenuated total reflectance (ATR) accessory). For each sample, 64 interferograms were recorded, averaged and Fourier-transformed to produce a spectrum with a resolution of  $4 \text{ cm}^{-1}$ .

### **Microstructure experiments**

The microstructure of the *tempera (grassa) paint* systems was captured using an inverted fluorescence microscope (Axio Observer D1, Carl Zeiss), equipped with a Fluar 100x objective (numerical aperture 1.3, 100x magnification, oil immersion lens, Carl Zeiss). The Brownian motion of green fluorescent polystyrene microspheres (Bangs Laboratories, USA, with  $d = 0.2 \text{ }\mu\text{m}$ , a density of  $1.06 \text{ g/cm}^3$  and a refractive index of 1.59 at 589 nm), used as tracer particles, was recorded with a sCMOS camera Zyla X (Andor Technology). 2D images ( $127 \times 127 \text{ }\mu\text{m}$ , frame rate 50 frames/s) of the fluorescent particles were recorded to obtain movies of the fluctuating microspheres. Rhodamin B, a dye usually employed to stain water, was used in UB-based *tempera (grassa)* samples to enhance the contrast between the oil droplets (where its solubility is poor) and the aqueous medium. 100  $\mu\text{L}$  of a diluted solution of Rhodamin B (1/200) and 14  $\mu\text{L}$  of tracer particles were added to 700  $\mu\text{L}$  of paint sample prepared according to the above-mentioned method and homogenized using a vortex.

### **Rheological measurements**

Rheological measurements were performed on a stress-controlled rheometer (Physica MCR 301, Anton Paar GmbH, Germany) equipped with a Peltier element to ensure a constant measuring temperature of 20 °C. A 3 min waiting period was included before starting the measurement to ensure structural recovery. Due to differences in structure, flow and drying properties of the different types of paints studied, different methods adapted to each type of paint were established. The methods associated for oil-based paints (oil paints, PCP paints and CapS paints) and water-based paints (*tempera* and TG paints) were set as follows (see below). The results shown were determined from at least three measurements of freshly prepared paints, the displayed data are average values and the standard deviations are shown as error bars.

- **Yield stress determination**

Creep experiments to determine the yield stress  $\sigma_y$  were performed using a vane-and-cup fixture (ST10-4V-8.8, diameter 10 mm).

### Oil-based paints

For yield stress measurements, the shear stress was increased between  $10^{-2}$  Pa and  $10^4$  Pa and the deformation was recorded during a total measuring time of 600 s, a time scale relevant for the application of artist paints. Preliminary experiments did not show a substantial variation of the extracted  $\sigma_y$ -values with measuring time. The vane-and cup fixture avoids disturbance of yield stress determination by slip phenomena. At stresses below  $\sigma_y$  a linear relationship between deformation  $\gamma$  and applied shear stress  $\sigma$  is found (Hooke's law) since the paint behaves like an elastic solid. At a critical stress level the deformation drastically increases and the yield stress  $\sigma_y$  is determined from the  $\gamma$  ( $\sigma$ ) -curves according to the tangent intersection method<sup>114</sup> as shown in Figure 2.13. Particularly, for CapS it is known that structural recovery after shear happens quickly (within seconds) and thixotropic phenomena are of minor relevance<sup>115</sup>.

### Water-based paints

The vane-and-cup fixture was used to avoid disturbance of yield stress determination by slip phenomena. Shear stress was increased from  $10^{-3}$  Pa to 5000 Pa in a logarithmic stress ramp within 480 seconds. The yield stress  $\sigma_y$  was determined from the sharp kink in the deformation  $\gamma$  versus shear stress  $\sigma$  curves according to the tangent intersection method.<sup>114</sup>

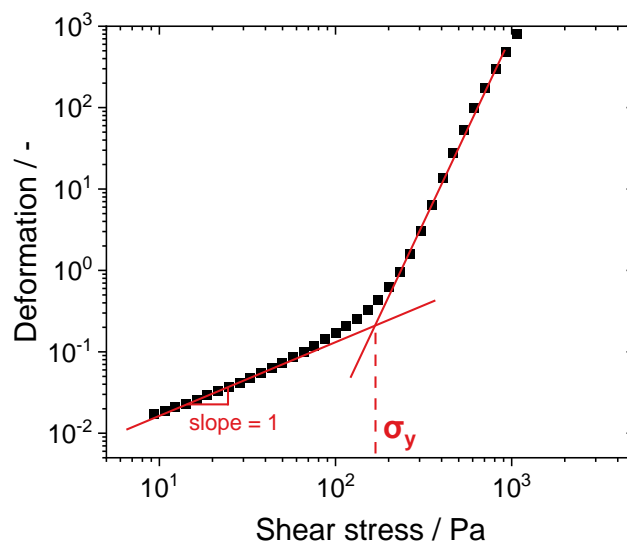


Figure 2.13 - Yield stress determination with the tangent intersection point method for a LW PCP paint sample ( $\varphi = 42$  vol% with 6 vol% of EY).

- **Viscosity at high shear**

### Oil-based paints

For the oil-based paints, a plate-plate geometry (diameter 25 mm, gap 0.5 mm) was used to perform steady shear viscosity measurements. The sample is placed between the two plates and is trimmed when the gap attains 0.525 mm to remove the excess of paint which might perturbates the measurement, then the gap is set at 0.5 mm for the measurement. The shear stress was increased between  $10^{-2}$  Pa and  $10^4$  Pa and the viscosity was recorded during a total measuring time of 1340 s.

#### Water-based paints

Concentric cylinder-and-cup geometries (Z10DIN, cylinder diameter  $d = 10$  mm, or Z27DIN  $d = 27$  mm) were used to determine the steady shear viscosity.<sup>116</sup> The cup was filled with a sufficient quantity of sample to fully cover the cylinder geometry, allowing viscosity measurements without significant modification of the paint composition due to the evaporation of water. The shear rate was increased in a logarithmic shear rate ramp from  $10^{-3} \text{ s}^{-1}$  to  $4200 \text{ s}^{-1}$  and the viscosity was recorded during a total measuring time of 484 s.

#### *2.3.3. Drying experiments and characterization of the solid films*

The environmental conditions were fixed ( $T = 20 \text{ }^\circ\text{C}$ , relative humidity 30-50%) for the storage of the samples for the (long-term) drying experiments.

#### **Gravimetric measurements**

Fresh paint samples were poured in circular custom-made aluminum sample holders (diameter 25 mm, thickness 0.4 mm, 0.7 mm or 1.0 mm) and weighted regularly upon time. The weight of each sample was normalized to the oil content of the fresh paint for comparison.

#### **Paint hardness measurements**

The change of hardness of the paint sample films upon time was determined using a universal testing machine (Texture Analyzer TA.XT Plus, Stable Micro Systems, UK) equipped with a stainless steel tip (diameter 8 mm) and a custom-made sample holder plate (405 x 15 mm), allowing to keep the thickness of the paint layer at 0.4 mm. The tip penetrated into the sample at  $10 \text{ mm/s}$  at a depth of 0.3 mm from the paint surface (Figure 2.14A). The force required to penetrate the tip into the paint layer was recorded and its maximum value in a single penetration cycle normalized to the piston cross-sectional area was determined as the hardness of the layer. This quantity was monitored over time to characterize the drying kinetics (Figure 2.14C). Each experiment was performed in triplicate, the displayed data are average values and the standard deviations are shown as error bars. Alongside with the determination of the hardness (which is the force necessary

to penetrate the paint layer divided by the surface of the tip), the sample was considered as “dry-to-touch” by visual control of its surface (see Figure 2.14B).

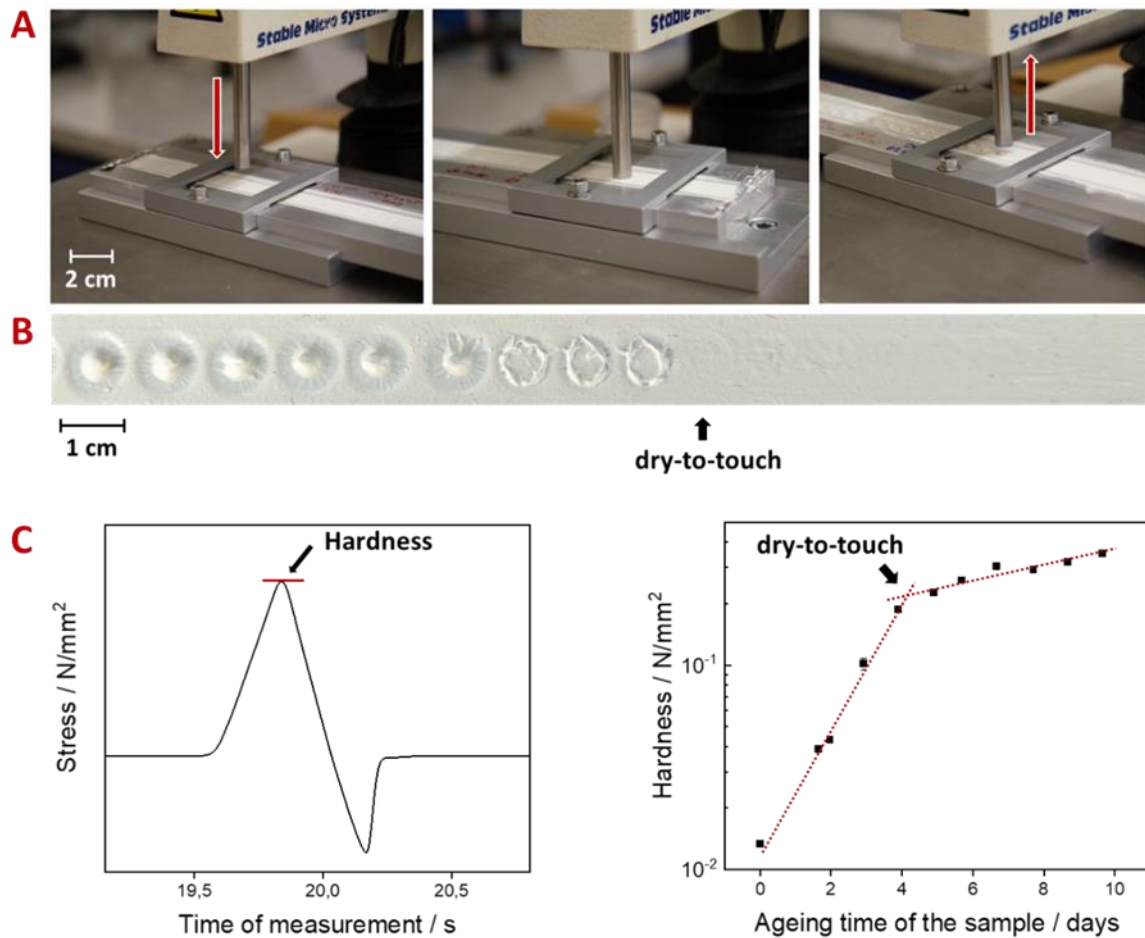


Figure 2.14 - (A) Custom-made equipment on a universal testing machine to determine the "dry-to-touch" state of the paints. (B) Traces left at the paint surface after measurements in triplicates, useful for the visual control of the "dry-to-touch" state. (C) Experimental determination of the hardness of a paint (left) and "dry-to-touch" determination from the hardness of the paint layer upon natural ageing (right).

### Colorimetric analysis

Custom-made aluminum paint sample holders, where fresh paint was poured in a holding surface of 48 x 68 mm and trimmed to ensure a paint thickness layer of 0.4 mm, 0.7 mm or 1.0 mm were used for colorimetric experiments. The sample holders were anodized in black to reduce the light reflection in the remaining gaps at the borders of the sample holder. A large microscope glass slide (1 x 52 x 76 mm) was placed on the sample holder, separated from the paint surface with a thin 0.1 mm gap to avoid the microscope glass to touch the paint surface when it is still liquid, and yet be as close as possible to the surface of the paint, which is recommended for colorimetric experiments. The glass slide was removed after each experiment to allow the paint to dry and cure further.

Colorimetric measurements were performed by means of a colorimeter PCE CSM 4, having a large sport diameter of 20 mm to reduce the influence of surface effects due to hand-made and imperfect

paint preparation (known to have effects on color changes<sup>117–120</sup>), using D65 as the illuminant and a 45°/0 geometry. The color of paints was characterized using CIELAB color space, measuring L\* (lightness), a\* and b\* (color coordinates), c\* (chroma) and h\* (hue), which could be converted into XYZ tristimulus values. The results shown were determined from at least seven measurements of freshly prepared paints, randomly performed on the entire surface of each mock-up paint to provide statistically consistent results; the displayed data are average values and the standard deviations are shown as error bars.

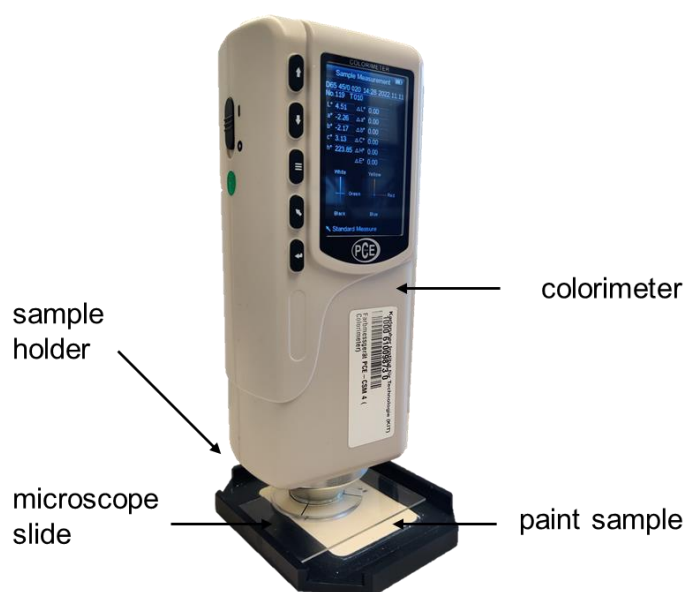


Figure 2.15 – Colorimeter and custom-made paint sample holder for colorimetric experiments

#### 2.3.4. Thermal and spectrometric analysis

##### Differential Scanning Calorimetry (DSC)

DSC measurements were performed with a differential scanning calorimeter (TA Instruments DSC 250) under constant nitrogen flow (80 mL/min) in the 25–250 °C temperature range, with a 10 °C/min heating rate. Paint samples (1–3 mg) were scratched from the cast of paint disposed on glass slides and placed in aluminum pans, then sealed. Since the oil is the only component susceptible to exhibit thermal effect in oil paints in the studied temperature range, DSC curves were normalized to the oil content. Temperature and heat flow were calibrated with indium, and the baseline was calibrated using two empty aluminum pans.

### **Evolved gas analysis coupled with mass spectrometry (EGA-MS)**

Evolved gas analysis coupled with mass spectrometry (EGA-MS) experiments were performed with a micro-furnace Multi-Shot Pyrolizer EGA/Py-3030D (Frontier Lab) coupled to the 6890 gas chromatograph (Agilent Technologies, Palo Alto, CA, USA) equipped with a deactivated and uncoated stainless-steel tube (UADTM- 2.5 N, internal diameter of 0.15 mm and length of 2.5 m, Frontier Lab). The GC system was equipped with a 5973 Mass Selective Detector (Agilent Technologies), a single quadrupole operating in Electron Impact (EI) mode at 70 eV in the 50–600 m/z range.

About  $300 \pm 50$   $\mu\text{g}$  of sample was introduced in a stainless-steel cup, placed in the furnace chamber, covering the temperature range 50-700 °C at a rate of 20 °C.min<sup>-1</sup>. Analyses were carried out using helium as carrier gas (1 mL/min). The GC injector was used in the split mode at a ratio 50:1. The interface pyrolizer-GC was maintained at 100 °C higher than that of the furnace, until a maximum of 280 °C was reached. The inlet temperature was 280 °C, while the chromatographic oven was kept at 300 °C. The temperature of MS transfer line was set at 300 °C, the ionization source at 230 °C and the quadrupole at 150 °C.

### **Fourier-Transformed Infrared Spectroscopy (TRANS-FTIR)**

Infrared spectra were recorded using a Perkin-Elmer Spectrum 100 FTIR Spectrophotometer (Perkin Elmer, USA), equipped with a universal attenuated total reflectance (ATR) accessory and a triglycine sulphate TGS detector. To monitor the changes in the protein structure as well as the lipid oxidation upon time, fresh paint thin layers were applied on BF<sub>2</sub> windows (diameter 13 mm) and regularly analysed by direct transmittance spectroscopy (TRANS-FTIR) after defined periods of time. For each sample, 128 scans were recorded in the range of 4000-600 cm<sup>-1</sup>, averaged, and Fourier-transformed to produce a spectrum with a nominal resolution of 4 cm<sup>-1</sup>. The amide I peak (1600-1700 cm<sup>-1</sup>) was fitted with a frequency deconvolution procedure according to the method described in *Bramanti et al. (1994)*<sup>121,122</sup>.

### **Pyrolysis coupled with mass spectrometry (Py/GC/MS)**

The instrumentation consists of a microfurnace multishot pyrolyzer EGA/Py-3030D (Frontier Lab) coupled to a gas chromatograph 6890 N (Agilent Technologies, Palo Alto, CA, USA) and to an Agilent 5973 Mass Selective Detector. The split/split-less injector was used in split mode at 280 °C, with a split ratio 30:1. The chromatographic conditions were as follows: 50 °C isothermal for 2 min, 10 °C/min up to 280 °C and isothermal for 2 min, and 15 °C/min up to 300 °C and isothermal for 30 min. The carrier gas (He, purity 99.9995%) was used in the constant flow mode at 1.0 mL/min. The temperatures of the MS transfer line, MS ion source, and MS quadrupole were 280, 230, and 150 °C, respectively. The mass spectrometer was operated in EI positive mode (70 eV) with a scan range m/z 50–600. MS spectra were recorded in TIC mode. Ca. 150  $\mu\text{g}$  of the sample were placed

in a pyrolysis cup where 4  $\mu\text{L}$  of 1,1,1,3,3,3-hexamethyldisilazane (HMDS) were added as a silylating agent for the in-situ derivatization of pyrolysis products. The temperature of the furnace for pyrolysis was set at 550 °C.

### **Thermogravimetric analyses (TGA)**

TGA was carried out with a TA-Instruments thermo-balance, model Q5000IR, at constant nitrogen flow (25 mL/min) in the 25–900 °C temperature range for UB-containing samples and 25-300 °C for LW-containing samples at a heating rate of 20 °C/min. Temperature calibration was based on the Curie point of paramagnetic metals (Alumel, Ni, Ni<sub>83%</sub>Co<sub>17%</sub>, Ni<sub>63%</sub>Co<sub>37%</sub>, Ni<sub>37%</sub>Co<sub>63%</sub>). Paint samples (c. 3 mg) were scratched from the cast of paint disposed on glass slides and placed in platinum pans (and in aluminum crucibles in on the platinum pans for LW-containing samples)

Isothermal thermogravimetric analyses (also called *oxygen uptake*) were performed on the same instrument for recording the oxygen uptake curve under a constant air flow (25 mL/min). The freshly prepared samples (c. 7-19 mg) were placed in platinum crucibles and analyzed at 80 °C for 5500 min.





### 3. A holistic view on the role of egg yolk in Old Masters' oil paints

*Full title:* A holistic view on the role of egg yolk in Old Masters' oil paints

*Authors:* Ophélie Ranquet, Celia Duce, Emilia Bramanti, Patrick Dietemann, Ilaria Bonaduce and Norbert Willenbacher

*Status:* published<sup>123</sup>

*Bibliographic data:* Nature Communications, **14**, 1534 (2023),  
DOI: 10.1038/s41467-023-36859-5

*The text has been adapted in this thesis to change the citation and figure numbering. Additionally, the material and method sections have been removed to avoid repetition and confirm with the other chapters.*

#### 3.1. Abstract

Old Masters like Botticelli used paints containing mixtures of oils and proteins, but “how” and “why” this was done is still not understood. Here, egg yolk is used in combination with two pigments to evaluate how different repartition of proteinaceous binder can be used to control the flow behavior as well as drying kinetics and chemistry of oil paints. Stiff paints enabling pronounced impasto can be achieved, but paint stiffening due to undesired uptake of humidity from the environment can also be suppressed, depending on proteinaceous binder distribution and colloidal paint microstructure. Brushability at high pigment loading is improved via reduction of high shear viscosity and wrinkling can be suppressed adjusting a high yield stress. Egg acts as antioxidant, slowing down the onset of curing, and promoting the formation of cross-linked networks less prone to oxidative degradation compared to oil alone, which might improve the preservation of invaluable artworks.

## 3.2. Introduction

It is usually assumed that traditional Old Masters' oil paints only contain oil as a binding medium, possibly with varying additions of some resins<sup>4-6,124</sup>. However, also proteins have been detected in oil paints by Sandro Botticelli (Figure 3.1, Supplementary Table 3.1), Leonardo da Vinci and other Italian Renaissance masters<sup>8,60</sup>, as well as in Northern oil painting, e.g. late medieval Cologne paintings, and those by Albrecht Dürer, Johannes Vermeer, Rembrandt and many others<sup>61-63,125</sup>. So far it is difficult to decide where and when egg additives to oil paints have been used, because oil paints are often not analyzed for small amounts of proteins to minimize sample size, analytical time and cost. However, the cited literature shows that such additives were identified in several centuries and countries, and they are not limited to specific pigments or layers.

What was the role of these proteins, how and why were they introduced into oil paints? The technical knowledge of the Old Masters, how paints had to be prepared, was initially passed down in workshops, but is lost today. It is known what pigments, binders and techniques were used in general, but in insufficient detail. There is clearly more to the preparation of a paint than just mixing the pigment with a binder. For example, when in the 15<sup>th</sup> century Italian artists started to turn from egg *tempera* towards adopting Northern oil painting in one of the art-historically most important technical transitions in painting, they seemed to have had some problems, as the wrinkling in an early painting by Leonardo da Vinci testifies (cf. below). This is surprising, because oil paints had been known in Italy for more than 100 years: oil paints are described in Cennino Cennini's famous treatise written c. 1400<sup>2</sup>, and oil binders have been identified in Italian 14<sup>th</sup> century paints<sup>4,6,7</sup>. However, these oil paints were usually monochrome colors applied on silver or gold leaf that did not need blending or complex paint application. Thus, oil painting seems to be more than painting with oil paints: protein additions might have been helpful to modify the oil paints' properties in a beneficial way, allowing more sophisticated paint handling.

For painting, it is essential how liquid paints can be applied, whether they can be mixed wet-in-wet or not, and how they look after drying, which includes aspects like opacity and gloss, but also wrinkling or crack formation. Thus, flow properties of paints and the drying/curing of paint layers are crucial, which are correlated both to the chemical composition, and the colloidal microstructure of the wet paint. Sandro Botticelli used both egg *tempera* and oil painting techniques in some of his paintings<sup>6,8</sup>, as in the Lamentation of Christ (Figure 3.1). Gas chromatography-mass spectrometry (GC/MS) and amino acid analysis (AAA) revealed mixtures of varying proportions of egg protein and oil in all six paint samples analyzed, most of them showing the appearance of oil paints (Supplementary Table 3.1)<sup>8</sup>, which confirms that other aspects than the exact composition are important for the classification of paints, as it was discussed for other types of paintings<sup>22</sup>.



Figure 3.1 - Sandro Botticelli, *The Lamentation of Christ*, c. 1490/95, 140 x 209,2 cm, Bavarian State Painting Collections, Inv. No. 1075. Although the flesh and some draperies are painted in egg tempera, the grass foreground and the stone tomb background are painted with oil paints containing proteins. © Bavarian State Painting Collections, Munich

But what possibilities of combining egg and oil did the Masters have, and what would have been the advantages with regard to rheology and stability of the resulting paints? Written sources such as Cennini do not describe the addition of proteinaceous materials to oil paints, but this is not surprising because the preparation of a pigment – a labor-intensive and time-consuming process – is often described in a different chapter, or not at all. The pigments, many of them deriving from minerals, had to be crushed and dispersed, cleaned and purified. There are many recipes describing the cleaning and preparation of pigments such as azurite or natural ultramarine, which sometimes involve addition of materials like glue, egg, but also polysaccharide gums or honey<sup>2,13,24</sup>. However, often these procedures are only mentioned for blue pigments and in context of painting techniques based on aqueous binders. The *Liber diversarum arcium*, presumably the most complete codification of medieval traditional oil painting, compiled c. 1300 and copied in Italy c. 1400, gives the only recipe according to our knowledge that is more explicit and directly links the addition of a proteinaceous binder to oil painting (recipe 1.3.9B)<sup>13</sup>: “[...] first grind with water and combine with three drops of glaire, and leave to dry in the sun, and once with time it is dried, repeat, and do this three or four times; afterwards temper it with oil [or] gum water, and use it.” Here we address the question whether such additions might also be useful for other pigments than the delicate and expensive blue pigments.

The cited recipe results in a protein coating of the pigments, before they are dispersed in oil, but various other systems may be formed with egg yolk or other aqueous proteinaceous solutions, drying oil and pigments, depending on paint preparation, as depicted in Figure 3.2. Small amounts of egg yolk, mixed into an oil paint with a brush directly on the palette, can result in very stiff paints.

This can be attributed to the formation of a fractal, percolating particle network induced by strong capillary forces acting in such a ternary system of solid particles and two immiscible fluids. In such systems, termed capillary suspensions, the immiscible secondary fluid phase forms pendular bridges (pendular state) or droplets incorporated into particle clusters (capillary state) which are much smaller than the suspended particles<sup>126</sup>. This sets capillary suspensions apart from emulsions where solid particles are added either to the continuous or disperse phase as well as from Pickering emulsions: in all these cases the particles are significantly smaller than the dispersed droplets<sup>127</sup>. Capillary suspensions, first described by Koos and Willenbacher<sup>126</sup>, have been observed for a wide variety of ternary solid/fluid/fluid systems<sup>128–131</sup>. If egg yolk, oil and pigments are ground together with water, an oil-in-water emulsion is formed (not depicted in Figure 3.2), which can be diluted with water. Such aqueous paints are labelled “*tempera*”, and, if oil is added the Italian term “*tempera grassa*” (i.e. fatty *tempera*) is used by technical art historians. Because *tempera* paints are significantly different from oil paints, particularly with respect to their drying behavior, they will be discussed in a subsequent paper (see chapter 4).

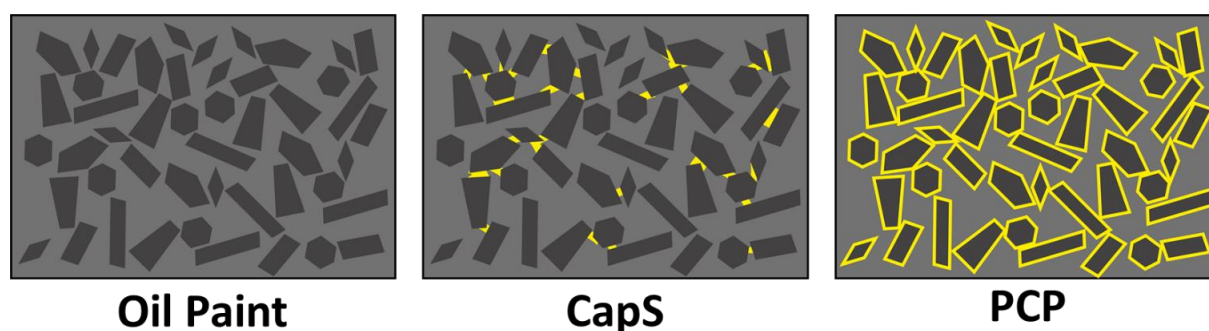


Figure 3.2 - Proposed scheme of the paint model systems' microstructure. The pigments are represented in black; the oil is in grey and the egg yolk is in yellow.

Coating of pigments with proteins was said to stabilize the pigments preventing accelerated catalytic break-down of the oil binder and subsequent discoloration<sup>63</sup>. Beyond that proteinaceous additives might have further advantages for many aspects of paint preparation, application and drying.

In this work, we report the first systematic study on the effect of adding proteinaceous materials to oil paints. For simplicity, only egg yolk is considered here. We investigated oil paints made from protein coated pigments and oil paints with a small amount of added egg yolk (capillary suspensions), to better understand Old Masters' paintings, their techniques and art historical developments. This research is seen as a proof of concept, demonstrating that such proteinaceous binders can be important additives. They can strongly influence the flow behavior of paints, i.e. their brushability and impasto, and hence the initial painting process. Egg yolk also affects the paints' drying, i.e. the complex oxidation and chemical crosslinking process. Furthermore, it can affect the chemical and physical stability of aging paints, possibly reducing wrinkling and crack formation, yellowing and darkening. This holistic view covers a wide range of different time scales

of paint handling and aging, but also different length scales: from the molecular level, which determines oxidation and cross-linking, to the mesoscopic length scale of colloidal structures, which influence both wet paint flow and drying, to the macroscopic scale, which reflects brushwork and impasto, but also wrinkling and cracking. This provides new insights which may contribute to a better conservation and preservation of invaluable artworks.

### 3.3. Results and discussion

Model paints were prepared using linseed oil (LO), a drying oil commonly used for artists' painting<sup>132</sup>, egg yolk (EY) and either lead white (LW) or ultramarine blue (UB) as pigments (see Chapter 2.1). These pigments were selected for their extensive use in the artistic field through history and because they differently affect the curing and ageing of an oil paint layer<sup>47</sup>. Synthetic ultramarine blue was used instead of the natural one, available to Italian Renaissance artists. The choice was driven by the need of ensuring a constant pigment composition, which was necessary for the preparation of large batches of paints, replicated measurements and several sets of systematic experiments that lasted about four years. It is well known that pigment shape and size distribution, exact chemical composition and pre-treatment may all affect paint rheology, drying and viscoelastic properties of dry paint layers.<sup>133,134</sup> As the focus of this work is on the effect of adding egg yolk to an oil paint, we selected two chemically very different, but readily available pigments to perform the comprehensive series of experiments and varied paint preparation only to achieve different repartition of egg yolk. The differently prepared model systems are schematically depicted in Figure 3.2:

An **oil paint** consists of a pigment which is ground with linseed oil, to form a pure suspension..

A **capillary suspension** (*CapS*) is an oil paint in which a few drops of egg yolk are added and mixed together with a palette knife. The egg yolk triggers the formation of a percolating particle network<sup>126,135</sup>, resulting in a very stiff paint.

A **protein coated pigment** (*PCP*), is prepared by first grinding the pigment with a solution of diluted egg yolk and subsequent drying. After evaporation of water, pigment particles coated with an egg yolk layer remain, and are then ground and dispersed with oil.

#### 3.3.1. Wet paint rheology

Rheological properties of paints have to be carefully adjusted to achieve the desired artistic expression. To paint impasto, i.e. with a visible, thick brushstroke, the paint must exhibit a sufficiently high yield stress preventing levelling after brush passage. Brushability, i.e. the force required to apply a paint layer, and the resulting layer thickness, are related to the high shear viscosity. These parameters can be easily changed by varying the pigment content<sup>30</sup>. Below we

will discuss the complex effects of added egg yolk on these features depending on paint composition and preparation. Our first focus will be on impasto and yield stress, which is the critical stress required to break up the paint structure and enable flow. Yield stress determination and brush stroke analysis are described in the Materials and methods section (2.3.2).

Paint formulations of identical solids volume fractions  $\phi$  (including the pigment and in case of PCP also the egg yolk dry matter volume) were compared with respect to the brush profiles and roughness of dry paint layers obtained from automatically applied brush strokes (Figure 3.3).

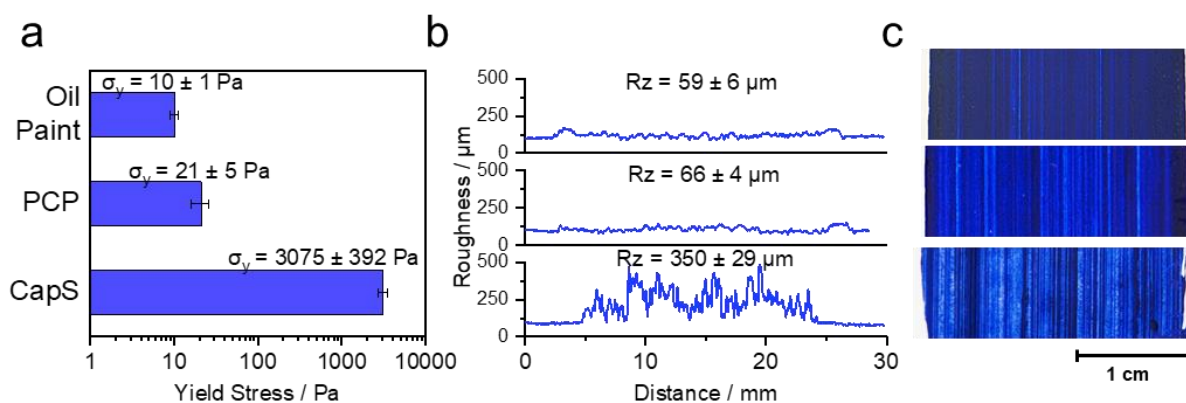


Figure 3.3 - Wet paint yield stress and brush stroke profile. Ultramarine paints, relationship between **a** yield stress  $\sigma_y$ , **b** roughness  $R_z$  and profile of the paint brush strokes and **c** appearance of the paint layer. The paints were prepared at a solid fraction of  $\phi = 32$  vol%, including 2 vol% of egg yolk solids for the paints containing proteins. The error interval denotes the standard deviation calculated from measurements performed at least in triplicate. PCP stands for protein coated pigment paint and CapS for capillary suspension paint.

The two pure suspension paint models (oil paint and PCP) showed similar, very regular paint profiles with low roughness  $R_z$  ( $< 100 \mu\text{m}$ ) in accordance with their low yield stress values ( $\sigma_y \approx 10$ – $20$  Pa) at a solids content of  $\phi = 32$  vol%. The addition of 2 vol% of egg yolk as a coating of the UB pigment surface did not significantly modify the impasto. Yield stress data not only inform us about brushstrokes or impasto. They also provide valuable insight into the interactions among suspended particles and the strength and microstructure of the corresponding particle network<sup>136–139</sup>. The addition of the same volumetric amount of pure egg yolk into the oil paint as a secondary liquid phase leads to a strong increase of the yield stress ( $\sigma_y \approx 3,000$  Pa). We attribute this to the formation of a percolating particle network induced by capillary forces inferred by the addition of a second, immiscible fluid phase, a generic phenomenon recently discovered and confirmed for a broad variety of colloidal systems<sup>126,131,135</sup>. Thus, levelling is prevented and the brush stroke profile exhibits strong fluctuation, i.e. the brushstroke is preserved with the CapS paint and this is a direct consequence of its orders of magnitude higher yield stress compared to the oil and PCP paints. Note, the capillary particle network is destroyed at high shear stresses  $\sigma \gg \sigma_y$  and hence the high shear viscosity of the suspension is the same as for the corresponding binary suspension<sup>135</sup>, therefore the artist can apply the paint as easily despite the higher yield stress.



The presence of egg yolk (in PCP paints), has distinctly different effects on yield stress, depending on the pigment type. The yield stress increases in UB oil paints when the pigment particles are coated with egg, while it decreases in LW oil paints. Moreover, when increasing the amount of egg yolk in UB based PCPs (Figure 3.4a) the yield stress increases, but it does not significantly vary with EY content for LW based PCPs (Figure 3.4b). This different behavior can be rationalized assuming the egg layer essentially remains on the pigment (see Figure 3.2 and Figure 2.8) also after dispersion in the oil since proteins are not oil soluble. Untreated, both pigments are very well wetted by the linseed oil ( $\Theta_{\text{UB or LW-LO}} = 9 \pm 2^\circ$ ), but the hydrophilic egg yolk coating leads to a significant increase in contact angle ( $\Theta_{\text{EY-LO}} = 38 \pm 7^\circ$ ), see Supplementary Table 3.2. For the UB-based paint, this results in an additional steric attraction<sup>140</sup> among particles, due to the hydrophilic surface layers attempting to minimize the contact with oil molecules (Figure 3.4c). Accordingly, the strength of the particle network, and hence the yield stress increases. Note, the hydrophilic character of the coating layer is decisive. A hydrophobic layer would act as a dispersing agent providing repulsive interaction leading to a reduction or complete elimination of the yield stress<sup>127,140</sup>. We are aware that a 2  $\mu\text{m}$  protein layer on a pigment with 2  $\mu\text{m}$  diameter is not a real artist paint, but such model systems are helpful to gain insight into the colloid-physical phenomena relevant for oil paints.

For the LW pigments another phenomenon prevails: the uptake of water from the ambient environment. Since external conditions (temperature, relative humidity) vary with the time of the day, the season and the geographical location, this challenges artists' paint preparation and egg yolk may modify the effect of water adsorbed during pigment storage or paint application. We attribute the high yield stress of the LW oil paint to the formation of a CapS due to humidity uptake from the environment and we hypothesize, that the lower yield stress of the PCP is due to a uniform distribution of the absorbed water in the hydrophilic EY layer preventing the formation of CapS. Obviously, a 0.2  $\mu\text{m}$  EY layer is sufficient to suppress this phenomenon. To further confirm this, the effect of humidity on paint yield stress was studied systematically.

Both pigments took up about the same amount of water when stored under controlled conditions of humidity and temperature (two weeks at relative humidity RH% of < 1 %, 50 % and 76%, and temperature  $T = 20^\circ\text{C}$ , for comparison the pigments used to determine the oil paint data shown in Figure 3.4a-b were stored at a relative humidity fluctuating around 50%) prior to preparation of the oil paints (see in Materials and methods, Figure 2.11). The effect on yield stress, however, is very different. For the UB pigment, water uptake does not affect the paint's yield stress (Figure 3.4d). In contrast, this quantity increases by almost two orders of magnitude for LW-based oil paints with an uptake of only 0.6 wt.% water when stored at 76 RH% (Figure 3.4e). Again, we attribute this to the formation of capillary suspensions similar as previously observed for other suspensions made from particles exposed to humid environment<sup>131</sup>. When exposed to the oil phase, the water on the particle surface creeps into the contact areas among adjacent particles and forms capillary bridge (Figure 3.4f). This is obviously not the case for the oil paint made with UB pigment: in this case

there seems to be no gain in free energy upon such a redistribution of water molecules. The phenomenon is further confirmed by adding 2 vol% of water as a secondary fluid to a  $\phi = 18$  vol% solids fraction LW oil paint, prepared with a previously dried pigment. Again, a capillary suspension with a yield stress two orders of magnitude higher than that of the corresponding oil paint is built (Figure 3.4g). However, this phenomenon which may greatly disturb paint preparation in an artist's workshop can be suppressed when the pigment surface is coated by a thin layer ( $\approx 0.2 \mu\text{m}$ ) of proteinaceous material, e.g. egg yolk. In this case, the yield stress of the resulting PCP paint does not change significantly when adding the same amount of water. A capillary suspension does not form, presumably because the added water is uniformly distributed in the hydrophilic EY surface layer (Figure 3.4g and i). Note, the pigments used to determine the oil paint data shown in Figure 3.4a-b, were stored at a relative humidity fluctuating around 50%, and the corresponding yield stress data agree fairly well with those obtained using pigments stored at a controlled humidity of 40% for two weeks (Figure 3.4d-e).

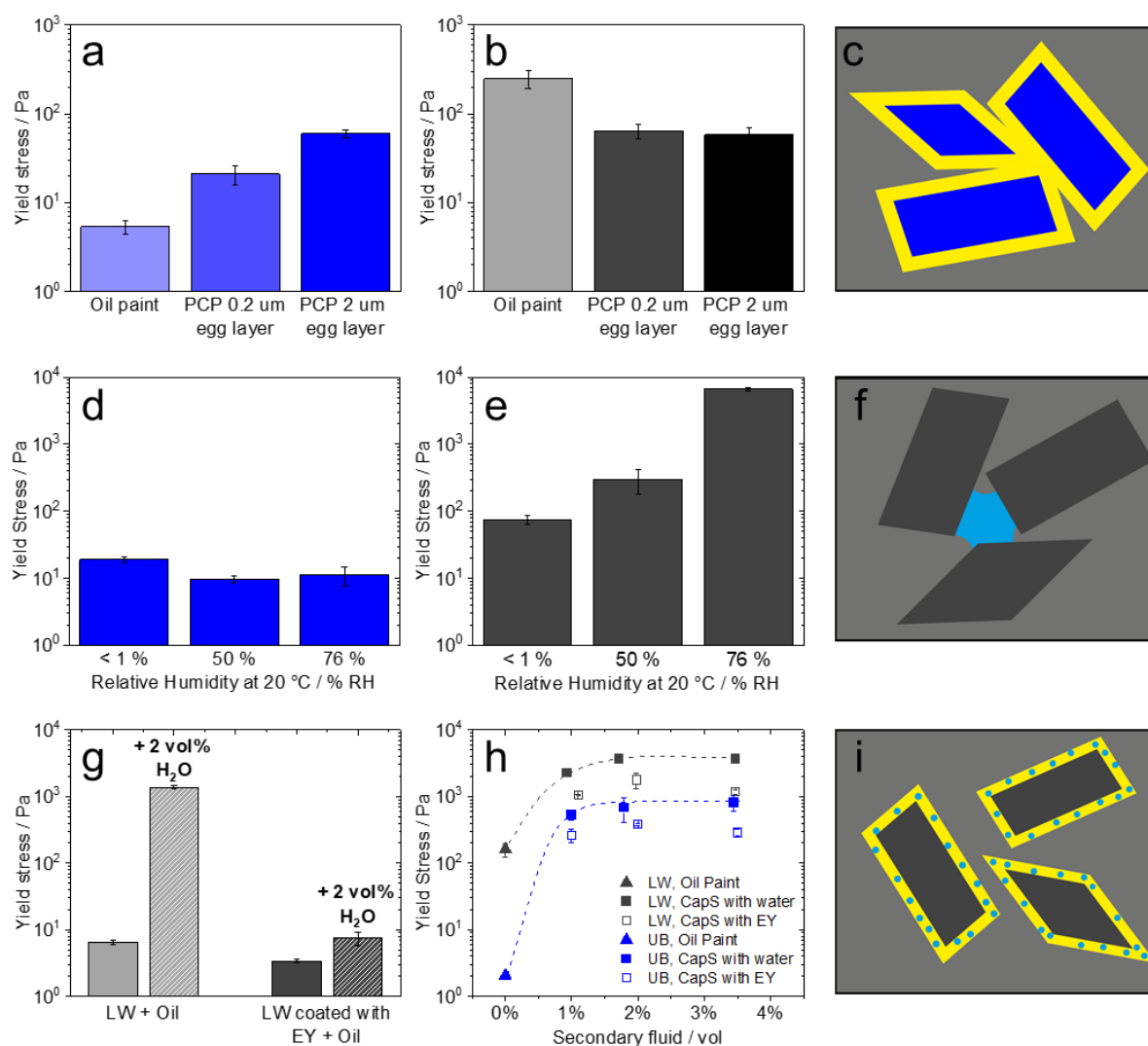


Figure 3.4 - Influence of proteinaceous coating and humidity on yield stress and microstructure. Ultramarine blue (UB) paints are displayed in blue, and lead white (LW) paints in black. **a** and **b**: yield stresses of paints prepared at a solids fraction of  $\phi = 32$  vol% with or without an egg yolk (EY) coating, dispersed in linseed oil. The pigments



were stored at a relative humidity of  $\approx 50$  RH% prior to be dispersed in oil. The thickness of the EY layer was calculated from the EY dry matter used to prepare the protein coated pigments (PCP) assuming ideal monodisperse spherical particles and was included when calculating  $\phi$  for the PCP paints. **c** representation of the steric attraction among pigment particles (in blue) due to the hydrophilic surface layers (in yellow), attempting to minimize the contact with oil molecules (in grey). **d** and **e**: yield stress of oil paints  $\phi = 32$  vol% prepared after a pigment storage of 2 weeks in humidity-controlled atmospheres prior to dispersion in oil. **f** representation of the formation of capillary bridges between pigment particles (in grey) due to humidity (water in cyan). **g** yield stress of LW oil paint  $\phi = 18$  vol% without (grey) and with EY coating (black), before and after addition of water as secondary fluid. **h** yield stress of LW (black) and UB (blue) suspensions (triangle) and capillary suspensions prepared with EY (hollow square) or water (full square) as a secondary fluid, all prepared at a solid fraction of  $\phi = 32$  vol%. **i** uniform distribution of water (in cyan) in the hydrophilic EY surface layer (yellow). The error interval denotes the standard deviation calculated from measurements performed at least in triplicate.

It is interesting to point out that *capillary suspension* paints can be formed if a sufficient amount of secondary fluid (either pure water, fresh EY, or another proteinaceous solution not miscible with the oil) is added to an oil paint, irrespective of the chemical structure and surface properties of the pigment. This phenomenon allows the yield stress to be varied over a wide range covering about three orders of magnitude (Figure 3.4h). Samples containing fresh egg yolk exhibit slightly lower yield stress values than the ones containing pure water. This is attributed to the amphiphilic low-density lipoprotein complexes (LDLs) lowering the surface tension of the yolk compared to pure water, thus weakening the strength of the capillary particle network<sup>105,107,141</sup>. In fact, the interfacial tension between oil and water ( $\Gamma_{\text{LO-H}_2\text{O}} \approx 11$  mN/m) is higher than that between oil and EY ( $\Gamma_{\text{LO-EY}} \approx 2$  mN/m), see Supplementary Table 3.3. The higher yield stress level of the LW CapS compared to the UB CapS is due to the larger fraction of fine particles in the LW samples<sup>135</sup> (see in Materials and methods, Figure 2.2 and Figure 2.5).

In conclusion, the addition of egg yolk can have a strong impact on yielding of oil paints depending on the paint preparation procedure. A dry proteinaceous layer covering the pigment surface results in an attractive steric interaction among pigment particles which then leads to an increase in yield stress. Pigments can take up water during storage or paint preparation depending on humidity conditions, but water is also introduced when egg yolk is added to an oil paint. Then so-called capillary suspensions with their distinct percolating fractal particle network can form, resulting in very stiff paints. The yield stress can vary in a wide range depending on the amount of added secondary liquid and controlled by the wetting behavior of the aqueous phase in the ternary system, i.e. on its three-phase contact angle on the pigment surface and its interfacial tension with the oil phase. When the pigment particles, however, are coated with a hydrophilic proteinaceous layer, the water uniformly distributes in that layer and a capillary suspension does not form, leaving the yield stress unchanged.

In past centuries, artists may not have been able to control the humidity taken up by their pigments. In case the paint was too stiff, they presumably added more oil. However, if too much oil is added, binder-related problems arise, such as stronger discoloring (attributable to a more visible yellowing of the binder) and darkening (fatty acids released from ageing oil tend to react with lead white, forming metal soaps, which results more transparent paint layers), but also crack formation and even worse, wrinkling, a problem even Leonardo da Vinci encountered (see discussion below).

Adding some proteinaceous material during pigment preparation, resulting in a coating layer, might have solved the problem of unintentional formation of capillary suspensions, resulting in better, more stable paints with higher pigment content. This surface treatment not only prevents the formation of capillary suspensions but also leads to a reduced increase of high shear viscosity with increasing solids content and hence allows for better brushability at high pigment loading (Supplementary Figure 3.11 and Figure 3.12).

### 3.3.2. *From wet paints to solid films*

Several complex mechanisms may control film formation. Egg proteins are commonly employed to form films and coatings in various products such as food or pharmaceuticals<sup>107,142</sup>. Evaporation of solvent in protein-based paints results in dry films.

The drying of an oil paint layer is a chemically driven process, which entails the oxidation and cross-linking of the constituting polyunsaturated triglycerides (curing). As the curing reactions progress, the oil gradually becomes viscous, tacky and finally dry to the touch, which is a process that may take from hours to several days (Supplementary Figure 3.13), allowing the artists to work on the impasto, mix the paints on the palette and work with wet-in-wet technique. Drying might be influenced by several factors<sup>17,47,48</sup>, such as the environmental conditions (light, temperature, humidity) and the intrinsic properties of the film such as its chemical composition (binder and pigment) and the layer thickness<sup>49,50</sup>.

We investigated how the natural air-drying of linseed oil paints is affected by the egg addition. In the curing of a drying oil, upon exposure to air, oxygen is added, with consequent formation of peroxide species, initiating the curing reactions<sup>48,143,144</sup>. Peroxide species may be detected and estimated with differential scanning calorimetry (DSC) and thermal gravimetry (TGA).

In a DSC experiment a sample collected from a paint layer is progressively heated under inert atmosphere, and in the temperature range 75-200 °C, an exothermic peak is observed, which is due to two main thermal effects. The first, endothermic, consists of the decomposition of hydroperoxides and peroxides formed by the action of oxygen on the triglycerides. The second, exothermic, is related to the recombination of radical species, both deriving from the decomposition of the same peroxides and hydroperoxides, and those formed upon the curing process. The area of the overall peak is proportional to the amount of peroxides and active radical species present in the paint at the moment of the experiment<sup>47</sup>. DSC curves are shown in Figure 3.5a, Supplementary Figure 3.14 and Figure 3.15.

In a TGA experiment we observe a mass loss in the temperature range corresponding to the DSC peak, due to the thermal decomposition of peroxide species and indicating the mass% of peroxide species present in the paint layer.

The formation of peroxides is also visible by monitoring the mass change of a paint layer over time. In particular, upon curing a mass increase is observed due to the addition of oxygen, with formation of peroxides. With time, other reactions follow, some of which may lead to the formation of small molecular weight species, which may evaporate from the paint film, leading to a mass decrease. We compared the gravimetric mass increase (wt%) with the quantity of peroxide decomposition (in wt%, deduced from TGA data)<sup>145</sup>, all normalized to the oil content. We could detect the presence of active radical species in linseed oil samples right before the onset of mass uptake of the macroscopic samples, see Supplementary Figure 3.13.

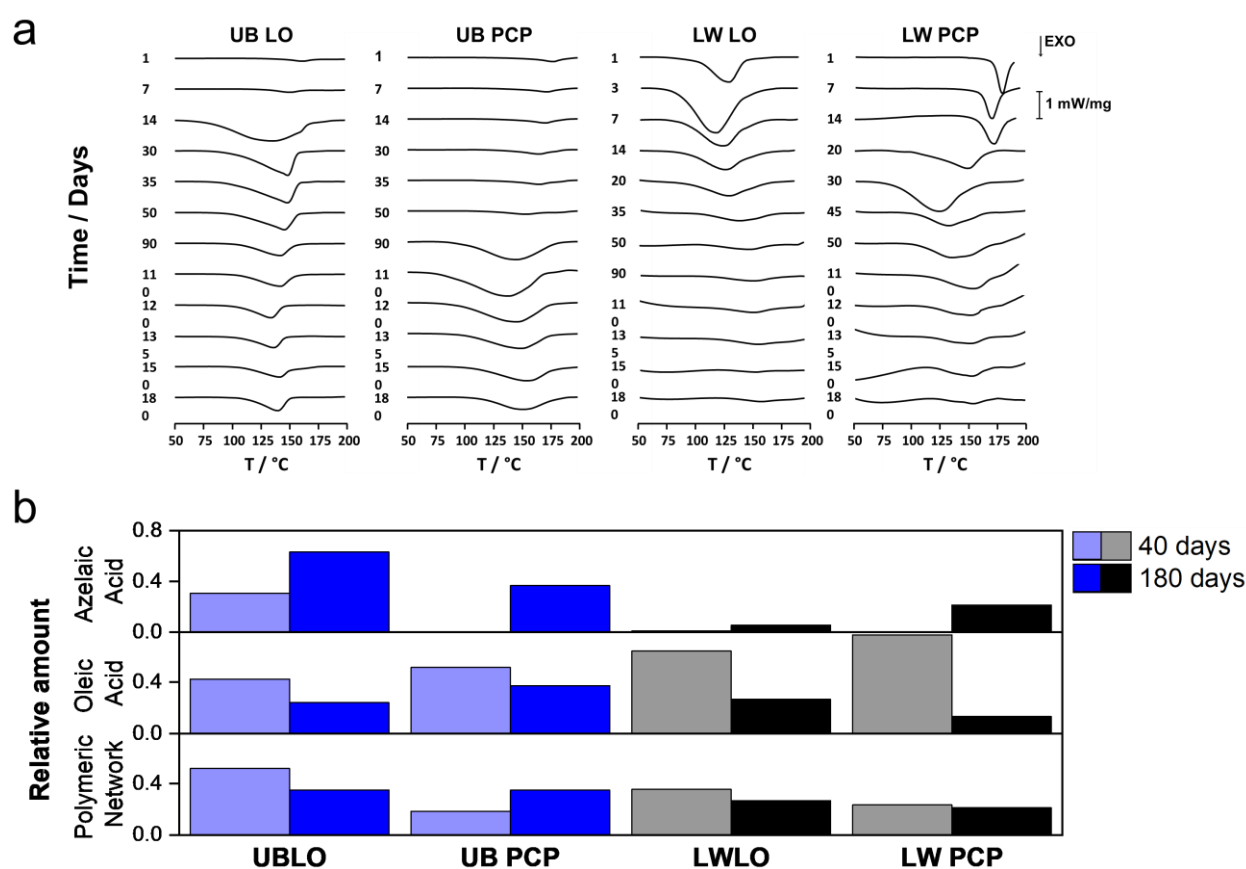


Figure 3.5 - Curing of oil paint layers. DSC curves **a** and relative amount Py/GC/MS extracted ion pyrograms **b** of ultramarine blue (UB) and lead white (LW) model paints up to 180 days of natural ageing. Solids content of UB LO, UB PCP, LW LO, LW PCP are  $\varphi = 6, 33, 31$  and  $29$  vol% respectively, including  $12$  vol% (UB PCP) and  $15$  vol% (LW PCP) of EY. **b** shows the evolution of the oil polymeric network ( $m/z$  129), the azelaic acid ( $m/z$  317) and the oleic acid ( $m/z$  339) of the different formulations at the same curing time. All DSC curves are normalized to the oil content and all the relative amount of the pyrolysis products to the palmitic acid peak  $m/z$  313. PCP stands for protein coated pigment paint and LO for oil paint.

Simultaneously, we measured the hardness of the paint surface at regular time intervals pushing a cylindrical piston into the layer at constant speed and depth, imitating the dipping of a finger into the paint. When the paint is still liquid, the hardness of the paint remains low ( $< 0.01$  N/mm<sup>2</sup>), but this value increases up to two decades upon film formation and approaches a plateau, which

characterizes the “dry-to-touch” state of the paint film when a solid film is formed. The mechanically determined “dry-to-touch” transition clearly corresponds to the steep increase of the sample mass indicating the onset of oxidation and chemical drying (Figure 3.6a). This has been suspected earlier, but quantitative mechanical data were lacking<sup>143</sup>.

The addition of pigments into raw linseed oil speeds up its drying kinetics: when a 0.4 mm thick layer of raw linseed oil takes up to 70 days to dry, this time is reduced to 20 and 4 days for paints including 32 vol% of UB and LW pigments (but no egg yolk), respectively (Figure 3.6b). Indeed, LW acts as a catalyst for curing reactions and thus allows for shorter drying times compared to the UB paints<sup>40,47</sup>.

When adding increasing amounts of EY as pigment coating, we observe a delay in the curing reactions and drying time (Figure 3.6b). This is also evident from the DSC (Figure 3.5a and Supplementary Figure 3.14), TGA (Supplementary Figure 3.13) and gravimetric data both at natural (Figure 3.5a and Figure 3.6c-d) and accelerated ageing at 80°C (Supplementary Figure 3.20). This can be ascribed to the antioxidant properties of egg yolk, which are exerted by phospholipids, representing 10 wt% of the yolk dry content, phosvitin, proteins and free aromatic amino acids, tending to inhibit oxidation of lipids by different mechanisms<sup>146</sup>. Moreover egg yolk contains carotenoids and vitamin E, which are lipophilic compounds preventing lipid per-oxidation by either radical transfer or by stabilization of peroxy radicals<sup>146</sup>. Such stabilization of peroxy radicals is also well evident from the onset temperature of the DSC peroxide decomposition/radical recombination peak. Supplementary Figure 3.16 and Figure 3.17 and Supplementary Table 3.4 show that the presence of egg shifts the onset temperature during the first days of natural aging especially for the PCP paints with their high EY content. With time, the onset temperature of the peak tends to reach the same value for all systems (Supplementary Figure 3.16), possibly because upon hardening of the paint layer, the reaction pathways might be more strongly affected by the mobility and chemical reactivity of active species present in the oil phase, away from the oil/pigment and oil/protein interfaces.

For UB-based paints, the latency time of drying is the same for CapS and PCP containing the same amount of EY solids (Figure 3.6c): the antioxidant effect of egg is exerted irrespective of the protein repartition in the microstructure of the UB paints. For the LW paints, however, the EY distribution has a significant impact: when EY is restricted to the small contact regions between adjacent particles in the capillary suspension paints, the drying time is close to that of the oil paint, in LW PCP paints, however, the drying time is longer (Figure 3.6d). If the assumption that the protein coating does not change with drying and curing is correct, this difference observed in the UB and LW paints may be explained by the fact that the catalytic effect of LW is exerted upon the dissolution of lead into the oil<sup>147</sup>. In CapS, most of the pigment particle surface is in direct contact to the oil phase, making it possible for the lead to dissolve into the oil and catalyze the curing reactions. As a result, LWLO and LW CapS behave very similarly from the curing kinetics point of view. In PCP the EY is evenly distributed on the pigment surface, serving as an “antioxidant shield”, delaying the

dissolution of lead into the oil, and possibly affecting the products of reaction between the metal and the binders. This feature has been used earlier to prevent the lipid peroxidation of linseed oil in o/w emulsions<sup>148</sup>. PCP-type LW paints, however, are faster to start the curing process than UB ones, but the differences tend to disappear when large amounts of egg yolk are added (Figure 3.6b). Our data show that CapS takes up less oxygen than PCP at given egg yolk content. As the interfaces oil/protein/pigment are different in the two systems we may expect a change in the oxidative reaction pathways and kinetics.

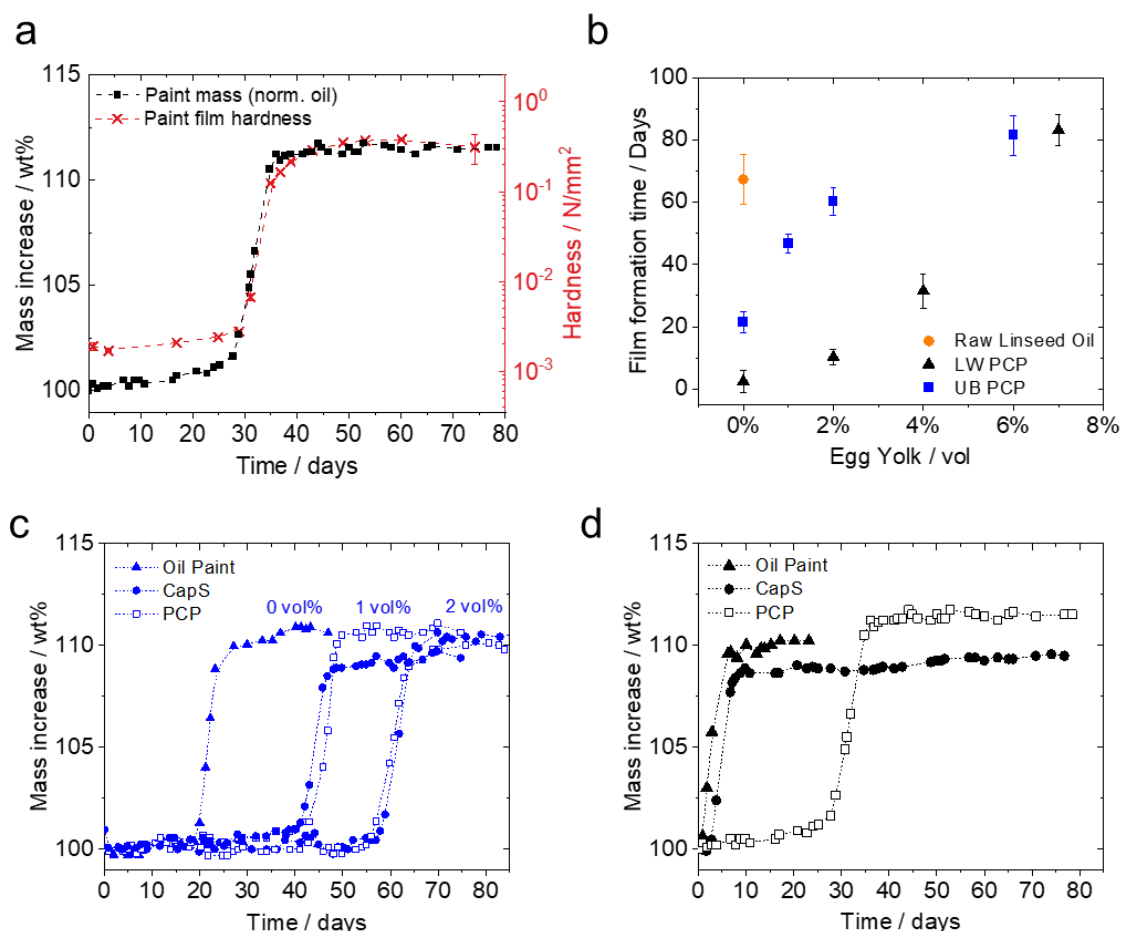


Figure 3.6 - Curing kinetics and film formation of oil paints. **a** Displays the comparison between the mass uptake (black square) of a protein coated paint film (LW PCP at 4 vol% of EY), normalized to its oil content, over time and the corresponding change in mechanical hardness (red cross). The error interval denotes the standard deviation calculated from measurements performed at least in triplicate. **b** Film formation time (the time at which the paint has reached its maximum weight change) vs. egg yolk content for PCP type paints; error bars represent the interval between the start and the maximum of the weight increase. **c** and **d**: Mass increase, normalized to the oil content, of UB (blue) or LW (black) paint samples prepared as oil paints (triangle), capillary suspension CapS (circle) or PCP (square) paints as a function of time. **c** UB CapS and PCP paints contain 1 and 2 vol% of EY solids. **d** LW CapS and PCP paints contain 4 vol% of EY solids. All studied paints contained a solids fraction (pigment and EY solids) of  $\phi = 32$  vol%.

The delay in the onset of the oil curing observed when EY is added, and the higher stability of peroxides produced, entails a delay in the formation of oxidation products of the oil as well as the oil polymeric network. This shows up in the analysis of oil paint films at different stages of curing by analytical pyrolysis coupled with GC/MS (Py/GC/MS) (Figure 3.5b and Supplementary Figure

3.18 and Figure 3.19). At 40 days, oil paint layers already show an extensively cross-linked oil network, a relatively high content of azelaic acid (stable product of oxidation), but the unsaturated oleic acid is still present, indicating the curing is not complete. With ageing, the amount of azelaic acid increases, and that of oleic acid decreases, furthermore the relative content of the polymeric network slightly decreases with time, due to oxidative degradation phenomena, as reported previously<sup>47</sup>. In PCP-type UB paints at 40 days the relative content of the polymeric network is very small, and increases steadily with time. On the other hand, and in agreement with the catalytic activity of LW, in LW PCP the cross-linked network is well present at 40 days and appears very stable over time. Concurrently the relative content of azelaic acid increases with time and that of oleic acid decreases. The data available at this stage seem to indicate that when egg is present oxidative degradation occurs to a smaller extent. TG experiments under accelerated conditions at 80°C confirm that egg preserves the oil paint from oxidative degradation: the mass loss is small also after several hours of accelerated curing in UB PCP and LW PCP compared to UBLO and LWLO (Supplementary Figure 3.20).

The addition of egg thus seems to favor the formation of a well cross-linked network. This might be due to the known reactivity between lipid oxidation products and proteins<sup>74–76</sup>, which may cause polymeric network modifications in the paint<sup>77</sup> and co-polymerization<sup>78</sup>. Indeed, egg proteins respond to the chemical environment generated by the oxidizing lipids in a paint layer as shown with secondary structure analysis of the protein component in PCP systems by peak fitting of the amide I band of TRANS-FTIR spectra<sup>121</sup>. CapS were not studied with this technique as the amount of added EY is below the detection limit. Previous research on model systems based on combinations of different pigments and proteinaceous materials showed that proteins undergo structural modifications which depend on the nature of the pigment and the age of the paint layer<sup>73</sup>. Our results here show that the relative content of beta structures, helix and random coils of proteins in PCP systems is subject to significant changes in correspondence to the maximum of the mass increase upon curing (Supplementary Figure 3.21), when the concentration of peroxide species is very high (Supplementary Figure 3.13).

The experiments on the drying/curing of the paint layers stressed out that formulations containing EY presented longer drying times compared to oil paints. These particularly long drying periods are unrealistic for artists' paintings, and inconvenient, but may be overcome by applying other well-known remedies, such as drying agents, or heat treatment of the oil<sup>2,40</sup>. On the other hand, the addition of proteinaceous materials seems to produce well cross-linked polymeric fractions, less prone to oxidative degradation, which may lead to conservation issues<sup>48</sup>.

### 3.3.3. Wrinkling

Wrinkling may occur during the transition from the wet paint to the dry layer, and may deteriorate the quality and appearance of a painting. Wrinkling occurs rather quickly, such within days, and thus areas were usually removed and improved by artists. As a result, examples of paintings showing wrinkling are rare. One of them is Leonardo da Vinci's *Madonna of the Carnation*, c. 1475, which shows extensive wrinkling on the flesh of Mary (Figure 3.7a and Supplementary Figure 3.23).

When linseed oil cures, a film may form at its surface due to a gradient of oxygen distribution in the paint layer, resulting in an uneven drying between the surface and its bulk. Because oxidation results in a volume increase of the oil, the surface area can be enlarged by wrinkling, as long as the oil below the dried skin is still liquid. This effect depends on the difference of film formation rate between the surface and the deeper layers<sup>38</sup>, which is especially strong if oils with very high drying rates are used, such as tung oil or linseed oil with too much added catalytic drier<sup>149,150</sup>, or they are applied in too thick layers<sup>38</sup> (see also Supplementary Figure 3.24). It is also well known that wrinkling is more likely to occur in paints containing too few pigments<sup>40</sup>. Increasing the solids fraction in oil paints thus prevents the formation of wrinkles (Supplementary Figure 3.25). The phenomenon is, however, not simply related to pigment loading.

Wrinkling of oil paints may also be avoided adding egg to the paint formulation. In Figure 3.7b, the oil paint with 32 vol% solids content exhibits similar wrinkling as the CapS with only 16 vol% particle loading adjusted to the same yield stress level ( $\approx 58\text{-}75$  Pa) adding 2 vol% EY. However, wrinkling can be suppressed when the mobility of the paint below the dry skin is drastically reduced as shown here for the oil paint with 32 vol% solids with 4 vol% EY added, thus increasing the yield stress to  $\sigma_y \approx 3,200$  Pa. The wrinkling phenomenon is tightly related to the paints' yield stress and can be strongly reduced by thoughtfully adjusting this material property. Moreover, adding egg yolk to oil paints is a skillful method to achieve this, especially when a high pigment loading is to be avoided, e.g. for reasons of artistic expression. This new insight may encourage further targeted investigations regarding the composition of paint layers with and without wrinkles.

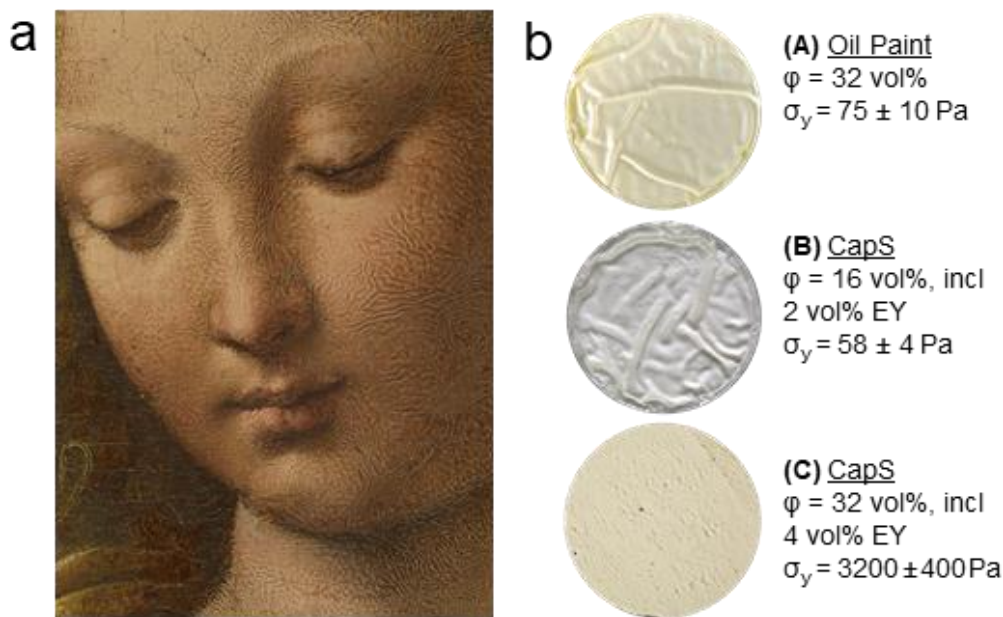


Figure 3.7 - Wrinkling and yield stress of paints. **a** Detail of Mary's face displaying wrinkling of the flesh paint in Leonardo da Vinci's *Madonna of the Carnation*, c. 1475, Inv. No. 7779, 62 x 48,5 cm, © Bavarian State Painting Collections, Munich, the whole painting is shown in Supplementary Figure 3.23. **b** Photographs of LW paint surface structures after film formation (thickness = 1.0 mm) depending on pigment content  $\phi$  and yield stress  $\sigma_y$ . CapS denotes capillary suspension and EY denotes egg yolk.

### 3.4. Conclusion

This holistic study combines knowledge from conservation science, rheology and analytical chemistry to understand in which various ways Old Masters like Botticelli, da Vinci or Rembrandt might have used proteinaceous binders to modify oil paints to create their artworks. Exemplarily using two major pigments employed for painting during many centuries, lead white and ultramarine blue, we discuss various ways to produce different microstructures (protein-coated pigments vs. capillary suspensions) and how this can be used to control the flow behavior of paints, as well as their drying kinetics and mechanisms according to the artist's requirements. It was shown how artists might have used proteinaceous materials to influence impasto of their fresh oil paints, to overcome unexpected problems with humidity, produce paint layers stable against wrinkling and oxidative degradation, giving us the opportunity to admire their masterpieces still today.



### 3.5. Acknowledgments

This research was supported by the Consorzio Interuniversitario Nazionale per la Scienza e Tecnologia dei Materiali (INSTM), the German Academic Exchange Service France (DAAD), and the KIT Campus Transfer GmbH (KCT). The experiments were performed in part at the Karlsruhe Institute of Technology (KIT) in Germany and at the University of Pisa in Italy. We thank H. Telle Jiménez (KIT) for the realization of the contact angle and interfacial tension experiments, R. Carosi (University of Pisa) for the support and the realization of thermal analyses, E. Cantisani (ICVBC, CNR in Florence) for the realization of XRD analyses and Dr. L. Bernazzani (University of Pisa) for helpful discussion.

### 3.6. Competing interests

The authors declare no competing interests.

### 3.7. Supplementary information

#### 3.7.1. Egg yolk and oil in a historic artwork

#### Sandro Botticelli's Lamentation of Christ

Table 3.1 - Results of binding media analyses of Sandro Botticelli's Lamentation of Christ, Bavarian State Painting Collections, Inv. No. 1075, published in Diemann et al. 2017.<sup>8</sup> For sample positions A and B cf. Figure 3.8. The classification of paints into oil and tempera has been performed by an interdisciplinary team of conservators and scientists mainly based on the appearance of the paints, which include optical and rheological aspects (cf. Figure 3.9 and Figure 3.10.) as well as knowledge from sources and chemical analysis. +++ large quantity, ++ intermediate quantity, + small quantity, (+) very small amount.

Area	Paint layer	Classification	Oil (GC/MS)	Protein (AAA)	Contaminations from varnish
A: Green meadow on red dress of mourner on the right	Light green grass	Oil	++	(+)	
	Yellow-green grass	Oil	++	++	
	Dark green background of grass	Oil	+++	+	Linseed oil, dammar, mastic, copaiba balsam
	Red from dress, with white highlight layers	Egg <i>tempera</i>	+++	+++	
B: Stone of tomb	Dark grey paint of shadow	Oil	++	++	Dammar, mastic, Strasbourg turpentine, copaiba balsam, beeswax, linseed oil
	Light brownish paint of stone	Probably oil	+++	++	



Figure 3.8 - Sandro Botticelli, the Lamentation of Christ, with indication of sampling positions for binding medium analyses reported in Table 3.1, and details displayed in Figure 3.9 and Figure 3.10. © Bavarian State Painting Collections, Munich.



Figure 3.9 – The flesh, details of Christ's head (left) and St. John's feet (right) show the typical egg tempera layer build-up and paint application by hatching. In contrast, the grass foreground (including the dark green (almost black) paint layer) shows typical properties of oil paints. Pictures: © Wibke Neugebauer, Munich.



Figure 3.10 – Two details of the stone background of the tomb in Botticelli's Lamentation of Christ show wet-in-wet mixing of paints, typical for oil painting, which allows a fast and efficient painting process, creating varying, vivid surface impressions of stone in one painting step. Pictures: © Wibke Neugebauer, Munich.

### 3.7.2. Results

Table 3.2 - Contact angle measurements according to ISO 19403-2:2017

Contact angle / °	Dried EY	Lead White	Ultramarine Blue
Linseed Oil	38 ± 7	9 ± 1	9 ± 2
Water	29 ± 7	84 ± 3	55 ± 6

Table 3.3 - Interfacial tension measurements according to ISO 19403-3:2017

Interfacial tension / mN/m	Water	Liquid EY
Linseed Oil	10.8 ± 0.7	1.9 ± 0.3

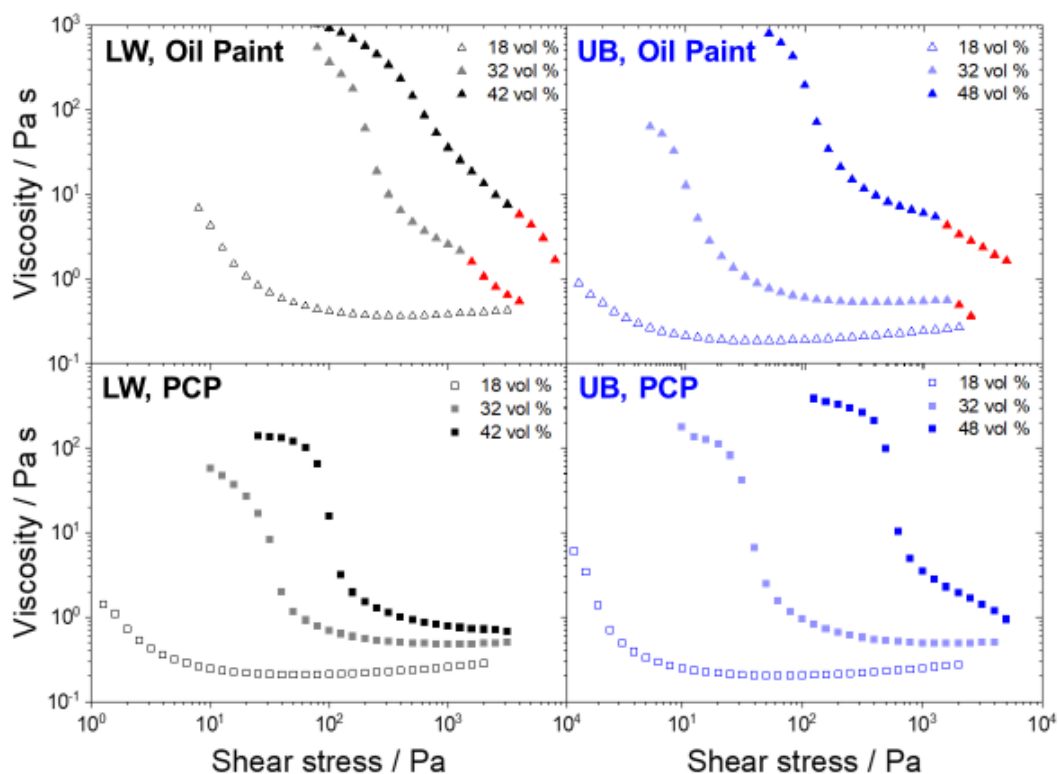


Figure 3.11 - Viscosity measurements as a function of the shear stress of lead white LW (black) and ultramarine blue UB (blue) oil paints (▲) and pigment coated paints PCP (■) at different solids content. In red are displayed the values obtained due to the spillage of the paint in plate-plate geometry.

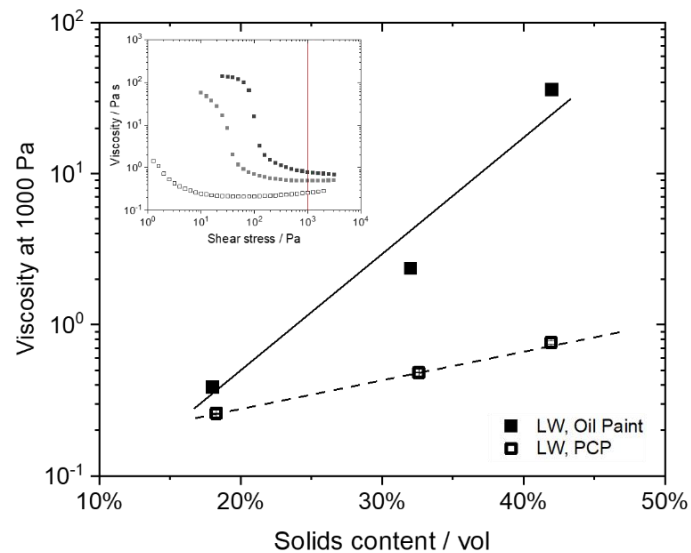


Figure 3.12 - Viscosity measurements at 1000 Pa of LW oil paints (■) and LW PCP (□) as a function of the solids content. Coating the pigment with an egg yolk layer reduces the viscosity of LW paints at high shear, hence allows for better brushability at high pigment loading. Similar results were obtained for ultramarine blue pigment paints (data not shown).

We measured the viscosity at high shear stresses well above the yield stress of paints with increasing solids content, prepared with or without pigment coating. The viscosity measurements of paints prepared with the raw pigments dispersed in the oil showed spillage at high shear stresses (red symbols in Figure 3.11). When the pigments are coated with egg yolk, the high shear regime is accessible and the data show that the increase in high shear viscosity is much less pronounced for the PCP systems than for the oil paints (Figure 3.12).

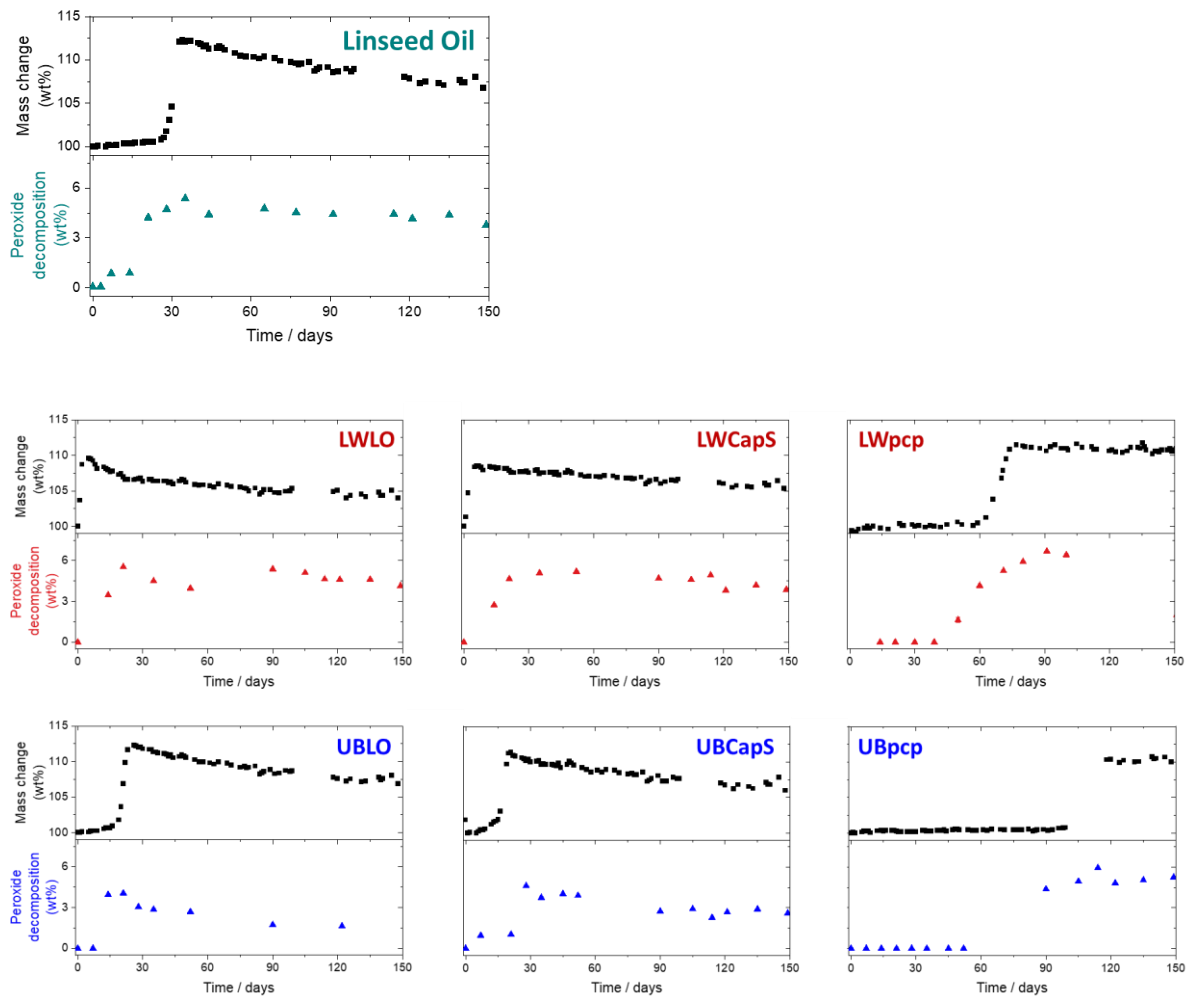


Figure 3.13 - Comparison of the mass increase of linseed oil-based samples (above) and the associated peroxide decomposition performed by TGA measurements (below, at  $T = 135\text{-}180\text{ }^{\circ}\text{C}$  depending on the paint composition), all normalized to the oil content. Solids content of LW LO and LW PCP are  $\varphi = 31$  and  $29\text{ vol}\%$  respectively, including  $15\text{ vol}\%$  (PCP) of EY. Solids content of UB LO and UB PCP are  $\varphi = 6$  and  $16\text{ vol}\%$  respectively, including  $12\text{ vol}\%$  (PCP) of EY. Solids content of LW CapS and UB CapS are  $\varphi = 31$  and  $33\text{ vol}\%$  respectively, including  $2\text{ (LW)}$  and  $3\text{ vol}\%$  (UB) of EY. PCP stands for protein coated pigment paint, CapS for capillary suspension paint and LO for oil paint.

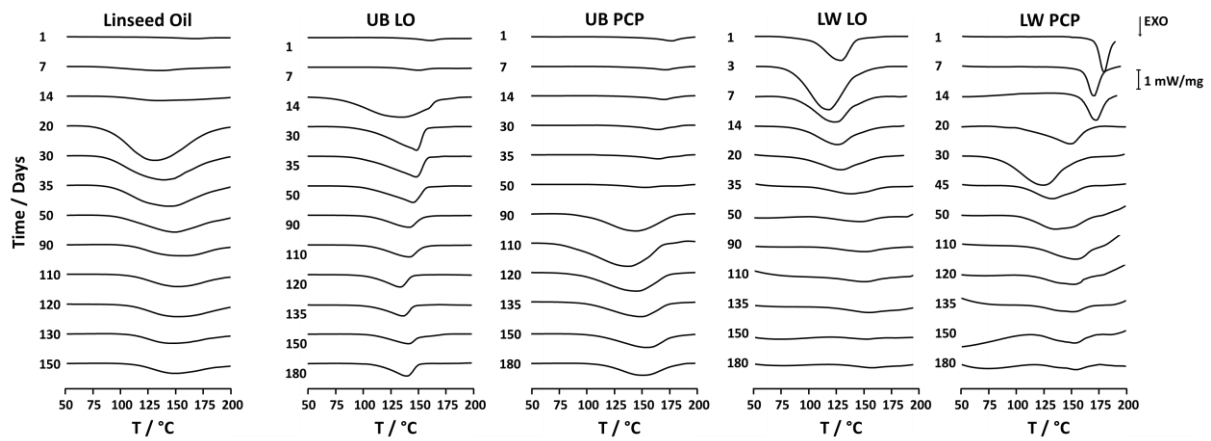


Figure 3.14 - DSC curves (normalized to the oil content) of raw linseed oil and mock-up paints exposed to natural ageing. Solids content of LW LO and LW PCP are  $\phi = 31$  and 29 vol% respectively, including 15 vol% (PCP) of EY. Solids content of UB LO and UB PCP are  $\phi = 6$  and 16 vol% respectively, including 12 vol% (PCP) of EY. PCP stands for protein coated pigment paint and LO for oil paint.

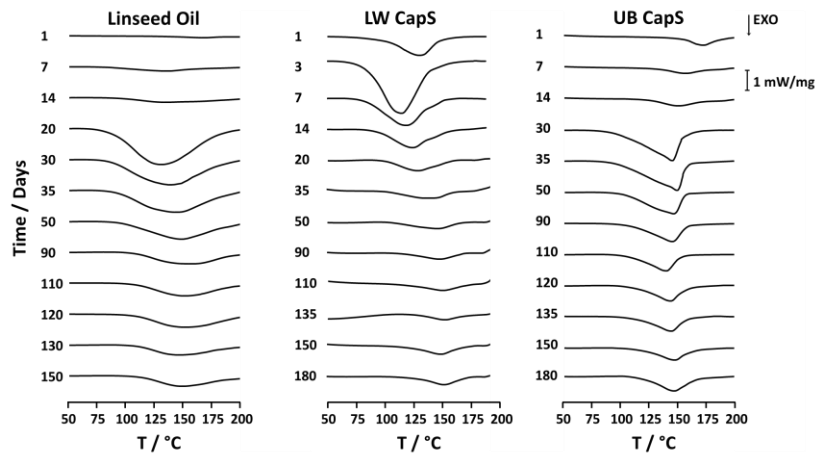


Figure 3.15 - DSC curves (normalized to the oil content) of linseed oil and mock-up capillary suspension paints CapS exposed to natural ageing. Solids content of LW CapS and UB CapS are  $\phi = 31$  and 33 vol% respectively, including 2 (LW) and 3 vol% (UB) of EY.

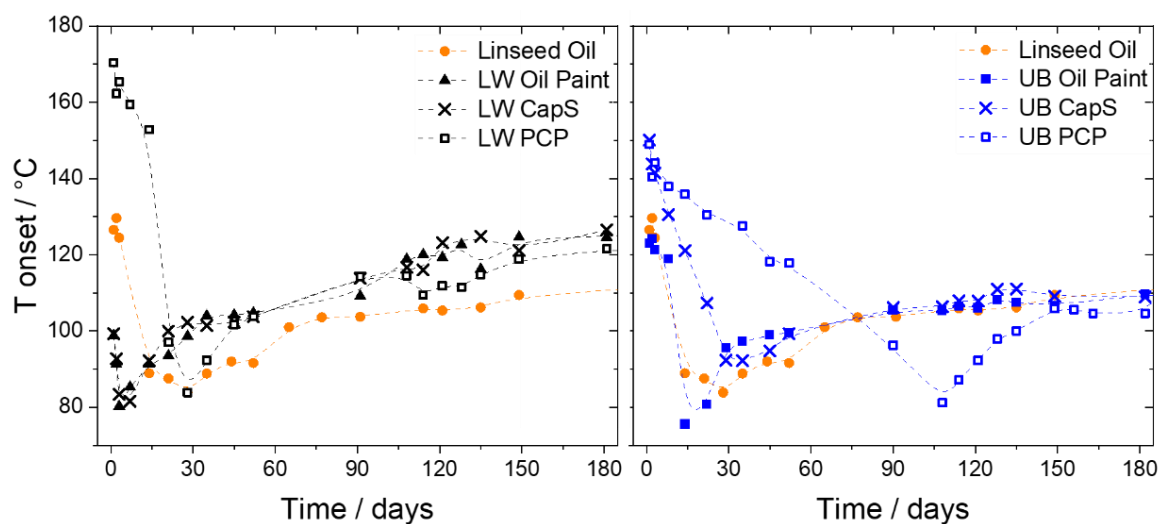


Figure 3.16 - Onset temperature of the overall exothermic peak associated to the decomposition of peroxides and hydroperoxides (endothermic) and the recombination of radical species (exothermic) as a function of the evaluation time. Solids content of LW LO, LW CapS and LW PCP are  $\varphi = 31, 31$  and  $29$  vol% respectively, including  $2$  (CapS)  $15$  vol% (PCP) of EY. Solids content of UB LO, UB CapS and UB PCP are  $\varphi = 6, 33$  and  $16$  vol% respectively, including  $3$  (CapS) and  $12$  vol% (PCP) of EY. PCP stands for protein coated pigment paint, CapS for capillary suspension paint and LO for oil paint.

Table 3.4 - Onset temperature of the normalized DSC curves for linseed oil (LO). Solids content of LW LO and LW PCP are  $\varphi = 31$  and  $29$  vol% respectively, including  $15$  vol% (PCP) of EY. Solids content of UB LO and UB PCP are  $\varphi = 6$  and  $16$  vol% respectively, including  $12$  vol% (PCP) of EY.

Time / days	T onset / °C				
	Linseed Oil	UB LO	UB PCP	LW LO	LW PCP
1	127	123	149	99	170
2	130	124	140	91	162
3	124	121	144	80	165
7	78	119	138	85	159
14	89	76	136	91	153
20	88	81	130	94	97
30	84	96	134	99	84
35	89	97	128	104	92
50	92	100	118	105	104
90	104	105	96	109	114
110	106	105	81	119	114
120	105	106	92	119	112
135	106	108	100	116	115
150	109	107	106	125	119
180	110	110	105	125	122

Table 3.5 - Onset temperature of the normalized DSC curves for linseed oil (LO). Solids content of LW CapS and UB CapS are  $\phi = 31$  and 33 vol% respectively, including 2 (LW) and 3 vol% (UB) of EY.

Time / days	T onset / °C		
	Linseed Oil	LW CapS	UB CapS
1	127	99	150
2	130	93	144
3	124	83	141
7	78	82	131
14	89	92	121
20	88	100	107
30	84	102	92
35	89	101	92
50	92	104	99
90	104	114	106
110	106	117	106
120	105	123	108
135	106	125	111
150	109	121	109
180	110	127	109

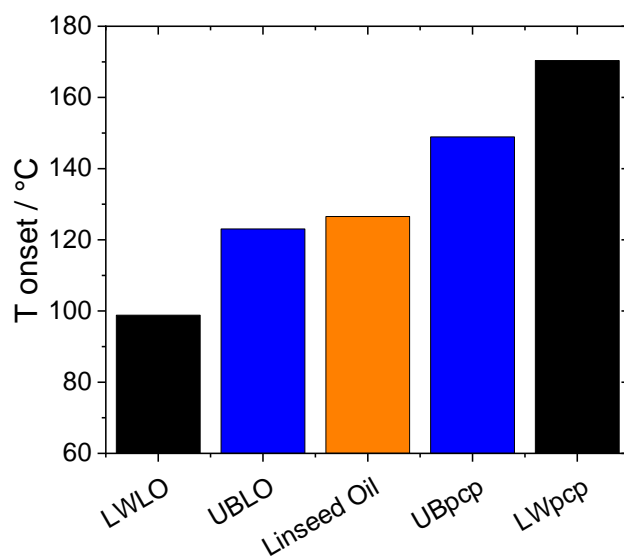


Figure 3.17 - Onset temperature of the overall exothermic peak on the first day of natural ageing. Solids content of LW LO and LW PCP are  $\phi = 31$  and 29 vol% respectively, including 15 vol% (PCP) of EY. Solids content of UB LO and UB PCP are  $\phi = 6$  and 16 vol% respectively, including 12 vol% (PCP) of EY. PCP stands for protein coated pigment paint and LO for oil paint.



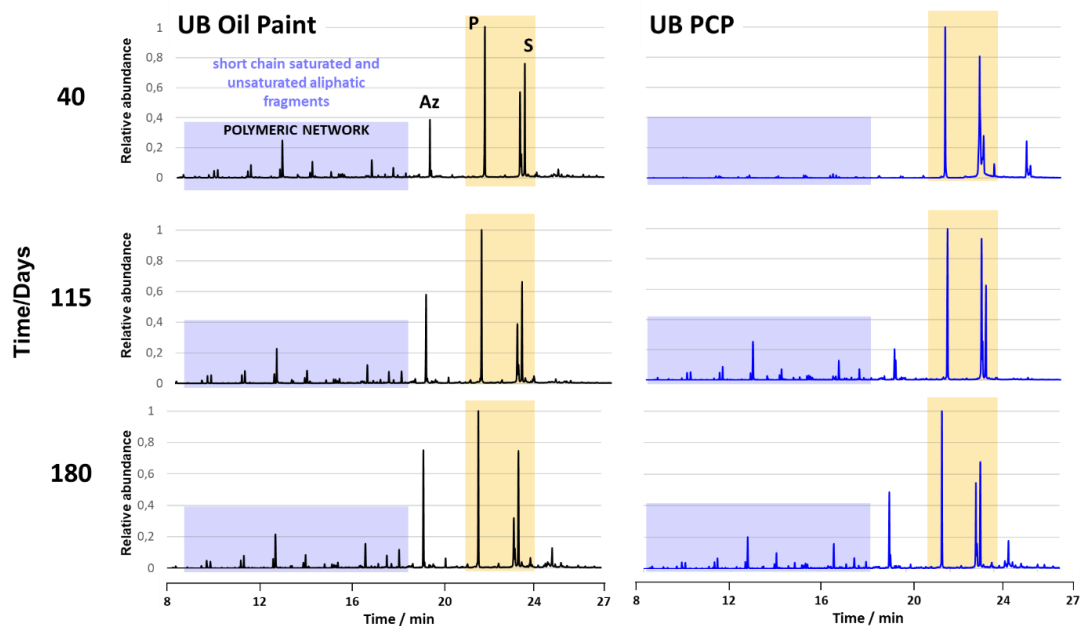


Figure 3.18 - Extracted ion pyrograms of  $m/z$  129 of model oil paintings after 40, 115 and 180 days of natural aging. Solids content of UB oil paint and UB PCP are  $\varphi = 6$  and 16 vol% respectively, including 12 vol% (PCP) of EY. All the paints have been normalized to the palmitic acid peak (P). (S) represents the stearic acid and (Az) the azelaic acid peak. The evolution of the polymeric network upon time is visible in the blue rectangle, more details can be found in Figure 3.5 in the main manuscript (see text for an explanation).

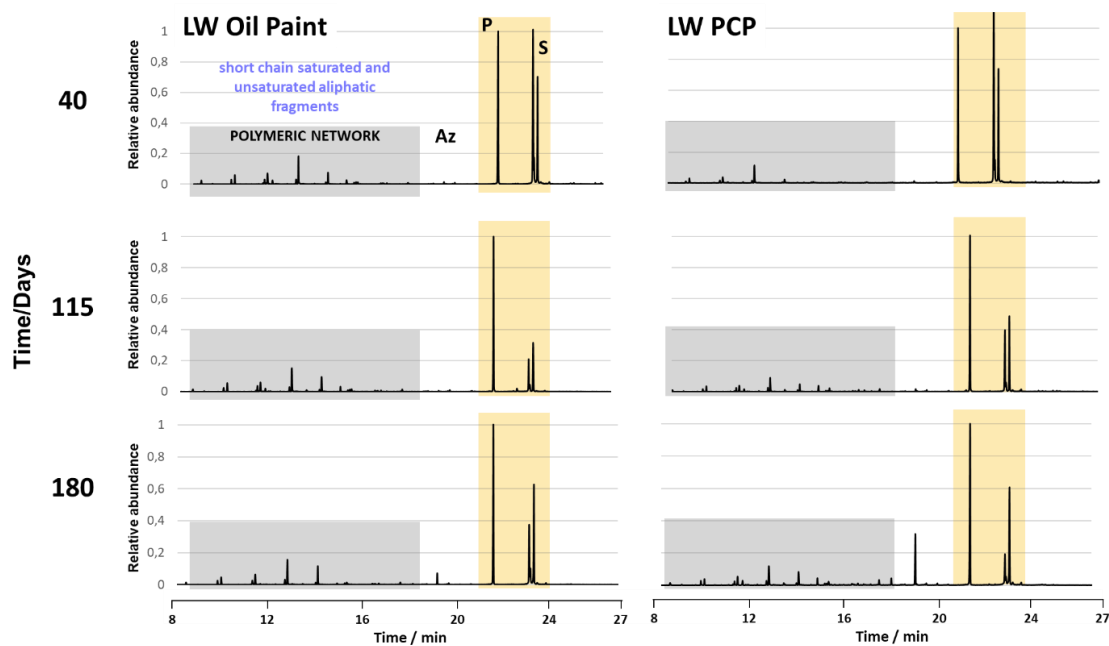


Figure 3.19 - acted ion pyrograms of  $m/z$  129 of model oil paintings after 40, 115 and 180 days of natural aging. Solids content of LW oil paint and LW PCP are  $\varphi = 31$  and 29 vol% respectively, including 15 vol% (PCP) of EY. All the paints have been normalized to the palmitic acid peak (P). (S) represents the stearic acid and (Az) the azelaic acid peak. The evolution of the polymeric network upon time is visible in the grey rectangle, more details can be found in Figure 3.5 in the main manuscript (see text for an explanation).

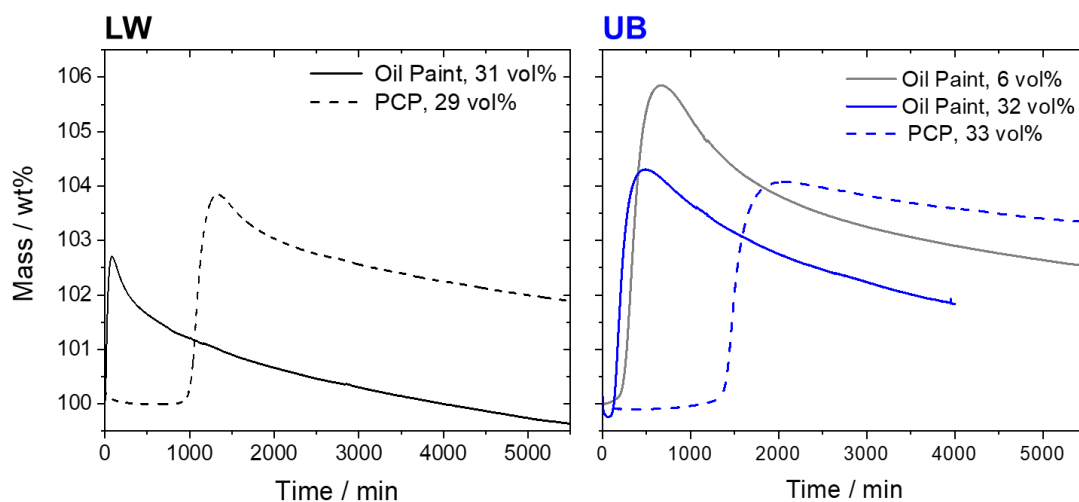


Figure 3.20 - Oxygen uptake experiments in TGA in accelerated conditions at 80 °C. Solids content of UB oil paint and LW oil paint is only composed on pigments. Solids content of UB protein coated paint (PCP) is composed of 21 vol% of UB and 12 vol% of egg yolk and LW PCP is composed of 14 vol% of LW and 15 vol% of egg yolk.

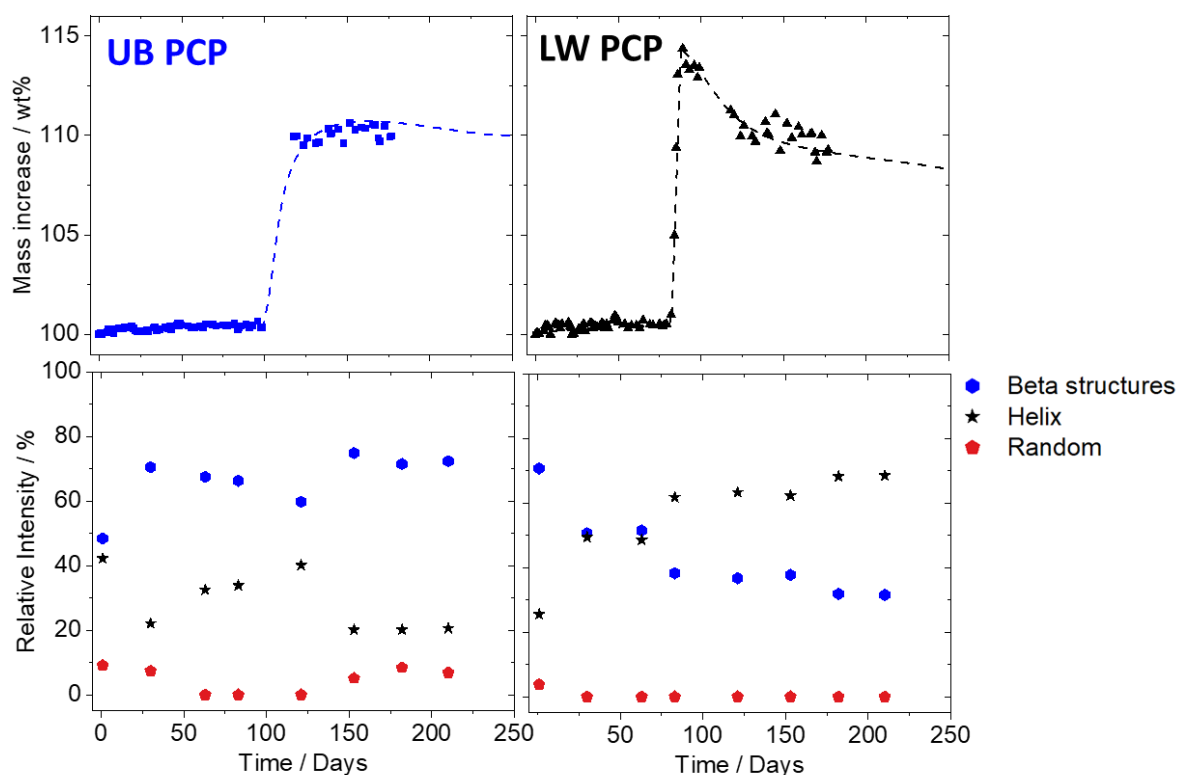


Figure 3.21 - Above: mass increase normalized to the oil content of UB protein coated paint PCP (blue) and LW PCP (black) as a function of time. Below: relative intensity % of the optical density of the peaks assigned to beta structures, helix and random coils, obtained by fitting the amide I band of TRANS-FTIR spectra of the PCP samples as a function of time. Solids content of UB PCP is  $\phi = 33$  vol%, including 12 vol% of EY and LW PCP is  $\phi = 29$  vol%, including 15 vol% of EY.

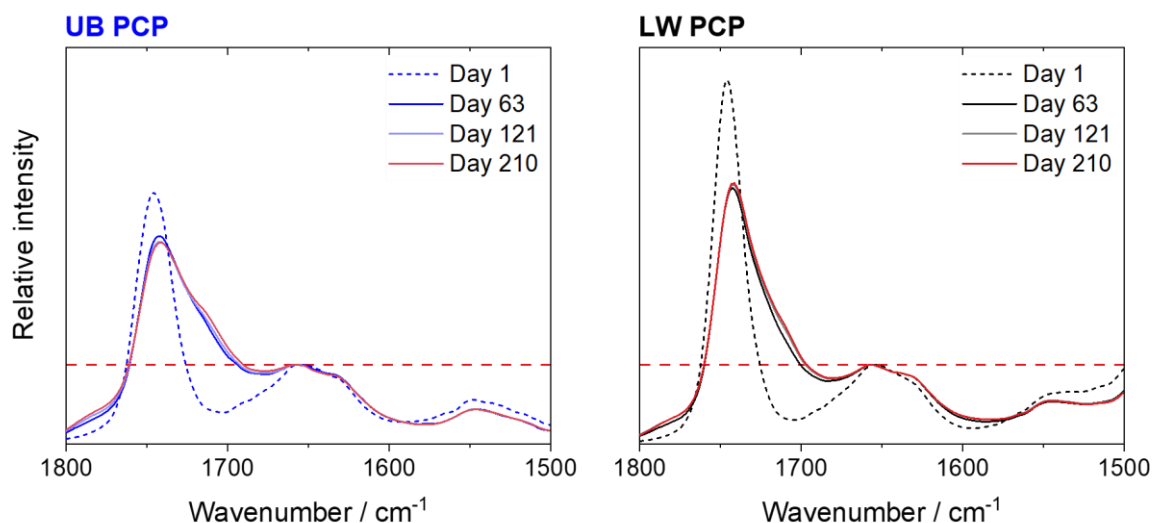


Figure 3.22 - TRANS-FTIR spectra of UB PCP (blue) and LW PCP (black) paints at 1, 63, 121 and 210 days of natural ageing. Solids content of UB PCP is  $\phi = 33$  vol%, including 12 vol% of EY and LW PCP is  $\phi = 29$  vol%, including 15 vol% of EY.

Table 3.6 - Peak attribution according to Bramanti et al. (1996)<sup>122</sup>

Helices		$\beta$ -structures		Random	
1658 cm <sup>-1</sup>	$\alpha$ -helix	1610 cm <sup>-1</sup>	intermolecular $\beta$ -sheets	1644-47 cm <sup>-1</sup>	Random coil
1667 cm <sup>-1</sup>	extended helix	1615 cm <sup>-1</sup>	anti-parallel $\beta$ -sheets		
		1630 cm <sup>-1</sup>	$\beta$ -turns		
		1677 cm <sup>-1</sup>	anti-parallel $\beta$ -turns		
		1681-91 cm <sup>-1</sup>	anti-parallel $\beta$ -sheets		

We followed the mass change of egg-based samples upon time on aluminum pans and the modification of the protein conformation on BF<sub>2</sub> pellets to understand how the conformation changes of egg proteins are related to the curing of the linseed oil.

When egg yolk coats the UB pigment prior to be dispersed into the oil, the proteins are present mostly  $\beta$ -structures ( $\approx 70$  %), helices ( $\approx 30$  %) at less extent and no random conformation. The oil undergoes curing reactions at around 100 days of ageing, causing no major changes of the secondary structure of the polypeptide chain upon curing.

In LW PCP, the proteins change their conformation in correspondence with the mass uptake of the oil (from 50% helix and 50%  $\beta$ -structures with the “fresh” oil to a majority of helicoidal structures ( $\approx 65$  %) over  $\beta$ -structures when the oil undergoes curing reactions). This change of protein structure upon curing suggests that the egg proteins interact with the LW pigment upon the oil curing, provoking a modification in the secondary structure of the polypeptide chain, leading to a reorganization of the polymeric network in the paint.



Figure 3.23 - Leonardo da Vinci, *Madonna of the Carnation*, c. 1475, 62 x 48,5 cm, Inv. No. 7779, © Bavarian State Painting Collections, Munich

This artwork painted by Leonardo da Vinci shows wrinkling in the shadows of the flesh paint of Mary and the child shown in Figure 3.7 of the main text. Unfortunately the paints in the flesh could not be sampled and therefore no discussion of the paint composition is possible.

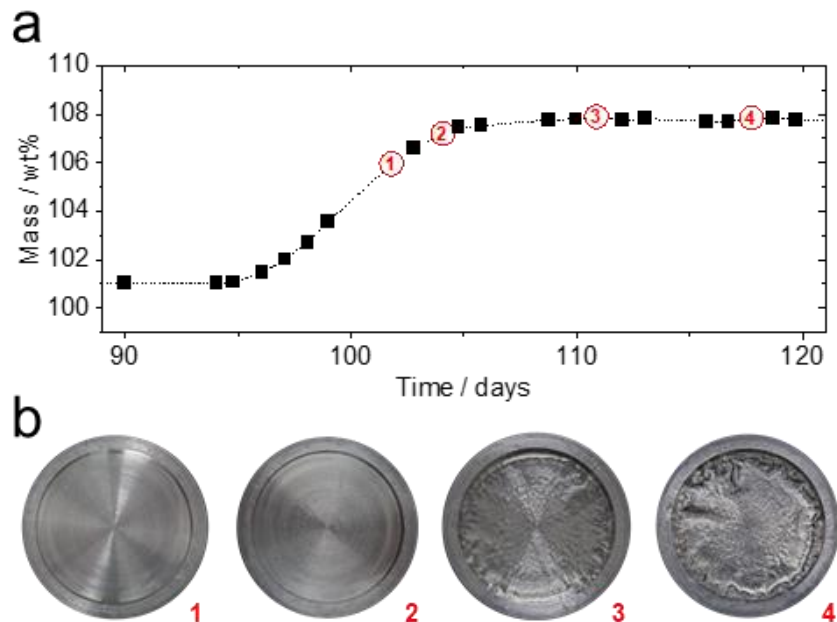


Figure 3.24 – **a** Mass increase of raw linseed oil at a thickness layer of 1.0 mm and **b** corresponding photographs of the wrinkling at the time indicated.

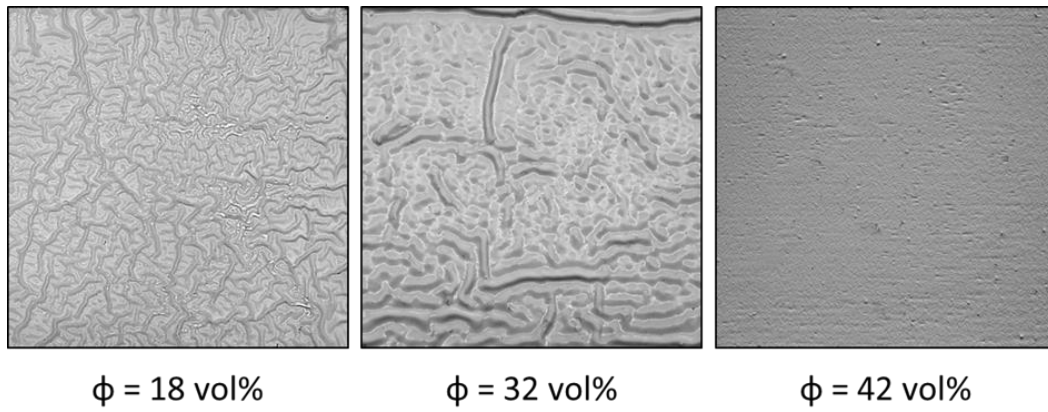


Figure 3.25 - Surface of LW oil paint samples (thickness 1.0 mm) at increasing pigment content after several months of natural ageing.



## 4. *Tempera* and *Tempera Grassa* – from wet paints to solid films

*Full title:* *Tempera and Tempera Grassa – from wet paints to solid films*

*Authors:* Ophélie Ranquet, Celia Duce, Giulia Caroti, Patrick Dietemann, Ilaria Bonaduce and Norbert Willenbacher

*Status:* published<sup>151</sup>

*Bibliographic data:* *ACS Applied Polymer Materials*, **5**, 4664–4677 (2023),  
DOI: 10.1021/acsapm.3c0017

*The text has been adapted in this thesis to change the citation and figure numbering. Additionally, the material and method sections have been removed to avoid repetition and confirm with the other chapters. Reprinted (adapted) with permission from *Tempera and Tempera Grassa – From Wet Paints to Solid Films*, Ophélie Ranquet, Celia Duce, Giulia Caroti, Patrick Dietemann, Ilaria Bonaduce, and Norbert Willenbacher, *ACS Applied Polymer Materials*, 2023, 5, (7), 4664-4677, DOI: 10.1021/acsapm.3c00179. Copyright 2023 American Chemical Society.*

### 4.1. Abstract

Old Masters frequently used paints containing both egg and oil binders to create their paintings. These two binders can be combined in the paint in many different ways resulting in substantially different behaviors of the wet paint but also affecting drying and curing reactions. This paper focuses on paints bound with egg (*tempera* paints), and the influence of added oil on microstructure, rheology, drying kinetics, and chemistry is discussed. Such egg *tempera* paints with oil are called fatty *tempera*, or *tempera grassa* (TG), and are sometimes believed to play an intermediate role between oil and *tempera* paints. Despite their hydrophobic nature, pigments do not enter into the oil droplets emulsified in a TG due to the adsorption of egg proteins on the pigment surface. We further show that the flow behavior of both paint types can be described using classical suspension rheology concepts. When combining the pigment, the egg yolk, and the oil into the calculation of the disperse phase volume fraction  $\phi$ , minor differences in viscosity and onset of percolating network formation are attributed to the broader particle size distribution for TG. The dry-to-touch is controlled by the evaporation of water in both cases and reached within minutes. The added oil does not change the painting behavior in general; however, different brushability is observed on absorbent substrates when water is lost quickly and the remaining oil in TG keeps the paint soft. After the dry-to-touch state is reached, the oil cross-linking sets in, leading to a second hardening step. Egg components exert an antioxidant effect of the oil, which does affect not only

the kinetics of the curing process but also its chemistry and is dependent on the microstructure of the paint film.

## 4.2. Introduction

The classical binding media of Italian artists in the 14<sup>th</sup> century was usually egg, and the corresponding paintings are classified as egg *tempera*. In the transition of egg *tempera* to oil painting in 15<sup>th</sup> century Italy, one of the most important and influential technical transitions in art history, famous Masters such as Antonello da Messina, Giovanni Bellini, Sandro Botticelli, Leonardo da Vinci or Domenico Ghirlandaio and their workshops sometimes combined and modified materials and techniques to create their artworks.<sup>3-6,10</sup> Some artworks were made using both *tempera* and oil techniques in parallel in different areas of the same painting, (Figure 4.1 and Supplementary Figure 4.14), and some paintings show properties of both *tempera* and oil paints at the same time.<sup>23</sup>

In classical egg *tempera*, paints dry within seconds to minutes, due to water evaporation. To achieve complex color transitions, paints with different hues were thus not blended on the painting, but applied on top of each other in many thin, translucent layers by hatching. The color transition is thus achieved by modulating the hiding power of a paint layer by its thickness, which results from the hatching density of several layers of quick-drying paint. For example flesh was painted by applying brownish, pink and white paints in many brushstrokes on top of a greenish paint that still shines through in some areas (Figure 4.1a).<sup>21,152</sup> In contrast, oil paints take days to dry by chemical cross-linking, and thus color transitions can be achieved by wet-in-wet painting, i.e. several different colors can be applied and blended into each other with a soft brush to create continuous color transitions (Figure 4.1b).<sup>23</sup>

In the transition phase of *tempera* to oil painting, sometimes paints with intermediate properties are found. E.g. in Jacopo del Sellaio's *Martyrdom of St Sebastian* (Supplementary Figure 4.15), some typical *tempera* paints surprisingly do not show differences in layer thickness or color in places where one or several brushstrokes were applied on top of each other (light blue-green paint in Figure 4.2). It seems that the paints were liquid long enough to fuse and level after application, quite opposite to the behavior of traditional *tempera* paints as seen in Figure 4.1.<sup>23</sup> Also the impasto of the white paint of the crossbow reminds of oil rather than *tempera* paint.

It is sometimes assumed that adding oil to *tempera* is delaying its drying process, thus such paints are explained as "*tempera grassa*" (Italian for "fatty *tempera*"), a mixture of egg yolk with (emulsified) drying oils. To the best of our knowledge, though, "*tempera grassa*" is not described in art technical treatises. Whereas collections with a scientific laboratory may hypothesize the use of a *tempera grassa* by chemical analysis, based on the presence of oil with egg in the same paint layer, such extensive chemical analysis (and sampling) is often not possible. In contrast, there is a tendency to label uncommon *tempera* paints with somewhat oil-like properties as *tempera grassa*



in art technological studies, without actual analysis certifying the simultaneous presence of egg and oil binders<sup>4</sup>.

Therefore, the term “*tempera grassa*”, although defined by its composition, is often applied based solely on visual examination of paintings by comparing the appearance of the respective paints with common practical experience with materials and methods, as is done in Figure 4.1 and Figure 4.2. However, paint systems exhibit complex colloidal interactions and microstructural properties, it is thus not necessarily expected that paints change gradually from *tempera*-like to oil-like<sup>153</sup> if oil is added to *tempera* paints. In this paper we study the microstructure, rheological properties, drying kinetics and chemical behavior of *tempera* and *tempera grassa* in comparison with oil paints. The aim is to provide a framework to rationalize the influence of paint composition and preparation on the final aspect of paintings we can still enjoy in museums and churches.



Figure 4.1 – Domenico Ghirlandaio and workshop, *Mary with Child and Saints*, c. 1490/94, detail of St Thomas' eye in tempera (left) and his finger in oil technique (right). The full painting is depicted in Supplementary Figure 4.14. In classical tempera, color transitions were created with hatching brushstrokes of various colors, e.g. brownish, pink and white paints over a greenish layer still visible below the eye (left), and color transitions are achieved by superimposing thin layers of limited hiding power. In contrast, paints were mixed wet-in-wet in oil to obtain continuous color transitions (right), final white highlights were added with a rather stiff paint. © Bavarian State Painting Collections, Inv. No. 1078, pictures: Daniela Karl. Reproduced with Permission.



Figure 4.2 - Jacopo del Sellaio, *The Martyrdom of St Sebastian*, c. 1465/73, detail of water and a bowstring. The full painting is depicted in Supplementary Figure 4.15. Generally painted in egg tempera technique, the light blue-green paint shows untypical behavior for tempera, because the color does not change in areas with several superimposed brushstrokes, quite in contrast to Figure 4.1 (left), and also the white impasto brush strokes show

### 4.3. Results and discussion

#### 4.3.1. Microstructure of tempera and tempera grassa paints

Hen egg yolk (EY) contains  $\approx 50$  wt% of dry matter, composed of about 31 wt% of lipids, 17 wt% of proteins and 2 wt% of carbohydrates and ash.<sup>32</sup> These are gathered as protein-lipid complexes in two major forms: insoluble granules aggregates ( $d = 0.3\text{-}2 \mu\text{m}$ ) containing high density lipoprotein complexes (HDL) and water-soluble plasma, composed mostly of low-density-lipoprotein (LDL) micelles ( $d = 13\text{-}50 \text{ nm}$ ).<sup>33,34,104</sup> The complex microstructure of EY is a dispersion of protein-stabilized lipid particles and droplets, and the entire system can be described as a concentrated o/w emulsion, stabilized by proteins.<sup>105,106</sup> This type of system can thus be diluted with water.

In this work, model paints were prepared using fresh EY, distilled water, either lead white (LW) or ultramarine blue (UB) as pigments, and linseed oil (LO), a drying oil commonly used for artists' painting.<sup>132</sup> The two pigments were selected for their extensive use in the artistic field through history and because they differently affect the curing and ageing of oil paint layers<sup>47,123</sup>. Synthetic ultramarine blue was used instead of the natural one. The choice was driven by the need of ensuring a constant pigment composition, which was necessary for the preparation of large batches of paints, replicated measurements and several sets of systematic experiments that lasted about three years. Model systems were prepared to be analyzed with different techniques in their wet, dried and aged states. The composition of the paints prepared is specified in Table 4.1.

Table 4.1 – Composition of tempera and tempera grassa (TG) paints (in vol%) in the wet and dried state

		<b>Egg yolk dried matter</b>	<b>Pigment (LW or UB)</b>	<b>Linseed Oil</b>	<b>Water</b>
<b>EY-rich Tempera</b>	Wet	29	16	-	55
	Dry	64	36	-	-
<b>EY-rich TG</b>	Wet	24	13	17	46
	Dry	45	24	31	-
<b>EY-poor TG</b>	Wet	3	17	40	40
	Dry	4	28	68	-

The structure of freshly prepared water-based paints was investigated using fluorescence microscopy (Figure 4.3): hydrophilic polystyrene tracers ( $d = 0.2 \mu\text{m}$ ) were added to the LW-based liquid paints to better localize the aqueous phase. For UB-based paints (Figure 4.3a-b), this strategy did not work, thus a water-soluble fluorescent dye (Rhodamin B) was added to enhance the contrast between the UB pigment particles, the aqueous EY matrix, and the linseed oil droplets.

The microscope images (Figure 4.3a) show that a *tempera paint* is a suspension of pigment particles ( $d \approx 2 \mu\text{m}$ ) in the aqueous continuous phase. The microstructure of the EY itself, described above, is not resolved by optical microscopy. When oil is mixed into the *tempera* paint, an o/w emulsion is formed: large-size oil droplets can be distinguished by contrast from the continuous phase containing tracer and pigments particles (Figure 4.3b) in *tempera grassa (TG) paints*. When LW is used instead of UB, similar o/w emulsions are formed (Figure 4.3c<sub>1-2</sub>). *TG paints* contain oil droplets of different sizes within the continuous aqueous EY-phase, the largest of which are easily discernable in the microscopic images (Figure 4.3b-c). During paint preparation, the microstructure of EY might have been disrupted through mixing and grinding, and although not visible in fluorescence microscopy, we cannot exclude that some EY lipids were extracted by the oil phase, or that flocculation and coalescence occurred between the different lipid droplets. However, in a first approximation, this would not affect the flow properties of the paints because the lipids are part of the disperse phase of the paints either way.

Contact angle data indicate that both pigments are much better wetted by linseed oil ( $\Theta_{UB \text{ or } LW-LO} = 9 \pm 2^\circ$ ) compared to water ( $\Theta_{UB-H_2O} = 55 \pm 6^\circ$  and  $\Theta_{LW-H_2O} = 84 \pm 3^\circ$ ). However, in *TG* paints, both pigments are located in the aqueous continuous phase and do not mix with linseed oil droplets. This aspect distinguishes *tempera grassa* from *oil paints* where the pigment particles are dispersed in the oil. It also explains why *tempera grassa* paints are *tempera* paints: they are diluted with water, as oil is in the disperse phase. The difference in microstructure between *tempera* and *oil paints* indicates that some components of the fresh yolk increase the affinity of the pigments towards the aqueous phase. Presumably some EY proteins adsorb onto the pigment particles during paint preparation, which is strongly expected since proteins are surface active materials.<sup>106,127,140</sup> To investigate into this, we prepared EY-rich *tempera* and *TG paints* with either UB or LW pigments. After homogenization, we centrifugated the paints, and the corresponding images are shown in Figure 4.3d. In the centrifugated *TG paints*, linseed oil is separated from the other phases and has the lowest density (A in Figure 4.3d). The turbid fraction B is an oil-rich emulsion containing a small fraction of proteins (see Supplementary Figure 4.16). ATR-FTIR experiments of dried aliquots of each separated phase disclosed the presence of proteins in the pigment-rich phase (E and E\* in Figure 4.3d, for UB and LW pigments respectively), in the transparent interphase region (D in Figure 3d) and in the yellow phase (C in Figure 4.3d) underneath the oil phase (A in Figure 4.3d) (see Supplementary Figure 4.16). It may be assumed that proteins tend to adsorb at the pigment particle surface, however, further spectroscopic investigations would be necessary for direct

experimental evidence. In both types of paints, EY was homogeneously dispersed, its colloidal ingredients (granules and LDL micelles) did not separate under the experimental conditions.

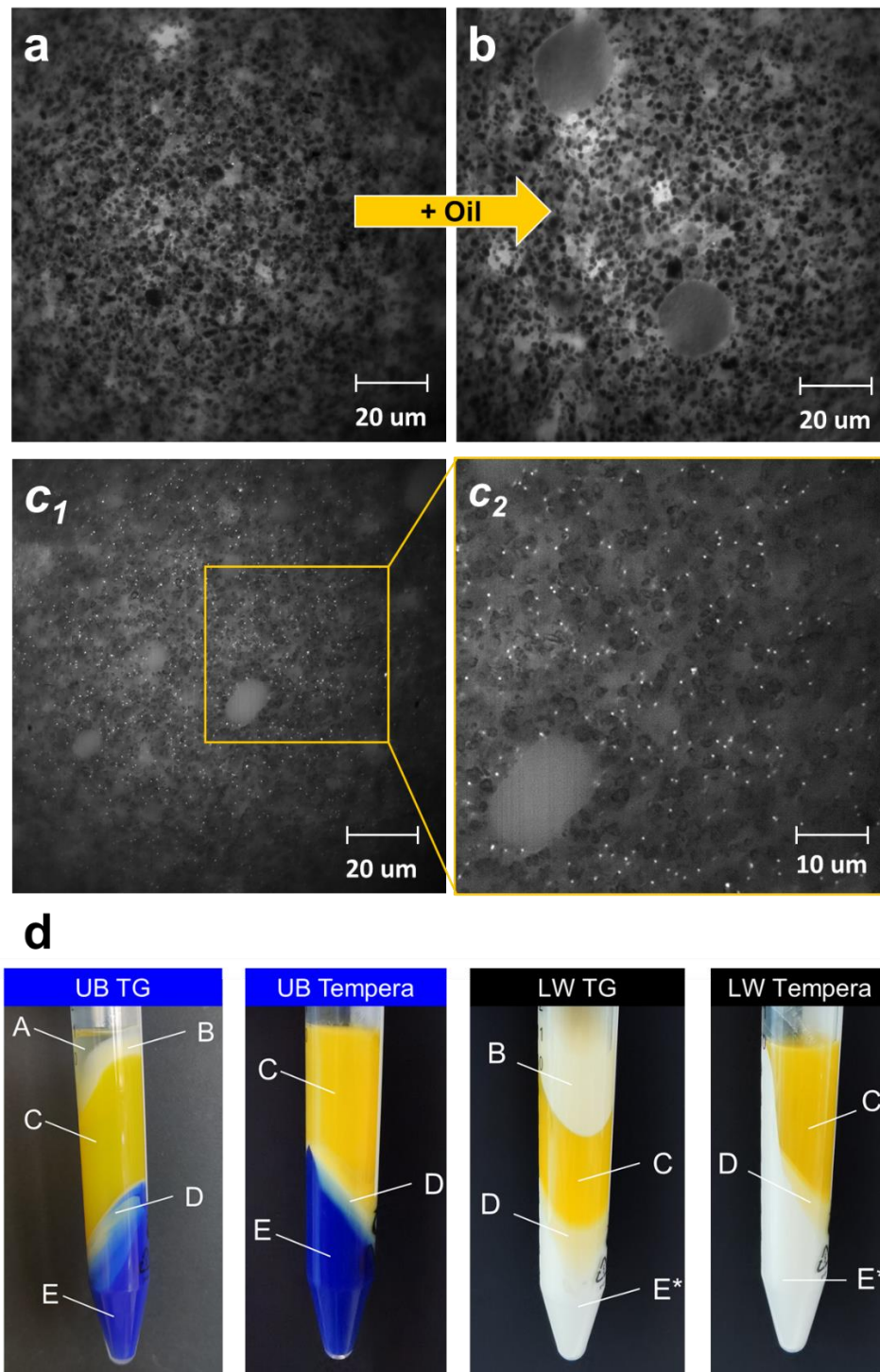


Figure 4.3 – Fluorescence microscopy images of the microstructure of UB-EY-rich Tempera **a**, UB-EY-rich TG **b**, LW-EY-rich TG **c<sub>1</sub>-c<sub>2</sub>**. The images were taken 5 minutes after placing the paints onto microscope glass slides. Green fluorescent, hydrophilic polystyrene tracers ( $d = 0.2 \mu\text{m}$ ) were added to the LW-based liquid paints whereas a water-soluble fluorescent dye (Rhodamin B) was added to UB-based paints to better localize the aqueous phase. **d**: pictures of centrifuged EY-rich tempera and TG samples. A is the oil fraction, B is an oil-rich emulsion, C is an EY-rich phase, D is a transparent interphase region, E and E\* are UB and LW pigment-rich phases. We could detect the presence of proteins in each fraction except for the oil fraction A.

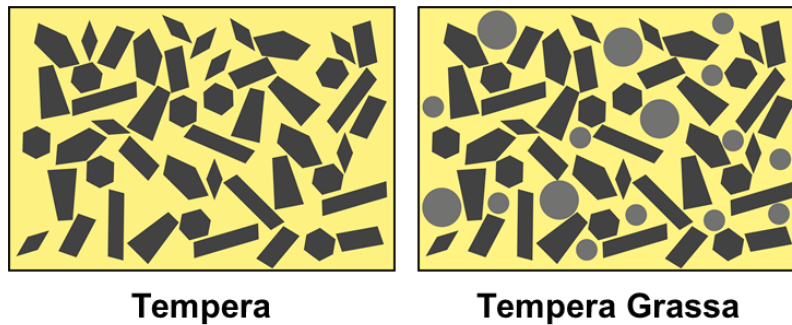


Figure 4.4 – Proposed scheme of the microstructure of the tempera and tempera grassa model systems. The pigments are represented in black; the oil is in grey and the fresh liquid egg yolk containing water is in yellow. These models are simplified and are based on the microscope images (Figure 4.3) not resolving the colloidal microstructure of the EY.

In conclusion, the differently prepared model systems can be schematically depicted as shown in Figure 4.4, and are described as follows:

- A **tempera paint** consists of pigment particles dispersed in an egg yolk and water (o/w) emulsion. On a micrometer length scale the egg yolk/water mixture is treated as a homogeneous fluid.
- A **tempera grassa paint (TG)**, i.e. a fatty *tempera*, comprises pigment particles and micron-sized oil droplets dispersed in fresh egg yolk and water (o/w) emulsion.

#### 4.3.2. Rheology of tempera (grassa) paints

How do the flow properties of *tempera paints* change when the artist adds some linseed oil to form an o/w emulsion, a so-called *tempera grassa*? Does it correspond to an “in-between” system, with intermediate properties, making the link between a *tempera* and an *oil paint*?

The disperse phase volume fraction  $\phi$  is the dominant parameter controlling the flow behavior of suspensions and emulsions. Here, it is calculated from the pigment and the gravimetrically determined dry mass of the EY after water evaporation and the density of these ingredients. This approximation has to be carefully interpreted: proteins and lipids contained in fresh EY and in *tempera (grassa) paints* in the wet state only partly exist as aggregates dispersed in the aqueous phase, but are partly dissolved on a molecular level.<sup>33,104</sup> We do, however, not know the fraction of proteins and lipids existing as aggregates or being adsorbed at the surface of the pigment particles. Nevertheless, we will consider the dried matter of the EY as part of the disperse phase volume fraction of the paint, which seems to be a good first approximation, as the correlation of the data below will show. For this rheological study, paints different to those described in Table 4.1 are studied: the volume ratio of pigment and EY dry matter was fixed to 1:2, and the oil content was varied. This ratio was found to be useful in preliminary tests with regard to rheology of paints, film formation as well as drying kinetics, and it is consistent with a statement by the Renaissance artist Cennino Cennini (chapter 157): “[...] bind your pigments with egg yolk, and bind them thoroughly,



always as much egg yolk as the pigment [...],<sup>2</sup> considering that half of the yolk is water and pigment powder apparent densities are in the range of c. 15-30 % of bulk densities. The EY-poor TG paint is not discussed in this section due to the very low EY content.

The viscosity, but also the color intensity of a paint increases strongly with its pigment content. If paints are very diluted, they will appear very light and transparent, but might also be too liquid. Here, we investigated the flow properties of *tempera (grassa) paints* at disperse phase volume fraction mostly between 50-70 vol% and varying oil content (10-30 vol%) as part of the disperse phase fraction. We focused on two rheological properties particularly relevant for painting: yield stress and high shear viscosity. The yield stress of a paint expresses the force necessary to break up the rest structure and make the paint flow. The viscosity at high shear rates or stresses reflects its resistance to flow when brushing it vividly.

Figure 4.5a shows that a *tempera paint* with a disperse phase volume fraction  $\varphi = 40$  vol% exhibits Newtonian flow behavior at a low viscosity level. When oil is added, i.e. upon changing from *tempera* to *tempera grassa*, the paints exhibit shear thinning behavior and the viscosity level as well as the degree of shear thinning increase with increasing oil content. The viscosity at low shear rates is controlled by a complex interplay of thermodynamic and hydrodynamic interactions, but here we focus on the high shear viscosity  $\eta_\infty$  dominated by hydrodynamics and thus solely determined by the disperse phase volume fraction<sup>154</sup>. This parameter has been deduced from the viscosity functions of these paint samples at shear rates above  $500 \text{ s}^{-1}$ , when the viscosity data approached a constant limiting value.

Figure 4.5b displays the  $\eta_\infty$  values determined for *tempera* and *TG paints* with different solids and oil content as a function of disperse phase volume fraction. The dramatic increase of  $\eta_\infty$  with disperse phase volume fraction is very well captured by the empirical model proposed by Maron and Pierce<sup>155</sup> which includes the maximum packing fraction  $\varphi_m$  as adjustable parameter:

Equation 1

$$\eta_\infty = \eta_s \left(1 - \frac{\varphi}{\varphi_m}\right)^{-2}$$

Where  $\eta_s$  is the viscosity of the continuous phase and  $\varphi_m$  the disperse phase fraction at which the dispersed particles/droplets are densely packed. Here,  $\eta_s \approx 2 \text{ mPas}$  mainly determined by the EY components molecularly dissolved in water.

The data for the *tempera paints* are matched using  $\varphi_m = 63$  vol%, the value expected for random close packing of equally sized spheres. This result justifies the approximation to treat the dry matter of EY as solid phase when calculating  $\varphi$ , not including it would result in an unphysically low value for  $\varphi_m$  considering the nearly isometric shape of the pigment particles (see in chapter 2 Figure 2.1 and Figure 2.4). Apparently, the effects of the deviations from the non-ideal spherical shape and the deviations from a monodisperse particle size distribution balance each other with respect to the

maximum packing fraction. The dependence of  $\eta_\infty$  on  $\phi$  for *TG paints* is also captured using Equation 1, but higher  $\phi_m$  values up to  $\phi_m = 74$  vol% have to be used (see Figure 4.5b). This is expected, since in this case the disperse phase comprises pigment particles and oil droplets. This results in a broad size distribution of the disperse phase which corresponds to an increase in  $\phi_m$ .<sup>156,157</sup>

All in all, it means that the high shear viscosity of *tempera* and *TG paints* can be equally tuned either by varying the solids content (pigment or EY dried matter) or by adding oil.

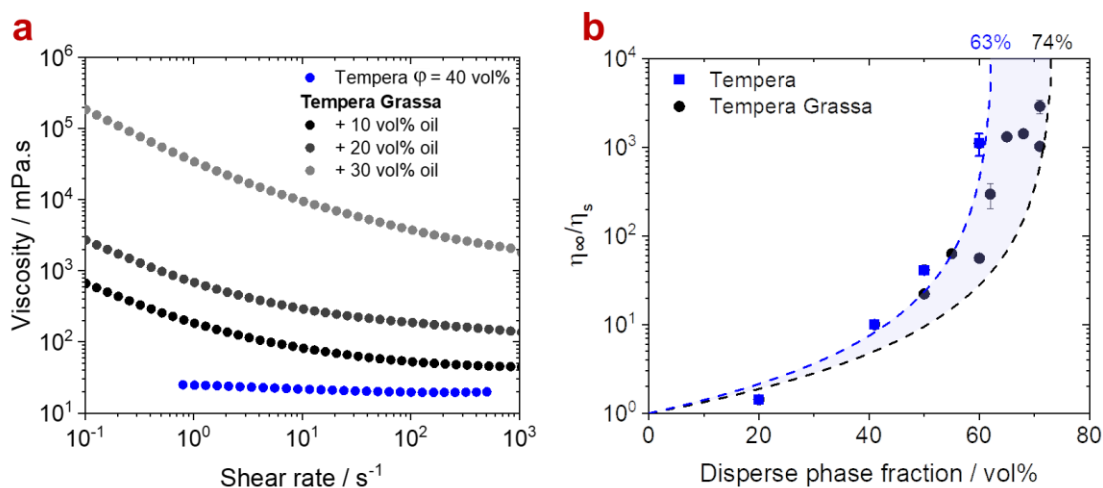


Figure 4.5 – a: viscosity curves of tempera and tempera grassa paints with a fixed pigment + EY fraction  $\phi_{\text{pigment+EY}} = 40$  vol% but increasing oil content. Water was partly substituted with linseed oil for TG paints. b: reduced high shear limiting viscosity  $\eta_\infty/\eta_s$  of tempera and TG paints as function of the disperse phase volume fraction  $\phi$ . The high shear limiting viscosity  $\eta_\infty$ , i.e. a constant viscosity level at high shear rates, here is typically reached at shear rates  $\geq 500$  s<sup>-1</sup>, and accordingly we set  $\eta_\infty = \eta(1000$  s<sup>-1</sup>). Here and in all following figures the error interval always denotes the standard deviation calculated from measurements performed at least in triplicate.

Creep experiments at varying shear stresses were performed to further elucidate the yielding and flow behavior of the paints. Figure 4.6a shows the deformation versus shear stress data for a *tempera* and two corresponding *tempera grassa* paints. At low disperse volume fractions, paints such as the *tempera* with  $\phi = 40$  vol% exhibit large absolute values of deformation, as expected for a low viscosity Newtonian fluid. Paints with intermediate volume fraction, like the *TG* paint made with additional 20 vol% of oil, show a weak shear thinning behavior but no measurable yield stress. However, when a critical volume fraction  $\phi_c$  is exceeded, like for the *TG* paint prepared with 30 vol% added oil (corresponding to a total disperse volume fraction of 70 vol%), a yield stress is observed: the paint responds linearly to the applied stress as expected for an elastic solid (slope = 1 in log-log representation) until a strong deformation occurs in the system, indicating viscous flow. The critical stress at which flow sets in is called yield stress  $\sigma_y$  (Figure 4.6a) and here it is determined using the tangent intersection method<sup>114</sup>. Similar results have been obtained for other paints differing in pigment and oil content. The critical volume fraction  $\phi_c < \phi_{\text{max}}$  at which the yield stress starts to occur marks the disperse phase volume fraction at which particle separation is small

enough and attractive particle interactions are strong enough to induce the formation of a sample-spanning particle network. For *TG paints*, this critical value slightly increases with increasing oil fraction (Figure 4.6b) which may be attributed to the broadening of the disperse phase size distribution.

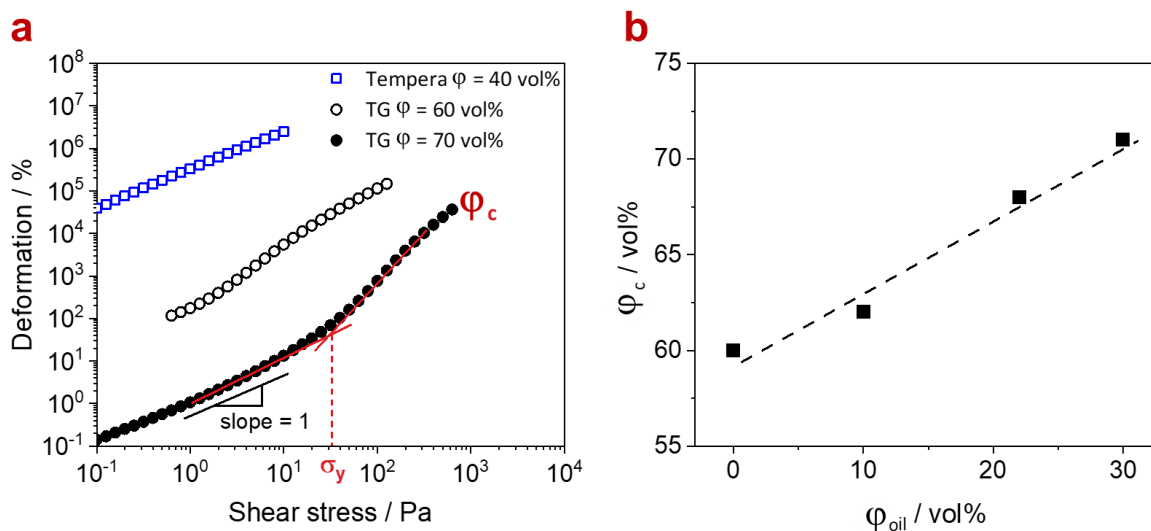


Figure 4.6 – **a** deformation vs. shear stress curves for tempera with  $\phi = 40$  vol% and TG paints with  $\phi = 60$  and  $70$  vol% (including 40 vol% UB and EY + 20% and 30 vol% of linseed oil respectively) as obtained from creep experiments performed at increasing shear stresses; **b** critical disperse phase volume fraction  $\phi_c$  for tempera and TG paints as a function of oil volume fraction.

We compared the viscosity of different *tempera* and *tempera grassa* paints below and above  $\phi_c$ . In the latter case the minimum applied stress during the viscosity measurement was set larger than the yield stress  $\sigma_y$ , which in both cases was  $\approx 50$  Pa. Selected data are shown in Figure 4.7a, which displays viscosity curves for two *tempera* paints and two *tempera grassa* paints. The viscosity curves demonstrate that the same flow behavior and viscosity level can be achieved with both types of paints. The disperse phase volume fraction, however, has to be set somewhat higher for a *TG paint* again due to the broader size distribution of the dispersed objects which has a significant impact on flow behavior of dispersions at volume fractions typically  $> 50$  vol%.<sup>154</sup> For comparison, it should be noted that oil paints (including prepared with the same pigment) exhibit a yield stress (and the formation of a percolating particle network) at much lower volume fractions  $\phi \approx 20$  vol%.<sup>123</sup> This again underpins that the pigment particles in *tempera* and *TG paints* are sterically stabilized due to adsorbed EY ingredients preventing particle network formation up to disperse phase volume fractions around 50 vol%.

These results also correlate with the appearance of visible brush strokes when the paint is applied to paper with a brush (Figure 4.7b). The paints with  $\phi > \phi_c$  have a yield stress, which is a prerequisite for creating impasto, i.e. an intentional visible brushing profile, giving a texture to the paint. In contrast, samples with low disperse volume fraction yield a smooth uniform paint film.



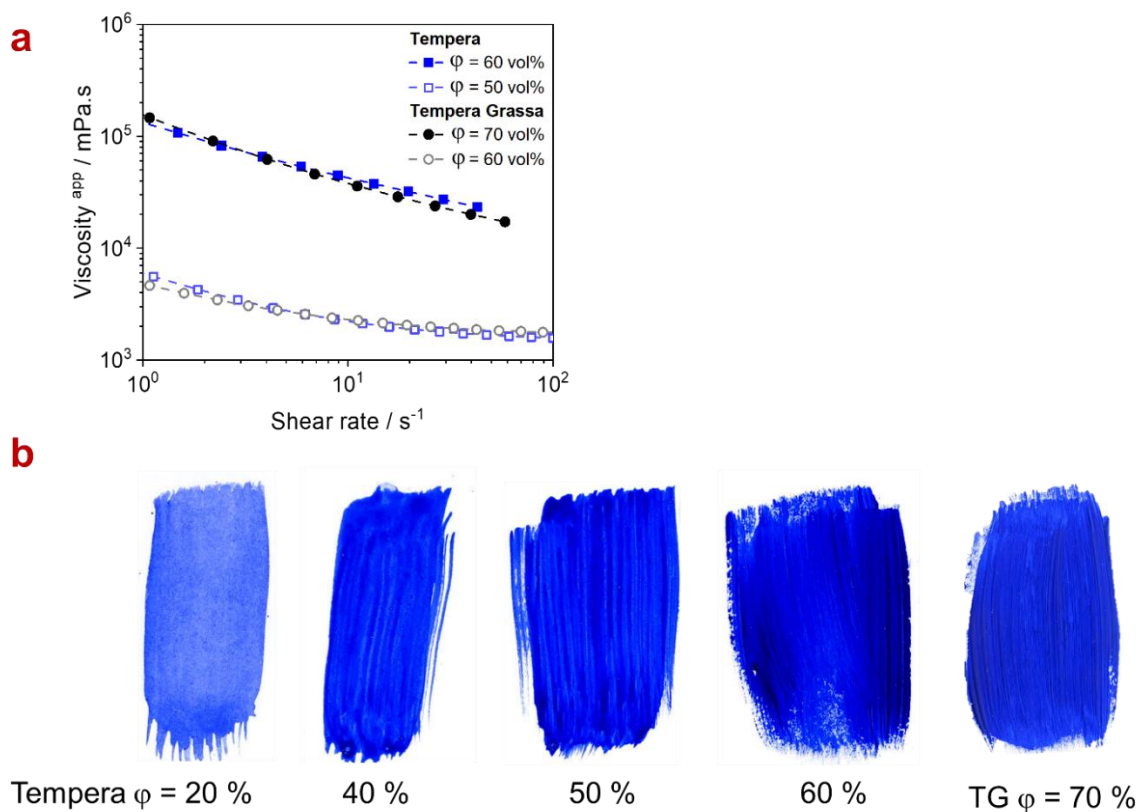


Figure 4.7 – **a**: apparent viscosity curves of tempera with  $\phi = 50$  and  $60$  vol% (blue symbols) and TG (black symbols) paints with  $\phi = 60$  and  $70$  vol% (including  $40$  vol% UB and EY +  $20\%$  and  $30$  vol% of linseed oil respectively). **b**: brush strokes of tempera paints with different disperse phase volume fraction between  $20$  vol% and  $60$  vol% and a TG paint including  $40$  vol% pigment and EY as well as  $30\%$  added linseed oil.

Interestingly, even if two paints exhibit similar flow properties, differences in the brushing texture may be observed on absorbent substrates. Here, we compared the brushing behavior of a *tempera* with  $\phi = 60$  vol% and a corresponding *tempera grassa* with  $30$  vol% added oil ( $\phi = 70$  vol%) on paper as well as on glass (Figure 4.8, left). Both samples exhibit a similar yield stress and viscosity curve (filled symbols in Figure 4.7a). When the *tempera grassa* is brushed on paper, however, it seems to flow better than the pure *tempera*. We attribute this to the penetration of water into the hydrophilic, open porous paper substrate. The paper easily soaks the water contained in the aqueous paint, leaving a concentrated disperse phase on the paper surface. After loss of water, the *tempera* contains a higher solids fraction, it is more pigmented than the TG, which also includes oil droplets, deformable at high shear force and thus helpful for brushing. When the paints are brushed on the non-absorbing glass surface, they both keep a sufficient quantity of water and their brushing texture is similar (Figure 4.8, right, see also Figure 4.17 and Figure 4.18), consistent with their similar flow properties. The uptake of water by the open porous paper substrate also shows up in the short drying time. The dry-to-touch state was reached within  $4$  minutes on paper, whereas it took  $10$  minutes on glass, for both *tempera* and TG, respectively.

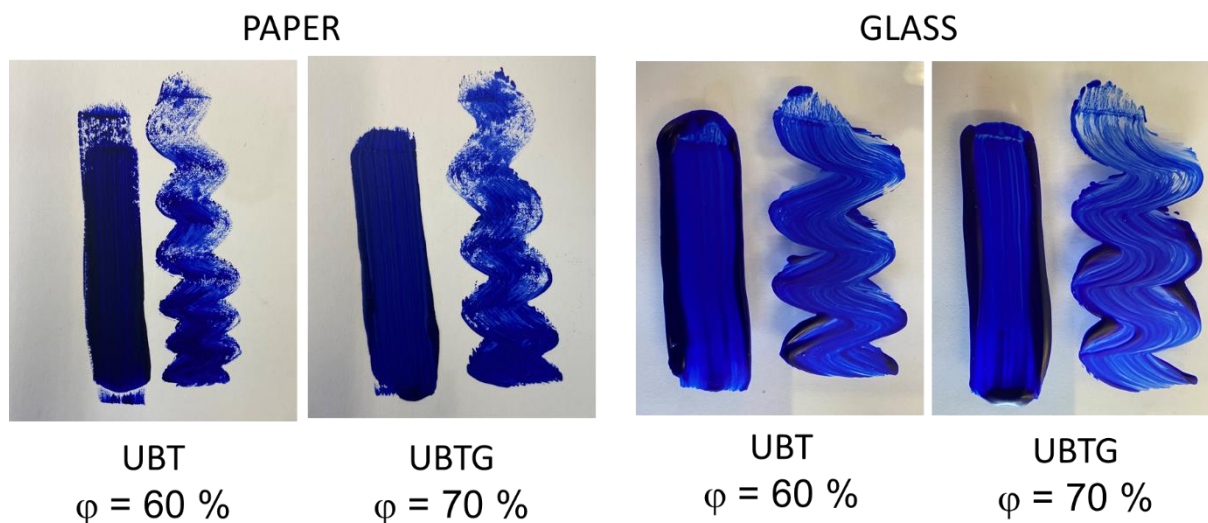


Figure 4.8 - Brush strokes of a *tempera grassa* with  $\phi = 70$  vol% (including 40 vol% UB and EY + 30% of linseed oil) and a *tempera* at  $\phi = 60$  vol%, having a similar yield stress and complete flow curve, applied with a brush on glass and on paper.

Addition of oil to the *tempera* can make it stiffer without increasing the pigment content, but also allows the artist to tune and adapt the flow properties of a paint depending on the painting surface, such as a ground layer or another layer of paint for example. Due to the shear-thinning effect, the paint can be brushed nicely onto the painting. Nevertheless, the paint remains soft with a limited yield stress, thus a brushstroke can be maintained, but no pronounced impasto is possible if we compare it e.g. to oil paints forming a strong capillary network.<sup>123</sup>

All in all, *tempera* and *TG paints* exhibit similar flow properties: shear thinning behavior is observed at intermediate disperse phase volume fraction and when a critical disperse volume fraction  $\phi_c$  is exceeded also a yield stress occurs. To achieve similar flow behavior, the total volume fraction of the disperse phase (including pigment, EY, and oil) of a *TG* must be higher than that of a *tempera* paint (containing only pigment and EY).

#### 4.3.3. Film formation and drying kinetics

*Tempera paints* are known for their quick drying times: a thin *tempera* layer forms a solid film within seconds or minutes, allowing the artist to apply the next layers on top of it quickly to obtain the desired appearance. This drying mechanism is physically driven, with the evaporation of water as the main solvent<sup>22,158</sup>. A drawback of this technique is the need for the artist to add regularly water on his palette in order to continue painting, and cracks may form during drying (Supplementary Figure 4.21). It is sometimes believed that addition of oil allows the artist to apply *tempera grassa* paint layers wet-in-wet, similar as oil paints.<sup>153</sup> This, however, would require long drying times. Therefore, the drying kinetics of *tempera* and *TG* paints whose compositions are given in Table 1, were compared.

We investigated the natural air-drying of *tempera* and *tempera grassa* paints. The kinetics of water loss was monitored gravimetrically and the change in hardness of the paint surface was tested at regular time intervals pushing a cylindrical piston into the layer at constant speed and depth, imitating the dipping of a finger into the paint<sup>123</sup>. Parallel experiments were carried out on paint layers of the same thickness and composition. Typical results for UB EY-poor TG paint layers are shown in Figure 4.9. The water content in the paint layer decreases linearly until a plateau is reached indicating that water evaporation is completed. As long as the paint is still liquid, the hardness of the paint surface remains low ( $\leq 0.001$  N/mm<sup>2</sup>), but this value increases by more than two orders of magnitude when film formation sets in and approaches a plateau, which characterizes the “dry-to-touch” state of the paint when a solid film is formed (Supplementary Figure 4.19). Similar results for LW EY-poor TG paint layers are found in Supplementary Figure 4.20.

Both *tempera* and *tempera grassa* paints (regardless of the pigment type and the quantity of EY) are “dry-to-touch” after  $\approx 25$  min of drying: a solid film is formed, and another layer of paint can be applied on top of it (Supplementary Table 4.2). It should be noted that paint layers were applied here on sample holders made of stainless steel at a paint layer thickness of  $h = 0.4$  mm (in the wet state). During painting, brush strokes are typically much thinner and the paint is commonly applied onto an absorbent substrate. Under such conditions drying times are usually much shorter, as discussed in the context of the brush stroke experiments shown in Figure 8. Here, experiments were carried out with unusually thick paint layers to ensure a good reproducibility. When the “dry-to-touch” state is reached, the paint still contains water, which continues to evaporate until drying is completed (around twice the time needed to reach the “dry-to-touch” state). Obviously, a complete evaporation of water is not necessary to obtain a solid film. Our data suggest, that the “dry-to-touch” state happens when the dense packing of the disperse phase is reached. In the example displayed in Figure 4.9, the “dry-to-touch” state occurs when the paint reaches a disperse phase volume fraction of  $\phi_{\text{dry-to-touch}} \approx 75$  vol%.

Most importantly, similar drying times for both *tempera* and *tempera grassa* systems are observed, showing that in both cases the formation of a solid film is controlled by the water evaporation, and that the presence of oil droplets does not significantly interfere with this physical mechanism. In contrast, the drying of oil paints is controlled by oxidation and typically takes much longer.<sup>123</sup> This information is crucial for painting, because it means that a *tempera grassa* does not differ significantly from a *tempera* in terms of drying: adding oil does not help to increase the drying time, thus the artist will not be able to work wet-in-wet as with an oil paint.

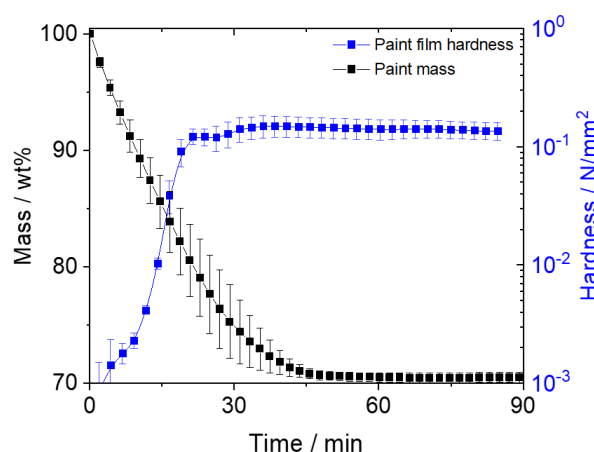


Figure 4.9 - Water loss (black) and mechanical hardness (blue) versus time for UB EY-poor TG paint layers. Layers have a controlled thickness of  $h = 0.4$  mm. All experiments were performed in triplicate (Supplementary Figure 4.19). Displayed data points refer to the average value at a given time and the error bars represent the standard deviation.

Although the *tempera grassa* paint dries by evaporation of water in the first place, the drying oil included in the paint is expected to undergo chemical changes upon time. In a drying oil, peroxide formation occurs upon curing by addition of oxygen, and results in a gravimetrically detectable mass increase. For oil paints, this onset of oxidation and cross-linking corresponds to the “dry-to-touch” state of the paint film, accessible via hardness measurements.<sup>123</sup> Accordingly, for *tempera grassa* paints, a mass increase is expected when the oil curing sets in, and thus, a second hardening step is expected. This was measured experimentally: after the first plateau in hardness, corresponding to the dry-to-touch state (as discussed above, see Figure 4.9), a second steep increase and subsequent plateau in hardness occurs long after water loss is complete, simultaneously with a significant increase in mass (Figure 4.10).

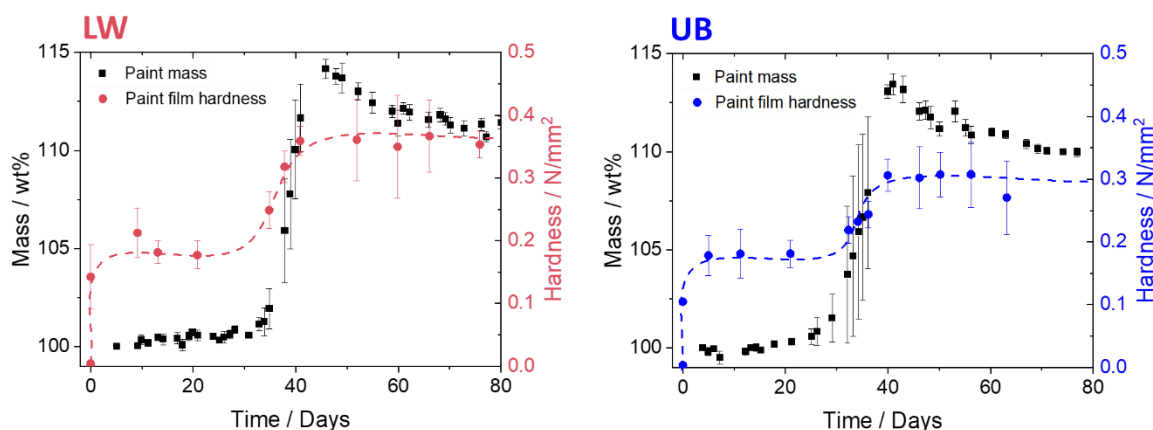


Figure 4.10 – Kinetics of mass increase (black symbols) and film hardening (LW in red, UB in blue) for EY-poor TG paint films (composition as described in Table 1). The paints thickness layer is  $h = 0.4$  mm. Note, the mass uptake is normalized to the oil content.

In EY poor TG paint films (thickness  $h = 0.4$  mm) the second mass increase step occurs about 35-40 days after film formation irrespective of whether LW or UB are used as pigment.

A dependency is observed though as a function of the EY content. This is shown in Figure 4.11 where the time of the second step mass increase for different UB *TG paints* is shown as a function of increasing amounts of EY. EY considerably postpones the mass increase, and at a dry EY content of about 55 vol%, the onset of oxidation of the oil is delayed for about 1 year.

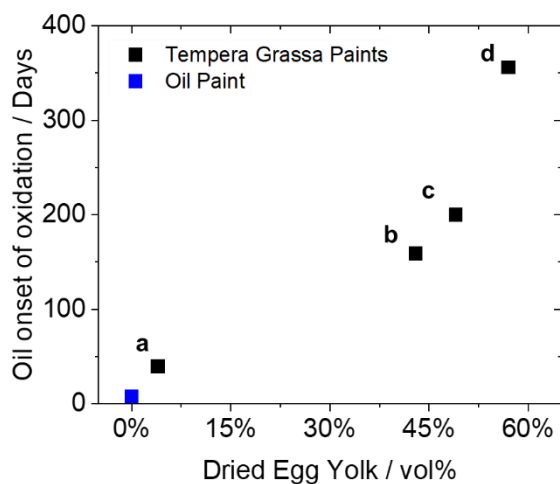


Figure 4.11 – UB-based tempera grassa and oil paint's onset of oxidation from gravimetric measurements at a layer thickness  $h = 0.4$  mm. The oil paint contains 48 vol% of UB and 52 vol% of linseed oil. TG paints were prepared with the following composition, after evaporation of water: (a) is the EY-poor TG in Table 1 and contains 28 vol% of UB, 4 vol% of EY and 68 vol% of LO, (b) is the EY-rich TG and contains 24 vol% of UB, 45 vol% of EY and 31 vol% of LO, (c) contains 15 vol% of UB, 49 vol% of EY and 36 vol% of LO and (d) contains 3 vol% of UB, 57 vol% of EY and 41 vol% of LO.

To prove that the second mass increase can be ascribed to the oil curing, evolved gas analysis – mass spectrometry (EGA-MS) was used. When peroxide species are present in a paint layer, their thermal decomposition occurs at around 140-180°C.<sup>123</sup> Moreover, when a polyunsaturated lipid undergoes oxidation, several volatile molecules, such as short chain alcohols, aldehydes and acids are produced<sup>48,55,100,101,159,160</sup>. These evaporate at relatively low temperatures ( $T < 200$  °C).<sup>56</sup> Such effects, the decomposition of peroxide species and evaporation of relatively volatile species, are both visible in TGA and EGA-MS measurements. Figure 4.12 shows the initial portion of the EGA-MS curves of LW EY-rich TG at 30 days and 160 days of natural ageing, with the corresponding mass spectra at 160 days (the complete curves, in extracted ion mode are shown in Supplementary Figure 4.27 and Figure 4.29). The mass spectra relative to the same region at 30 days are shown in Supporting Figure 4.26. At 30 days the evolution of volatile species up to 200°C is negligible, while a peak is clearly visible at 160 days. For comparison, a LW oil paint prepared as described in (Ranquet et. al)<sup>123</sup> shows a similar peak, characterized by similar mass spectral features, both at 30 days (Supplementary Figure 4.26d,f) and 160 days (Figure 4.12d,f). In particular, the mass spectra of LW EY-rich TG in the region between 130 and 210 °C at 160 days (Figure 4.12c,e) and those of LW oil paint in the same region both at 30 days (Supplementary Figure 4.26d,f) and at 160 days (Figure 4.12d,f) are characterized by fragment ions which are abundant in the mass spectra of short chain alcohols ( $m/z$  57 – 1 penten-3ol and 1-hydroxyl butanone;  $m/z$  53, 72, 99 – 1-octen-3-ol), 2-pentyl furan ( $m/z$  91, 98, 138), unsaturated aldehydes ( $m/z$  70, 83, 97 112 – 2-heptenal;

m/z 70,83, 97, 108, 125 -2-octenal; m/z 70, 83, 96, 111 – 2-nonenal; m/z 70, 83, 98, 110, 125 – 2-decenal) and polyunsaturated aldehydes (m/z 81, 110 – 2,4-heptadecadienal; m/z 81, 109, 138 – 2,4-nonadienal). These are typical products of autoxidation of polyunsaturated lipids<sup>56</sup>, which are not observed among the compounds evolved below 210 °C in EY-rich TG at 30 days of ageing (Supporting Figure 4.26c,e).

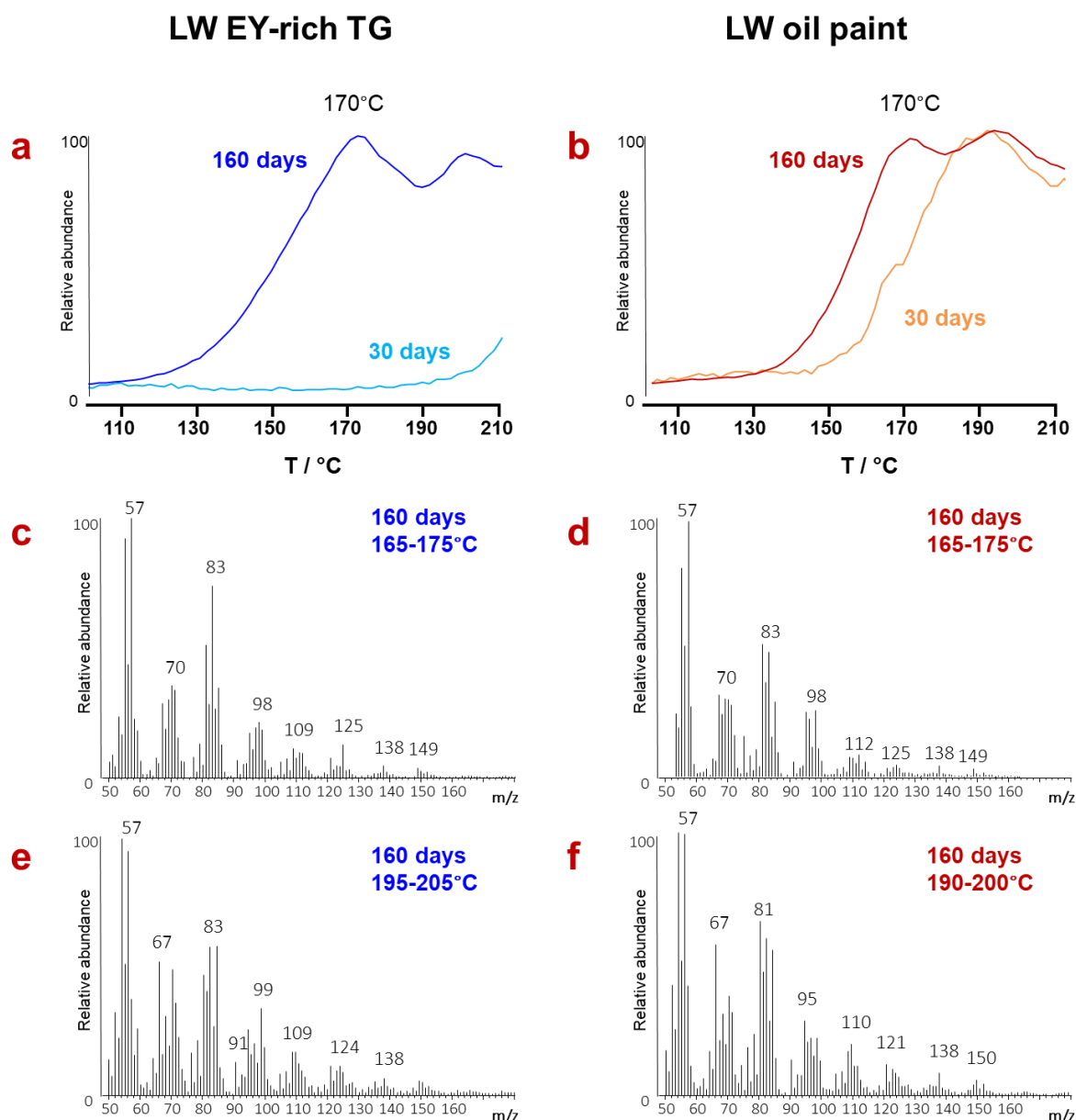


Figure 4.12 – – **a-b** EGA-MS total ion chromatogram curves of LW EY-rich TG (left) and LW oil paint (right) at 30 and 160 days of ageing; **c-d** average mass spectra corresponding to the paints at 160 days in the temperature range 165-175 °C; **e** average mass spectrum of LW EY-rich TG at 160 days in the temperature range 195-205 °C; **f** average mass spectrum of LW oil paint at 160 days in the temperature range 190-200 °C. Both paints have the same pigment : oil ratio ( $\approx 0.5$  in volume).

The mass loss due to peroxide decomposition and evaporation of volatile molecules was monitored by TGA on multiple samples collected at different time intervals. The mass loss% as observed by TGA experiments was then compared to the mass increase measured gravimetrically and

Supplementary Figure 4.22 shows the data of the LW EY-rich TG paint layer: the mass increase is clearly synchronized to the lipid oxidation.

As already shown for oil paints, peroxide and other active radical species appear in the paint layer before the mass uptake sets in: the presence of antioxidants in the oil itself, the natural antioxidant effect of proteins, the presence of phospholipids, phosvitin, carotenoids, vitamin E, and free aromatic amino acids in egg<sup>123,146</sup> prevent the establishing of autoxidative radical chain reactions. We can detect the presence of peroxide species and other active radical species with differential scanning calorimetry (DSC). DSC of curing of oil paintings shows an exothermic peak at temperatures below 200°C, which is due to the overall superposition of two phenomena: the decomposition of peroxides (endothermic) and the recombination of radicals (exothermic).<sup>123</sup> Note, evaporation of low molecular weight compounds also occurs < 200 °C, as described above, but in DSC experiments it is not observed as the pans where measurements are carried out are sealed, impeding evaporation. The DSC curves obtained from a LW EY-rich TG paint sampled at regular intervals are shown in Supplementary Figure 4.22. The detection of a clear exothermic DSC peak below 200°C – which thus indicates the presence of active species (peroxides and radicals) - is observed before (Supplementary Figure 4.22c, at 90 days) the second overall gravimetric mass increase takes place (Supplementary Figure 4.22b, at 140 days). The antioxidant effect operated by egg components may be explained in several ways, which include the inactivation of reactive oxygen species, free radicals scavenging, reduction of hydroperoxides, and stabilization of peroxides.<sup>161</sup> In TG paints the stabilization of radical species is very clear: the onset temperature of the DSC peroxide decomposition/radical recombination peak in the first stages of curing is significantly higher than the one of oil paints containing no proteins (Supplementary Figure 4.23). The lowest onset temperature in the TG system is observed exactly when the maximum intensity of the exothermic peak is registered, and when the mass increase reaches a plateau, as was observed in oil paints. On the longer term, the onset temperature of this peak reaches the same value for all systems, irrespective of their composition.

#### 4.3.4. Complex oil-proteinaceous material interactions

We investigated the role of the paint microstructure, resulting from different paint preparation techniques (Supplementary Figure 4.24), on the natural air-drying kinetics and further curing reactions of the oil. In particular a set of paints of almost identical composition in the dried state with little EY amount were prepared (4 vol% of EY dried matter in the dry paint, to allow short curing times - see Figure 4.11) following different preparation procedures. In addition to a *tempera* grassa TG, two oil paints were prepared, the first one called Protein Coated Pigment (PCP) and the other Capillary Suspension (CapS). PCP and CapS are oil-based paints prepared as described in (Ranquet et.al).<sup>123</sup> Briefly, in PCP the pigment particles are uniformly coated by a layer of EY, and are subsequently dispersed in the oil, which is the continuous phase. In CapS, the oil paint is added



with small amounts of egg, which forms capillary bridges among pigment particles: EY is unevenly distributed in the contact regions between adjacent particles. A schematic representation of the paint microstructures following the different preparation procedures is proposed in Supplementary Figure 4.24. We compared the curing kinetics of these paints gravimetrically as shown in Figure 4.13. The formation of peroxides and the resulting mass uptake of the oil is monitored via mass change of a paint layer over time. LW is a known catalyst for the oxidation of drying oils<sup>162</sup> and its catalytic action is presumably carried out mostly upon dissolution into the oil, with formation of lead soaps acting as actual catalysts.<sup>163,164</sup> We previously showed that when egg yolk is used as a pigment coating (*PCP*), it acts as an antioxidant shield and blocks direct interactions between the pigment and the oil, strongly delaying the curing process. In *CapS* paints, the majority of the pigment surface is in direct contact with the oil resulting in paints having drying times close to the ones of pure oil paints. In both oil paints (*PCP* and *CapS*), the profile of the mass change is characterized by a steep increase, followed by a plateau.<sup>47</sup>

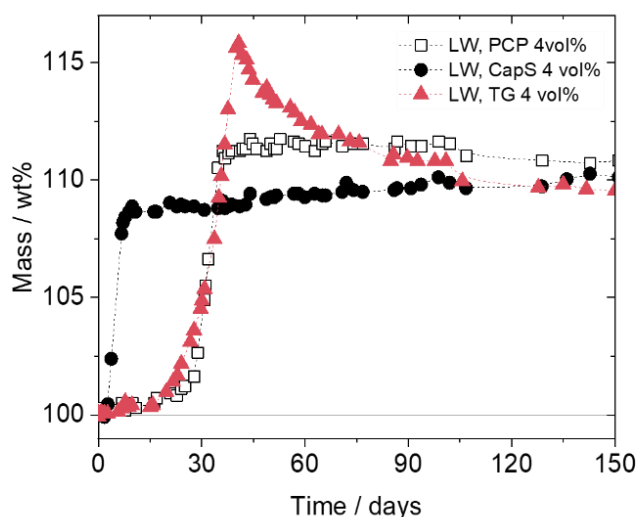


Figure 4.13 – Kinetics of mass increase, normalized to the oil content, for LW paints prepared as *CapS* (●), *PCP* (□) or *TG* (▲) at a layer thickness  $h = 0.4$  mm. Each paint is composed of 4 vol% of EY dry matter, 28 vol% of LW and 68 vol% of linseed oil in the dried state.

In the *TG*, a significant delay in the mass uptake is also observed, similar, to the delay found in *PCP*. This late onset of oxidation is expected since the pigment is not in direct contact with the oil. The shape of the curves is different though: the *TG* curve exhibits a pronounced maximum immediately after its steep increase and declines to approach a plateau gradually upon time (Figure 4.13). This gradual mass loss observed after 40 days of natural ageing cannot be attributed to the loss of residual water, which is confirmed by thermal gravimetric analyses: although water is present in *TG* paints at day 0, it is fully evaporated by the time the oil curing sets in (Supplementary Table 4.3 and Figure 4.25). In the range of  $T = 50$ - $150$  °C, no significant mass loss other than the one ascribed to the peroxide decomposition/evaporation of oxidation products (at  $T \approx 150$  °C, also present in pure oil paints) could be detected (Supplementary Figure 4.22). The different shape of



the mass profiles of *PCP* and *TG* paint in Figure 4.13 is a clear indication that the chemical reactions occurring in these paints, which have the same composition after evaporation of water, are affected by the wet paint microstructure. Further investigations are necessary to reveal the chemistry behind the different curve shapes observed in Figure 4.13, and the microstructural differences between *TG* and *PCP* paints after evaporation of water, which is most likely responsible of the different chemical reactions occurring among EY and oil components.

#### 4.3.5. Aging

Evolved gas analysis coupled with mass spectrometry (EGA-MS) was used to analyze the evolution of compounds produced upon thermal decomposition by the paint layers over 3 years of natural ageing<sup>56</sup>.

The thermograms of the egg containing paints present three main thermodegradative regions (Supplementary Figure 4.27 and Figure 4.28):

- The first, up to about 320°C, is dominated by 2,5-diketopiperazines – (DKPs,  $m/z$  154), and nitriles, such as hexa- and octadecanonitrile (characteristic fragment ions including  $m/z$  110, 194, 208, 222, 236)<sup>165–168</sup>. DKPs are the products of depolymerization of proteins upon pyrolysis<sup>81,168,169</sup>. Aliphatic nitriles are yielded by the thermal decomposition of the products of chemical interactions between lipids and proteins.<sup>168</sup> Most likely these products contain imine groups formed between the acidic moiety of fatty acids belonging to the egg lipid fraction and amine groups present on the polypeptide chain, and produce nitriles upon pyrolysis.
- The second region – between about 320°C and 390°C – is due to the thermal decomposition of di- and triglycerides containing palmitic, oleic and stearic acids (with characteristic fragment ions at  $m/z$  129, 185, 213, 241, 256, 264 and 284, see Supplementary Figure 4.27 and Figure 4.28). EY is naturally composed of a great quantity of mono-unsaturated ( $\approx$  49%) and saturated fats ( $\approx$  35%)<sup>170</sup>. The temperature at which thermal decomposition occurs indicates that these are non-polymerized lipids.
- The third thermodegradative region, above about 390°C, is due to the thermal decomposition of the cross-linked fraction. This can be concluded from the mass spectral features of the compounds evolved in this region, which present fragments ions ascribable to the tropylium ion ( $m/z$  91) and  $C_6H_5-C\equiv O^+$  ( $m/z$  105)<sup>56,81</sup>. Such cross-linked fraction is observed in the pyrolysis of proteinaceous materials, and is ascribed to the thermal decomposition of the residual material formed in a protein when loss of side chain and depolymerization have taken place.<sup>81</sup>

For comparison, the EGA-MS data of oil paints are presented as well (Supplementary Figure 4.29). The oil paint layer analyzed at increasing ageing time presents very little changes. The shape of the curves and the mass spectral features associated with the different thermodegradative zones are typical of a cured oil paint.<sup>56,171</sup> In particular, besides the relatively low molecular weight

products of oxidation, which are evolved below 200-250 °C, two main – partially superimposed - thermodegradative regions are observed at all ageing times, the first between about 300 and 400°C and the second above  $\approx 390^\circ\text{C}$ . The first region presents the mass spectral features of products of thermal decomposition of glycerides (fragment ions at  $m/z$  129, 185, 213, 241, 256, 264 and 284, see Supplementary Figure 4.28). Given the temperature at which thermal decomposition occurs, we can conclude that these derive from the pyrolysis of cross-linked glycerides. It must be noted that free glycerides are not observed in LW oil paint, even at 30 days of ageing, due to the fast curing of LW-based oil paints.<sup>47</sup> The last thermodegradative region above  $\approx 390^\circ\text{C}$  is due to the thermal decomposition of the highly cross-linked polymeric network, which shows the same mass spectral features of the last thermodegradative region of the *tempera*-based paints ( $m/z$  91,  $m/z$  105).<sup>171</sup> This is because in an EGA-MS experiment, the sample is progressively heated ( $20^\circ\text{C}/\text{min}$ ), undergoing progressive evaporation and thermal decomposition. When the temperature increases to high values (above  $\approx 380\text{-}400^\circ\text{C}$ ) the residual sample is a highly cross-linked charred material, which produces aromatic compounds upon further heating.

Differences are observed between the glyceride fractions of *oil* and *tempera grassa* paint layers, and different changes occur with time. At 30 days, LW EY-rich TG presents both free glycerides – egg lipid fraction – and cross-linked glycerides – those deriving from the cross-linking of polyunsaturated fatty acids of linseed oil. This cross-linked fraction is unexpectedly not detected in the analyses carried out at longer ageing times, while it remains visible also after 3 years in LW oil paint.

Differences are also observed between the *tempera* and *tempera grassa* paint layers, and different changes occur with time, although they become evident only after three years of ageing. In the *tempera* paint, carbonyl groups of egg lipids chemically interact with amine groups in proteins, and this interaction increases with time. As a result, a significant relative increase in the evolution of nitrile species upon pyrolysis is observed at 1200 days. This is comparable to what is observed in very ancient paintings (e.g. 18<sup>th</sup> century B.C.E mural paintings from Tel Kabri)<sup>172</sup>. At the same time, the thermal decomposition of the glycerides is significantly, relatively decreased, and shifted to higher temperature, indicating cross-linking. The relative increase in the signal relative to the evolution of nitrile species is not observed in TG paints, at least in the time period investigated here. A possible explanation is that proteins have reacted with the oil lipids, and are thus not available for further reactions with the egg lipids. This is in agreement with the fact that the signal relative to the oil cross-linked glycerides in the TG paints (peaking at around  $400^\circ\text{C}$ ) is visible at 30 days, but it is not observed at longer curing times: co-polymerization between proteins and polyunsaturated oil lipids has possibly taken place, as hypothesized for historical *tempera grassa* paints of the 20<sup>th</sup> century<sup>78</sup>.

#### 4.4. Summary and Conclusion

*Tempera* and *tempera grassa* artists' paints based on lead white or ultramarine blue pigments have been investigated with respect to their microstructure, flow behavior and drying characteristics. Fluorescence microscopy, centrifugation and IR-spectroscopy revealed that pigment particles remain in the continuous aqueous EY phase and, despite their hydrophobic nature, they do not enter into the oil droplets emulsified in a *tempera grassa*, which may be attributed to the adsorption of proteins from the EY on the pigment surface.

Both, *tempera* and *TG*, exhibit flow properties typical for colloidal dispersions. The disperse phase volume fraction  $\varphi$  is a most important parameter controlling the rheology of such systems. Our data suggest that for a *tempera* paint,  $\varphi$  should be calculated including the pigments as well as the EY dry matter, and for the *TG* the oil volume fraction has to be added as well. The high shear limiting viscosity diverges as predicted by the well-known Maron-Pierce model, with  $\varphi_m = 63$  vol% as maximum packing fraction for the investigated *tempera* paints, whereas higher  $\varphi_m$  values up to 74 vol% were found for the *TG* due to the broad size distribution of the oil droplets. Beyond a critical value  $\varphi_c < \varphi_m$ , in both *tempera* and *TG*, a sample spanning network forms and the samples exhibit a yield stress. The value for  $\varphi_c$  increases monotonically with increasing oil content. To achieve similar flow behavior, the total volume fraction of a *TG* must be higher than that of *tempera* paint. But even if yield stress and viscosity function match, this does not necessarily lead to similar brush texture and appearance. On absorbent substrates, such as paper or traditionally primed supports, water is soaked up quickly, and the remaining oil droplets in *TG* keep the paint soft. Although this does not allow for working wet in wet, it may enable color transitions not achievable with pure *tempera*.

*Tempera* paints are known to dry quickly. As a *tempera grassa* is a *tempera*, with water being the continuous phase, the dry-to-touch state is reached for both paints even prior to complete evaporation of water, at about  $\varphi = 75$  vol%, and the oil does not affect water evaporation. Drying of these paints with their aqueous continuous phase happens within minutes and is hence much faster than for oil paints. Accordingly working wet-in-wet is not possible.

Hardness measurements and gravimetry showed that in *TG* a second hardening step occurs, accompanied by a significant mass uptake. At low EY content 4 vol% and paint thickness of 0.4 mm on non-absorbent substrate, this happens after 35-40 days. Thermoanalytical techniques and mass spectrometry demonstrated that the second hardening step is due to the oil curing, which is significantly delayed by the presence of egg. This antioxidant effect was also observed when egg is used as a pigment coating in an oil paint. Data show that the paint microstructure affects the chemistry of the oil curing and different reactions take place when oil is the disperse phase rather than the continuous phase. More research is necessary to better clarify the chemistry of these systems. Mass spectrometry finally showed that oils and proteins chemically interact with each

other with time, probably leading to copolymerization between the oil poly-unsaturated lipids and proteins moieties.

The study clearly demonstrates that a *tempera grassa* remains a *tempera*. For example, the drying time and thus the possibilities to create color transitions, do not change significantly when adding oil to a *tempera* paint. Thus, a *tempera grassa* cannot be considered a paint medium with intermediate properties between *tempera* and oil paints, although this is sometimes assumed.<sup>153</sup> More research is clearly necessary at this point in order to distinguish whether *tempera grassa* was the technique used, rather than an oil paint in which protein coated pigment particles were dispersed, when egg and oil are found in the same paint layer. If it will be proven that *tempera grassa* was actually used by artists, we still need to understand why this was done - possibly to achieve specific artistic effects, such as handling and optical properties, which Old Masters took advantage of to optimize their paints.

#### **4.5. Acknowledgments**

This research was supported by the University of Pisa (BIHO 2018 - MAMO), the German Academic Exchange Service France (DAAD), and the KIT Campus Transfer GmbH (KCT). The experiments were performed in part at the Karlsruhe Institute of Technology (KIT) in Germany and in part at the University of Pisa in Italy. We thank S. Baroni for helpful discussion concerning the paint preparations, H. Telle Jiménez (KIT) for the realization of the dry-to-touch experiments, R. Carosi (University of Pisa) for the support and carrying out some thermal analyses, and K. Bertsch (KIT) for the sample photographs.

#### **4.6. Competing interests**

The authors declare no competing interests.

## 4.7. Supplementary information

### 4.7.1. *Tempera (grassa) and oil paints in historic artworks*



Figure 4.14 - Domenico Ghirlandaio and workshop, *Mary with Child and Saints Dominic, Michael, John the Baptist and Thomas*, c. 1490/94, 221.1 x 198.4 cm, Bavarian State Painting Collections, Inv. No. 1078. The painting is in tempera technique, but the cloths of St Thomas (on the right) with his hands and foot, the foot of St John the Baptist and the hands of Saint Dominic (on the left) are painted in oil. Picture: Sibylle Forster. Reproduced with Permission. See chapter 1 for more information.



Figure 4.15 - Jacopo del Sellaio, *The Martyrdom of St Sebastian*, c. 1465/73, 122.5 x 81.6 cm, Inv. No. 1352, © Bavarian State Painting Collections. Reproduced with Permission.

#### 4.7.2. Microstructure of tempera and tempera grassa paints

##### Centrifugation

We employed centrifugation and FTIR measurements to gain deeper insight into the phase composition of EY-rich *tempera* and *TG* paints. Samples including either UB or LW were centrifugated to separate the different phases of the paint, which were then analyzed by ATR-FTIR. Corresponding results are shown in Figure 4.16:

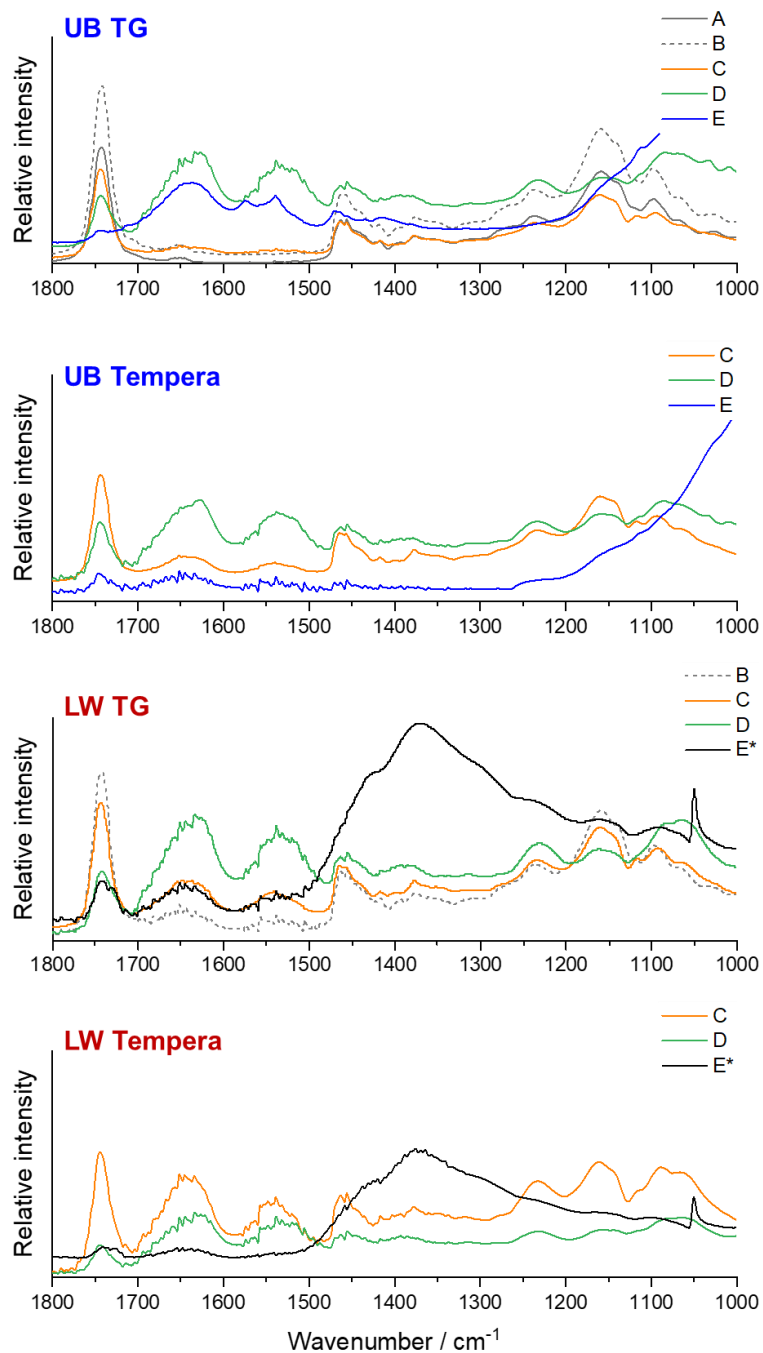


Figure 4.16 - ATR-FTIR spectra of EY-rich tempera and tempera grassa samples (Figure 4.3). After centrifugation, each phase was extracted and naturally air-dried, a piece of each sample was then analyzed with ATR-FTIR spectroscopy. Characteristic absorption bands for proteins are centered at  $1650\text{ cm}^{-1}$  and  $1540\text{ cm}^{-1}$ , identified as the amide I and II bands. A is the oil fraction, B is an oil-rich emulsion, C is an EY-rich phase, D is a transparent interphase region, E and E\* are respectively UB and LW pigment-rich phases. We could detect the presence of proteins in each fraction except for the oil fraction A.



### 4.7.3. Rheology of tempera (grassa) paints

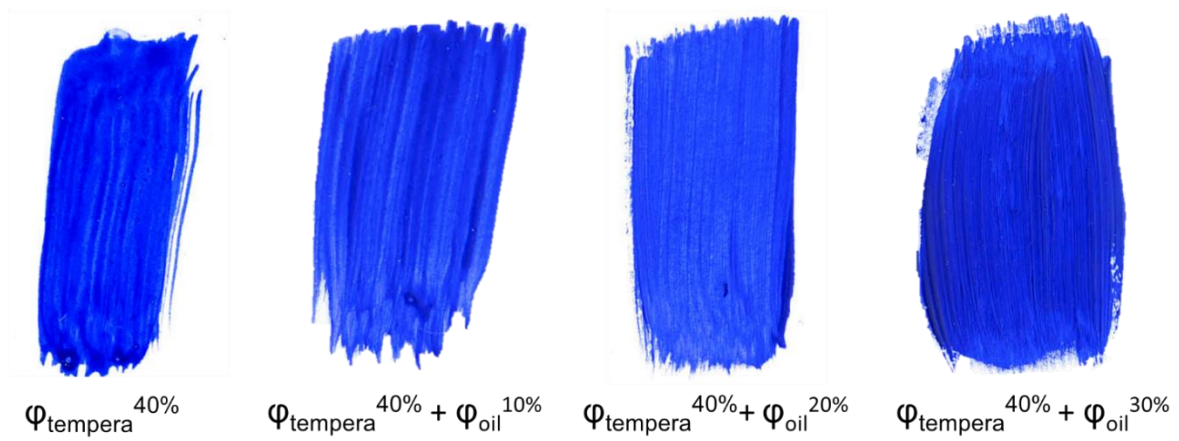


Figure 4.17 - Brush strokes of tempera and tempera grassa paints at a disperse fraction  $\varphi_{\text{tempera}} = 40 \text{ vol}\%$  with increasing oil content  $\varphi_{\text{oil}}$ . The paint with  $\varphi_{\text{tempera}}^{40\%} + \varphi_{\text{oil}}^{30\%}$  shows a clearly visible brush stroke profile after application on the paper, whereas the others are rather smooth.

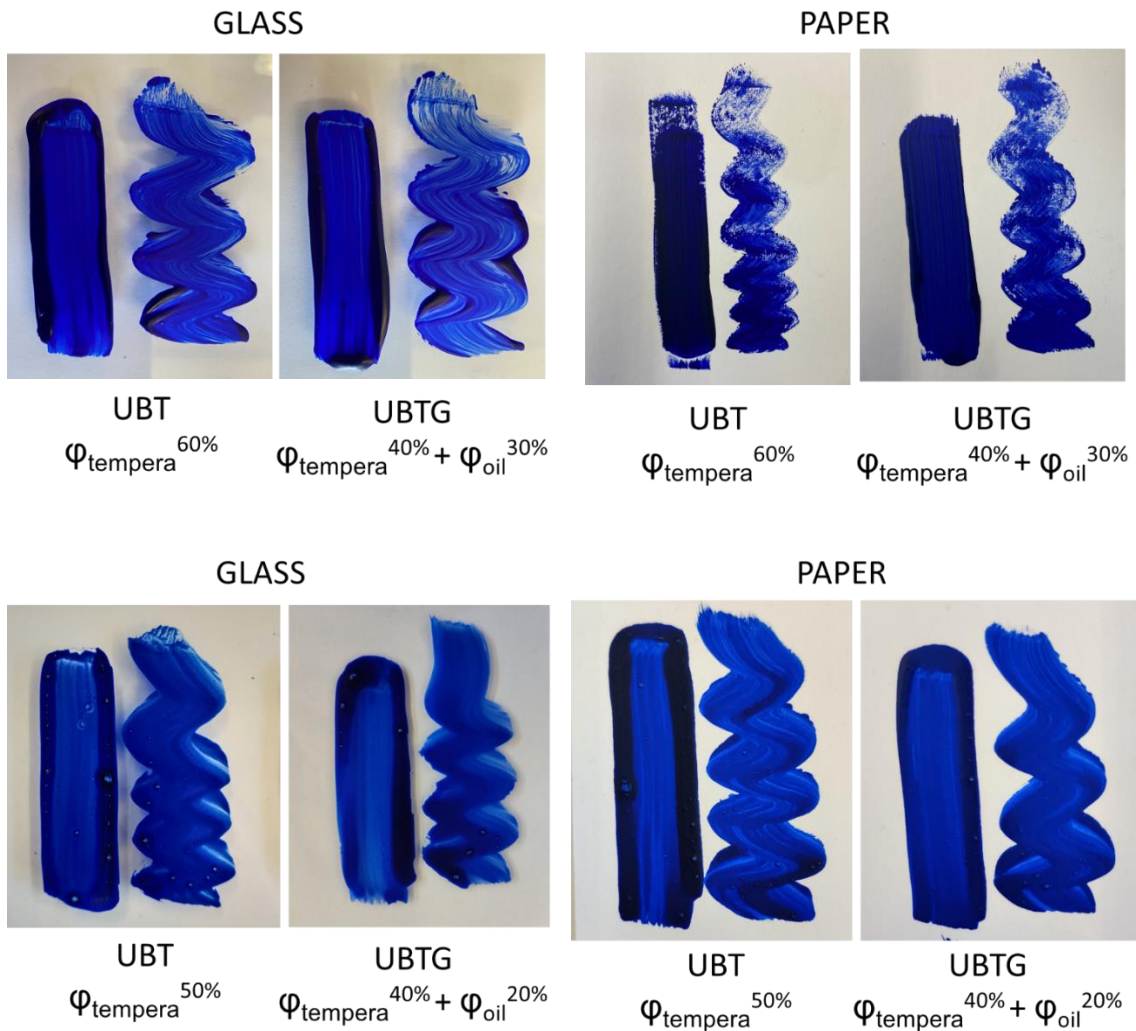


Figure 4.18 - Brush strokes of tempera and tempera grassa paints on glass and on paper.



#### 4.7.4. Film formation and drying kinetics

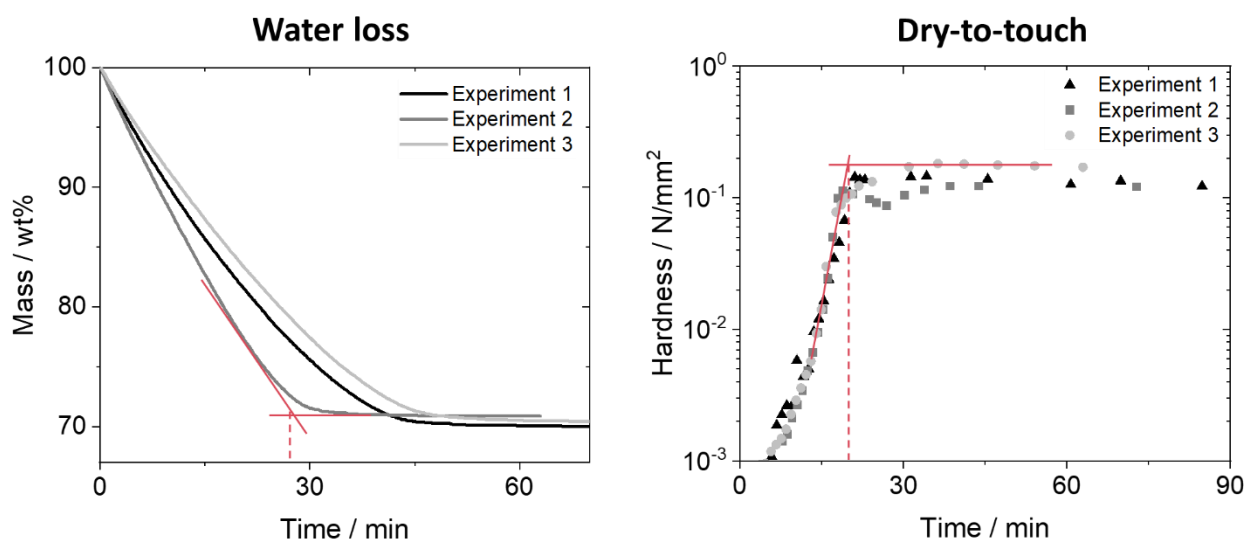


Figure 4.19 - (Left): gravimetric experiment for the determination of the water loss. (Right): change in mechanical hardness of the layer paint surface upon time. Water loss and dry-to-touch processes are considered as completed when the variation of mass and hardness are not significant anymore, represented by the dashed red lines. All experiments were performed in triplicates. The above-mentioned experiments were conducted with UB EY-poor TG paint having a controlled thickness of  $h = 0.4$  mm.

Table 4.2 - Drying time of EY-rich tempera and tempera grassa paints films of thickness  $h = 0.4$  mm in the liquid state. The error interval represents the standard deviation calculated from measurements performed at least in triplicate. Note that drying times can be much shorter when paints are applied on absorbent grounds.

Time / min	Dry-to-touch	Water loss
UB EY-rich <i>Tempera</i>	$27 \pm 10$	$79 \pm 7$
UB EY-rich TG	$25 \pm 3$	$47 \pm 10$
UB EY-poor TG	$20 \pm 3$	$37 \pm 9$
LW EY-rich <i>Tempera</i>	$27 \pm 4$	$78 \pm 4$
LW EY-rich TG	$30 \pm 8$	$82 \pm 10$
LW EY-poor TG	$20 \pm 2$	$54 \pm 7$

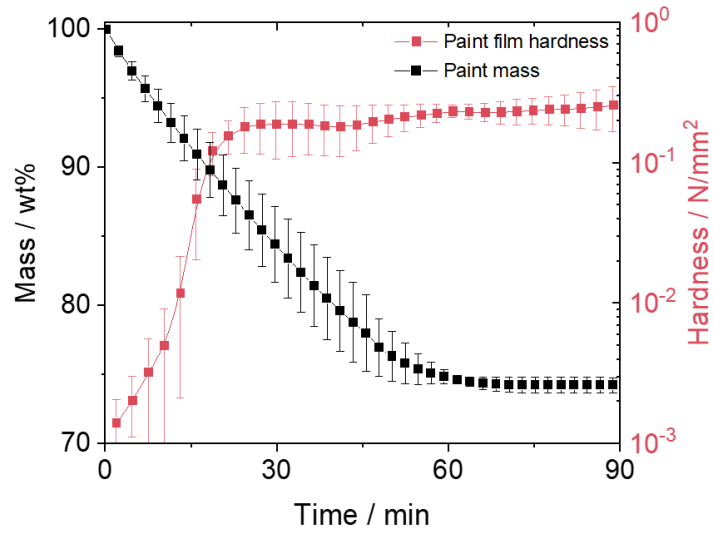


Figure 4.20 - Water loss (black) and mechanical hardness (red) versus time for LW EY-poor TG paint layers. Layers have a controlled thickness of  $h = 0.4$  mm. All experiments were performed in triplicate (Figure 4.19). Displayed data points refer to the average value at a given time and the error bars represent the standard deviation.

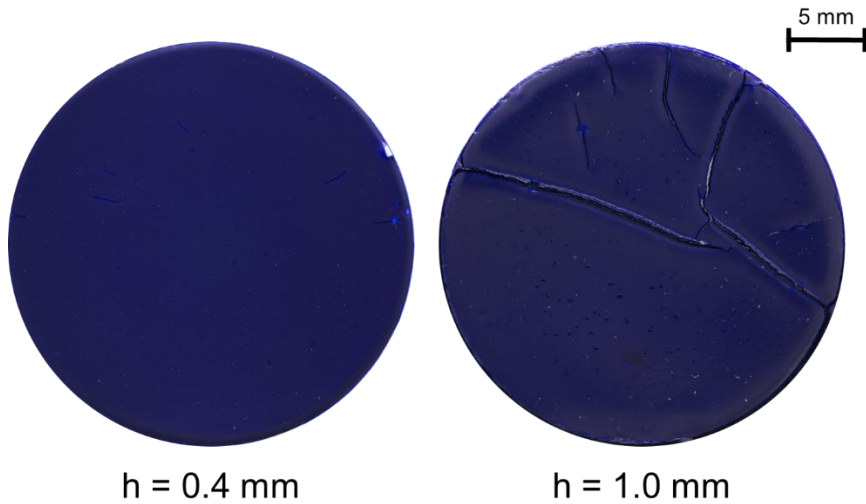


Figure 4.21 – Surface of dried UB-based TG samples with  $\varphi_{\text{tempera}}^{40\%} + \varphi_{\text{oil}}^{30\%}$  with a thickness layer of  $h = 0.4$  mm (left) and  $h = 1.0$  mm (right) in the wet state. The sample at a high thickness layer shows formation of cracks due to the evaporation of water upon drying.

#### 4.7.5. Complex oil-proteinaceous material interactions

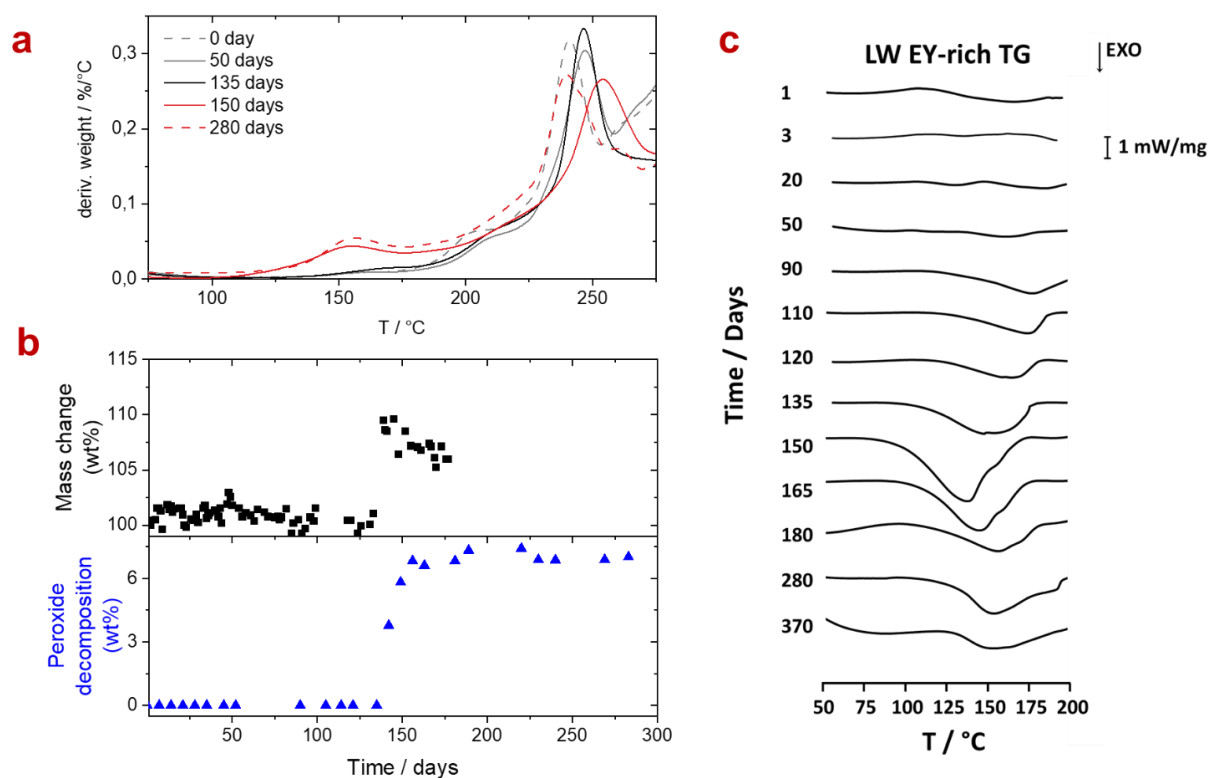


Figure 4.22 – **a** TGA curves derivatives, **b** comparison of the mass increase of the paint sample (above) and the associated peroxide decomposition performed by TGA measurements and **c** DSC curves under N<sub>2</sub>, normalized to the oil content, of a LW EY-rich TG (16 vol% of LW, 48 vol% of EY and 36 vol% of LO).

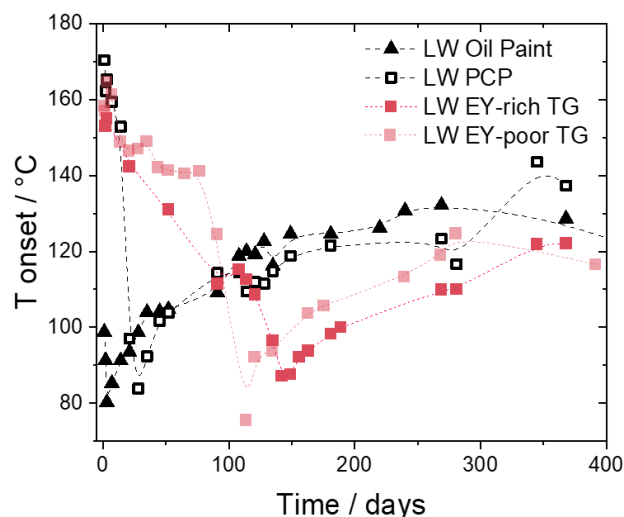


Figure 4.23 - Onset temperature of the overall exothermic peak associated to the decomposition of peroxides and hydroperoxides (endothermic) and the recombination of radical species (exothermic) as a function of the evaluation time. In the dried state, LW LO contains 31 vol% of LW and 69 vol% of LO, LW PCP is composed of 31 vol% of LW, 15 vol% (PCP) of EY and 54 vol% of LO, LW EY-rich TG contains 16 vol% of LW, 48 vol% of EY and 36 vol% of LO and LW EY-poor TG contains 27 vol% of LW, 13 vol% of EY and 60 vol% of LO.

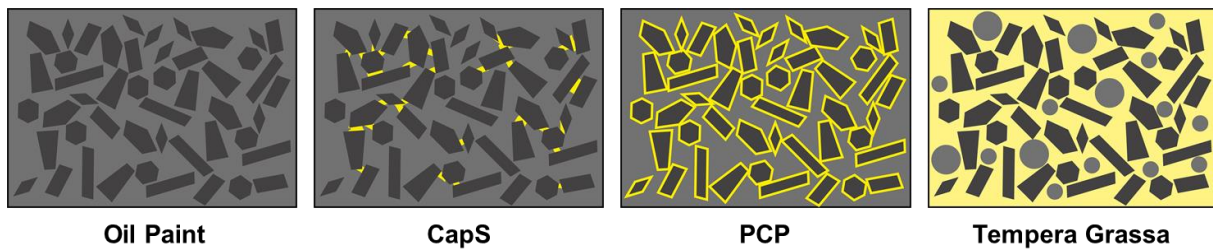


Figure 4.24 - Proposed scheme of the microstructure of the paint model systems in the dried state. The pigments are represented in black; the oil is in grey, the EY is in yellow (schemes from chapter 3 and Ranquet et. al)<sup>123</sup>. The oil paint, capillary suspension (CapS) and protein coated pigment (PCP) are oil-based paints. The tempera grassa is a tempera paint including emulsified oil droplets.

Table 4.3 - Mass loss from thermograms at 125 °C under N<sub>2</sub> of naturally air-dried samples. All values are displayed in wt%. The following compositions are given in the dried state: UB LO is composed of 6 vol% of UB and 94 vol% of LO. UB TG contains 3 vol% of UB, 56 vol% of EY dried matter and 41 vol% of LO. LW LO is composed of 31 vol% of LW and 69 vol% of LO. LW TG contains 16 vol% of LW, 48 vol% of EY dried matter and 36 vol% of LO. Raw data to be found in Figure 4.25.

Time / Days	UB LO	UB TG	LW LO	LW TG
0	< 0.1 %	26.2 %	< 0.1 %	0.4 %
21	1.0 %	1.5 %	0.5 %	0.6 %
269	1.3 %	1.5 %	0.3 %	0.5 %

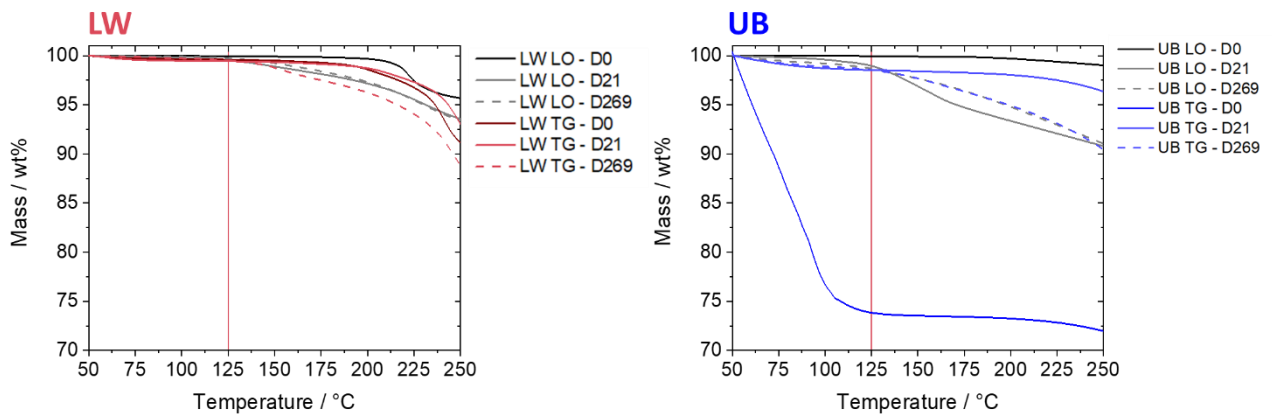


Figure 4.25 - Thermogravimetric data under N<sub>2</sub> at a heating rate of 20 °C/min of naturally air-dried samples upon time at day 0, 21 and 269 (respectively D0, D21 and D269).

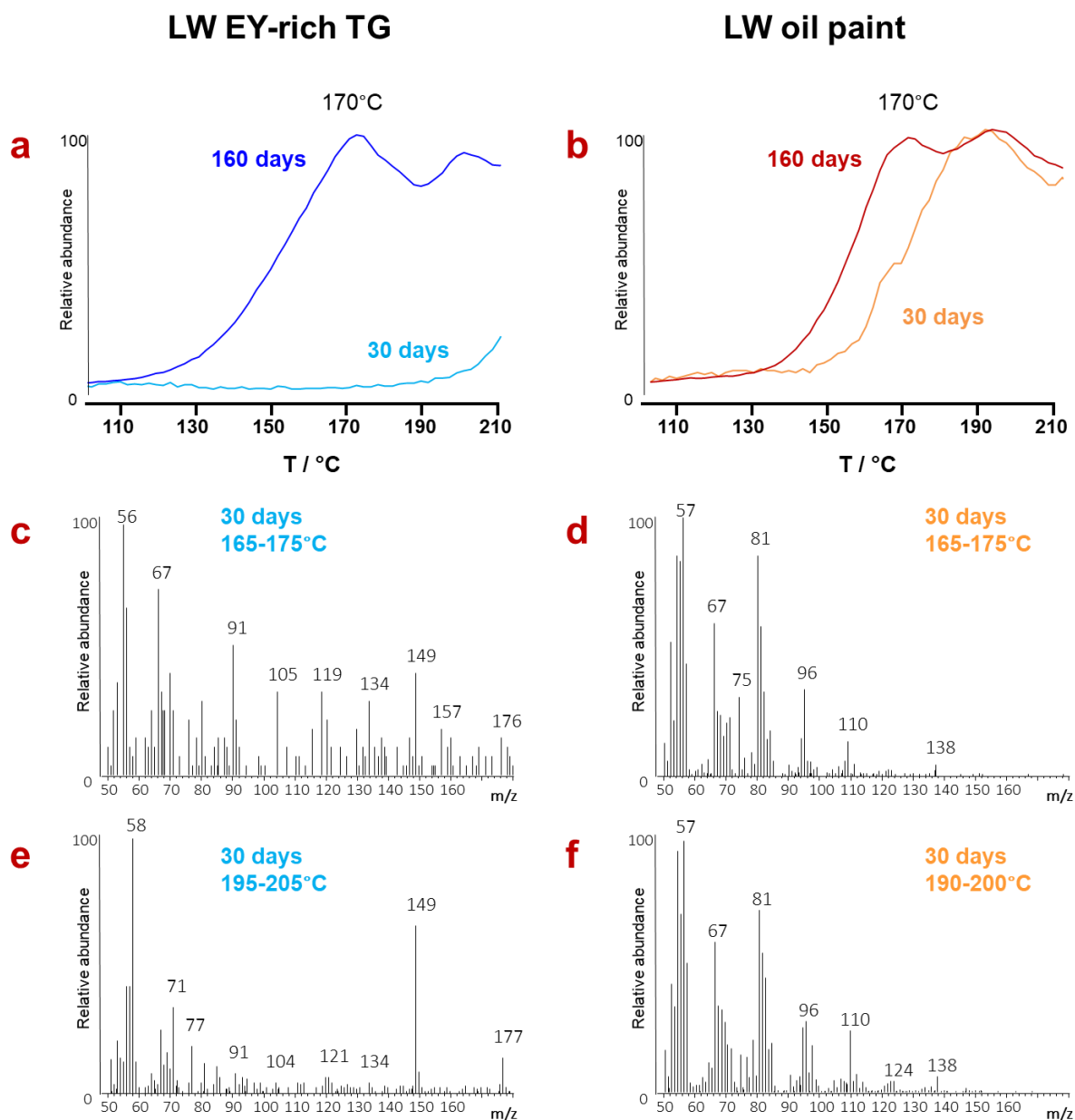


Figure 4.26 - **a-b** EGA-MS total ion chromatogram curves of LW EY-rich TG (left) and LW oil paint (right) at 30 and 160 days of ageing; **c-d** average mass spectra corresponding to the paints at 30 days in the temperature range 165-175 °C; **e** average mass spectrum of LW EY-rich TG at 30 days in the temperature range 195-205 °C; **f** average mass spectrum of LW oil paint at 30 days in the temperature range 190-200 °C.

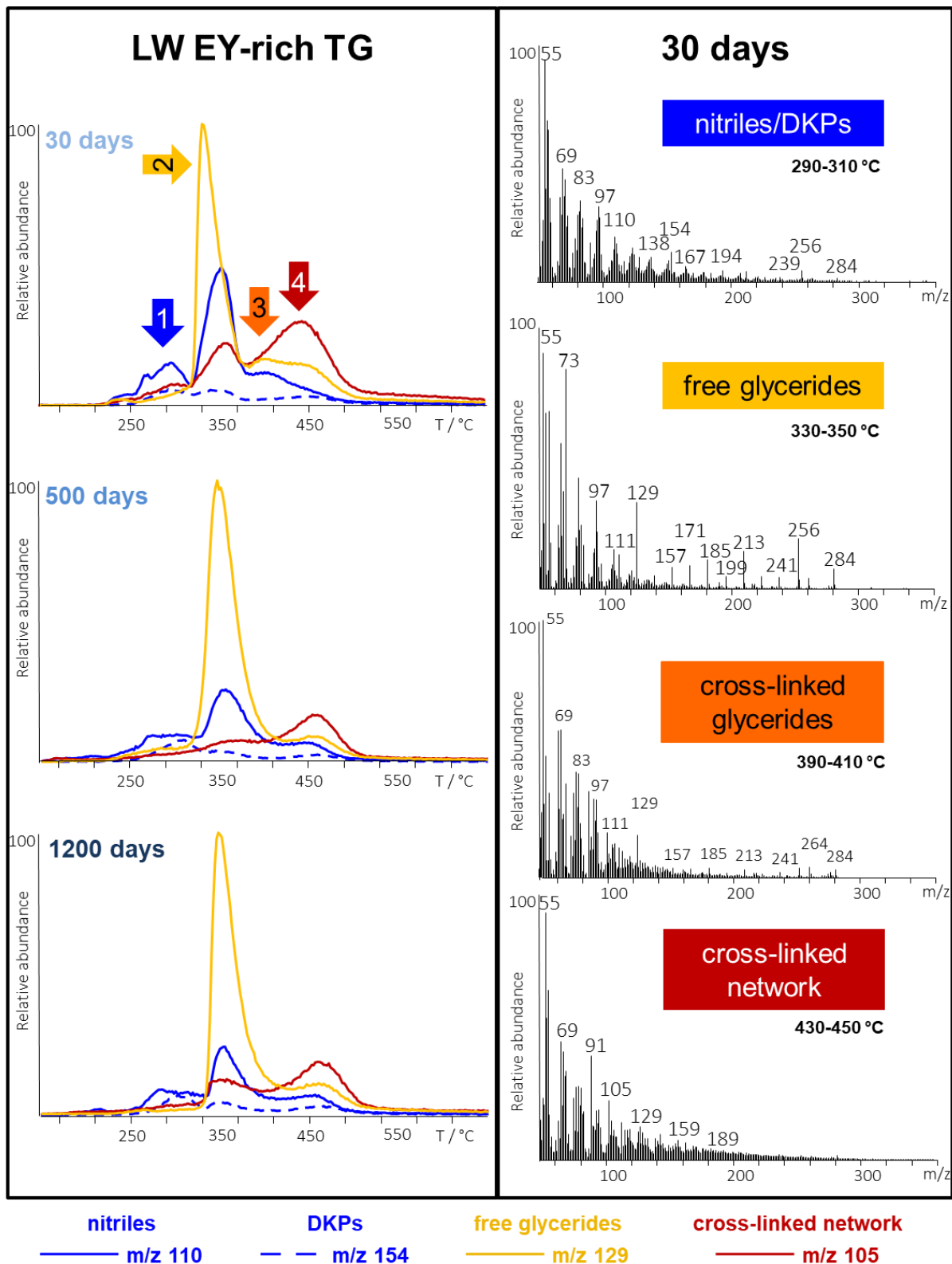


Figure 4.27 - Extracted ion thermograms of selected fragments of a LW EY-rich TG (left) and its corresponding mass spectra at 500 days of ageing at the indicated temperatures (right).

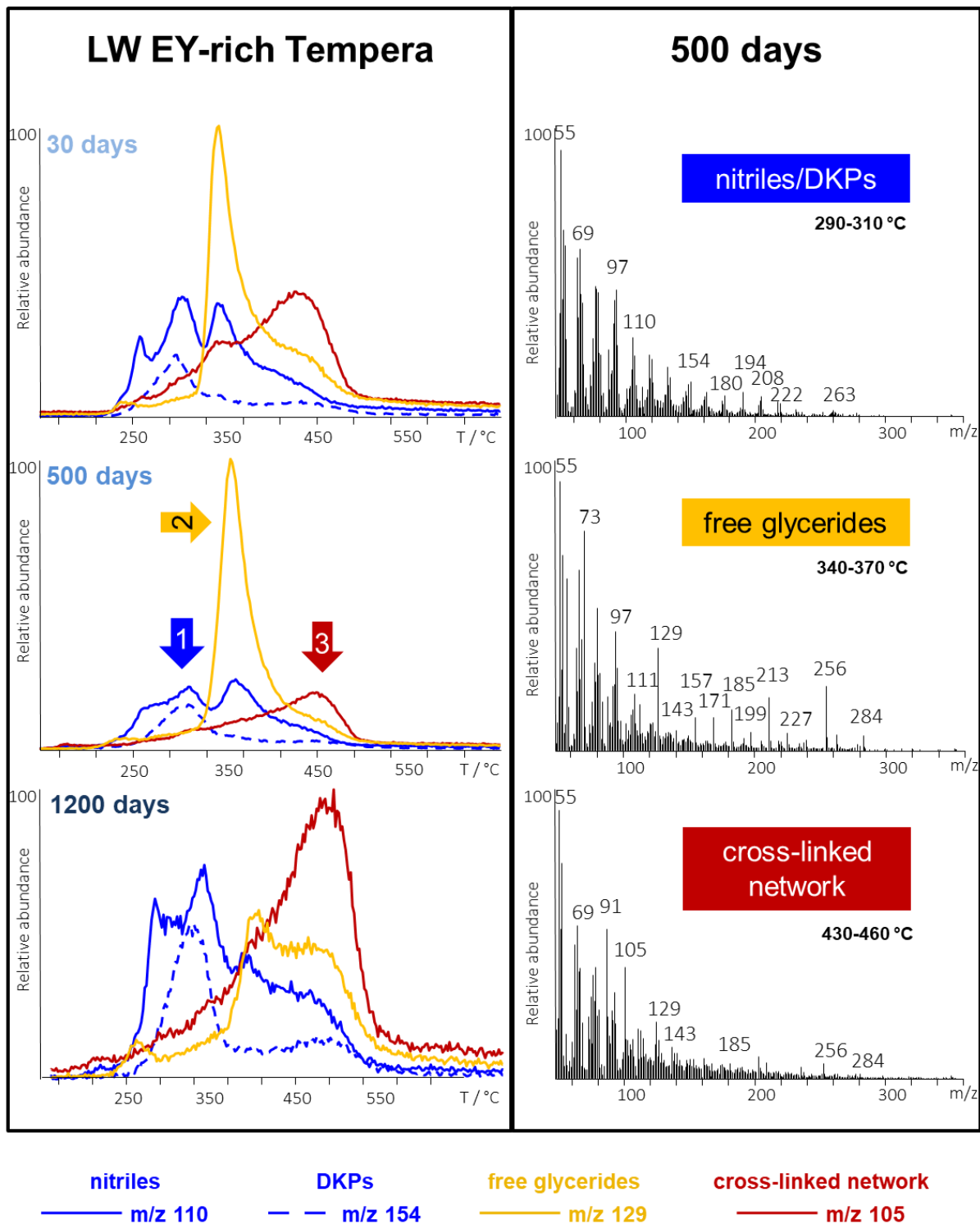


Figure 4.28 - Extracted ion thermograms of selected fragments of a LW EY-rich tempera (left) and its corresponding mass spectra at 500 days of ageing at the indicated temperatures (right).

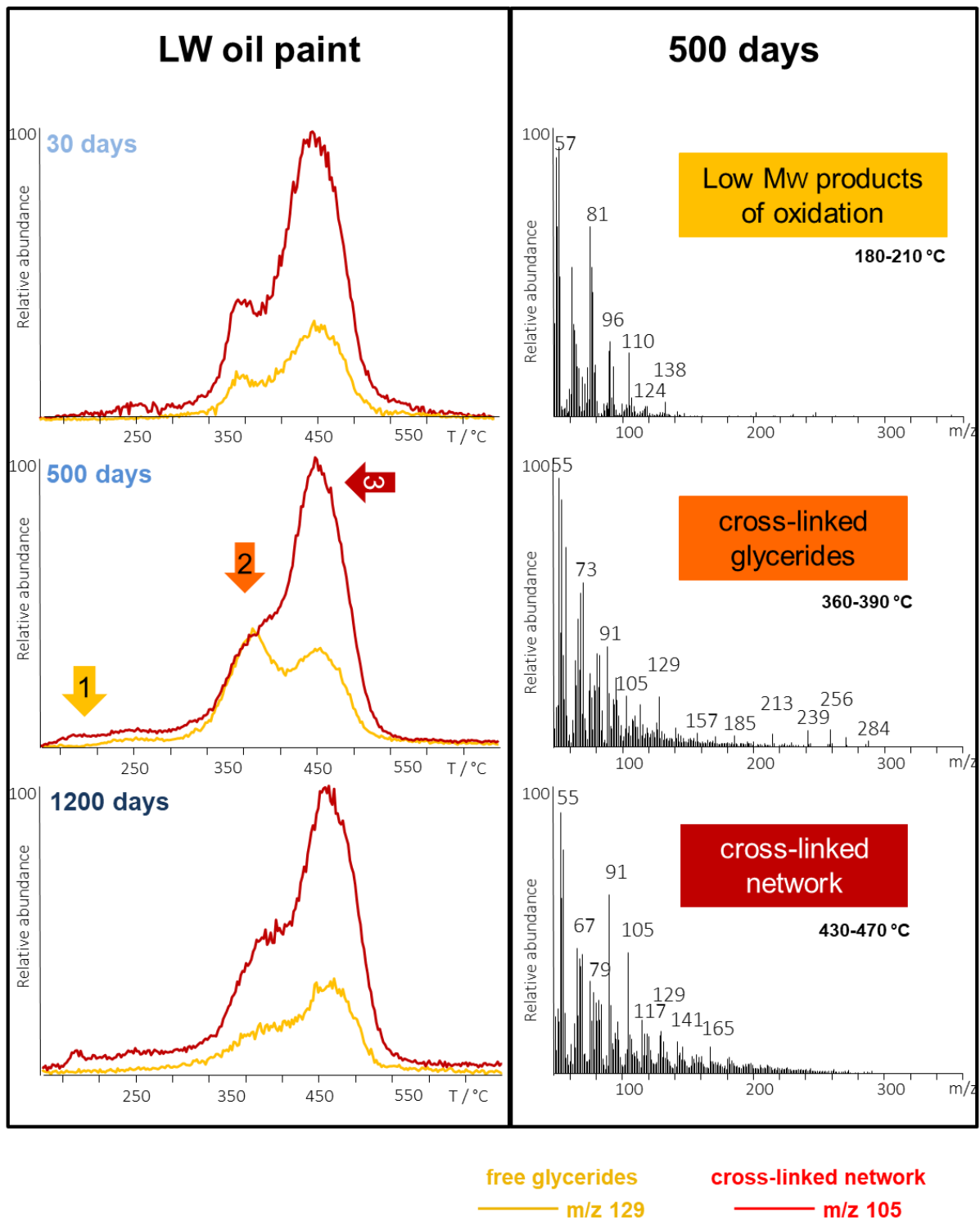


Figure 4.29 - Extracted ion thermograms of selected fragments of a LW oil paint (left) and its corresponding mass spectra at 500 days of ageing at the indicated temperatures (right).



## 5. From the flow properties to the final aspect of paints: complementary investigations on paint modifications

In this chapter, further topics investigated in the framework of this thesis are presented in different sections.

Additional information regarding the flow properties and drying behavior of oil paints is investigated in the first part of this chapter. First, the flow properties of oil paints with different volume concentrations of pigment covered with egg yolk are investigated and compared in terms of drying kinetics, in order to extend the understanding of this surface modification over a wider range of systems. Then, the influence of the thickness of the paint layers on drying and aging will be discussed. This parameter is an aspect not considered in most of the studies on the topic. However, it has been shown that the drying of thin films is influenced by the intrinsic properties of the paint such as its chemical composition (binder and pigment) and the thickness of the layer.<sup>49,50</sup> A large variation in layer thickness due to uncontrolled thickness of paint samples can therefore lead to significantly different results in the mechanical properties and in the chemical reactions taking place in the paint during the oil curing.<sup>39</sup>

Yellowing is an aspect particularly interesting in paintings because it contributes to the premature and unwanted aging of oil-containing paints over time. Therefore, we studied the influence of the preparation of paints with identical compositions (in CapS, PCP, TG) on the evolution of their color over time, to understand the role of their microstructure on yellowing.

It is often believed that other parameters than the modification of the paint's chemical composition, in particular the pigment shape and its particle size distribution might influence the flow and drying properties of the obtained paints.<sup>35,50,120,158</sup> Here we evaluate the role of the particle size distribution in the flow properties of ultramarine blue oil paints, their drying kinetics and color modification upon drying.

Finally, the last section of this chapter focuses on understanding the influence of protein distribution in the curing of oil-containing paints. This part is an extension of the work presented in both chapter 3 and 4. Particularly, artificial ageing is used to study the kinetics of drying of capillary suspensions paints, but also of *tempera grassa* paints with a significant quantity of egg yolk, which is more representative of the compositions found in TG paints typically described in historical recipes.

This chapter should, by its diversity, complement the other works presented in this thesis and offer a wider angle of understanding on the physico-chemical properties of paints containing both oil and egg yolk, both in their wet state and upon drying and curing.

## **5.1. Further investigation on the flow behavior, drying kinetics and wrinkling of oil paints**

This section summarizes further investigations regarding oil paint properties. It completes the information gathered and explained in the chapter 3 of this manuscript. Here, we examine the relationship between the flow properties of oil-based paints, with and without egg yolk additions, and their onset of drying at different solids content. Then, we investigate the influence of the thickness layer of oil paints on their “dry-to-touch” time, which may lead to the appearance of wrinkles at their surface.

### *5.1.1. Influence of the volume solids fractions on the flow behavior and drying kinetics of oil paints*

We showed in Chapter 3 that covering the pigment surface with a dry protein layer (*PCP paints*) might change the flow properties of these same oil paints prepared with uncovered pigments in paints formulations at identical solids fractions. However, increasing the amount of egg yolk in *PCP* paints can have a distinctly different effect depending on the pigment properties. The yield stress increases with increasing egg yolk layer thickness for UB pigments but decreases for LW pigment-based *PCPs*. For the UB-based paint, the increase of the yield stress results in an additional steric attraction<sup>140</sup> among the pigment particles, due to the hydrophilic surface layers attempting to minimize the contact with oil molecules. As a result, the particle network gets stronger and the yield stress of the paint increases accordingly. For LW paints, covering the pigment with a protein layer avoids the formation of a capillary network, which may form upon storage of the pigment in the ambient environment, resulting in a decrease of the yield stress.

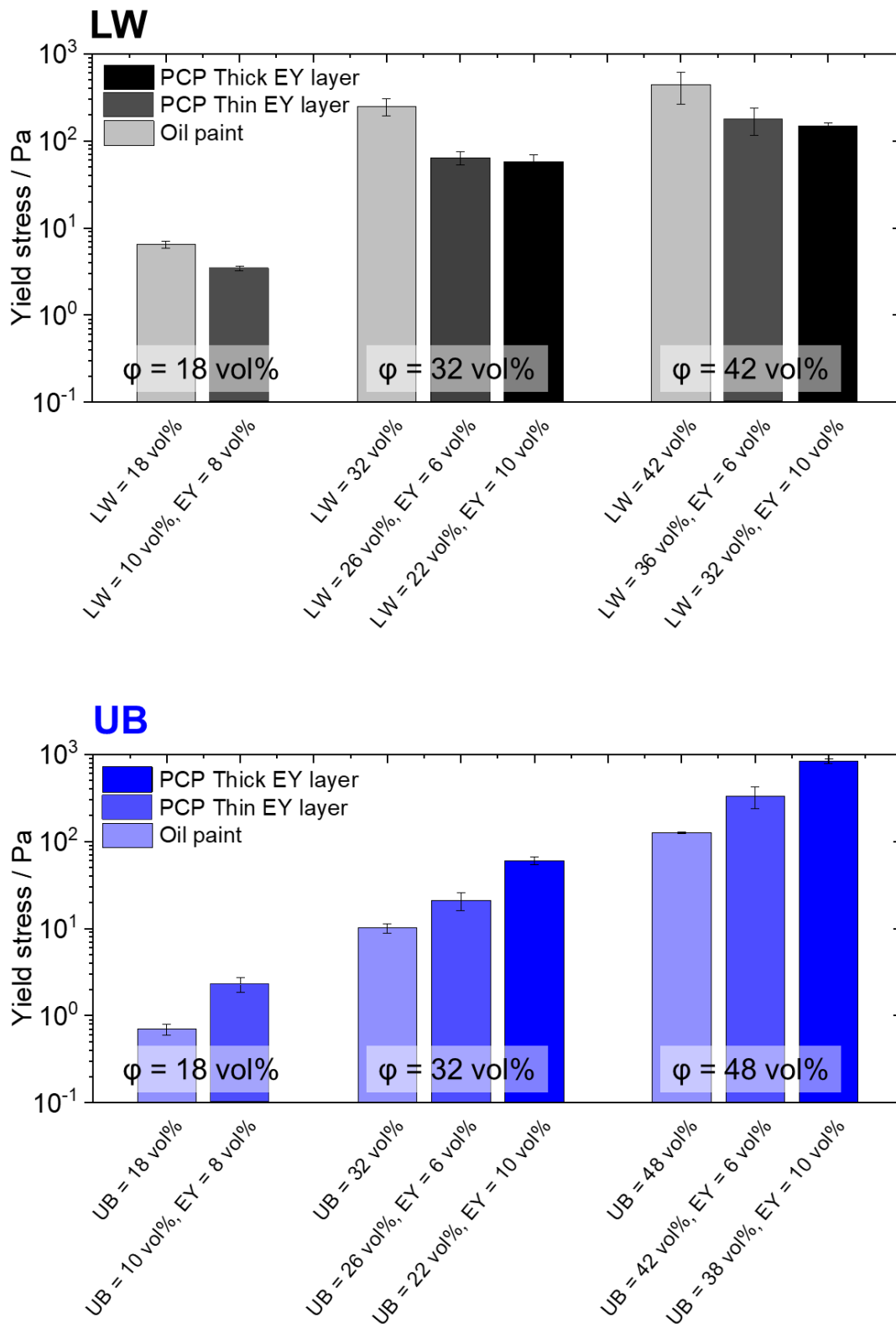


Figure 5.1 – Overview of the yield stress of LW (above) and UB (below) oil and PCP paints at different solids content. The composition of each paint is indicated below each paint data. The error interval here and the following figures always denotes the standard deviation calculated from measurements performed at least in triplicate.

We measured the yield stress of oil paints and varied the solids content and the pigment coating with egg yolk. This set of data presented for paint formulations at  $\phi = 32$  vol% in chapter 3 is now extended in Figure 5.1 for paints at solids fractions  $\phi = 18$  vol% (LW and UB),  $\phi = 42$  vol% (LW) and 48 vol% (UB) in order to understand the effect of pigment coating with EY in a wider range. As for oil paints<sup>9,30</sup> and suspensions in general<sup>127,173</sup>, increasing the solids content should lead to an increase of the yield stress of the suspension.

We determined the yield stress  $\sigma_y$  of oil paints at low solids fraction  $\phi = 18$  vol%, where the paint could flow without being too liquid - a paint one can paint with - and at high pigment loading, where the paint could still be applied with a brush but any additional pigment grains would result in forming aggregates than could not be dispersed again. The maximum pigment loading achieved for LW oil paints with pigment stored in laboratory conditions was  $\phi = 42$  vol%, and  $\phi = 48$  vol% for UB. Figure 5.2 displays the relationship between the pigment loading and the yield stress of uncoated LW- and UB-based oil paints. This set of data confirms the general trend exposed in chapter 3 for paints prepared at  $\phi = 32$  vol%, where LW oil paints form stiffer paints than UB ones, due to the influence of the humidity on LW pigment's surface.

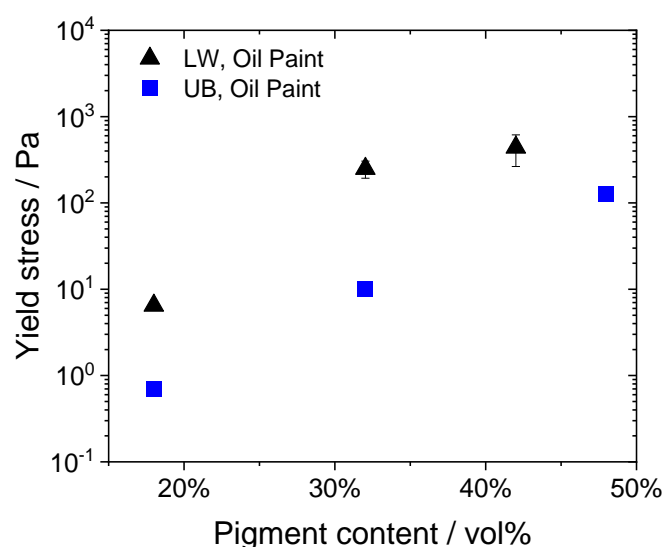


Figure 5.2 - Yield stress of LW and UB oil paints at different pigment loading.

Covering the pigment with a proteinaceous layer, e.g. dried egg yolk, changes the particle surface properties and lead to a modification of the flow behavior of these *PCP* paints. This is shown for the full range of paints prepared at different solids fractions in Figure 5.1. These effects are even more pronounced for paints with a higher egg yolk coating layer around the pigments. We investigated the flow properties of these paints at the indicated solids content (18, 32, 42-48 vol%) but at identical pigment volume fraction  $\phi_{\text{pigment}} = 10$  vol% for both pigments. In these systems, the proportion of egg yolk is larger than the one of the pigments, unrealistic for an artist paint, but helpful to gain insight into the role of EY in these colloidal systems. The results shown in Figure 5.3 demonstrate that the surface properties of the egg yolk in these oil paints are massively dominant,

and totally eclipse those of the pigments. The yield stress of LW-based PCP paints is no longer larger than that of UB ones, because the pigments are fully covered by EY and cannot form a capillary suspension anymore.

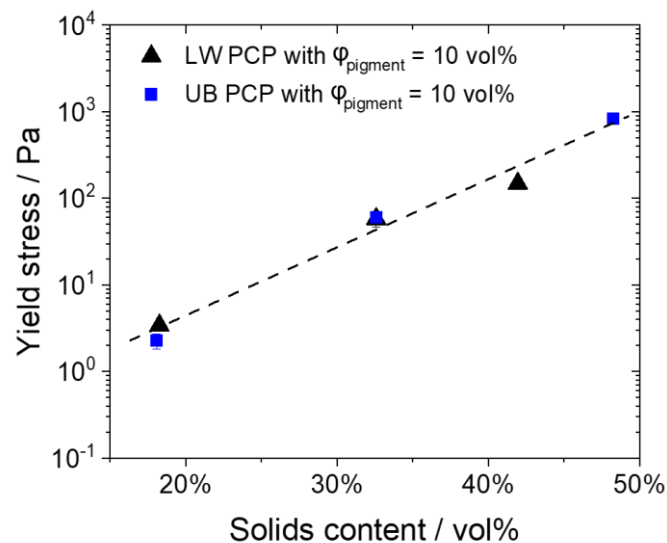


Figure 5.3 - Yield stress of PCP paints at different solids content. All paints contain  $\phi_{\text{pigment}} = 10 \text{ vol}\%$  and the quantity of egg yolk dried matter is adapted to each paint so that  $\phi = \phi_{\text{pigment}} + \phi_{\text{EY}}$

Increasing the solids content in oil paints (without EY) also influences the kinetic of drying/curing of the oil paints. We measured the film formation time, which is the time at which the paint has reached its maximum weight change, see chapter 3, for oil paints at different solids fractions (Figure 5.4) at a paint thickness layer  $h = 0.4 \text{ mm}$ . In LW oil paints, due to the LW pigment catalytic activity towards the curing of linseed oil, the film formation time is rapid and is not strongly influenced by the paint pigment loading. However, for UB paints, the volume pigment concentration has a strong impact on the kinetic of drying of the linseed oil: film formation is achieved in a more rapid way in paints at high pigment loading compared to dilute oil paints. This can be easily explained by the fact that pigments speed up the drying of raw linseed oil due to catalytic effects which are, however, weaker than for LW (see Figure 3.6 in chapter 3). In the dilute paint systems, there is less contact between the oil and the pigment compared to the concentrated paints, and thus the paints at lower pigment loading show longer drying times.

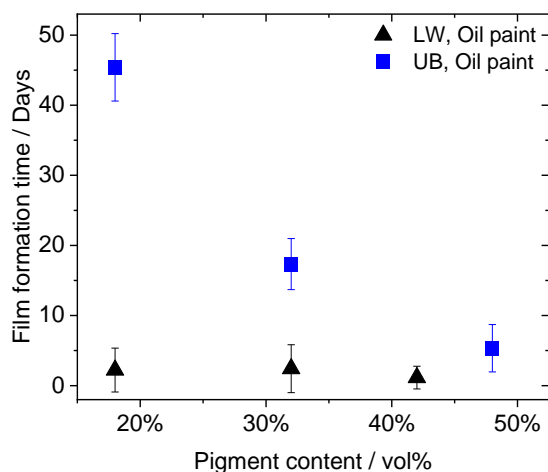


Figure 5.4 - Film formation time of oil paints at different solids fractions. Error bars represent the interval between the start and the maximum of the weight increase.

Larger quantities of EY in PCP paints (here only LW is investigated) increase the film formation time due to the dominating antioxidant properties of the EY (see chapter 3), in the full range of the studied concentrations. However, for PCP paints including only a thin layer of EY, the catalytic effect of the pigment dominates. These results are compiled in Figure 5.5 and summarize the contribution of both pigment loading and egg yolk coating in the drying time of oil paint film layers of 0.4 mm.

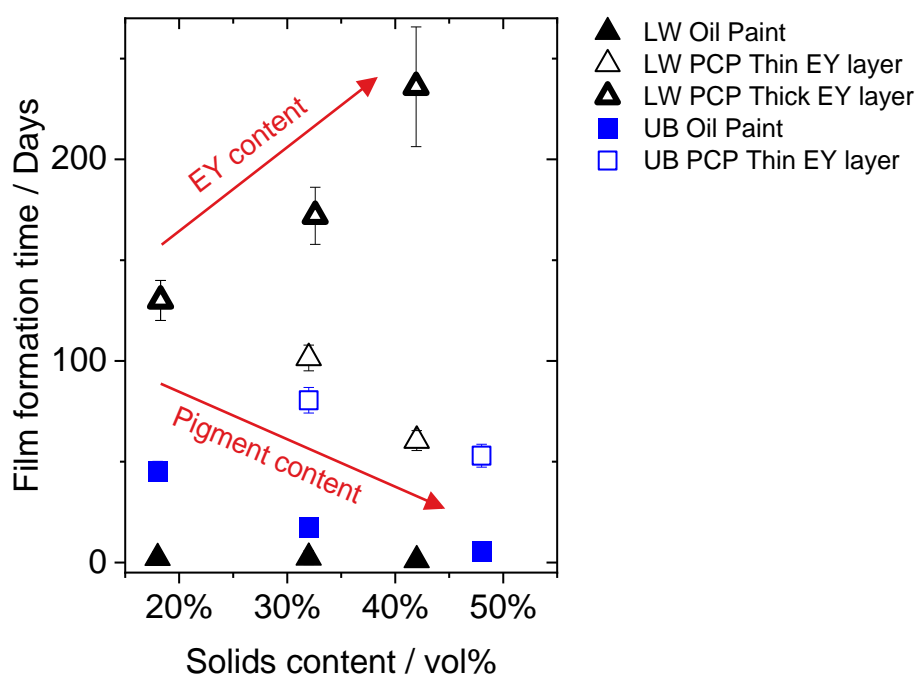


Figure 5.5 – Overview of the film formation time of both oil and PCP paints at different solids fractions. Error bars represent the interval between the start and the maximum of the weight increase. Detailed paint concentrations are to be found in Figure 5.1.

### 5.1.2. Correlations between the thickness layer of an oil paint, its drying time and wrinkling

As seen in chapter 4, to create impasto, a paint needs to have a yield stress: the brushing profile is intentionally visible, creating brush strokes with a certain texture, a visible roughness. We showed previously that oil paints at high yield stress values can be achieved by adjusting the paint pigment loading, by modifying the pigment particle surface, but also by forming a percolating particle network<sup>126,135</sup> through the addition of a second immiscible fluid phase, resulting in a capillary suspensions paint *CapS*. We also showed that wrinkling can be reduced and even suppressed by adjusting the yield stress of paints to high values (see in chapter 3 Figure 3.7 and Figure 3.25).

A paint with impasto forms though naturally thicker paint layers than more dilute paints (see in chapter 3 Figure 3.3), which leads to question the influence of the layer thickness of an oil paint on its drying time and on the apparition of wrinkles at the surface of its dried film. This last point has been mentioned in some books and publications, reporting the appearance of visible wrinkles on surfaces of paints with too little pigment<sup>40</sup> or when the layer thickness of a paint is too important<sup>38,39</sup>. However, no systematic study on the subject in the context of oil paints has been conducted, and no emphasis was done concerning the microstructure of these systems.

We showed previously that the drying time of an oil paint is strongly connected to its microstructure (Chapter 3). The change of mass of oil-containing paint samples at different layer thickness (0.4 mm, 0.7 mm and 1.0 mm) was monitored gravimetrically upon time according the procedure described in Methods, section 2.3.3. Here in Figure 5.6, we observe that the mass increase of a UB oil paint is delayed with the thickness of its paint layer, whereas the film formation time is almost identical for a *CapS* paint (made with water to avoid a delay because of the antioxidant properties of the EY) at the same pigment concentration. This difference in drying time can be ascribed to the paint microstructure: the UB oil paint is a suspension of pigment particles, which has a low yield stress  $\sigma_y \approx 10$  Pa. On the other hand, the UB *CapS* forms a more compact paint, with a strong impasto (typical yield stress values  $\sigma_y > 1000$  Pa). The UB *CapS* forms a strong percolating network, which favors contact between the oil and the pigment particles, whereas the UB oil paint forms a weaker network in which the pigment particles might sedimentate at a too high thickness layer, with a gradient of oxygen distribution within the paint: the oxygen may not be able to penetrate deep into the paint layer, leading to a lower relative mass increase in thin films (Figure 5.6). In addition to this, the oil paint is quite liquid, and no strong impasto can be achieved, thus a thickness layer of 1.0 mm is unrealistic for such a paint in a real artist paint. A drying gradient such as in this UB oil paint is systematically applicable for paints at low yield stress values (data not shown).

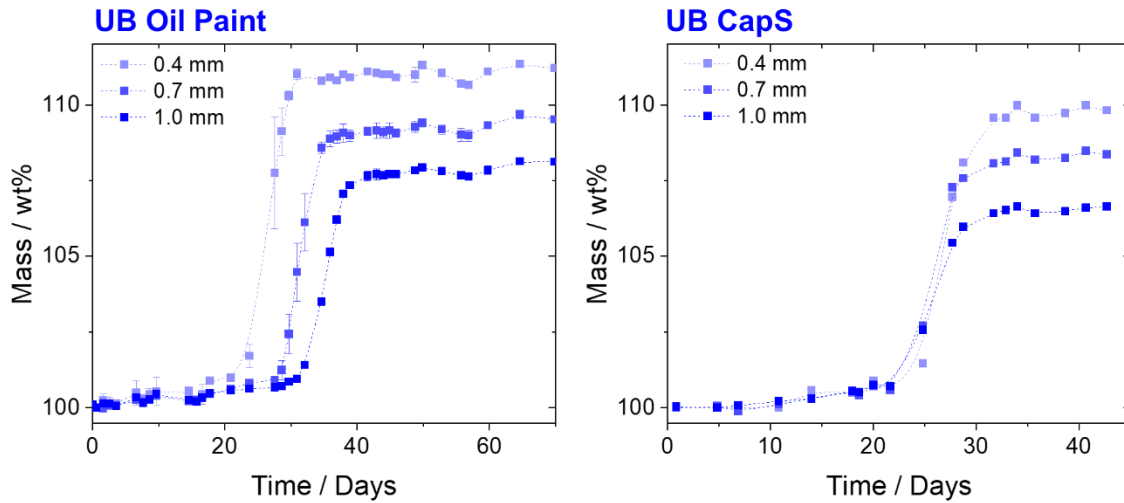


Figure 5.6 – Mass increase, normalized to the oil content, of UB paint samples at  $\varphi = 32$  vol% at different thickness layers prepared as oil paints (left) or CapS (right) as a function of time. The fresh CapS contains 4 vol% of water as a secondary fluid, which evaporates within the first day (data not shown) and does not delay the film formation time like EY with its antioxidant properties.

Also, this same paint shows a pronounced wrinkling for layer thickness  $h = 0.7$  mm and 1 mm upon drying (Figure 5.7). This confirms that this paint, which has a low yield stress in the liquid state, has a strong mobility below the dry skin, with a gradient of oxygen distribution in the paint layer, resulting in an uneven drying between the surface and its bulk, which caused wrinkles (chapter 3).

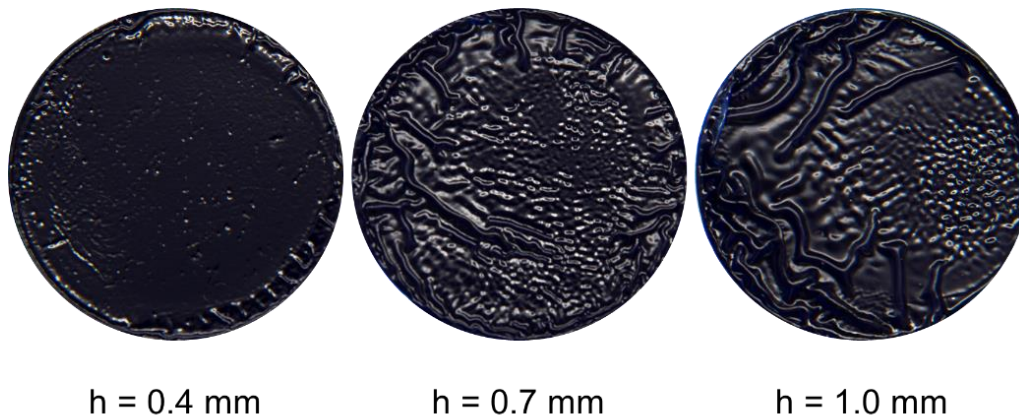


Figure 5.7 - Dried paint sample surface of UBLO paints at  $\varphi = 32$  vol% ( $\sigma_y \approx 10$  Pa) with different layer thickness. Each sample has a diameter of 25 mm.

As for the UB CapS, the LW oil paint at  $\varphi = 42$  vol% is a paint with a high yield stress ( $\sigma_y \approx 440$  Pa). It dries faster when the layer thickness is thin, and its surface after drying is almost wrinkle-free, independent of its layer thickness in the 0.4-1.0 mm range (Figure 5.9), which confirm our assumptions concerning the strength of the particle network in the paint and its consequences regarding the kinetic of drying and aspect of its dried surface at different layer thicknesses.



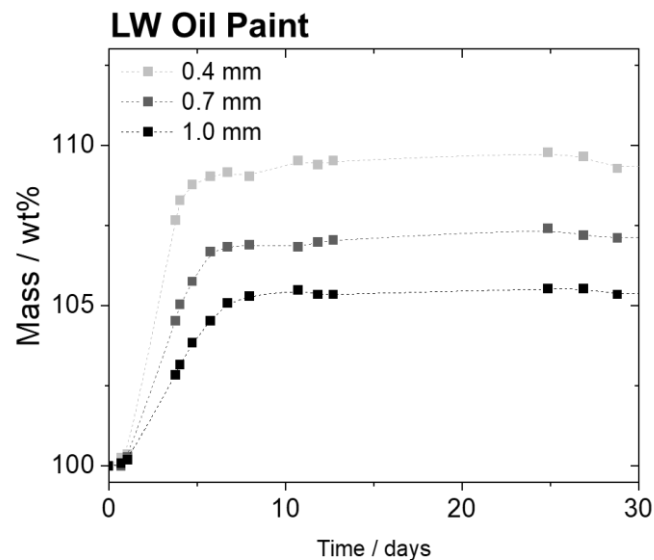


Figure 5.8 - Mass increase, normalized to the oil content, of LW paint samples at  $\phi = 42$  vol% at different thickness layers prepared as oil paints.

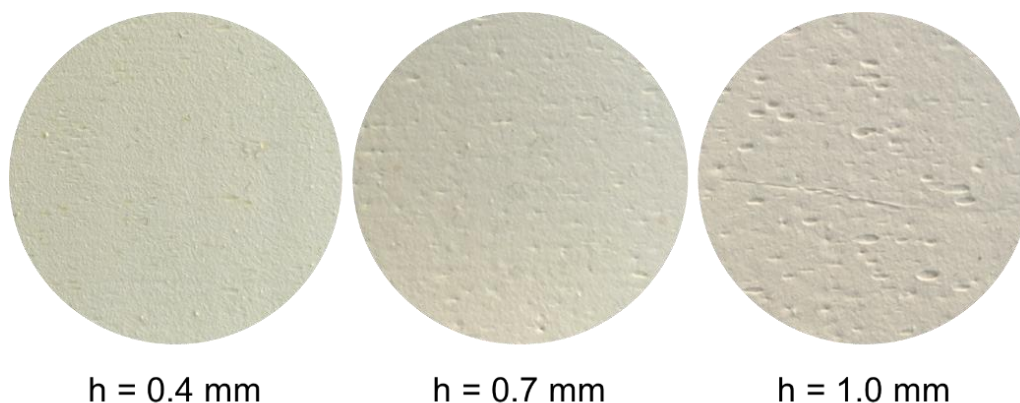


Figure 5.9 - Dried paint sample surface of LWLO paints at  $\phi = 42$  vol% ( $\sigma_y \approx 440$  Pa) with different thickness layer. Each sample has a diameter of 25 mm.

### 5.1.3. Conclusions

The flow behavior, drying kinetics and wrinkling of oil paints are strongly connected. First, we showed that the flow properties of oil paints can be tuned by varying the pigment loading or by coating the pigment with a proteinaceous material such as egg yolk. This results in changes of the paint microstructures, but also in their drying kinetics. At very high EY concentrations, the effect of the pigment on paint drying is eclipsed by the proteinaceous coating layer, resulting in very long drying times. On the contrary, UB paints at high pigment concentration dry faster than more diluted paints because of the important quantity of linseed oil which is not in direct contact with the pigment, accelerating the oil curing reactions, but also due to the more pronounced catalytic effect at higher

particle-oil interfacial area. For LW paints, the catalytic effect of the pigment is such, that the influence of its concentration is neglectable compared to the case of UB.

Also, paints at low yield stress are more inclined to show a drying time gradient with increasing thickness layer compared to paints having a strongly connected network. These latter can produce wrinkle-free paint surfaces, independent of the paint layer thickness. These new insights may encourage further investigations regarding the microstructure of paint layers with and without wrinkles.

## **5.2. Colorimetric study of paints having a similar composition but different microstructures**

Colorimetric measurements were performed on three LW-based oil paints of same composition but different microstructures upon time. The thickness layer of each paint was set to 0.7 mm. One CapS, one PCP and one TG paint were prepared, having 32 vol% of solids content and including 3 vol% of EY in the dried state. The aim is to determine if the microstructure of these systems influences the color of the paint upon time, particularly regarding yellowing, which may be a huge drawback for artistic painting<sup>101,174</sup>.

Lead white has been chosen for this study due to its catalytical properties, allowing a faster oil curing upon time than UB pigment, but also because of the color of the paint: yellowing in white paints can be easily detected due to the modification of the paint color on the  $b^*$  axis with our instrument. The color yellow is located in the CIE  $L^*a^*b^*$  color space in the  $+b^*$  axis, by opposition to the blue color ( $-b^*$ ). Yellowing of UB oil paints consequently results in paints becoming grayer/blacker, and may reach the detection limit of the instrument.

Gravimetric data of these paint systems at a layer thickness of 0.4 mm, presented in chapter 3, already showed different drying times due to the paint microstructures: the CapS paint's mass uptake occurs after 6 days, whereas it takes place after 35 days for TG and PCP paints (see in chapter 4 Figure 4.13). Due to these different drying times, the data presented below display the color recorded of the solid films, with time = 0 days corresponding to the first day at which the paint has dried, which may differ from one paint to another. However, this simplifies the evaluation of the data and the color comparison.

Figure 5.10 displays the colors associated to the paint surfaces upon time, the numbers indicated correspond to their yellowness index, which is calculated using Equation 2 below and corresponds to "the degree of departure of an object color from colorless or from a preferred white, toward yellow"<sup>175</sup>.

The yellowness index (YI) can be calculated using the following equation<sup>176</sup>:

Equation 2 – Yellowness index (YI) according to Francis and Clydesdale, comparable to the  $YI_{E313}$ <sup>175,177</sup>

$$YI = 142.86 \times \frac{b^*}{L^*}$$

	CapS	PCP	TG
0	14.9 ± 0.2	13.8 ± 0.5	15.0 ± 0.3
50	25.1 ± 0.4	28.3 ± 0.2	24.4 ± 0.4
100	29.6 ± 0.2	33.7 ± 0.2	31.5 ± 0.5
150	34.7 ± 0.4	34.9 ± 0.7	33.4 ± 0.4
200	37.7 ± 0.5	38.2 ± 0.3	33.2 ± 0.3
250	38.6 ± 0.4	42.4 ± 0.2	35.3 ± 0.1

Figure 5.10 - Evolution of the yellowness index of LW-based paints with 32 vol% of solids content, including 3 vol% of EY in the dried state upon time, and visualization of the corresponding measured color.

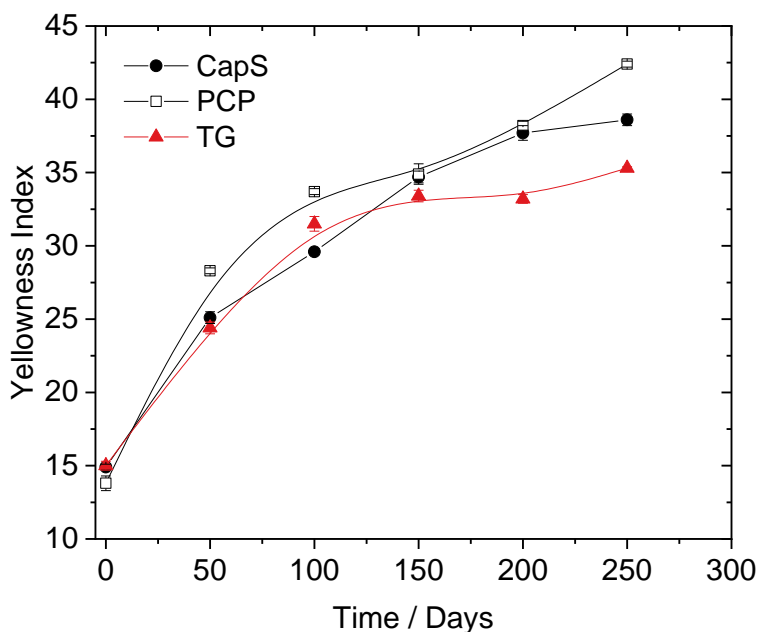


Figure 5.11 – Yellowness index calculated from the CIE  $L^*a^*b^*$  color coordinates (Equation 2) of each sample upon time. The results shown were determined from at least 7 measurements randomly made on the entire paint surface, the displayed data are average values and the standard deviations are shown as error bars.

The three evaluated paints appear white on their drying day (time = 0 day) and evolve progressively towards the color yellow. However, the perception of the color is slightly different from one system to another, and also here shown either printed on paper or visualized digitally on a non-calibrated display. For this reason, the YI value is used to quantify the color change and show the evolution of the color upon time. We can see in Figure 5.11 a non-linear evolution of the color towards yellow, independently of the system studied. However, 250 days after the paints film formation, the YI value of the TG paint is lower than both CapS and PCP respectively. At this stage, the PCP system seems to be more prone to yellowing compared to the two other paints, which have either strong attractive interaction between the particles (the CapS has a high yield stress in the wet state) or have a completely different oil distribution in the paint (the TG is an o/w emulsion in the wet state and the pigments are located in the egg yolk phase). These interesting preliminary results need however additional measurements upon longer ageing times to conclude on the possible relationship between yellowing and paint microstructure.

### 5.3. Study of the influence of the particle size distribution of ultramarine blue pigment on the flow behavior, drying kinetics and color of oil paints

Ultramarine blue pigment is a deep blue color pigment, made originally from the semi-precious stone lapis lazuli, highly requested for painting during Renaissance despite its expensive price. It became more affordable since the 19<sup>th</sup> century thanks to the production of synthetic ultramarine blue. Pigments with different size and shape as well as different surface coatings have been used since then. These physico-chemical specifications affect not only texture, flow and drying kinetics, i.e. the workability of the paint, but also the color impression of the dry layer.<sup>35,117,119,120</sup>

The preparation of pigments to formulate artist paints was sometimes described in ancient recipes, but these recipes depend on many aspects such as the type of paint, for example in oil or in *tempera*. The grinding process of pigment particles, which delivers pigments of different size and size distribution, is of a great importance because it leads to formulate paints having different properties: in the wet state, these parameters should have an effect on the pigment dispersion or aggregation within the paint, which is then strongly connected to the microstructure of the paint film after completing its drying process. Grinding the pigments traditionally by hand is a long and extensive task, leading to the production of pigments particles having a broad size distribution, compared to the modern pigment production methods using a mechanical grinding process. Gueli et. al<sup>119</sup> and Fanost<sup>35</sup> studied the effect of particle size on the resulting pigments color, where sieving and grinding were the techniques used to achieve different pigment particles sizes. However, these studies were performed on the raw pigments, prior to disperse them with a binder to form proper paints.

The study conducted by Pozo-Antonio et. al (2018)<sup>120</sup> has shown the importance of the pigment composition, grain morphology as well as their particle size and size distribution on the paints color and roughness in dried *tempera* paints. However, the quantity of binder used for the experiments, egg yolk or rabbit glue, was constantly varied depending on the type of pigment used (the binder demand), and no correlation could be made between the binder demand for each pigment and its corresponding particle size distribution (PSD). In addition to this, we showed in chapter 4 that egg yolk itself has a complex microstructure, a dispersion of protein-stabilized lipid particles, which can be ascribed to a concentrated o/w emulsion in the fresh state. The binder alone, because of its complex structure, might influence strongly the paints color and roughness. It is though necessary, in order to understand the importance of the PSD, size and morphology of pigments in paint systems, to evaluate this series of criteria in a systematic way.

Fundamental work has to be done to correlate colloidal properties, rheological parameters and the final appearance of the paints we can observe in museums. This section focuses on understanding the role of the ultramarine blue pigment particle size distribution, size, morphology and pigment surface treatment in oil paints. Seven different UB pigments, from two different manufacturers, were

evaluated and compared in terms of flow properties, color and drying kinetics in oil paints at the same pigment volume concentration.

### 5.3.1. Materials

In this section, a variety of different synthetic ultramarine blue pigments have been used. In addition to the pigment particles from *Abralux Colori Beghè* (Italy) employed for chapters 3 and 4, six other blue pigments purchased from *Kremer Pigmente* (Germany) were studied, as summarized in Table 5.1.

The manufacturers describe the pigments in terms of color, density, average particle size. No information is given concerning the methods employed, neither at which precision and conditions it has been done. The synthesis of pigment particles varies from one manufacturer to another, as well as their characterization methods, which might lead to huge differences in terms of products and properties the users face when using these pigments to prepare their paints.

Table 5.1 – Synthetic ultramarine blue pigments description according to the manufacturers

Name	Name (manufacturer)	Manufacturer	Density	Color	Average particle diameter / $\mu\text{m}$	Oil absorption value
<b>UB0</b>	Blu Oltramare Puro M (6018)	Abralux Colori Beghè	2.35	Blue	-	35-37
<b>UB1</b>	45000	Kremer Pigmente	2.35	Dark blue	3.80	32.0
<b>UB2</b>	45020	Kremer Pigmente	2.35	Blue, reddish	2.43	35.0
<b>UB3</b>	45030	Kremer Pigmente	2.35	Blue, greenish	1.44	40.0
<b>UB4</b>	45040	Kremer Pigmente	2.35	Light blue, greenish	1.24	37.5
<b>UBS</b>	45010	Kremer Pigmente	2.30	Blue	2.5	45.0
<b>UBCC</b>	45080	Kremer Pigmente	2.35	Light blue	0.85	31.0

However, the oil absorption value should in principle (it is not indicated) respect the European norm *ISO 787-5:1980*, which is by definition “The amount of varnish oil absorbed by a pigment or filler sample under specified conditions”<sup>178</sup>. Yet this number corresponds to a quantity – in mass or in volume – which is not indicated in the pigments’ characterization description, leaving uncertainties regarding the unit employed which can be thus misleading. Moreover, we have shown in chapter 3

that some pigments can be more hygroscopic than others: the absorption of oil by the pigment will then be different when it is stored in more humid or drier conditions, which can also disturb the measurement if no attention is paid to storage conditions.

Also, the average particle size is indicated as such in the pigments' description. Yet this information needs to be carefully interpreted: particles always have a size distribution, which might not always be monomodal. For example, a batch of pigment particles can have the same particle size average value  $x_{50}$  than another one, and yet the first batch has a bimodal distribution whereas the second one shows a monomodal distribution; this may result in materials having different colloidal properties. For instance, a change in particle size distribution results in a modification in the maximum particle packing fraction in suspension systems<sup>179</sup>, and a broadening in particle size distribution (PSD) in suspension rheology leads to an increase in relative viscosity of the fluid.<sup>154,180</sup> It might also influence the kinetics of a chemical reaction due to a modification of the surface interactions between the different materials in those systems.<sup>181,182</sup> Thus, it is crucial to determine not only the average size of pigment particles, but also their size distribution to understand the effects influencing their use in suspensions.

Table 5.2 – Size and size distribution characteristics of the UB pigments described in this chapter

Name	Sv / m <sup>2</sup> /cm <sup>3</sup>	x <sub>16</sub> / µm	x <sub>50</sub> / µm	x <sub>84</sub> / µm	Size distribution profile	Specifications
<b>UB0</b>	3.6	1.2	<b>2.0</b>	3.0	Narrow monomodal dispersion	-
<b>UB1</b>	2.5	1.6	<b>3.2</b>	7.1	Monomodal dispersion	-
<b>UB2</b>	2.8	1.4	<b>2.9</b>	7.0	Monomodal dispersion	-
<b>UB3</b>	5.2	0.7	<b>1.5</b>	6.0	Monomodal dispersion	-
<b>UB4</b>	2.9	1.1	<b>4.2</b>	13,5	Bimodal dispersion	-
<b>UBS</b>	2.5	1.8	<b>2.8</b>	4.6	Narrow monomodal dispersion	Pigment coated with silica
<b>UBCC</b>	5.2	0.8	<b>1.5</b>	4.5	Monomodal dispersion	Contains calcium carbonate

Additional measurements to characterize these pigments in terms of particle shape, size, size distribution, and chemical composition were completed according to the methods described in chapter 2 in order to obtain a deeper understanding of the parameter characteristics of each pigment, which might influence the paint flow properties and drying kinetics.

Because of the different size distribution profiles (Figure 5.12) and average size  $x_{50}$  (Table 5.2), the pigments could be categorized in four different groups:

- **Group A:** Narrow monomodal dispersion (UB0 and UBS)
- **Group B:** Monomodal distribution with a larger average size (UB1 and UB2)
- **Group C:** Monomodal distribution with a smaller average size (UB3 and UBCC)
- **Group D:** Bimodal distribution (UB4)

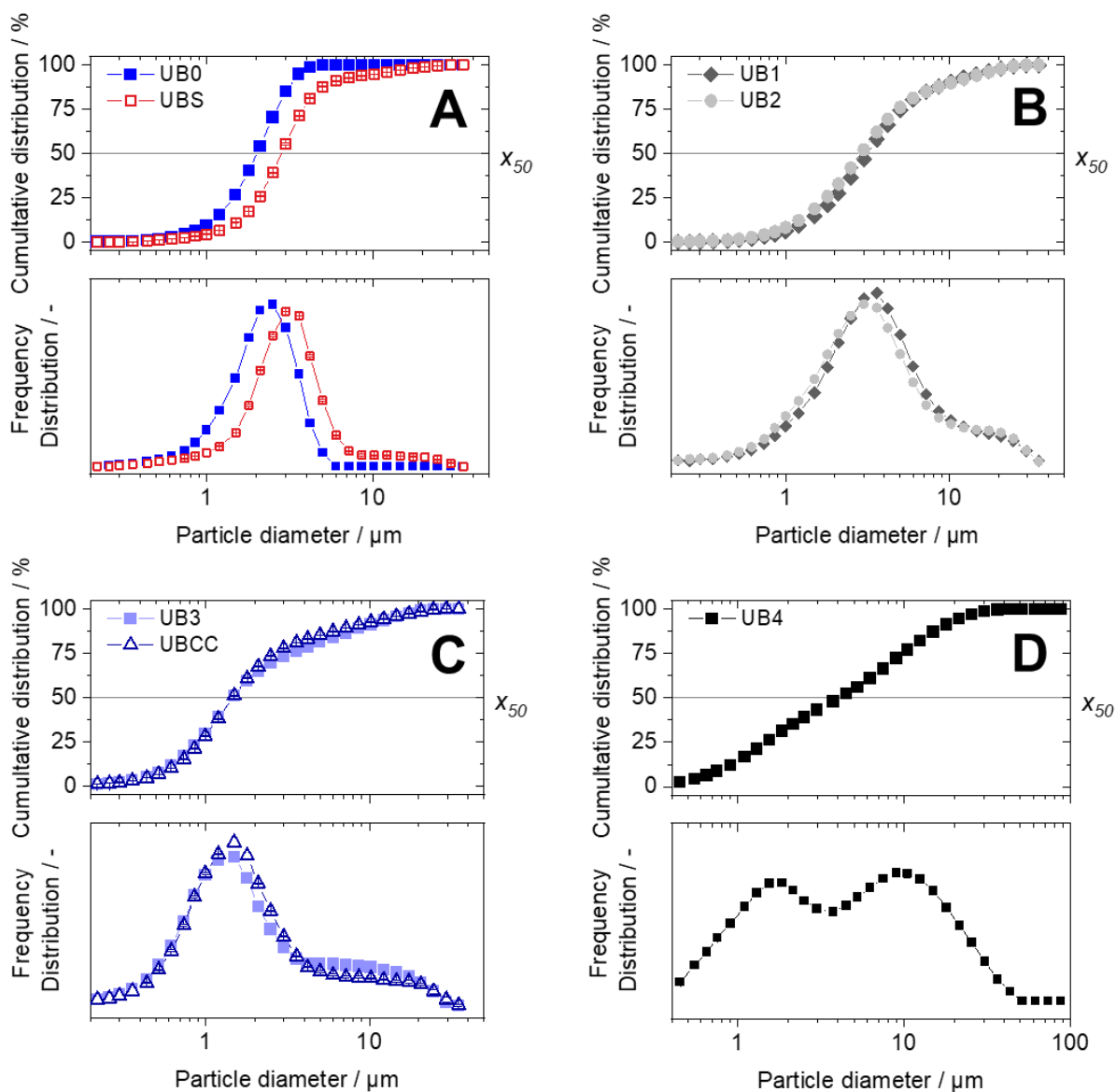


Figure 5.12 - Cumulative and frequency distribution of UB pigments particle diameter ( $\mu\text{m}$ ) described in Table 5.2.

In addition to this, two pigments have a different chemical composition from the other ones: according to the manufacturer, UBCC contains calcium carbonate to ensure a light blue color of the pigment, and UBS is coated with silica, which is supposed to protect the pigment against acidic reactions and thus increase its stability. As mentioned in Chapter 1, UB pigment is known to be sensitive towards acidic media, which can cause the so-called “ultramarine disease” or “ultramarine sickness”: the pigment degrades and loses its intense color in the painting<sup>42,183,184</sup>. This is a particular issue for blue oil painting where both UB pigment and a drying oil are dispersed together:



the oil dries through an oxidative radical process<sup>48</sup> which leads to the contact between the pigment and acidic moieties of the oil produced upon hydrolysis and oxidation . However, Li et al. (2011) could increase the resistance of UB pigment against acidity by coating the particles with a uniform silica film<sup>185</sup>, which is probably the reason why the manufacturer prepared the pigment UBS with this feature.

Scanning Electron Microscopy (SEM) images (Figure 5.13) support the PSD data: the pigment particles in UB0, UBS, UB1 and UB2 show a homogeneous isometric size, the particles of UB3 and UBCC are also isometric but smaller, whereas the pigment UB4 contains both small particles and bigger aggregates. The morphology of the different pigments is comparable.

Contact angle measurements were performed according to the European norm *ISO 19403-2:2017* with different solvents to characterize the surface properties of the studied pigments.<sup>186</sup> However, this set of experiments did not deliver exploitable results, probably due to the measuring conditions. The pigments, pressed under vacuum and/or at high temperatures did not form stable and flat compact pellets. As a consequence, the drops of solvents which were deposited on the surface were instantly adsorbed onto the porous pellet, and no measurement was possible. Another approach was considered, which consisted in depositing a pigment layer on double-sided tape, which was taped on a microscope slide. The pigments were previously dried overnight at 170 °C to remove any excess of water due to the natural air humidity upon storage (see in Materials and methods chapter 2). However, the data could not be used because of the large standard deviation concerning most of the experiments, together with a lack of data coherence.

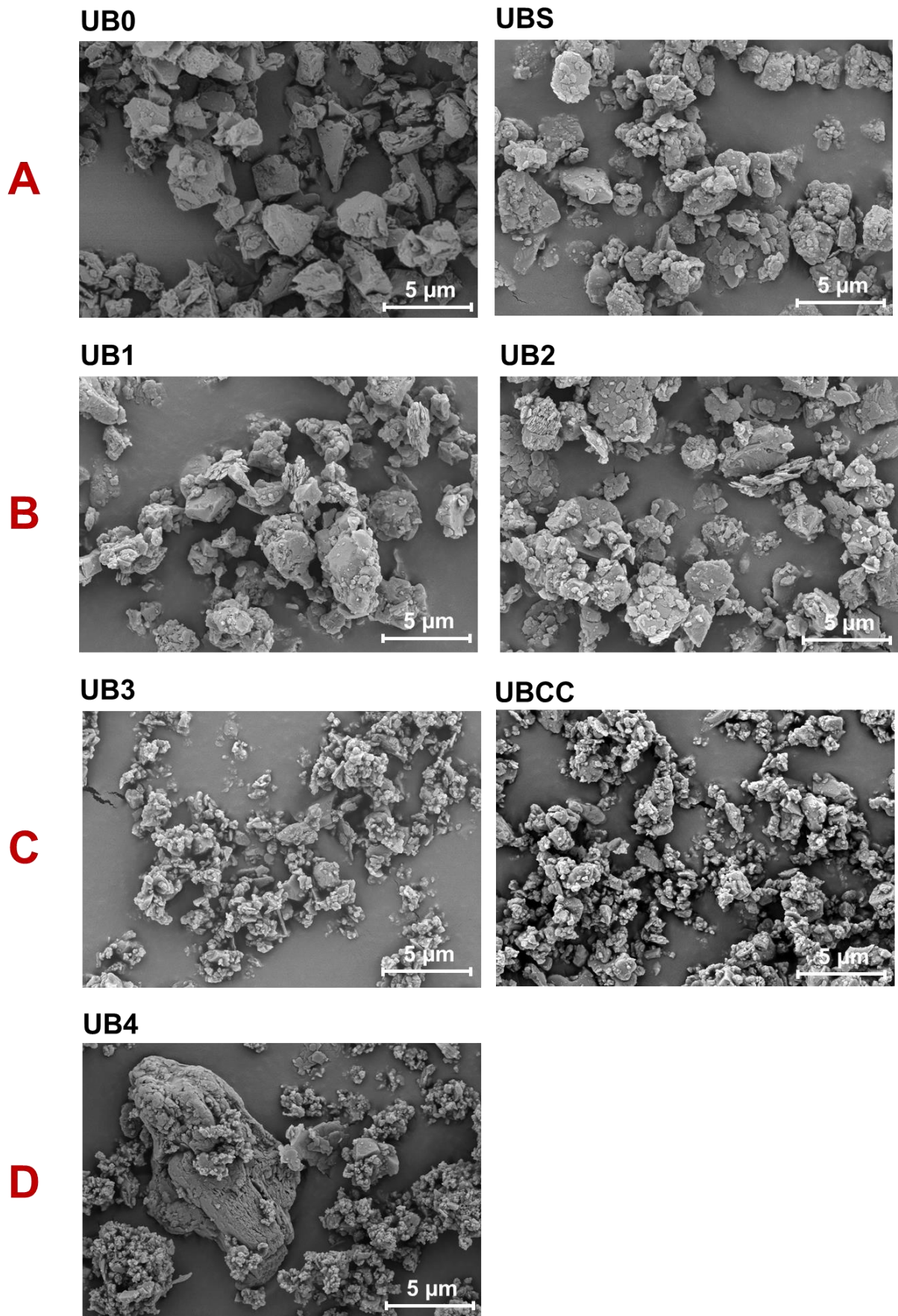


Figure 5.13 - SEM images of the ultramarine blue pigments studied in this chapter

### 5.3.2. Flow behavior of UB-based oil paints

The pigment fraction used for the following study in all experiments is set at  $\phi = 32$  vol%, which was chosen for comparison purposes with the systems prepared in the chapter 3 of this manuscript. Also, at this concentration, the paint is easy to prepare and to apply on different surfaces. On the other hand, oil paints prepared at these pigment concentrations can lead to paint surface layers presenting unwanted effects such as wrinkling if the yield stress of the liquid paint is not high enough (chapter 3).

We showed that this effect can be attenuated by increasing the solids content of the oil paint. For this reason, the maximum pigment fraction was also experimentally determined, compared to the corresponding maximum pigment fraction indicated by the manufacturer as “Oil absorption value” if we consider this value as being given in wt%. This set of measurements (Figure 5.14) shows a significant difference between the experimental and theoretical data, which may come from the manufacturers’ experimental procedure (unknown). For example, important parameters such as the oil used for the experiment or the pigment storage conditions are not indicated.

From the experimental data, we can recognize that the maximum solids content (MSC) that can be mixed with linseed oil from pigments previously dried is generally higher than the one determined from pigments stored at RT conditions. This is not surprising if we consider that some pigments might be hygroscopic (chapter 3), thus already partly saturated by the water contained naturally in a RT “humid” atmosphere ( $RH \approx 50\%$ ). The pigment UB0, which is the same used as standard UB pigment for this thesis, shows similar MSC values in both dried and humid conditions, which means that is not influenced by the humidity content as already stated in chapter 3. However, all the other pigments, produced by *Kremer*, have MSC values which are significantly different for particles which were stored either in dried or at RT conditions. Except for UB2, the MSC could be significantly increased by drying the pigments prior to use them. This shows a strong sensitivity of these pigments towards humidity, which influences the MSC value, and might also have an impact on the flow properties of oil paints prepared with these pigment particles as described in chapter 3 for the lead white pigment, also purchased from the same manufacturer.

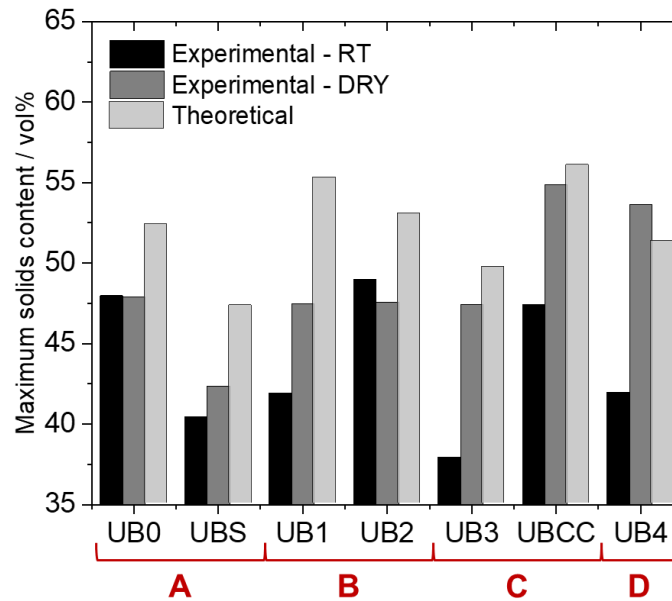


Figure 5.14 – Maximum pigment content (vol%) for all investigated UB pigments, determined experimentally from the dried pigments or pigments stored at room temperature (RT) conditions (experimental values) or calculated from the manufacturers' information datasheets (theoretical value)

To avoid the possible formation of unwanted CapS due to the water sensitivity of the pigments, we investigated the flow behavior of oil paints using these UB particles after drying them overnight to remove traces of water and compared them to the ones with the pigments stored under laboratory conditions. Oil paints at solids fraction  $\phi = 32$  vol% were prepared and their flow properties were compared in terms of viscosity at high shear and yield stress (Figure 5.15).

The yield stress  $\sigma_y$  of a paint expresses the force necessary to break up the rest structure and make the paint flow. At the same solids fraction, the yield stress of the paints prepared with the different UB pigments varies from one type of blue to another. First of all, the yield stress value of the paint prepared with UB0, manufactured by *Abralux Colori Beghè*, shows the lowest value ( $\approx 10$  Pa), independently from its storage condition. All the paints prepared with pigments from *Kremer Pigmente* display yield stress values  $\sigma_y > 100$  Pa, which is one order of magnitude higher than for the standard pigment UB0, even at similar particle size (like UB3 or UBCC) or particle size distribution (UBS). This general trend, independent of particle size, size distribution or particle shape, suggests that other parameters, most likely the surface energy of the pigment particles, determines the yield stress values. A hint can be found from the pigments UBS and UBCC, which composition (addition of calcium carbonate for UBCC) and surface treatment (UBS is coated with silica) are for sure different from the others and exhibit particularly high yield stress values.

We showed in (chapter 3) that covering the pigment surface with a dry protein layer (*PCP paints*) might lead to an increase in the paint yield stress due to an attractive steric interaction among hydrophilic surface layers. It is also known that each manufacturer production procedure is different, incorporating different additives which can also influence the pigment particle surface

properties. The general trend in which the pigments produced by *Kremer* results in paints with a higher yield stress than the one from *Abralux* supports the hypothesis that these pigments were produced differently, using probably components playing a role in the surface treatment of the pigment particles. The pigment UB3 stands out from the others: the yield stress of this paint (with pigments stored in both dry and laboratory conditions) is one order of magnitude higher ( $\sigma_y > 1000$  Pa) than the other *Kremer* pigment-based paints. UB3 and UBCC have the same size and size distribution (Figure 5.12), however the  $\sigma_y$  value of the UB3-oil paint is much higher than the one of the UBCC, which confirms that the effect of the surface properties/composition of the pigment particles might be of a great influence concerning the flow properties of the paints. In the frame of this study, this effect has, as a matter of fact, more influence than the PSD itself at this suspension concentration.

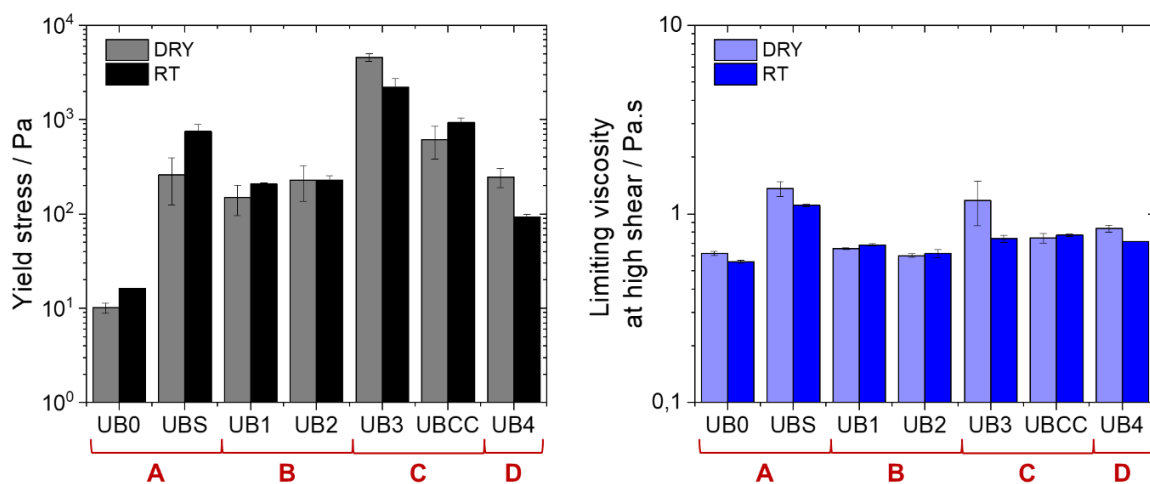


Figure 5.15 - Yield stress (left) and viscosity at high shear (right) of UB pigments paints  $\phi = 32$  vol% with pigments stored under dried (DRY) and laboratory (RT) conditions.

The viscosity at high shear (rate or stress) represents the resistance of the paint to flow after shearing/brushing it strongly, and the limiting high shear viscosity  $\eta_\infty$  of a suspension, such as an oil paint, depends exclusively on the solids volume fraction of its particles or aggregates<sup>154</sup>. The entire set of oil paints was prepared at the same solids fraction  $\phi = 32$  vol% and indeed, the resulting limiting high shear viscosity of the samples is almost identical for all of them ( $\approx 0.7$  Pa.s). Some small differences can be pinpointed for UB3 and UBS samples, where  $\eta_\infty$  shows higher values, which can reside in the fact that the high shear regime is not completely achieved at the term of the measurement for these samples showing higher yield stress values: the particle network is not completely broken at this stage, resulting in higher effective volume fraction and hence higher viscosity values. Our data support, that the particle size distribution has no effect on the limiting high shear viscosity, and thus on the vividly applied brush strokes of an oil paint at this concentration. This is expected since the particle loading of the paints was far below the maximum packing fraction and accordingly the PSD does not affect viscosity.<sup>154</sup>

As a conclusion, neither the PSD nor the size of the used UB pigments particles have a significant effect on the flow properties of the oil paints at a solids fraction  $\phi = 32$  vol%. The dominating effect seems to be rather related to the surface properties and/or the pigment composition, which can significantly influence the yield stress of these oil paints.

### 5.3.3. Oxidation and curing of UB-based oil paints

Curing of a drying oil and the formation of peroxides results in gravimetrically detectable uptake of mass of an oil paint layer. For oil paints, this onset of oxidation and crosslinking corresponds to the “dry-to-touch” state of the paint film, also accessible via hardness measurements (see chapter 3 and 4). In this section, we investigate the effect of the different UB pigments used for this study on the curing kinetics of oil paints, under both natural ageing and accelerated ageing conditions according to the methods described in chapter 2 of this manuscript.

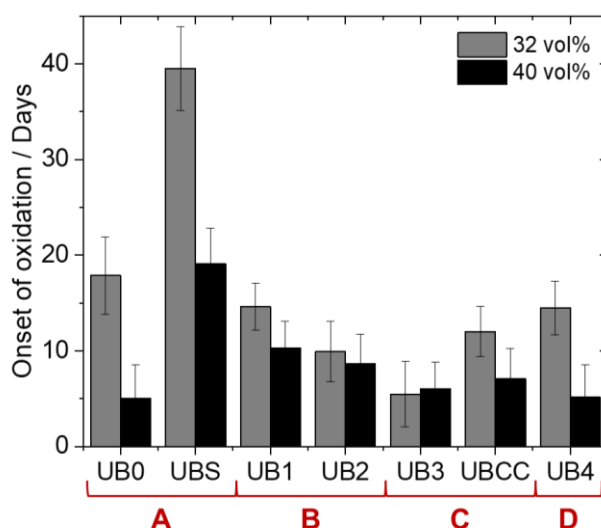


Figure 5.16 – Drying time of UB oil paints under natural ageing conditions at  $\phi = 32$  and 40 vol%. Error bars represent the interval between the start and the maximum of the weight increase.

Two sets of paints have been prepared, at pigment concentration  $\phi = 32$  and 40 vol%, as proof of concept. Paints at higher solids content dry faster than the more diluted ones, which is expected since we showed in chapter 3 that the addition of pigments into raw linseed oil speeds up its drying kinetics. In addition to this, except for UBS-paint the mass uptake for all other oil paints takes place in a narrow time range and the paints dry within  $\approx 10$  days at  $\phi = 32$  vol% despite their different PSD and size (or composition). UBCC dries as fast as the other pigments despite its known different surface chemistry, since it contains calcium carbonate.. UBS-containing paint takes twice as much time to dry as the other paints at the same solids content (32 vol%), which is apparently due to the silica surface coating.



We showed in chapter 3 that changing the surface properties of pigments by coating them with an egg yolk layer can strongly delay the kinetics of drying of oil paints. In the case of EY coating (*PCP paints*), the coating layer serves as an “antioxidant shield”, preventing oxidation reactions catalyzed by the direct contact between the pigment particle surface and the oil phase. Some of these experiments were repeated in accelerated conditions at 80°C (oxygen uptake) by thermogravimetric analysis to confirm these observations. Alongside with gravimetric experiments performed on samples upon natural ageing, the onset of mass uptake corresponds to the onset of the overall oil curing reactions, which can be detected gravimetrically by the increase of the sample’s mass. The mass of the UBS-oil paint at 32 vol% starts to increase after  $\approx 350$  min while this onset was detected at  $\approx 100$  min for both UB0 and UB4-oil paint samples.

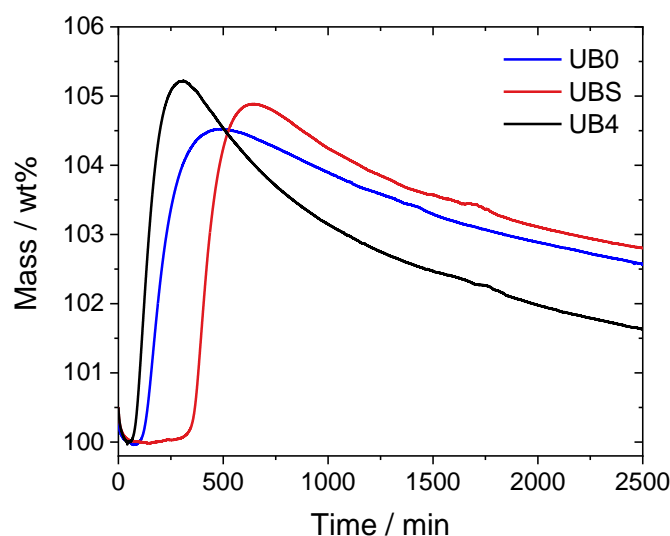


Figure 5.17 - Oxygen uptake experiments in accelerated conditions at 80 °C of UB-based oil paints with  $\phi = 32$  vol%.

The oxygen uptake data displayed in Figure 5.17 corroborate that a modification of the pigment surface with a coating silica layer delays the curing reactions of the oil. The kinetic of onset of the mass increase UB4-based paint is as rapid as the UB0-based paint, even if both pigments size distribution are different: UB4 has a bimodal PSD and a higher average particle size than UB0, with a narrow PSD. These results are consistent with those obtained gravimetrically under natural ageing conditions.

All in one, the drying kinetics of oil paints in the conditions of this study are not significantly influenced by the PSD of the studied ultramarine blue pigments, even at higher pigment concentration in the suspension. However, changing the pigment surface properties by coating it with a silica layer delays the onset of the curing reactions, which echoes with a similar effect discovered in chapter 3 with *PCP paints* and their EY coating layers.

### 5.3.4. Colorimetric study of UB-based oil paints

We showed in chapter 3 that the paint mechanically determined “dry-to-touch” transition corresponds to the steep increase of the sample weight indicating the onset of oxidation and chemical drying. This transition from a liquid paint to a solid film also leads to surface changes of the paint: the paint might shrink, leading to modifications of the light reflection of the paint, the color might change due to further physico-chemical transformations, the surface might appear glossy or matt, etc.<sup>50,187</sup>

We measured the color of the UB-based oil paint samples with a colorimeter according to the method described in chapter 2, from their wet state until their transformation into solids films at a paint layer thickness  $h = 0.7$  mm. Simultaneously, the mass change of the corresponding paint layers was monitored over time (method described in chapter 2). The steep increase of the mass, corresponding to the onset of oxidation and chemical drying, but also to the “dry-to-touch” transition as stated previously corresponds with the total change of the color  $\Delta E^*$  of the paint layer. An example is given in Figure 5.18, which is applicable for the entire set of UB oil paints in this present chapter. This experiment confirms the previous statements where the surface of a paint layer undergoes surface modifications upon drying, that we can measure by means of a colorimeter. The value  $\Delta E^*$ , corresponding to the difference between the paint sample and the black standard (see chapter 2), decreases upon time, which indicates that the color difference between the standard and the samples diminishes upon drying.

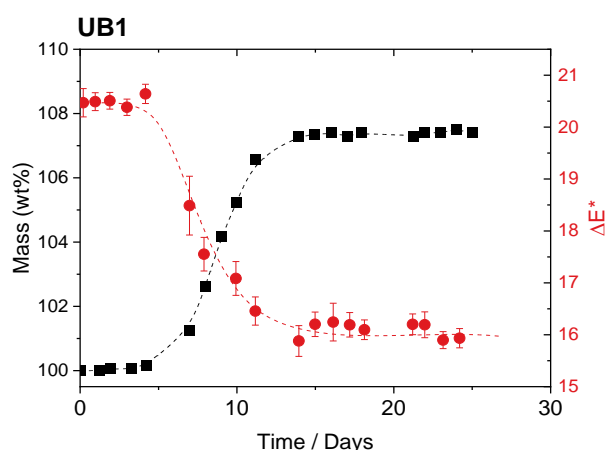


Figure 5.18 – Mass and total color change  $\Delta E^*$  upon drying time of UB1-oil paint at  $\phi = 32$  vol%, at a paint thickness layer  $h = 0.7$  mm under natural ageing condition.

The  $L^*a^*b^*$  values were recorded upon drying time. The values of the  $b^*$  coordinate (Figure 5.19, left), which is located on the yellow (+ $b^*$ ) – blue (- $b^*$ ) axis and of the lightness  $L^*$  (black-white axis, Figure 5.19, right) are of particular interest due to the blue color of the paints. Selected data for two kinds of paints are reported in Table 5.3. It shows that both in the wet and dried state, all UB paints have similar  $b^*$  and  $L^*$  values, except for the UBCC-oil paint. Upon drying, the  $b^*$  values are increasing, indicating a change of chroma. The paints contain all about 68 vol% of linseed oil, which



is subject to yellowing upon drying<sup>43</sup>. As such, the evolution of the  $b^*$  value towards  $+b^*$  (yellow) is consistent. The  $b^*$  coordinate of the UBCC-oil paint is lower than the ones of the other paints. The paint appears as a result “bluer”. This difference might be ascribed to a different pigment composition since this very pigment contains calcium carbonate.

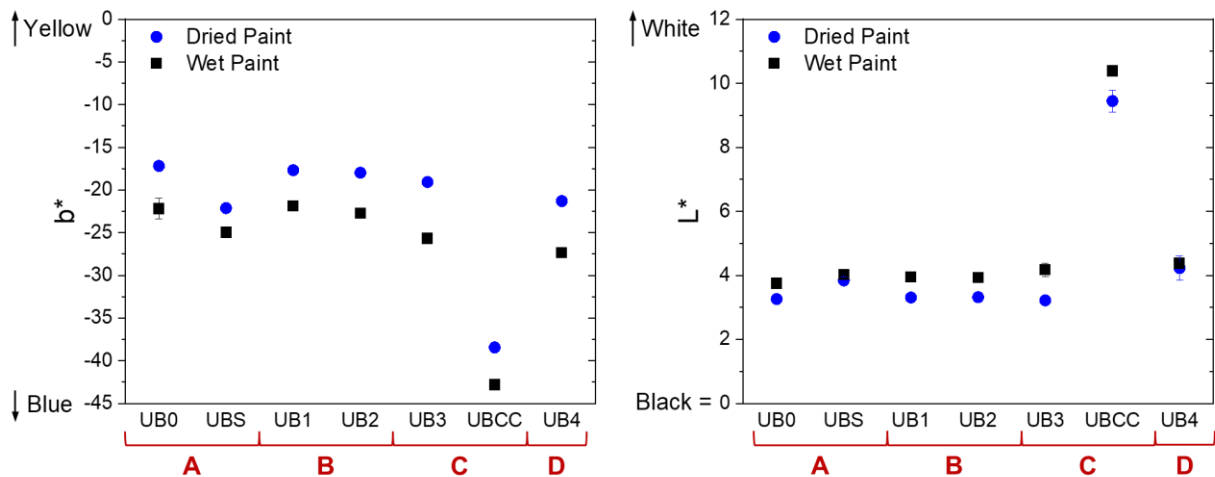






Figure 5.19 –  $b^*$  and  $L^*$  coordinates of UB oil paints samples at 32 vol% with a thickness layer  $h = 0.7$  mm, in the color space  $L^*a^*b^*$  CIE 1976 in the wet and dried state.

The lightness value  $L^*$  of the paints are low ( $\approx 3-4$ ), close to the lightness value of black ( $L^* = 0$ ). Upon drying, the  $L^*$  value slightly decreases, probably due to changes in the paint surface. However, the  $L^*$  coordinate of the UBCC-oil paint is higher than for the other paints ( $\approx 10$ ). The addition of calcium carbonate in the pigment synthesis of the UBCC had the purpose of delivering a lighter blue color than the other ones according to the manufacturer, which has equally been measured in the resulting oil paints. Reconstitution of the paint colors based on their coordinates is visible in Table 5.3.

The color of the oil paints containing UB pigments, despite having different PSD, pigment size or manufacturer, is not significantly affected in the frame of this study. However, the modification of the pigment composition with addition of white compounds such as calcium carbonate greatly influence the color of the paint, as is already influenced the color of the raw pigment (see Table 5.1). The addition of a silica layer does not significantly influence the paint color on the short term, but it might be of a great interest to investigate this effect on the long term on aged UBS oil paint layers, since silica is believed to protect the UB pigment against acidic reactions, leading to the pigment degradation.

Table 5.3 – Colorimetric values of UBCC and UB1 oil paints at a 32 vol% pigment loading and with a 0.7 mm thickness paint layer.

	$\Delta E^*$	$L^*$	$a^*$	$b^*$	Color
UB1 (wet)	$20.5 \pm 0.2$	$3.9 \pm 0.1$	$3.0 \pm 0.1$	$-21.9 \pm 0.2$	
UB1 (dried)	$16.2 \pm 0.2$	$3.3 \pm 0.1$	$1.9 \pm 0.1$	$-17.7 \pm 0.2$	
UBCC (wet)	$42.9 \pm 0.2$	$10.4 \pm 0.1$	$9.9 \pm 0.1$	$-42.8 \pm 0.2$	
UBCC (dried)	$38.2 \pm 0.2$	$9.4 \pm 0.3$	$8.5 \pm 0.1$	$-38.4 \pm 0.2$	

These results differ from the observations made by Pozo-Antonio et. al (2018)<sup>120</sup> with *tempera* paints, where the study showed that surface physical properties including the pigment morphology, size, PSD had important effects on the paints' roughness, reflectance intensity and color. However, in this study involving numerous pigments such as Lapis Lazuli and azurite, the variation in PSD and average particle size was more pronounced (e.g. PSD = 0.6-95  $\mu\text{m}$  and  $x_{50}$  = 47  $\mu\text{m}$  for Lapis lazuli). Moreover, the binder in *tempera* (egg yolk, which contains also an important disperse fraction and water) behaves differently from oil, in terms of flow properties of the paint but also regarding the chemical reactions taking place (see chapter 4). These effects have an important impact on the microstructure of the resulting paint, which influence their physical properties as a solid film, investigated in this study. The main conclusions of this above-mentioned study reveal that the composition of the pigment (UB containing calcium carbonate) is the most important parameter controlling the color of the paint, which confirm our findings in this study on UB-containing oil paints.

### 5.3.5. Conclusions

In the frame of this study where UB oil paints at a solids fraction  $\phi = 32$  vol% were prepared using seven different pigments, neither the PSD nor the size of the used UB pigment particles has a significant effect on their flow properties, drying kinetics or paint color.

The dominating effect influencing the yield stress of these oil paints seems to be rather related to the surface energy determined by surface treatment or pigment composition. The oil paint drying kinetics is affected mostly by modifying the chemical composition of the pigment surface. We observed a delayed onset of the curing reactions when using a UB pigment coated with a silica

layer, whereas all the other paints have similar drying times, even at higher pigment packing fractions. The color of the oil paints was mostly affected by the modification of the pigment composition (addition of calcium carbonate, a white compound). The addition of a silica layer did not influence the paint color significantly on the short term, but it might be of a great interest to investigate this effect on the long term, since silica is believed to increase the stability of the UB pigment against degradation.

The pigment with the broadest particle size distribution (from 0.1 to 50  $\mu\text{m}$ ) did not particularly show major differences from the pigments with narrow size distributions in terms of flow properties, color and drying behavior in the conditions of the experiments. However, the PSD range might still be narrow compared to traditional pigment preparation techniques with mechanical grinding, and the pigment particles were isometric and of similar morphology.

## **5.4. Oxidation, crosslinking and complex oil-protein interactions in *tempera grassa* and oil paints**

### *5.4.1. Materials*

The paints studied in this section have been prepared in the proportions indicated in Table 5.4 (the formulations are indicated there in the dried state). Each fresh paint was prepared by hand, applied as a thin relatively uniform layer on a microscope slide (layer thickness  $h \approx 0.2$  mm) and stored under controlled laboratory conditions ( $T \approx 25$  °C and relative humidity  $\approx 50\%$ ). The preparation methodology for each type of paint as well as the analytical techniques used in the following section are detailed in chapter 2.

It is important to keep in mind that most of the UB-based paints evaluated in the following study have a low pigment content ( $< 10$  vol%), which does not correspond to paints one can paint with. As a consequence, the pigment binder interactions are small. However, general trends in the curing reaction of linseed oil are investigated, which is possible also for these types of paints taking these parameters in consideration.

Table 5.4 – Paints compositions (in the dried state) studied in this section

Type of paint	Paint sample	Solids content / vol%	Pigment content / vol%	EY dry matter content / vol%	Linseed oil content / vol%
<i>Tempera Grassa</i> Paints	UB-poor EY-rich TG	58	3	55	42
	UB EY-rich TG	64	16	48	36
	UB EY-medium TG	22	5	17	78
	LW EY-rich TG	65	16	49	35
	LW EY-medium TG	40	27	13	60
Oil-based Paints	UB-poor Oil Paint	6	6	-	94
	UB Oil Paint	32	32	-	68
	UB CapS Paint	33	30	3	67
	UB PCP Paint	16	4	12	84
	LW Oil Paint	31	31	-	69
	LW CapS Paint	31	29	2	69
	LW PCP Paint	29	20	9	71

#### 5.4.2. Artificial accelerated ageing of paints in isothermal conditions

The curing of the oil contained in freshly prepared paints samples was followed by thermogravimetric analysis (TGA) under accelerated conditions at 80 °C. This work is an extension of the data presented in chapter 3, Supplementary Figure 3.20, to other paint systems investigated in this manuscript (CapS and *Tempera Grassa*).

We compared the curing kinetics of linseed oil contained in CapS paints under accelerated conditions. We showed in chapter 3 that these systems form a strong structure at rest with a very high yield stress value (> 1000 Pa). In natural ageing conditions, LW CapS shows similar drying kinetics as the LW oil paint, at the same solids fraction (chapter 3 Figure 3.6): the catalytic effect of the lead white pigment has a greater influence than the antioxidant properties of the EY, which is located in small quantities at the junction between pigment particles and does not influence the kinetics of drying of the oil. In accelerated conditions (Figure 5.20), the onset of mass uptake of the LW CapS is also similar as for the corresponding oil paint. However, differences in the mass loss profile are visible, where the LW CapS mass loss is less pronounced than the one of the LW oil paint. In a general way, the mass loss is ascribed to the decomposition of peroxides and is a

consequence of oxidative degradation of the oil, which occurs in parallel to cross-linking<sup>48,55</sup>. The differences observed here may correspond to different reaction pathways which establish when proteins are present in the paint layer, which we were not able to detect with gravimetry. However, further investigations are needed to better understand the reactions taking place in these paints.

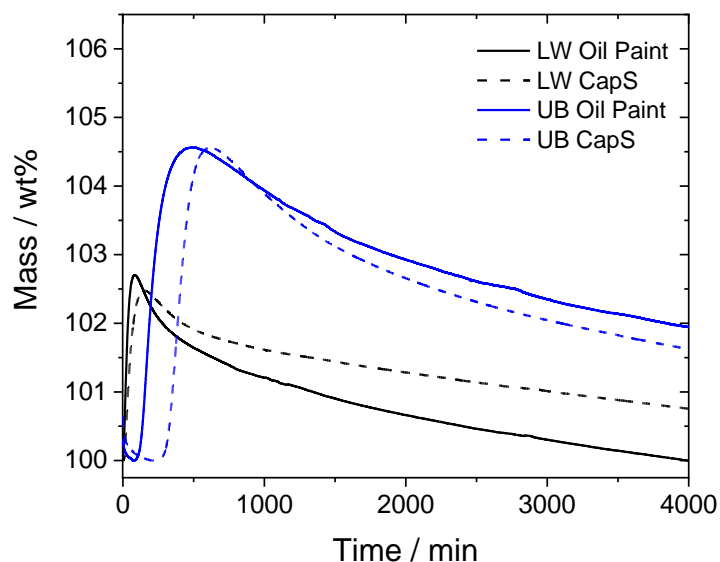


Figure 5.20 - Oxygen uptake experiments in TGA in accelerated conditions at 80 °C for LW (black) and UB (blue) Oil (fill line) and CapS (dashed line) paints.

In accelerated conditions, oil paints containing UB as pigment add more oxygen (twice as much) than LW, probably due to a high degree of oxidation and a different evolution of the unsaturated fatty acids in the cross-linking reactions.<sup>47,171</sup> Because of this, UB and LW oil paints are not directly compared with each other.

Under natural ageing conditions, the onset of mass uptake of UB CapS (but also UB PCP at the same composition) was delayed compared to the UB Oil Paint (chapter 3 Figure 3.6), due to the antioxidant effect of EY, exerted irrespective of the protein repartition in the microstructure of the UB paints. Under accelerated conditions, a delay in the onset of the mass uptake of the CapS compared to the oil paint is also observed (Figure 5.20), in accordance to the results obtained under natural ageing conditions. However, the mass loss profiles are similar, which suggests that similar chemical reactions are taking place upon time in both of these paints.

The same experiments were repeated for *tempera grassa* paints, which are systems behaving differently than oil paints in terms of drying due to their different microstructure. In chapter 4, we showed that the pigments are located in the continuous EY-phase and do not mix with the linseed oil droplets: the pigments do not exert their catalytic effect on the curing on the linseed oil, which is particularly visible for LW-based paints due to the known catalytic influence of the pigment on the

curing of drying oils. Yet these experiments performed both on LW and UB TG paints had short curing times, because these paints contain little amount of egg. Most of the gravimetric experiments at higher EY content were done almost exclusively on UB TG paints under laboratory conditions. Here, accelerated ageing experiments allow to pursue these investigations faster for TG paint systems with a higher egg content.

Under accelerated conditions, the onset of drying time depends on the amount of egg yolk contained in the paint, but the type of pigment used does not seem to influence it (Figure 5.21, left). At similar compositions, both UB and LW EY-rich TG paints' mass uptake occurs almost simultaneously, supporting the assumption that the pigment hardly modifies the drying kinetics of the oil. If these pigments are not (strongly) involved in the curing of the oil, it might indicate that they are protected from it, and its further oxidative degradation reactions which might deteriorate the pigment particles (such as the dissolution of lead into the oil<sup>147</sup> and ultramarine degradation through acidic reactions with the oil<sup>183</sup>).

By extension, this is an important factor for the understanding of the ageing of *tempera grassa* paints: the pigments contained in these types of paints are known to be very well preserved, especially ultramarine pigments, which we know are very sensitive towards acidic reactions leading to strong pigment degradation and color damage. Yet blue pigments are generally very well preserved in *tempera* paints, and our results indicate that this could be due to a protection of the particle by the EY.

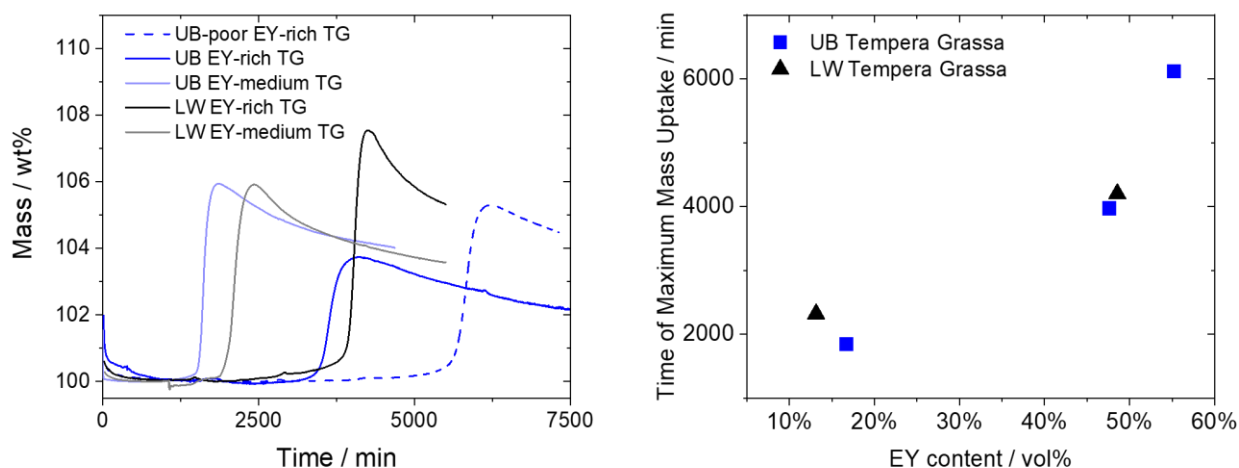


Figure 5.21 - Oxygen uptake experiments in TGA in accelerated conditions at 80 °C (left) and time at which the paints' mass reach the maximum value as function of the volume content of EY in the paint (right) for LW (black triangle) and UB (blue square) tempera grassa paints.

### 5.4.3. DSC of paints

The curing of the oil contained in the paint samples described in Table 5.4 was also followed by DSC under laboratory conditions (natural ageing). We characterized the decomposition and recombination of peroxides in these paints with DSC over time (Figure 5.23). This work is an extension of the data presented in chapter 3, Supplementary Figure 3.14 and Chapter 4 to *TG paint* systems.

As mentioned previously, the antioxidant effect exerted by EY can be clarified in various ways, including the inactivation of reactive oxygen species, free radicals scavenging, reduction of hydroperoxides, and stabilisation of peroxides.<sup>161</sup> As such, we observed that the onset temperature of the peroxide decomposition/radical recombination peak  $T_{\text{onset}}$  in the first stages of curing is significantly higher for LW EY-rich TG paint than the one of paints containing no proteins (Figure 5.24). In addition to this, the lowest  $T_{\text{onset}}$  in these systems is always observed simultaneously with the maximum intensity of the exothermic peak in DSC, which corresponds to the completion of the mass increase determined by gravimetric measurements (data shown in chapter 3 Figure 3.13-15 and in chapter 4 Figure 4.22).

We learned that increasing the quantity of EY, also in TG paints, results in a postponing of the mass increase (see Chapter 3 also detected in accelerated ageing conditions in Figure 5.21). This is also verified by DSC on various TG paints at different EY and pigment concentrations, displayed in Figure 5.22 and Figure 5.23. For the LW EY-medium TG paint, the early stages exothermic peak is clearly detectable in the first days of ageing, whereas this value is not easily visible at this scale for the corresponding EY-rich TG. For the UB TG paints, the quantity of pigment also seems to play a role in the curing reactions: the overall enthalpy of reaction, but also the onset temperatures of these peaks are different between both TG paints studied, where the UB-poor EY-rich TG has much less pigment compared to the UB EY-medium TG, having slightly higher onset temperature values.

The  $T_{\text{onset}}$  of UB-paints containing egg yolk is always lower than that of LW-paints, especially during the first stages of curing (Figure 5.24 and Figure 5.25). However, this difference detected is difficult to attribute to the UB pigment alone, since the quantity of UB is here very low compared to LW. We showed indeed that the pigment concentration had an influence on the  $T_{\text{onset}}$  values obtained in UB paints, when we compared a UB CapS with a high pigment loading with a UB-poor UB oil paint in Chapter 3, Figure 3.14 and Figure 3.15. In this case, UB CapS had higher  $T_{\text{onset}}$  values than the UBLO, but also than the LW CapS at similar volume concentrations, in accordance with the results obtained by Pizzimenti and al. (2021)<sup>47</sup>. On the longer term, however, the onset temperature of this overall exothermic peak reaches the same value for all systems having the same pigment, which is  $\approx 110$  °C for UB paints and  $\approx 120$  °C for LW paints.

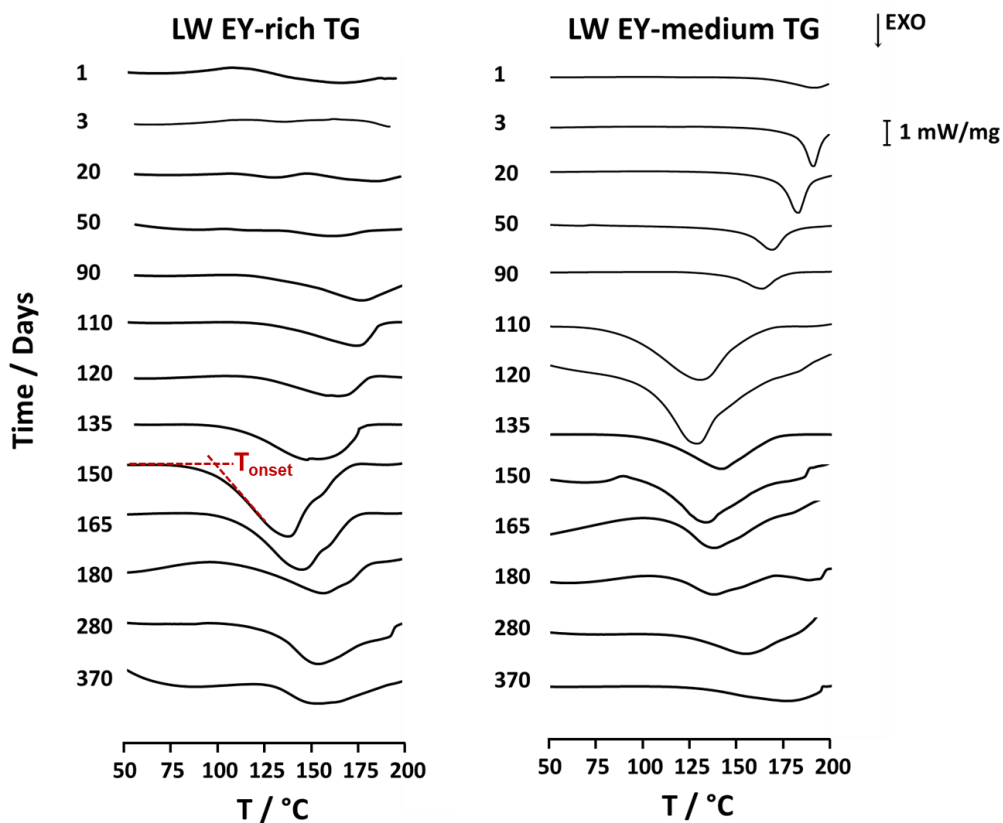


Figure 5.22 - DSC curves of LW-based TG paints upon time.

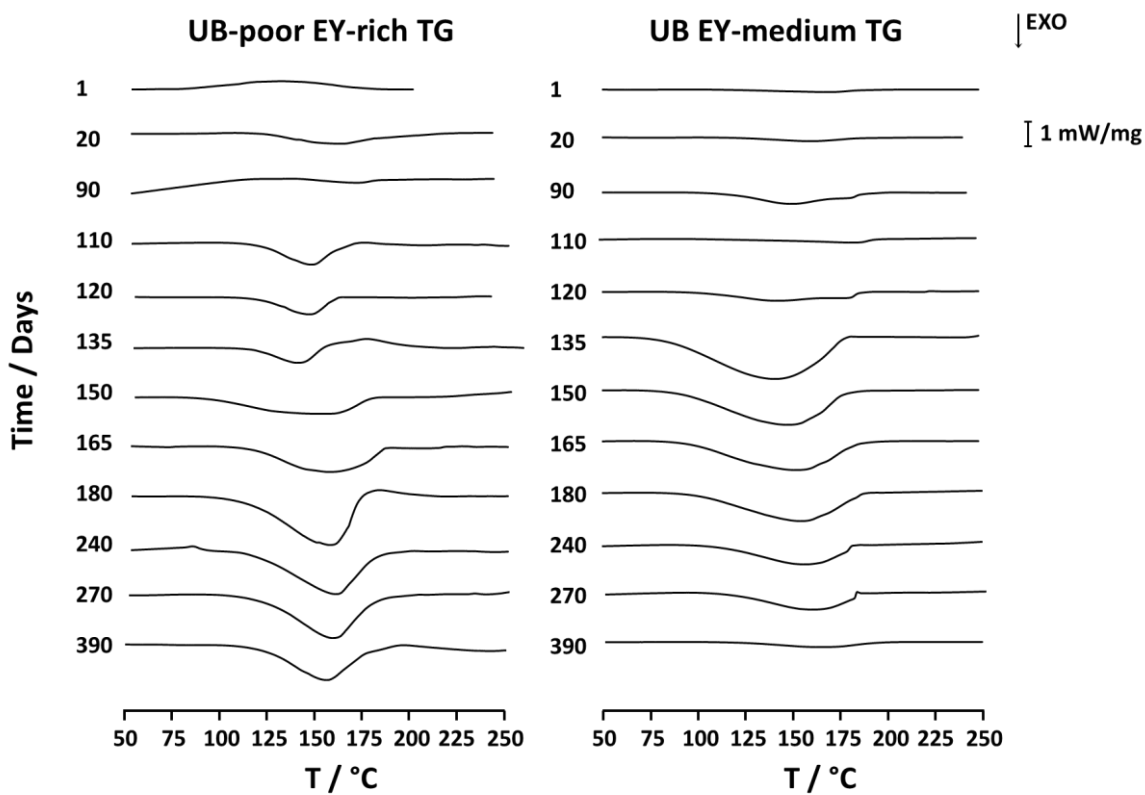


Figure 5.23 - DSC curves of UB-based TG paints upon time.



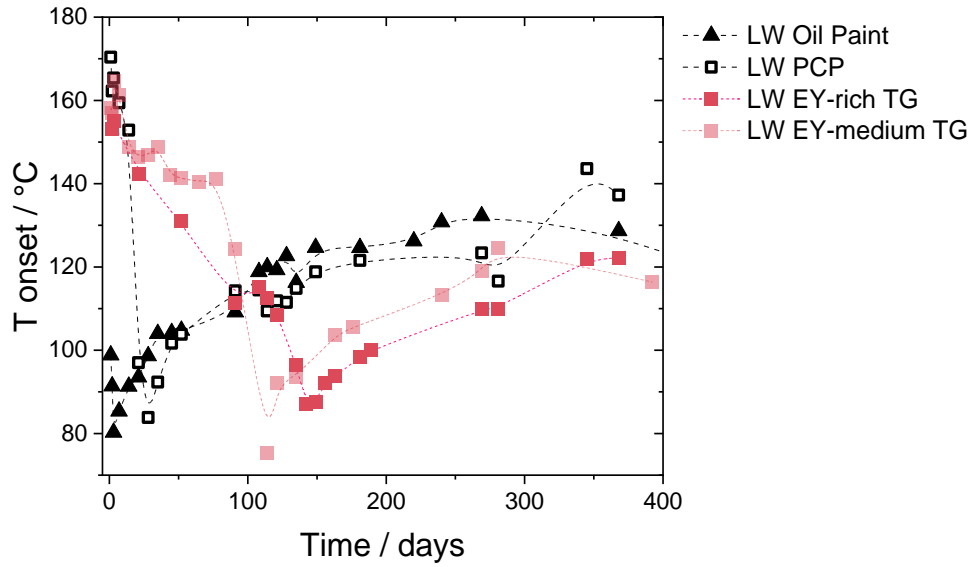


Figure 5.24 - Onset temperature of the overall exothermic peak associated to the decomposition of peroxides and hydroperoxides (endothermic) and the recombination of radical species (exothermic) as a function of the evaluation time of LW paints.

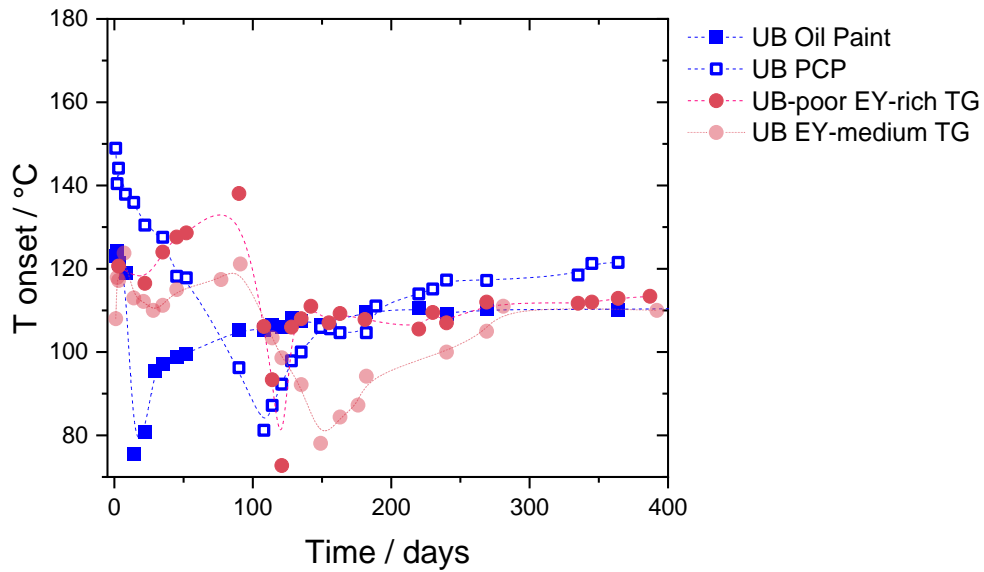


Figure 5.25 - Onset temperature of the overall exothermic peak associated to the decomposition of peroxides and hydroperoxides (endothermic) and the recombination of radical species (exothermic) as a function of the evaluation time of UB paints.

#### 5.4.4. EGA/MS of paints

The EGA-MS technique was used to determine and characterize the components with different thermal stability, from the products of the oxidative degradation of the oil to the highly crosslinked networks<sup>56</sup> of the same paint samples described in Table 5.4. This final section is an extension of the data presented in chapter 4 to the other paints systems studied in this chapter. Here we focus on the mass spectral features of LW oil-based paints (Figure 5.26). The average mass spectra associated to the data presented here are to be found in the Appendix, together with the full dataset carried out on UB-based paints upon time.

The thermograms of these paints present 3 main thermodegradative regions:

- Up to  $\approx 320$  °C, dominated by 2,5-diketopiperazines – (DKPs,  $m/z$  154), and the hexa- and octadecanonitrile (characteristic fragment ions including  $m/z$  110, 194, 208, 222, 236): these are the products of chemical interactions between lipids and proteins, and of depolymerization of proteins upon pyrolysis.<sup>81,168,169</sup> Most likely these products contain imine groups formed between the acidic moiety of fatty acids belonging to the egg lipid fraction and amine groups present on the polypeptide chain, and produce nitriles upon pyrolysis (see section 4.3.5).
- Between  $\approx 320$  and 390 °C, di- and triglycerides containing palmitic, oleic and stearic acids are thermally decomposed. The temperature at which this thermal decomposition occurs indicates that these are non-polymerised.
- The thermodegradative region above  $\approx 390$  °C, is due to the thermal decomposition of the cross-linked fraction, with characteristic fragment ions including  $m/z$  91 and 105 in the pyrolysis of proteinaceous materials. Such cross-linked fraction is observed in the pyrolysis of proteinaceous materials, and is ascribed to the thermal decomposition of the residual material formed in a protein when loss of side chain and depolymerization have taken place.<sup>81</sup>

Both the LW oil paint and the LW CapS paints analyzed at increasing ageing time present very little changes. The shape of the curves and the mass spectral features associated with the different thermodegradative zones are typical of a cured oil paint, with a high quantity of fragments associated to a crosslinked network. The presence of 2 vol% of EY in the CapS paint does not influence the thermal stability of the paints significantly, which remains essentially similar to the one of the cured LW oil paint. The corresponding mass spectra for the LW oil paint is to be found in chapter 4 (Figure 4.29) and the LW CapS in the Appendix (Figure A 3).

On the other hand, the LW PCP thermodegradative profiles evolve slightly differently upon time, with at first a different evolution of the shape of its total ion chromatogram curves (Figure 5.26, above). After 30 days of ageing, the paint formed freshly a solid film (according to the gravimetric data presented in chapter 3) and still contains a high quantity of free glycerides which are not part of a cross-linked network yet. Upon time, as for LW EY-rich TG which also contains a high content

of EY (chapter 4), the quantity of free glycerides remains relatively the highest compared to the other selected fragments, even if the cross-linked fraction increases up to 500 days of ageing, resulting from the curing reactions taking place (Figure 4.27). The LW PCP paint thermodegradative profiles show though both features which can be ascribed to the oil paint, yet not at the same state of curing, and to the TG paint, where the amount of free glycerides is still important even at long ageing times, due to its significant EY content. This correlates with the conclusions drawn in the previous chapters 3 and 4. The corresponding mass spectra for the LW PCP paint is to be found in the Appendix (Figure A 4).

The UB-containing oil and *tempera* paints studied in this section contain a very little amount of pigment and make it difficult to study conscientiously the mass spectral features of these paints undergoing complex curing reactions due to an extremely high content of binder and a reduced interaction between the binders and the pigments. Upon time, the relative abundance of the studied fragments does not evolve significantly. The EGA/MS data associated can be consulted in the Appendix (Figure A 1 and Figure A 2).

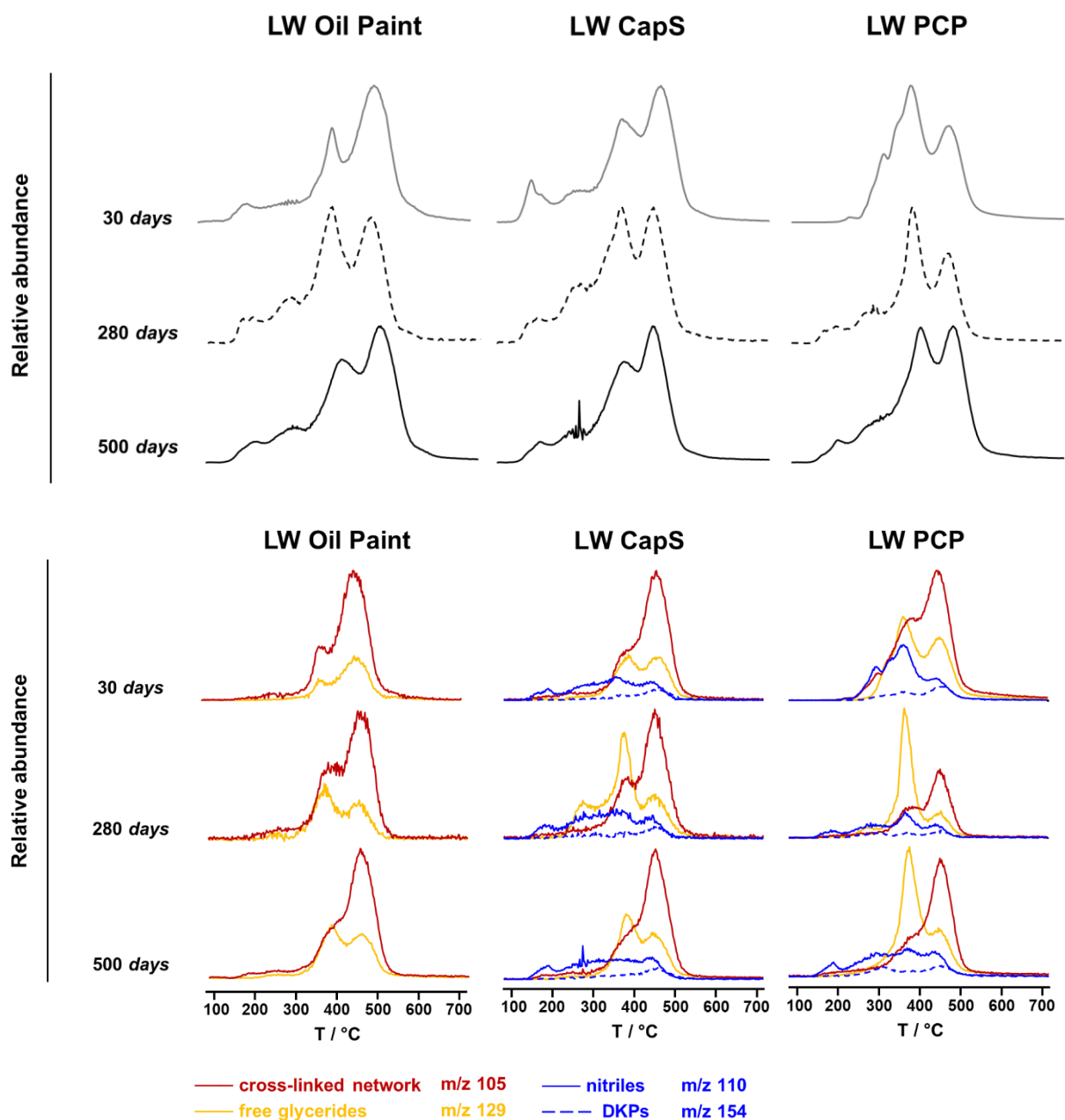


Figure 5.26 - Total ion chromatogram curves (above) and extracted ion thermograms of selected fragments (below) for LW oil paints.

# Summary

Old Masters and their workshops prepared paints containing complex mixtures of oils and proteins, but “how” and “why” this was done is still not understood. Understanding how paints have been prepared in the past, not only in terms of composition, but also in terms of the different steps of preparation and the mixing procedures, is important to identify and learn how technical and artistic development took place during centuries, and to support conservation treatments. This improvement in the understanding of these procedures is accompanied not only by a clear definition of the different terms describing the paints at different scales, i.e. the description of the materials, the flow properties during mixing or the final visual appearance, but also of the major physico-chemical phenomena that dominate the different stages of the preparation of these paints, their application on a surface and their aging behavior over time.

This thesis summarizes the results of around 3.5 years of experimental work focused on the rheological and chemical study of oil-based and *tempera*-based paints, prepared as mock-ups of artists paints. In this work, we examine the influence of the preparation of paints, focusing on the addition of egg yolk and linseed oil as binders, in the modification of the paints' microstructures and its repercussion on the flow behavior, drying and ageing properties of these complex systems. We characterize the systems by means of steady shear rheometry, thermal analysis, spectrometric techniques, microscopy, gravimetry, mechanical tests and colorimetry. The main body of this dissertation is divided into three parts, the first two consisting of peer-reviewed scientific papers.

In chapter 3, we discuss the different effects of adding proteinaceous materials (egg yolk) to oil paints. We prepared oil paints made from protein coated pigments and oil paints with a small amount of added egg yolk (capillary suspensions) and compared their behavior to pure oil paints. There, the pigments are located in the (continuous) oil phase, and the addition of EY has a strong impact on the modification of the flow properties depending on the paint preparation procedure. We could show that covering the pigment surface with a dry protein layer (PCP paints) might lead to an increase in the paint yield stress forming stiffer paints than oil paints due to an attractive steric interaction among hydrophilic surface layers. Pigments can take up water during storage or paint preparation depending on humidity conditions, but water is also introduced when egg yolk is added to an oil paint. Indeed, the addition of liquid EY as a secondary fluid leads to the formation of a capillary network resulting in the production of even stiffer paints (CapS paints). Yet, when the pigment particles are coated with a hydrophilic egg yolk layer, the water uniformly distributes in that layer and a capillary suspension does not form, leaving the yield stress unchanged. Furthermore, these different protein additions affect the chemical and physical stability of aging paints: the

experiments on the drying/curing of the paint layers stressed out that formulations containing egg yolk showed longer drying times compared to oil paints, and that addition of yolk seems to produce well cross-linked polymeric fractions, less prone to oxidative degradation. Finally, we could show that wrinkling, which may occur during the transition from the wet paint to the dry layer, can be suppressed when the mobility of the paint below the dry skin is drastically reduced, e.g. by increasing the paints' yield stress. This holistic view covers a wide range of different scales of paint handling and aging, from the molecular level, which determines oxidation and cross-linking, to the mesoscopic length scale of colloidal structures, which influence both wet paint flow and drying, to the macroscopic scale, which reflects brushwork and impasto, but also wrinkling and cracking.

These observations on oil-based paints motivate us to investigate different systems, where the egg forms the continuous medium and in which linseed oil was added and forms the disperse phase, i.e. *tempera* and *tempera grassa* paints. Chapter 4 focuses on the connection between their microstructure, flow behavior and drying characteristics. Microscopic and spectroscopic techniques revealed that the pigments remain in the continuous aqueous egg phase and do not enter into the oil droplets emulsified in a *tempera grassa*. This feature is attributed to the adsorption of proteins from the EY on the pigment surface. Also, the flow properties of both *tempera* and *tempera grassa* systems are typical for colloidal dispersions: the disperse phase volume fraction  $\varphi$  controls the flow properties and should be calculated including the pigments, the egg yolk dry matter and the oil volume fraction, if applicable. Beyond a critical value  $\varphi_c < \varphi_m$ , both *tempera* and *tempera grassa*, exhibit a yield stress. Also, the total volume fraction of a *tempera grassa* must be higher than that of *tempera* paint to reach similar rheological properties. However, even with similar yield stress and viscosity values, these paints do not necessarily lead to similar brush texture and appearance: on absorbent substrates such as paper, a *tempera* dries faster than a *tempera grassa*, in which the remaining oil droplets softens the paint. Yet these drying times are very short for both types of paints (minutes) due to their aqueous continuous phase, in comparison to oil paints (days). As a consequence, working "wet-in-wet" is not possible for *tempera*-based systems. Finally, also in *tempera grassa* paints with little egg yolk, the oil oxidizes and undergoes curing reactions similar to oil paints leading to a paint film hardening. However, the pigments do not affect this chemical drying since they are not in contact with the oil. The onset of oxidation is also strongly delayed with increasing amount of egg yolk, due to its antioxidant effect. Mass spectrometry finally showed that oils and proteins chemically interact with each other over time, probably leading to copolymerization between the oil poly-unsaturated lipids and proteins moieties.

Our results help to understand some key mechanisms ruling the flow properties and drying of these paint systems. Furthermore, additional parameters were investigated in chapter 5. Increasing the pigment content in oil-based paints speeds up the curing reactions leading to the formation of a solid film. Also, paints having at low yield stress are more inclined to show a drying time gradient with increasing thickness layer, whereas paints with a strongly connected network such as capillary suspensions dry homogeneously, independent of their layer thickness. These latter are also more

inclined to form a wrinkle-free paint. Paint yellowing seems to evolve differently depending on the systems' microstructures, but longer ageing times than one year are requested to confirm this statement. The particle size distribution is often held responsible for the modification of artist paint properties. However, the experiments conducted here on synthetic ultramarine blue did not show significant differences between pigments having a wide size distribution compared to the ones having narrow ones in terms of flow properties, color and drying behavior in the conditions of the experiments. Finally, the thermodegradative profiles as well as the DSC curves of the systems not presented in the sections based on the publications are presented to highlight further aspects that should be documented in this thesis. Particularly, the protein detection in paints prepared as capillary suspensions shows its limits, displaying thermodegradative profiles very similar to their corresponding oil paints containing yet no egg yolk.

The work presented in this thesis does not pretend to cover all the aspects involved in a paint preparation and its behavior upon ageing, but answers some key aspects raised on the topic over the years in the different communities studying painting in the field of cultural heritage. Particularly, the combination of knowledge from three fields of research which are Conservation Science, Analytical Chemistry and Rheology helps to connect interesting individual findings, which are, at the larger scale, necessary to understand the key aspects ruling these complex systems. This will help improving the conservation of unique and invaluable artworks in a near future. Connecting different fields of expertise for answering a common question is not an easy task, because usually the same technical language is not used, but this work proved that it can be a step forward to improve the efficiency of such research projects.





# Outlook

This thesis provides many new insights into the relationship between the microstructures of oil and *tempera* paints, from their wet state to their transformation into solid films and aged layers. This study is the first of its kind to address all these aspects, not only in a multi-analytical approach, but also with a multi-field view. As often in this case, well beyond the objective of answering the questions raised in the first place, it has also opened new doors for reflection: several aspects for further research are briefly presented here.

First of all, egg yolk is the only source of proteinaceous material used in the frame of this study. Despite its extensive use in paintings and interesting properties, it also strongly delays the curing of oil-based paints due to its antioxidant properties. At high concentrations when used as a pigment coating, it might delay the paint film formation up to one year compared to an oil paint containing no egg yolk, which is absolutely not realistic for the studied artistic purposes. However, it showed also great assets, such as modifying the pigment surface properties when used as a coating for instance, avoiding the formation of unwanted capillary suspensions and thus permitting to increase the solids fraction of the paint mixture if desired. It would be interesting to understand if these conditions might also be reached by using different types of materials containing proteins, without containing any antioxidants, such as for example egg white (containing ovalbumin), milk (casein) or different plant-based proteins.

However, this study encountered some technical difficulties regarding the sensitivity of some of the analytical techniques used, especially regarding the protein detection in both paints' microstructures (spatial recognition) but also with advanced spectrometric methods (such as EGA/MS or Py/GC/MS), which are despite their high sensitivity not fully adapted yet to detect small quantities of EY proteins in aged paints (chemical detection): other approaches, such as proteomics can be extremely sensitive, and may be used for these purposes instead. This was particularly the case for CapS paint systems, which contained very little amount of egg yolk, but also for other systems prepared at low egg yolk content. Highly-sensitive detection methods are requested to localize the species in a system's microstructure.

We could show the determining influence of the paint microstructure on the flow properties of the wet paints, but also on their kinetics of drying and on the longer term on the curing of the oil and the chemical stability of these dried layers. In addition to this, the mechanical properties of the paints containing oil are affected by the oil curing, resulting in an increase of the paint layer's hardness when the curing reactions have started. Depending on the paint microstructure, we have shown that the chemical activity and further oxidation and cross-linking reactions may vary from

one system to another, and this could lead to modifications of the film mechanical properties. We could also demonstrate that oil paints with high yield stress values formed wrinkle-free paint layers, compared to paints having a low yield stress. To support the mechanico-chemical set of experiments started here, a mechanical stability study on aged paint layers with the same compositions but various microstructures might be of great interest. Typical mechanical testing experiences such as tensile or fatigue testing which are widely used in industry for polymer-based films, are probably the most adapted methods for this purpose. Preliminary tests were conducted on lead white containing oil-based paints using dynamic mechanical analysis (DMA), giving interesting and promising results. However multiple parameters need to be considered regarding for instance the film geometry, testing time or time-scale, and this could not be completed in the frame of this research project. Combined with a chemical characterization, we could understand how and at which extent microstructure, curing and mechanical paint resistance are connected, particularly towards cracks or wrinkle formation. This would enable to come nearer to the reality experienced by the original artworks, and merged with an investigation including external factors such as weathering and temperature variations, which are determining factors for the paint modifications upon time, this could help to set a targeted conservation strategy for these precious artworks.

In this dissertation, all the ageing experiments were performed at a relatively high thickness layer for comparative reasons: it was necessary to produce films which were thick enough to measure their change of hardness upon time, and to measure the change of weight on comparable sample holders in the same conditions. However, we showed that there is a correlation between the thickness of a paint sample and its onset of drying, though it would be reasonable to study these parameters on thinner paint layers, comparable to artist paints' panel paintings, to get closer to real painting conditions. In addition to this, we could demonstrate that the type of substrate such as paper or a metallic plate plays a role on the drying kinetics of these paint layers. Particularly, some surfaces absorb typically any excess of solvent or liquid binder such as water or oil, modifying greatly the drying times determined experimentally in this thesis. Usually, artists' paints are not purely monochrome, and several layers of paints are added on top of each other and/or mixed together in the wet state. As a consequence, it is legitimate to assume that solvents and liquid binders might transfer to lower layers and thus influence the drying and curing properties of these other paint surfaces, but at which extent? And what happens for mixed media, such as adding a layer of an oil-based paint on the top of a *tempera*, and vice-versa?

Finally, the colorimetric study delivered some promising results, which need yet longer ageing times to conclude on the topic. However, *tempera paints* with higher egg yolk content than the ones studied in this colorimetric study seem to preserve better the blue color over time than oil-based ones. Knowledge about the correlation between the color changes and the paint binder distribution need to be accumulated by conducting a systematic and controlled colorimetric study on the long term.

# Appendix

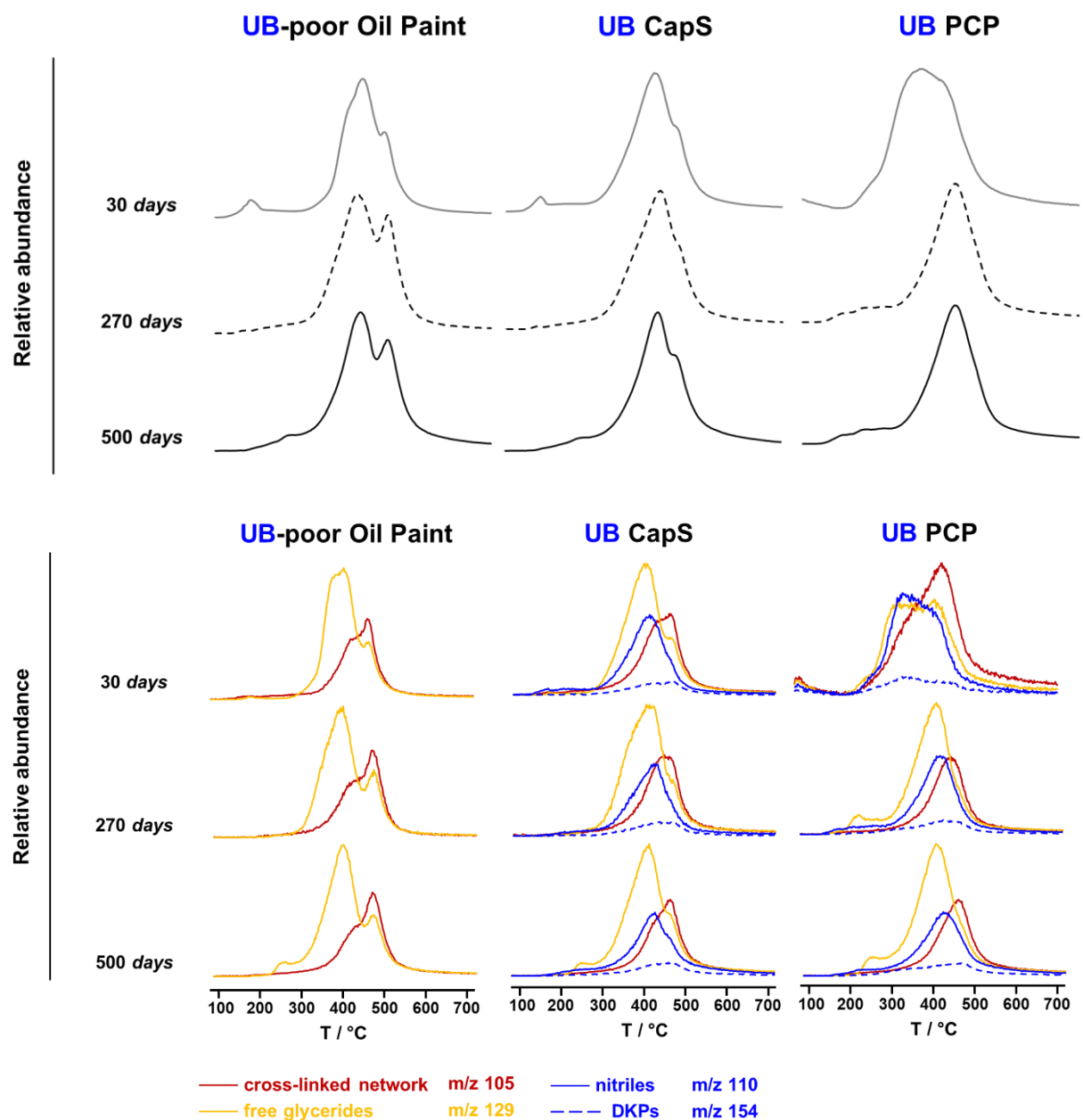


Figure A 1 - Total ion chromatogram curves (above) and extracted ion thermograms of selected fragments (below) for UB oil-based paints.

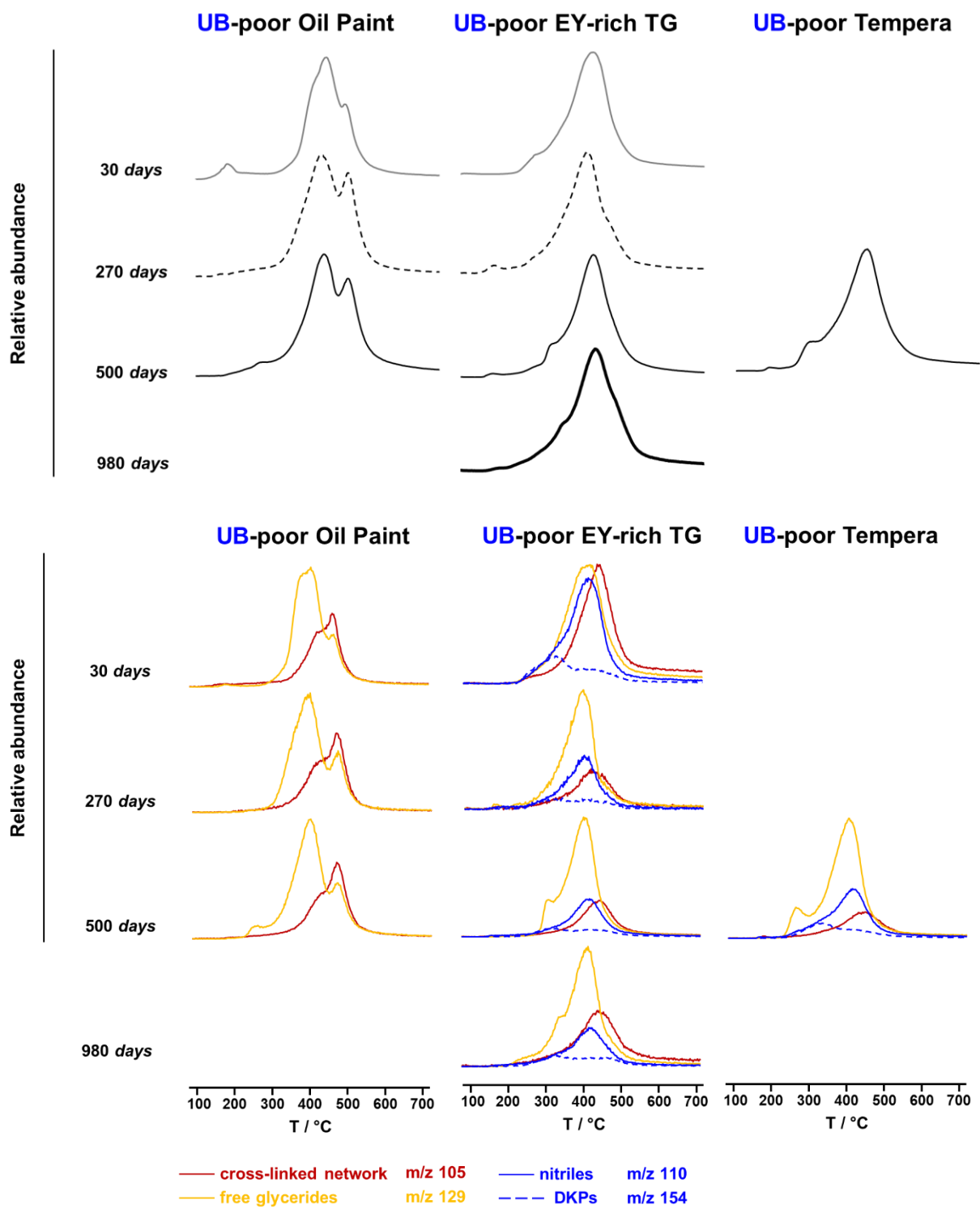


Figure A 2 - Total ion chromatogram curves (above) and extracted ion thermograms of selected fragments (below) for UB tempera-based paints.

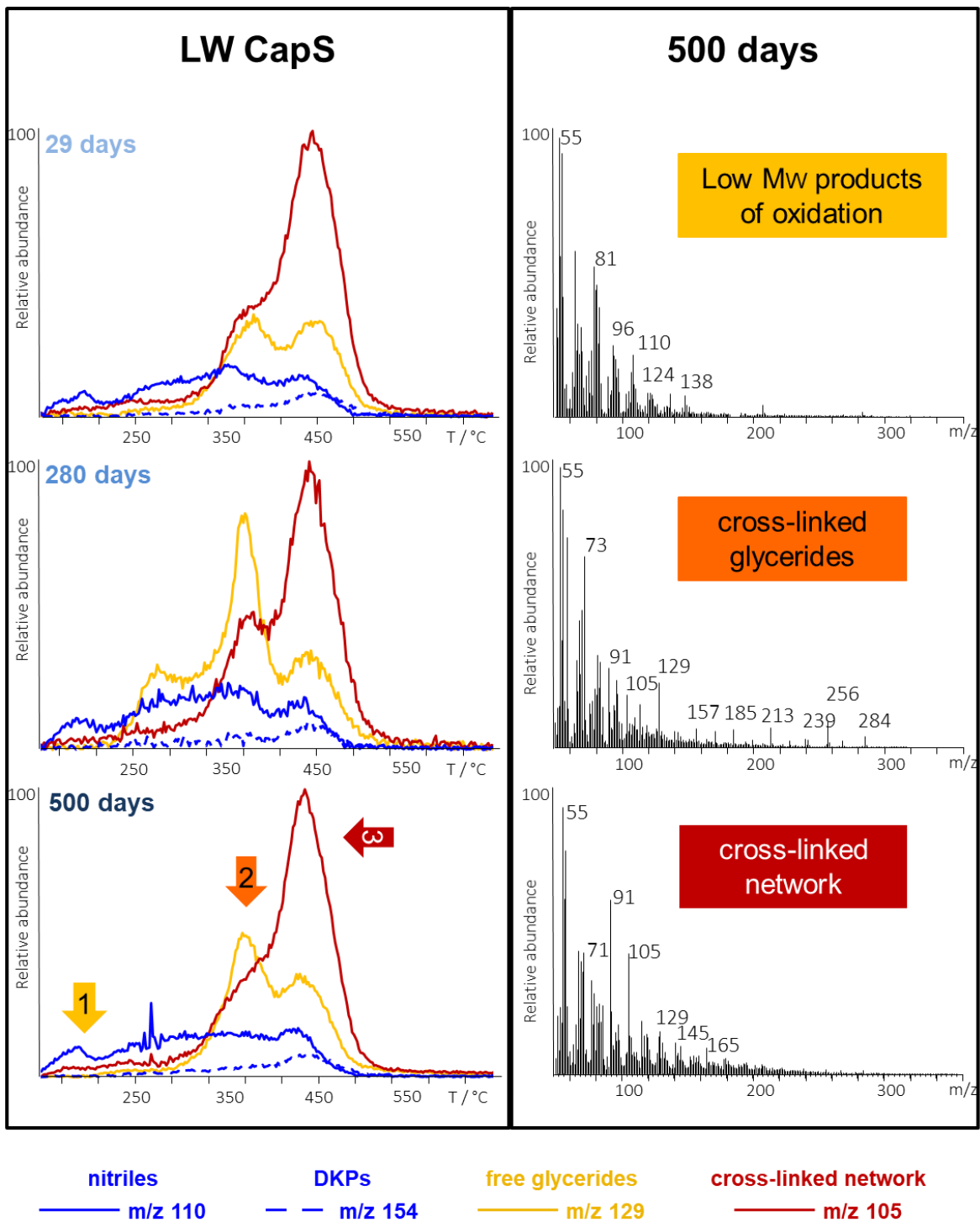


Figure A 3 - Extracted ion thermograms of selected fragments of a LW CapS paint (left) and its corresponding mass spectra at 500 days of ageing at the indicated temperatures (right).

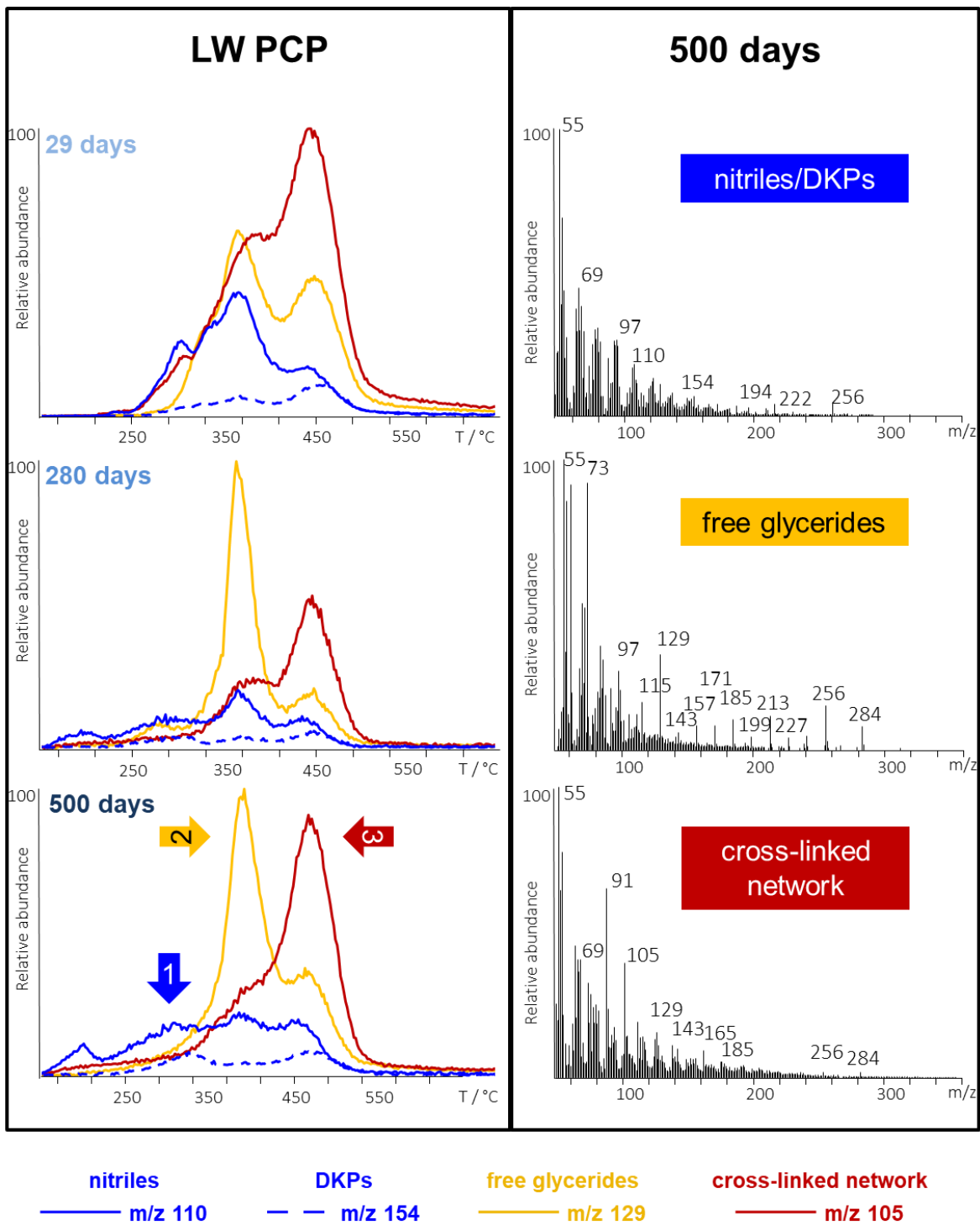


Figure A 4 - Extracted ion thermograms of selected fragments of a LW PCP paint (left) and its corresponding mass spectra at 500 days of ageing at the indicated temperatures (right).

# Notations

## Abbreviations

Abbreviation	Description
ATR	Attenuated total reflectance
CapS	Capillary suspension
CIE	Commission internationale de l'éclairage
DKPs	Diketopyperazines
DSC	Differential scanning calorimetry
EGAMS	Evolved gas analysis coupled with mass spectrometry
EY	Egg yolk
FTIR	Fourier-transform infrared
GC/MS	Gas chromatography coupled with mass spectrometry
HDL	High density lipoprotein
HMDS	1,1,1,3,3,3-hexamethyldisilazane
LDL	Low density lipoprotein
LO	Linseed oil
LSM	Confocal laser microscopy
LW	Lead white
LWLO	Lead white-based oil paint
MSC	Maximum solids content
MSD	Mean square displacement
NMR	Nuclear magnetic resonance
PCP	Protein coated pigment
pH	Potential of hydrogen
PSD	Particle size distribution
Py/GC/MS	Pyrolysis coupled with gas chromatography and mass spectrometry
RT	Room temperature
SEM	Scanning electron microscopy
TG	<i>Tempera grassa</i>

TGA	Thermogravimetric analysis
TRANS	Transmittance spectroscopy
UB	Ultramarine blue
UBLO	Ultramarine blue-based oil paint
XRD	X-ray diffraction
YI	Yellowness index

---

## Symbols

Symbol	Unit	Description
$\gamma$	[%]	Deformation
$\eta_{\infty}$	[Pa.s]	High shear limiting viscosity
$\eta_s$	[Pa.s]	Viscosity of the continuous phase
$\varphi$	[vol%]	Disperse fraction
$\varphi_c$	[vol%]	Critical volume fraction
$\varphi_{EY}$	[vol%]	Egg yolk disperse fraction
$\varphi_m$	[vol%]	Maximum packing fraction
$\varphi_{oil}$	[vol%]	Oil disperse fraction
$\varphi_{pigment}$	[vol%]	Pigment disperse fraction
$\rho$	[g/cm <sup>3</sup> ]	Density
$\sigma_y$	[Pa]	Yield stress
$\Delta E^*$	[ - ]	Total change of color compared to a reference
$a^*, b^*$	[ - ]	Color coordinates
$c^*$	[ - ]	Chroma
$d$	[mm], [ $\mu$ m], [nm]	Diameter
$h$	[mm]	Height
$h^*$	[ - ]	Hue
$L^*$	[ - ]	Lightness
$\Theta$	[°]	Incident angle
RH	[%]	Relative humidity
Rz	[ $\mu$ m]	Roughness
Sv	[m <sup>2</sup> /cm <sup>3</sup> ]	Specific surface
T	[°C]	Temperature
t	[s], [h], [days]	Time

---



$T_{\text{onset}}$	[°C]	Onset temperature of the peroxide decomposition/radical recombination peak in DSC
$x, y, z$	[ - ]	Cartesian coordinates
$X_{50}$	[ $\mu\text{m}$ ]	Volume-based average particle size diameter

---



# Bibliography

1. the Elder, P. *Pline l'ancien: histoire naturelle, livre XXXIV*. (Les Belles Lettres, 1953).
2. Broecke, L. *Cennino Cennini's Il libro dell'arte. A new English translation and commentary with Italian transcription*. (Archetype Publications, 2015).
3. DeGhetaldi, K. *From Egg to Oil: The early development of oil painting during the Quattrocento*. (University of Delaware, 2016).
4. Dunkerton, J. Modifications to traditional egg tempera techniques in fifteenth-century Italy. in *Early Italian Paintings: Techniques and Analysis* (eds. Hoppenbrouwers, R., Dubois, H. & Bakkenist, T.) 29–34 (1997).
5. Peggie, D. A. The Chemistry and Chemical Investigation of the Transition from Egg Tempera Painting to Oil in Italy in the 15th Century. in *Science and Art: The Painted Surface* (eds. Sgamellotti, A., Brunetti, B. & Miliani, C.) 209–229 (2014).
6. Higgitt, C. & White, R. Analyses of paint media: new studies of Italian paintings of the fifteenth and sixteenth centuries. *Natl. Gall. Tech. Bull.* **26**, 88–104 (2005).
7. Roy, A. & Dunkerton, J. Chemistry and conservation: changes in perception and practice at the National Gallery, London. in *Early Italian Paintings: Approaches to Conservation* (ed. Garland, P. S.) 120–131 (2003).
8. Dietemann, P., Fischer, U., Karl, D., Baumer, U. & Steuer, C. Die Bindemittel der Florentiner Malerei. in *Florentiner Malerei – Alte Pinakothek. Die Gemälde des 14. bis 16. Jahrhunderts* (eds. Schumacher, A., Kranz, A. & Hojer, A.) 92–105 (2017).
9. Salvant Plisson, J. Caractérisation des propriétés physico-chimiques des matériaux de peinture employés par Van Gogh : les peintures blanches. (Université Pierre et Marie Curie - Paris VI, 2012).
10. Koller, J. & Baumer, U. Leonardos Rolle in der frühen Ölmalerei. in *Leonardo da Vinci. Die Madonna mit der Nelke* (eds. Syre, C., Schmidt, J. & Stege, H.) 155–174 (Schirmer/Mosel, 2006).
11. White, R. Van Eyck's Technique. The Myth and the Reality, II. in *Investigating Jan van Eyck* (eds. Foister, S., Jones, S. & Cool, D.) 101–105 (2000).
12. Neugebauer, W. *Von Böcklin bis Kandinsky: kunsttechnologische Forschungen zur Temperamalerei in München zwischen 1850 und 1914*. (Pro Business, 2016).
13. Clarke, M. *Mediaeval painters' materials and techniques: the Montpellier 'Liber diversarum arcium'*. (Archetype Publications, 2011).
14. Dietemann, P., Neugebauer, W., Baumer, U., Fiedler, I. & Poggendorf, R. Edvard Munch's binding media of Street in Åsgårdstrand and a Woman in Red Dress and a suggestion for a threefold definition of the terms 'tempera' and 'oil'. in *Public paintings by Edvard Munch and his contemporaries – Change and conservation challenges* (eds. Frøysaker, T. & Streeton, N. L. W.) 279–293 (Archetype Publications, 2015).
15. Reinkowski-Häfner, E. Tempera: narratives on a technical term in art and conservation. in *Tempera Painting 1800 – 1950* 21–32 (2019).
16. Colombini, M. P. & Modugno, F. *Organic Mass Spectrometry in Art and Archaeology*. Wiley

- (2009).
17. Bonaduce, I. *et al.* A multi-analytical approach to studying binding media in oil paintings: Characterisation of differently pre-treated linseed oil by DE-MS, TG and GC/MS. *J. Therm. Anal. Calorim.* **107**, 1055–1066 (2012).
  18. Dietemann, P. *et al.* Analysis of complex tempera binding media combining chromatographic techniques, fluorescent staining for proteins and FTIR-FPA imaging. in *Painting in Tempera, c. 1900* 183–203 (2016).
  19. Reinkowski-Häfner, E. Tempera - Zur Geschichte eines maltechnischen Begriffs. *Zeitschrift für Kunsttechnologie und Konserv.* 297–317 (1994).
  20. Dietemann, P. & Neugebauer, W. Combining different types of sources for a better understanding of tempera painting around 1900. in *Making and Transforming Art: Technology and Interpretation, Postprints of the Art Technological Source Research (ATSR) working group conference* (eds. Dubois, H. *et al.*) 95–101 (Archetype Publications, 2014).
  21. Dunkerton, J., Foister, S., Gordon, D. & Penny, N. *Giotto to Dürer: Early Renaissance Painting in the National Gallery*. (Yale University Press, 1991).
  22. Dietemann, P. *et al.* A Colloidal Description of Tempera and Oil Paints , Based on a Case Study of Arnold Böcklin's Painting Villa Am Meer II (1865). *e-Preservation Sci.* **11**, 29–46 (2014).
  23. Karl, D. Die Maltechnik der Florentiner Meister. in *Florentiner Malerei – Alte Pinakothek. Die Gemälde des 14. bis 16. Jahrhunderts* 56–81 (2017).
  24. Bartl, A., Krekel, C., Lautenschlager, M. & Oltrogge, D. *Der "Liber illuministarum" aus Kloster Tegernsee*. vol. 8 (Franz Steiner Verlag, 2005).
  25. Schadler, K. *History of egg tempera painting*. <http://www.kooschadler.com/techniques.htm> (2017).
  26. de Viguerie, L., Ducouret, G., Lequeux, F., Moutard-Martin, T. & Walter, P. Historical evolution of oil painting media: A rheological study. *Comptes Rendus Phys.* **10**, 612–621 (2009).
  27. de Viguerie, L. *et al.* A 19th Century "Ideal" Oil Paint Medium: A Complex Hybrid Organic–Inorganic Gel. *Angew. Chemie - Int. Ed.* **56**, 1619–1623 (2017).
  28. Lim, S. & Ahn, K. H. Rheological properties of oil paints and their flow instabilities in blade coating. *Rheol. Acta* **52**, 643–659 (2013).
  29. de Viguerie, L. *et al.* Re-interpretation of the Old Masters' practices through optical and rheological investigation: The presence of calcite. *Comptes Rendus Phys.* **19**, 543–552 (2018).
  30. Salvant Plisson, J., de Viguerie, L., Tahroucht, L., Menu, M. & Ducouret, G. Rheology of white paints: How Van Gogh achieved his famous impasto. *Colloids Surfaces A Physicochem. Eng. Asp.* **458**, 134–141 (2014).
  31. Fanost, A. *et al.* Connecting Rheological Properties and Molecular Dynamics of Egg-Tempera Paints based on Egg Yolk. *Angew. Chemie* 1–6 (2021) doi:10.1002/ange.202112108.
  32. Stadelman, W. J. . & Cotterill, O. J. *Egg Science and Technology*. (Macmillan Education UK, 1986). doi:10.1007/978-1-349-09142-3.
  33. Anton, M. Egg yolk: Structures, functionalities and processes. *J. Sci. Food Agric.* **93**, 2871–2880 (2013).
  34. Chang, C. M., Powrie, W. D. & Fennema, O. Microstructure of Egg Yolk. *J. Food Sci.* **42**, 1193–1200 (1977).

35. Fanost, A. Formulation et propriétés physico-chimiques de peintures a tempera à base de jaune d'œuf et de terres vertes. (Sorbonne Université, 2020).
36. Van Der Kooij, H. M. & Sprakel, J. Watching paint dry; more exciting than it seems. *Soft Matter* **11**, 6353–6359 (2015).
37. dePolo, G., Walton, M., Keune, K. & Shull, K. R. After the paint has dried: a review of testing techniques for studying the mechanical properties of artists' paint. *Herit. Sci.* **9**, 1–24 (2021).
38. Kaufmann, H. P. & Strüber, K. Über die Runzelbildung bei der Verfilmung trocknender Öle. *Fette und Seifen* **53**, 543–544 (1951).
39. Basu, S. K., Scriven, L. E., Francis, L. F. & McCormick, A. V. Mechanism of wrinkle formation in curing coatings. *Prog. Org. Coatings* **53**, 1–16 (2005).
40. Mayer, R. *The Artist's Handbook of materials and Techniques. The Artist's Handbook of materials and Techniques* (Viking Penguin, 1991).
41. Janas, A. *et al.* Shrinkage and mechanical properties of drying oil paints. *Herit. Sci.* 1–10 (2022) doi:10.1186/s40494-022-00814-2.
42. Pozo-Antonio, J. S., Rivas, T., Dionisio, A., Barral, D. & Cardell, C. Effect of a SO<sub>2</sub> Rich Atmosphere on Tempera Paint Mock-Ups. Part 1: Accelerated Aging of Smalt and Lapis Lazuli-Based Paints. *Minerals* 1–24 (2020).
43. Mallégol, J., Lemaire, J. & Gardette, J.-L. Yellowing of Oil-Based Paints. *Stud. Conserv.* **46**, 121–131 (2001).
44. Van Der Kooij, H. M., Fokkink, R., Van Der Gucht, J. & Sprakel, J. Quantitative imaging of heterogeneous dynamics in drying and aging paints. *Sci. Rep.* **6**, 1–10 (2016).
45. Mecklenburg, M. F., Tumosa, C. S. & Vicenzi, E. P. The Influence of Pigments and Ion Migration on the Durability of Drying Oil and Alkyd Paints. *New Insights into Clean. Paint. Proc. from Clean. 2010 Int. Conf. Univ. Politec. Val. Museum Conserv. Inst.* 59–67 (2013).
46. Fuster-López, L., Izzo, F. C., Damato, V., Yusà-Marco, D. J. & Zendri, E. An insight into the mechanical properties of selected commercial oil and alkyd paint films containing cobalt blue. *J. Cult. Herit.* **35**, 225–234 (2019).
47. Pizzimenti, S. *et al.* Oxidation and Cross-Linking in the Curing of Air-Drying Artists' Oil Paints. *ACS Appl. Polym. Mater.* **3**, 1912–1922 (2021).
48. Bonaduce, I. *et al.* Conservation Issues of Modern Oil Paintings: A Molecular Model on Paint Curing. *Acc. Chem. Res.* **52**, 3397–3406 (2019).
49. Inyang, U. E., Oboh, I. O. & Etuk, B. R. Kinetic Models for Drying Techniques—Food Materials. *Adv. Chem. Eng. Sci.* **08**, 27–48 (2018).
50. Routh, A. F. Drying of thin colloidal films. *Reports Prog. Phys.* **76**, (2013).
51. Weger, M. Ueber die Sauerstoffaufnahme der Oele und Harze. *Chem. Rev. über die Fett- und Harz-Industrie* **5**, 236–250 (1898).
52. Sabin, A. H. Linseed Oil. *Ind. Eng. Chem.* **3**, 84–86 (1911).
53. Eibner, A. Sprung- und Rißbildung antrocknender Ölfarbenanstriche und auf Ölbildern. in *Monographien zur Maltechnik* (Deutsche Gesellschaft für rationelle Malverfahren, 1920).
54. Clark, G. . & Tschentke, H. L. Physico-Chemical Studies the Mechanism of the Drying of Linseed Oil. **1929**, (1929).
55. Lazzari, M. & Chiantore, O. Drying and oxidative degradation of linseed oil. *Polym. Degrad. Stab.* **65**, 303–313 (1999).
56. Vannoni, L. *et al.* Disclosing the chemistry of oil curing by mass spectrometry using methyl linoleate as a model binder. *Microchem. J.* **173**, 107012 (2022).

57. Bonaduce, I. *et al.* New Insights into the Ageing of Linseed Oil Paint Binder: A Qualitative and Quantitative Analytical Study. *PLoS One* **7**, (2012).
58. Oakley, L. H., Casadio, F., Shull, P. K. R. & Broadbelt, P. L. J. Modeling the Evolution of Crosslinked and Extractable Material in an Oil-Based Paint Model System. *Angew. Chemie - Int. Ed.* **57**, 7413–7417 (2018).
59. Juita, Dlugogorski, B. Z., Kennedy, E. M. & Mackie, J. C. Low temperature oxidation of linseed oil: a review. *Fire Sci. Rev.* **1**, 1–37 (2012).
60. Kalinina, K. B., Bonaduce, I., Colombini, M. P. & Artemieva, I. S. An analytical investigation of the painting technique of Italian Renaissance master Lorenzo Lotto. *J. Cult. Herit.* **13**, 259–274 (2012).
61. Groen, K. Investigation of the Use of the Binding Medium by Rembrandt. *Zeitschrift für Kunsttechnologie und Konserv.* **2**, 207–227 (1997).
62. von Baum, K. *et al.* *Let the Material Talk: Technology of Late-medieval Cologne Panel Painting*. (Archetype Publications, 2014).
63. Koller, J., Fiedler, I. & Baumer, U. Die Bindemittel auf Dürers Tafelgemälden. in *Albrecht Dürer: Die Gemälde der Alten Pinakothek* (eds. Goldberg, G., Heimberg, B. & Schawe, M.) 102–119 (Bayerische Staatsgemäldesammlungen München, 1998).
64. Sciutto, G. *et al.* Localization of proteins in paint cross-sections by scanning electrochemical microscopy as an alternative immunochemical detection technique. *Anal. Chim. Acta* **831**, 31–37 (2014).
65. du Boullay, C. T. *et al.* On the way to tempera grassa: unraveling the properties of emulsion-based paint binders. *Colloids Surfaces A Physicochem. Eng. Asp.* 131816 (2023).
66. Stacey, R. J. *et al.* Ancient encaustic: An experimental exploration of technology, ageing behaviour and approaches to analytical investigation. *Microchem. J.* **138**, 472–487 (2018).
67. Solazzo, C., Rolando, C. & Tokarski, C. Protéomique dans l'art et l'archéologie. *L'Actualité Chim. Matières Color. Org.* 1–6 (2008).
68. Chiavari, G., Gandini, N., Russo, P. & Fabbri, D. Characterisation of standard tempera painting layers containing proteinaceous binders by pyrolysis (/Methylation)-gas chromatography-mass spectrometry. *Chromatographia* **47**, 420–426 (1998).
69. Vagnini, M. *et al.* Identification of proteins in painting cross-sections by immunofluorescence microscopy. *Anal. Bioanal. Chem.* **392**, 57–64 (2008).
70. Orsini, S., Bramanti, E. & Bonaduce, I. Analytical pyrolysis to gain insights into the protein structure. The case of ovalbumin. *J. Anal. Appl. Pyrolysis* **133**, 59–67 (2018).
71. Dufrechou, M., Sauvage, F.-X., Bach, B. & Vernhet, A. Protein Aggregation in White Wines: Influence of the Temperature on Aggregation Kinetics and Mechanisms. *J. Agric. Food Chem.* **58**, 10209–10218 (2010).
72. Ren, F., Atlasevich, N., Baade, B., Loike, J. & Arslanoglu, J. Influence of pigments and protein aging on protein identification in historically representative casein-based paints using enzyme-linked immunosorbent assay. *Anal. Bioanal. Chem.* **408**, 203–215 (2016).
73. Duce, C. *et al.* Interactions between inorganic pigments and proteinaceous binders in reference paint reconstructions. *Dalt. Trans.* **42**, 5975–5984 (2013).
74. Gunstone, F. D. Bailey's Industrial Oil and Fat Products, Volume 1, Edible Oil and Fat Products: General Applications (5th edn). *Trends Food Sci. Technol.* **11**, 379–380 (1996).
75. Schaich, K., Shahidi, F., Zhong, Y. & Eskin, N. A. M. Lipid oxidation. in *Biochemistry of foods* (eds. Eskin, N. A. M. & Shahidi, F.) 419–478 (Academic Press, 2013).
76. Schaich, K. *Lipid co-oxidation of proteins : One size does not fit all.* *Inform vol.* 25 (2014).

77. van den Brink, O. F., Boon, J. J., O'Connor, P. B., Duursma, M. C. & Heeren, R. M. A. Matrix-assisted laser desorption/ionization Fourier transform mass spectrometric analysis of oxygenated triglycerides and phosphatidylcholines in egg tempera paint dosimeters used for environmental monitoring of museum display conditions. *J. Mass Spectrom.* **36**, 479–492 (2001).
78. Lluveras-Tenorio, A. *et al.* Development of a GC–MS strategy for the determination of cross-linked proteins in 20th century paint tubes. *Microchem. J.* **170**, 106633 (2021).
79. Chiavari, G. *et al.* Analysis of proteinaceous binders by in-situ pyrolysis and silylation. *Chromatographia* **57**, 645–648 (2003).
80. Corso, G. *et al.* Characterization of pigments and ligands in a wall painting fragment from Liternum archaeological park (Italy). *J. Sep. Sci.* **35**, 2986–2993 (2012).
81. Orsini, S., Duce, C. & Bonaduce, I. Analytical pyrolysis of ovalbumin. *J. Anal. Appl. Pyrolysis* **130**, 249–255 (2018).
82. Fujita, Y. & Noda, Y. The Effect of Hydration on the Thermal Stability of Ovalbumin as Measured by Means of Differential Scanning Calorimetry. *Bulletin of the Chemical Society of Japan* vol. 54 3233–3234 (1981).
83. Donovan, J. W., Mapes, C. J., Davis, J. G. & Garibaldi, J. A. A differential scanning calorimetric study of the stability of egg white to heat denaturation. *J. Sci. Food Agric.* **26**, 73–83 (1975).
84. Blume, K., Dietrich, K., Lilienthal, S., Ternes, W. & Drotleff, A. M. Exploring the relationship between protein secondary structures, temperature-dependent viscosities, and technological treatments in egg yolk and LDL by FTIR and rheology. *Food Chem.* **173**, 584–593 (2015).
85. Saitta, F. *et al.* DSC on ovalbumin-hematite “tempera” paints: the role of water and pigment on protein stability. *Thermochim. Acta* **694**, 1–17 (2020).
86. Odlyha, M., Cohen, N. S. & Foster, G. M. Dosimetry of paintings: Determination of the degree of chemical change in museum exposed test paintings (azurite tempera) by thermal and spectroscopic analysis. *Thermochim. Acta* **365**, 53–63 (2000).
87. Odlyha, M., Cohen, N. S. & Foster, G. M. Dosimetry of paintings: Determination of the degree of chemical change in museum exposed test paintings (lead white tempera) by thermal analysis and IR spectroscopy. *Thermochim. Acta* **365**, 45–52 (2000).
88. van den Brink, O. F., Ferreira, E. S. B., van der Horst, J. & Boon, J. J. A direct temperature-resolved tandem mass spectrometry study of cholesterol oxidation products in light-aged egg tempera paints with examples from works of art. *Int. J. Mass Spectrom.* **284**, 12–21 (2009).
89. Duce, C. *et al.* Physico-chemical characterization of protein-pigment interactions in tempera paint reconstructions: Casein/cinnabar and albumin/cinnabar. *Anal. Bioanal. Chem.* **402**, 2183–2193 (2012).
90. Martinetto, P. Cristallographie des matériaux hétérogènes ou partiellement cristallisés : application aux matériaux du Patrimoine et solides moléculaires organiques To cite this version : HAL Id : tel-00675961 Université Joseph Fourier Grenoble 1 Habilitation à Diriger . (2012).
91. Beck, L. *et al.* Absolute dating of lead carbonates in ancient cosmetics by radiocarbon. *Commun. Chem.* **1**, 1–7 (2018).
92. Welcomme, E., Walter, P., Van Elslande, E. & Tsoucaris, G. Investigation of white pigments used as make-up during the Greco-Roman period. *Appl. Phys. A Mater. Sci. Process.* **83**, 551–556 (2006).
93. Gonzalez, V., Wallez, G., Calligaro, T., Gourier, D. & Menu, M. Synthesizing lead white

- pigments by lead corrosion: New insights into the ancient manufacturing processes. *Corros. Sci.* **146**, 10–17 (2018).
94. Gliozzo, E. & Ionescu, C. Pigments — Lead-based whites, reds, yellows and oranges and their alteration phases. *Archaeol. Anthropol. Sci.* **14**, (2022).
  95. Plesters, J. 2. Ultramarine Blue, Natural and Artificial. *Stud. Conserv.* **11**, 62–65 (1966).
  96. Mertens, J. The History of Artificial Ultramarine (1787–1844): Science, Industry and Secrecy. *Ambix* **51**, 219–244 (2004).
  97. Borhade, A. V., Kshirsagar, T. A. & Dholi, A. G. Novel synthesis of ultramarine blue from waste coal fly ash via thiocyanate aluminosilicate sodalite. *J. Sulfur Chem.* **37**, 632–645 (2016).
  98. Boros, Ę. *et al.* On the dissolution of non-metallic solid elements (sulfur, selenium, tellurium and phosphorus) in ionic liquids. *Chem. Commun.* **46**, 716–718 (2010).
  99. Chukanov, N. V., Sapozhnikov, A. N., Shendrik, R. Y., Vigasina, M. F. & Steudel, R. Spectroscopic and crystal-chemical features of sodalite-group minerals from gem lazurite deposits. *Minerals* **10**, 1–23 (2020).
  100. Orlova, Y., Harmon, R. E., Broadbelt, L. J. & Iedema, P. D. Review of the kinetics and simulations of linseed oil autoxidation. *Prog. Org. Coatings* **151**, 106041 (2021).
  101. Mallégol, J., Gardette, J. L. & Lemaire, J. Long-term behavior of oil-based varnishes and paints. Photo- and thermooxidation of cured linseed oil. *JAOCS, J. Am. Oil Chem. Soc.* **77**, 257–263 (2000).
  102. Cairns, L. K. & Forbes, P. B. C. Insights into the yellowing of drying oils using fluorescence spectroscopy. *Herit. Sci.* **8**, 1–11 (2020).
  103. Nardelli, F. *et al.* The stability of paintings and the molecular structure of the oil paint polymeric network. *Sci. Rep.* **11**, 1–13 (2021).
  104. Daimer, K. & Kulozik, U. Oil-in-water emulsion properties of egg yolk: Effect of enzymatic modification by phospholipase A2. *Food Hydrocoll.* **23**, 1366–1373 (2009).
  105. Kiosseoglou, V. Egg yolk protein gels and emulsions. *Curr. Opin. Colloid Interface Sci.* **8**, 365–370 (2003).
  106. Anton, M. *et al.* Chemical and structural characterisation of low-density lipoproteins purified from hen egg yolk. *Food Chem.* **83**, 175–183 (2003).
  107. Anton, M. *Bioactive Egg Compounds*. (Springer, 2007).
  108. Cordobés, F., Partal, P. & Guerrero, A. Rheology and microstructure of heat-induced egg yolk gels. *Rheol. Acta* **43**, 184–195 (2004).
  109. Severa, L., Nedomová, Š. & Buchar, J. Influence of storing time and temperature on the viscosity of an egg yolk. *J. Food Eng.* **96**, 266–269 (2010).
  110. Sharp, P. F. & Powell, C. K. Increase in the pH of the White and Yolk of Hens' Eggs. *Ind. Eng. Chem.* **23**, 196–199 (1931).
  111. Sousa, R. de C. S. *et al.* Effect of pH and salt concentration on the solubility and density of egg yolk and plasma egg yolk. *LWT - Food Sci. Technol.* **40**, 1253–1258 (2007).
  112. Liu, J., Lv, Y., Mo, X., Duan, S. & Tong, Q. Effects of freezing and thawing treatment on the rheological and textural characteristics and micro-structure of heat-induced egg yolk gels. *J. Food Eng.* **216**, 144–150 (2018).
  113. Phenix, A. The composition and chemistry of eggs and egg tempera. *Early Ital. Paint. Tech. Anal.* 11–20 (1997) doi:10.1007/978-1-349-09142-3\_6.
  114. Yüce, C. & Willenbacher, N. Challenges in rheological characterization of highly



- concentrated suspensions — A case study for screen-printing silver pastes. *J. Vis. Exp.* **2017**, 1–17 (2017).
115. Koos, E., Kannowade, W. & Willenbacher, N. Restructuring and aging in a capillary suspension. *Rheol. Acta* **53**, 947–957 (2014).
  116. Viskosimetrie - Messung von Viskositäten und Fließkurven mit Rotationsviskosimetern - Teil 1: Grundlagen und Messgeometrie DIN 53019-1:2008-09.
  117. Benavente, D. *et al.* Influence of Surface Roughness on Color Changes in Building Stones. *Color Res. Appl.* **28**, 343–351 (2003).
  118. Ghinea, R. *et al.* Influence of surface roughness on the color of dental-resin composites. *J. Zhejiang Univ. Sci. B* **12**, 552–562 (2011).
  119. Gueli, A. M., Bonfiglio, G., Pasquale, S. & Troja, S. O. Effect of particle size on pigments colour. *Color Res. Appl.* **42**, 236–243 (2017).
  120. Pozo-Antonio, J. S. *et al.* Effect of tempera paint composition on their superficial physical properties- application of interferometric profilometry and hyperspectral imaging techniques. *Prog. Org. Coatings* **117**, 56–68 (2018).
  121. Bramanti, E., Bramanti, M., Stiavetti, P. & Benedetti, E. A frequency deconvolution procedure using a conjugate gradient minimization method with suitable constraints. *J. Chemom.* **8**, 409–421 (1994).
  122. Bramanti, E. & Benedetti, E. Determination of the secondary structure of isomeric forms of human serum albumin by a particular frequency deconvolution procedure applied to Fourier transform IR analysis. *Biopolymers* **38**, 639–653 (1996).
  123. Ranquet, O. *et al.* A holistic view on the role of egg yolk in Old Masters' oil paints. *Nat. Commun.* **14**, 1534 (2023).
  124. White, R. & Higgitt, C. Rembrandt's paint medium. in *Art in the making: Rembrandt* 48–51 (National Gallery Company, 2006).
  125. Koller, Johann; Fiedler, Irene; Baumer, U. Vermeers Maltechnik – eine Mischtechnik. in *Johannes Vermeer – Bei der Kupplerin* (ed. Neidhardt, Uta; Giebe, M.) 65–75 (Michael Sandstein Verlag, 2004).
  126. Koos, E. & Willenbacher, N. Capillary forces in suspension rheology. *Science (80-. )*. **331**, 897–900 (2011).
  127. Morrison, I. D. & Ross, S. *Colloidal dispersions: suspensions, emulsions, and foams*. (Wiley-Interscience New York, 2002).
  128. Okesanjo, O., Meredith, J. C. & Behrens, S. H. Structure-Property Relationship in Capillary Foams. *Langmuir* **37**, 10510–10520 (2021).
  129. Wang, G. S. *et al.* Formation of protein oleogels via capillary attraction of engineered protein particles. *Food Hydrocoll.* **133**, 107912 (2022).
  130. Domenech, T. & Velankar, S. Capillary-driven percolating networks in ternary blends of immiscible polymers and silica particles. *Rheol. Acta* **53**, 593–605 (2014).
  131. Hoffmann, S., Koos, E. & Willenbacher, N. Using capillary bridges to tune stability and flow behavior of food suspensions. *Food Hydrocoll.* **40**, 44–52 (2014).
  132. Eastlake, C. L. *Materials for a history of oil painting*. vol. 1 (Longman, Brown, Green and Longmans, 1847).
  133. Tiennot, M., Iannuzzi, D. & Hermens, E. Evolution of the viscoelastic properties of painting stratigraphies: a moisture weathering and nanoindentation approach. *Herit. Sci.* **9**, 1–10 (2021).

134. Almasian, M., Tiennot, M., Fiske, L. D. & Hermens, E. The use of ground glass in red glazes: structural 3D imaging and mechanical behaviour using optical coherence tomography and nanoindentation. *Herit. Sci.* **9**, 1–11 (2021).
135. Koos, E., Johannsmeier, J., Schwebler, L. & Willenbacher, N. Tuning suspension rheology using capillary forces. *Soft Matter* **8**, 6620–6628 (2012).
136. Bossler, F., Maurath, J., Dyhr, K., Willenbacher, N. & Koos, E. Fractal approaches to characterize the structure of capillary suspensions using rheology and confocal microscopy. *J. Rheol. (N. Y. N. Y.)* **62**, 183–196 (2018).
137. Bossler, F. & Koos, E. Structure of Particle Networks in Capillary Suspensions with Wetting and Nonwetting Fluids. *Langmuir* **32**, 1489–1501 (2016).
138. Piau, J.-M., Dorget, M., Paliarne, J.-F. & Pouchelon, A. Shear elasticity and yield stress of silica–silicone physical gels: Fractal approach. *J. Rheol. (N. Y. N. Y.)* **43**, 305–314 (1999).
139. Wu, H. & Morbidelli, M. Model relating structure of colloidal gels to their elastic properties. *Langmuir* **17**, 1030–1036 (2001).
140. Evans, D. F. & Wennerström, H. *The colloidal domain: where physics, chemistry, biology, and technology meet.* (Wiley-Vch, 1999).
141. Vincent, R., Powrie, W. D. & Fennema, O. Surface Activity of Yolk, Plasma and Dispersions of Yolk Fractions. *J. Food Sci.* **31**, 643–648 (1966).
142. Guérin-Dubiard, C. & Audic, J.-L. Egg-Protein-Based Films and Coatings. in *Bioactive Egg Compounds* (eds. Huopalahti, R., López-Fandiño, R., Anton, M. & Schade, R.) 265–273 (2007). doi:10.1007/978-3-540-37885-3.
143. Tumosa, C. S. & Mecklenburg, M. F. Weight changes on oxidation of drying and semi-drying oils. in *Collection Forum* 116–123 (2003).
144. Pizzimenti, S., Bernazzani, L., Tinè, M. R., Duce, C. & Bonaduce, I. Unravelling the effect of carbon black in the autoxidation mechanism of polyunsaturated oils. *J. Therm. Anal. Calorim.* **147**, 5451–5462 (2022).
145. Rudnik, E., Szczucinska, A., Gwardiak, H., Szulc, A. & Winiarska, A. Comparative studies of oxidative stability of linseed oil. *Thermochim. Acta* **370**, 135–140 (2001).
146. Nimalaratne, C. & Wu, J. Hen egg as an antioxidant food commodity: A review. *Nutrients* **7**, 8274–8293 (2015).
147. Tumosa, C. S. & Mecklenburg, M. F. The influence of lead ions on the drying of oils. *Stud. Conserv.* **50**, 39–47 (2005).
148. Lomova, M. V., Sukhorukov, G. B. & Antipina, M. N. Antioxidant coating of micronsize droplets for prevention of lipid peroxidation in oil-in-water emulsion. *ACS Appl. Mater. Interfaces* **2**, 3669–3676 (2010).
149. Stenberg, C., Svensson, M. & Johansson, M. A study of the drying of linseed oils with different fatty acid patterns using RTIR-spectroscopy and chemiluminescence (CL). *Ind. Crops Prod.* **21**, 263–272 (2005).
150. Nicholson, D. G. Drying of Linseed Oil Paint. *Ind. Eng. Chem.* **33**, 1148–1153 (1941).
151. Ranquet, O. *et al.* Tempera and Tempera Grassa—From Wet Paints to Solid Films. *ACS Appl. Polym. Mater.* **5**, 4664–4677 (2023).
152. Bomford, D., Dunkerton, J., Gordon, D., Roy, A. & Kirby, J. Italian Painting Before 1400. in *Art in the Making* 26–29 (1989).
153. Doherty, T. & Woollett, A. T. *Looking at paintings: a guide to technical terms.* (Getty Publications, 2009).

154. Mewis, J. & Wagner, N. J. *Colloidal suspension rheology*. (Cambridge university press, 2012).
155. Maron, S. H. & Pierce, P. E. Application of Ree-Eyring generalized flow theory to suspensions of spherical particles. *J. Colloid Sci.* **11**, 80–95 (1956).
156. Farris, R. J. Prediction of the Viscosity of Multimodal Suspensions from Unimodal Viscosity Data. *Trans. Soc. Rheol.* **12**, 281–301 (1968).
157. Sudduth, R. D. A generalized model to predict the viscosity of solutions with suspended particles. IV. Determination of optimum particle-by-particle volume fractions. *J. Appl. Polym. Sci.* **52**, 985–996 (1994).
158. *Tempera Painting 1800 – 1950*. (Archetype Publications, 2019).
159. Mallégo, J., Lemaire, J. & Gardette, J. Drier influence on the curing of linseed oil. *Prog. Org. Coatings* **39**, 107–113 (2000).
160. Meilunas, R. J., Bentsen, J. G. & Steinberg, A. Analysis of Aged Paint Binders by FTIR Spectroscopy. *Stud. Conserv.* **35**, 33–51 (1990).
161. Elias, R. J., Kellerby, S. S. & Decker, E. A. Antioxidant activity of proteins and peptides. *Crit. Rev. Food Sci. Nutr.* **48**, 430–441 (2008).
162. Rasti, F. & Scott, G. The Effects of Some Common Pigments on the Photo-Oxidation of Linseed Oil-Based Paint Media. *Stud. Conserv.* **25**, 145–156 (1980).
163. Boon, J. J., Van Der Weerd, J., Keune, K., Noble, P. & Wadum, J. Mechanical and chemical changes in Old Master paintings: dissolution, metal soap formation and remineralization processes in lead pigmented ground/intermediate paint layers of 17th century paintings. in *ICOM committee for conservation, 13th triennial meeting, Rio de Janeiro* 401–406 (James and James, 2002).
164. Cotte, M. *et al.* Lead soaps in paintings: Friends or foes? *Stud. Conserv.* **62**, 2–23 (2017).
165. Linn, R. *et al.* Evolved Gas Analysis-Mass Spectrometry to Identify the Earliest Organic Binder in Aegean Style Wall Paintings. *Angew. Chemie* **130**, 13441–13444 (2018).
166. Bonaduce, I. & Colombini, M. P. Gas chromatography/mass spectrometry for the characterization of organic materials in frescoes of the Momumental Cemetery of Pisa (Italy). *Rapid Commun. Mass Spectrom.* **17**, 2523–2527 (2003).
167. Sotiropoulou, S. *et al.* Advanced analytical investigation on degradation markers in wall paintings. *Microchem. J.* **139**, 278–294 (2018).
168. Orsini, S., Parlanti, F. & Bonaduce, I. Analytical pyrolysis of proteins in samples from artistic and archaeological objects. *J. Anal. Appl. Pyrolysis* **124**, 643–657 (2017).
169. Fabbri, D., Adamiano, A., Falini, G., De Marco, R. & Mancini, I. Analytical pyrolysis of dipeptides containing proline and amino acids with polar side chains. Novel 2,5-diketopiperazine markers in the pyrolysates of proteins. *J. Anal. Appl. Pyrolysis* **95**, 145–155 (2012).
170. Samman, S. *et al.* Fatty acid composition of certified organic, conventional and omega-3 eggs. *Food Chem.* **116**, 911–914 (2009).
171. La Nasa, J. *et al.* The role of the polymeric network in the water sensitivity of modern oil paints. *Sci. Rep.* **9**, 1–12 (2019).
172. Linn, R. *et al.* Evolved Gas Analysis-Mass Spectrometry to Identify the Earliest Organic Binder in Aegean Style Wall Paintings. *Angew. Chemie Int. Ed.* **57**, 13257–13260 (2018).
173. Wollgarten, S., Yuze, C., Koos, E. & Willenbacher, N. Tailoring flow behavior and texture of water based cocoa suspensions. *Food Hydrocoll.* **52**, 167–174 (2016).

174. Ioakimoglou, E. *et al.* Thin-film study on the oxidation of linseed oil in the presence of selected copper pigments. *Chem. Mater.* **11**, 2013–2022 (1999).
175. ASTM E 313 - 00 Standard Practice for Calculating Yellowness and Whiteness Indices from Instrumentally Measured Color Coordinates. *Annual Book of ASTM Standards* vol. 06 1–6 (2015).
176. Kremser, T., Susoff, M., Roth, S., Kaschta, J. & Schubert, D. W. Degradation studies of a commercial radiation-resistant polypropylene sterilized by gamma and electron beam technology before and after subsequent accelerated aging cycles. *J. Appl. Polym. Sci.* **137**, 1–7 (2020).
177. Hirschler, R. Whiteness, Yellowness, and Browning in Food Colorimetry. *Color Food Technol. Psychophys. Asp.* 93–104 (2012).
178. Allgemeine Prüfverfahren für Pigmente und Füllstoffe - Teil 5: Bestimmung der Ölzahl (ISO 787-5:1980).
179. Sohn, H. Y. & Moreland, C. The effect of particle size distribution on packing density. *Can. J. Chem. Eng.* **46**, 162–167 (1968).
180. Chong, J. ., Christiansen, E. B. & Baer, A. . Rheology of concentrated suspensions. *J. Appl. Polym. Sci.* **15.8**, 2007–2021 (1971).
181. Zhang, X. *et al.* Effects of particle size distributions on PMMA dust flame propagation behaviors. *Powder Technol.* **317**, 197–208 (2017).
182. Sun, G. & Grace, J. R. Effect of particle size distribution in different fluidization regimes. *AIChE J.* **38**, 716–722 (1992).
183. de la Rie, E. R., Michelin, A., Ngako, M., Del Federico, E. & Del Grosso, C. Photo-catalytic degradation of binding media of ultramarine blue containing paint layers: A new perspective on the phenomenon of “ultramarine disease” in paintings. *Polym. Degrad. Stab.* **144**, 43–52 (2017).
184. Schnetz, K. *et al.* Evidence for the catalytic properties of ultramarine pigment. *J. Cult. Herit.* **45**, 25–32 (2020).
185. Li, S., Liu, M. & Sun, L. Preparation of acid-resisting ultramarine blue by novel two-step silica coating process. *Ind. Eng. Chem. Res.* **50**, 7326–7331 (2011).
186. Paints and varnishes –Wettability – Part 2: Determination of the surface free energy of solid surfaces by measuring the contact angle (ISO 19403-2:2017).
187. Volz, H. G. & Simon, F. T. *Industrial color testing*. vol. 2 (Wiley-VCH New York, 2001).